UNIVERSITY OF SOUTHAMPTON

MOLECULAR FLEXIBILITY IN THE DESIGN OF LOW MOLAR MASS LIQUID CRYSTALS

by

Corrie Thomas Imrie

A dissertation submitted in partial fulfilment of the requirements for the degree of Doctor of Philosophy at the University of Southampton.

Department of Chemistry

May 1988

CONTENTS

UNIVERSITY OF SOUTHAMPTON

ABSTRACT

FACULTY OF SCIENCE

CHEMISTRY

Doctor of Philosophy

MOLECULAR FLEXIBILITY IN THE DESIGN OF LOW MOLAR MASS LIQUID CRYSTALS

by Corrie Thomas Imrie

This Thesis investigates the influence of molecular flexibility on the mesogenic behaviour and in particular, the properties of dimeric liquid crystals and their relationship to molecular structure. Dimers possess two semi-rigid anisometric units linked through a flexible alkyl spacer; this increased overall flexibility was thought to suppress smectic behaviour. In Chapter 2, however, the properties of several series of α,ω-bis(4-alkylanilinebenzylidine-4'-oxy)alkanes are presented and these serve as the first examples of dimers which exhibit a rich smectic polymorphism. Chapter 3 introduces a new class of dimer, the asymmetric dimeric liquid crystal, in which two different mesogenic groups are linked through a flexible spacer, and as examples, the α-(4-cyanobiphenyl-4'-oxy)-ω-(4-alkylaniline-benzylidine-4'-oxy)alkanes were synthesised. The dependence of the thermal stability of the smectic phase on the length of the terminal alkyl chain is very unusual because it does not simply increase on increasing chain length but instead passes through a minimum. This novel behaviour is rationalised by proposing that the structure of the smectic phase changes from being intercalated to interdigitated on increasing chain length. Chapter 4 investigates the properties of dimers and their relationship to molecular structure via the synthesis of a range of new compounds. In Chapter 5, the effect of a flexible core is examined in compounds which possess a mesogenic group linked via an alkyl chain to a small anisometric group. Finally, Chapter 6 presents the transitional properties of several series of mesogens which possess lateral alkyl chains; the observation of liquid-crystalline behaviour for this class of compound is rationalised by proposing that the lateral chain lies parallel to the molecular long axis and so is not in its all-trans conformation.

ACKNOWLEDGEMENTS

I must begin by thanking my supervisor, Professor G.R. Luckhurst, without whose enthusiasm, expertise and help this Thesis would not have been possible.

I am also grateful to B.D.H. Chemicals Ltd., and in particular Dr. I. Sage and Dr. B. Sturgeon, for many useful ideas as well as for supplying me with several essential chemicals.

I would like to thank all the members of the Chemical Physics group at Southampton, but in particular those who have helped directly with my work and the completion of this Thesis; Dr. J.W. Emsley, Mr. A.P. Singh, Mr. R.W. Date, Miss L. Taylor, Dr. G.N. Shilstone, Dr. B.A. Timimi, Dr. J.M. Seddon, Dr. G.S. Attard, and especially Miss J.L. Hogan.

I wish to thank my wife, Chris, for her unflagging support and encouragement, and my parents for their continued understanding.

Finally, I would like to acknowledge the SERC for the award of a CASE research studentship.

CHAPTER ONE: AN INTRODUCTION TO RELATIONSHIPS BETWEEN MOLECULAR STRUCTURE AND LIQUID CRYSTALLINITY

It is almost inconceivable that as recently as 1967 Dewar [1] stated, in a standard undergraguate chemistry text, that "liquid crystals are uncommon and of no practical importance" because the intervening years have seen such a dramatic increase in both the quantity and breadth of liquid crystal research which has resulted in the applications of liquid crystals being many and commonplace. Indeed, the study of liquid crystals now embraces such diverse and technologically important topics as display devices, liposomes, detergents, high tensile strength fibres and optical information storage. The design and synthesis of thousands of new liquid crystals has been stimulated by the demands of the device engineer and this resulted in the discovery of new mesophases as well as enhancing our understanding of relationships between the liquid-crystalline properties of a compound and its molecular structure. The primary aim of this thesis was to further our understanding of these structure-property relationships by the design and synthesis of new liquid crystals and in particular, to investigate the role of molecular flexibility in determining the liquid-crystalline properties of a compound. This introductory chapter, therefore, provides a brief outline of our current knowledge concerning structure-property relationships in liquid crystals. We begin with a brief historical account of the discovery of liquid crystals and then discuss the various liquid crystal phases that have been observed and the means by which they are identified. In the second half of this introduction, structure-property relationships are described in both low and high molar mass liquid crystals as well as in a new class of mesogens, dimeric liquid crystals. The application potential of this new class of compounds is also described. Finally, a brief qualitative account of a molecular theory that describes nematics composed of flexible molecules is given.

In 1888, an Austrian botanist called Reinitzer made the surprising discovery that cholesteryl benzoate had two distinct melting points; the solid first melted at 145 °C forming a turbid liquid which on

heating to 179 °C underwent a second transiton to give a clear liquid [2]. Some years later, Lehmann showed that the curious turbid fluid exhibited properties associated with both liquids and crystals. For example, the molten compound is birefringent, a property typical of a crystal and yet it flows like a liquid. This combination of properties prompted Lehmann into terming the fluid, amongst other names, a liquid crystal [3]. The phase interposed between the solid and the isotropic liquid is generally referred to as a mesophase and a mesogen is any compound that exhibits a mesophase.

Since Reinitzer's original discovery of liquid-crystallinity in 1888 many thousands of compounds have been shown to exhibit mesogenic behaviour [4,5]. Mesogens may be grouped according to how the mesophase is obtained and by molecular structure; such a classification is given in figure 1. At the root of this classification is the separation of thermotropic from lyotropic liquid crystals.

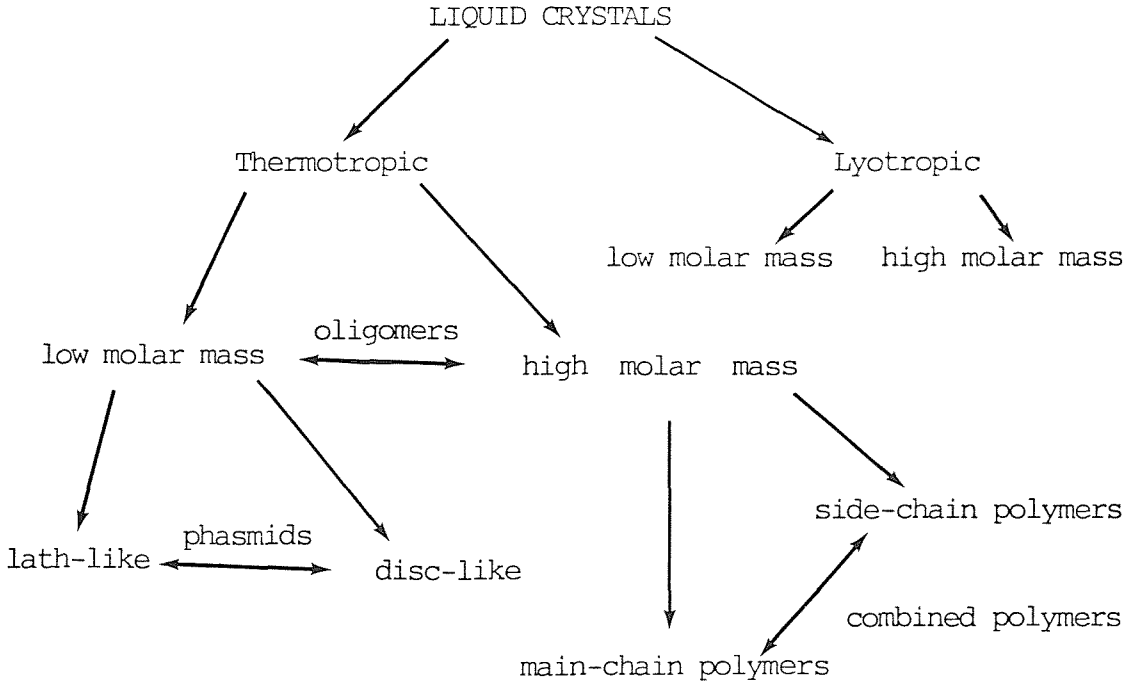

Figure 1 A classification of liquid-crystalline materials according to their molecular structure and the manner in which mesogenic behaviour is obtained.

Classically, thermotropic mesogens are considered to exhibit a mesophase as a result of a temperature change and by comparison a lyotropic mesogen is thought of as yielding a mesophase if dissolved in an appropriate solvent. This distinction, however, is no longer totally adequate and a more correct definition considers a lyotropic mesophase to consist of molecular aggregates or micelles whereas a thermotropic mesophase is a molecular and not a micellar system. It should be noted that a compound may be both a thermotropic and a lyotropic liquid crystal. Lyotropic liquid crystals are very important industrially encompassing such commercial products as detergents and liposomes. In this thesis, however, we restrict our attention to thermotropic liquid crystals. Thermotropic mesogens are further subdivided into two groups; compounds which exhibit a mesophase on heating the solid or cooling the isotropic liquid termed enantiotropic mesogens or those which form a mesophase only on supercooling the isotropic liquid denoted monotropic mesogens. Therefore, a mesophase exhibited by an enantiotropic mesogen is thermodynamically stable whereas that exhibited by a monotropic mesogen is thermodynamically unstable.

Over the last century many different types of mesophase have been discovered and these are classified according to the molecular arrangement present within the phase. In essence, there are three types of thermotropic liquid-crystalline mesophase formed by rod-like molecules; nematic, smectic and cubic. Recently, however, two new structural types of mesophase have been discovered and these will be mentioned briefly.

1.2.1 The nematic phase

The molecular arrangement within the nematic phase is the simplest of the three types. The molecular centres show only short range order but the molecules do possess a quasi-long-range orientational ordering of their long axes which tend to align parallel to a common axis called the director. A schematic representation of such an arrangement is given in figure 1.2.1.

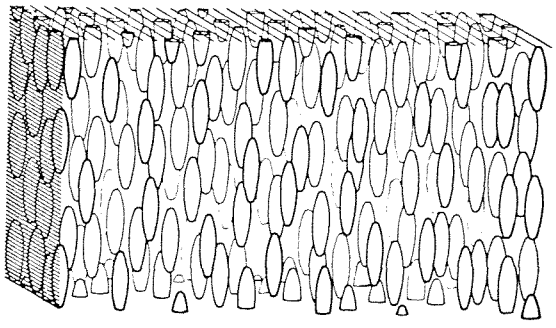

Figure 1.2.1 An idealised picture of the molecular organisation within the nematic phase.

1.2.2 The cholesteric phase

If a compound consisting of chiral molecules forms a nematic phase or if a chiral material is added to a nematic phase then the resulting phase exhibits a helical structure as illustrated in figure 1.2.2 and is termed a cholesteric phase. Thus, the molecules in a cholesteric phase tend to lie with their long axes parallel as in a nematic phase but on passing through the phase, the director is rotated through a constant angle. The cholesteric phase, therefore, can be thought of as being a twisted nematic with a definite periodicity or pitch length. Alternatively, the nematic phase may be considered to be a cholesteric phase in which the pitch length is infinite. It should be stressed that the helical structure present in a cholesteric phase is a consequence of the molecular chirality and is not induced by external constraints as it is, for example, in a twisted-nematic display device.

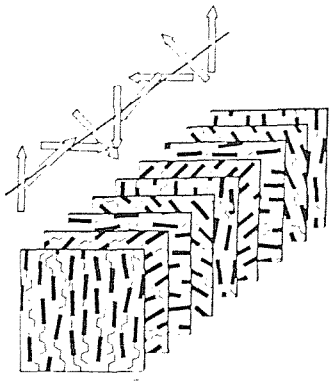

Figure 1.2.2 The helical structure within the cholesteric phase.

1.3 Smectic phases

A smectic phase differs from either a nematic or a cholesteric phase in that the positions of the molecular centres are correlated and arranged into layers. Clearly, it is easy to imagine a variety of molecular arrangements within the layers resulting in a range of possible smectic morphologies and indeed, many smectic modifications have been observed. Each different smectic phase has an associated letter, for example the smectic A phase. It should be stressed that this letter has no physical significance whatsoever. This nomenclature arose historically so that the first smectic phase to be discovered was assigned the letter A, the second B and so on. However, the same phase has sometimes been assigned differing letters by different groups and this resulted in considerable confusion. This situation has been remedied by the general acceptance of a system of nomenclature for the various smectic modifications [6]. More recently, it has been demonstrated that certain smectic mesophases actually possess long-range ordering of the molecular centres in three-dimensions and therefore, should strictly be termed crystals or perhaps, plastic crystals given the rotational motion of the molecules in these phases. Leadbetter [7] proposed that such smectic phases should be referred to by only their letter in order to distinguish them from "true" smectic phases: for example, the smectic E phase becomes simply the E phase. This nomenclature, however, has still to receive widespread acceptance and therefore, throughout this thesis such crystallline phases are still referred to as smectics. Any discussion of smectic phase structures must involve the concept of bond orientational order; a structure that possesses bond orientational order is one in which the direction of a unit vector which describes the lattice axis is preserved throughout the structure. It is important to note that long-range bond orientational ordering may exist without the presence of long-range positional ordering of the molecular centres.

1.3.1 The smectic A phase

Of all the various smectic modifications the smectic A phase possesses least order and if included in a smectic phase sequence then it is

always the highest temperature phase. The classical view of this phase has the molecules arranged into well defined layers with their long axes or more strictly, the director, perpendicular to the layer plane. The lateral distribution of the molecules within each layer is random and the molecules are able to rotate freely about their long axes. This simple model, however, fails to explain a number of experimental observations including, for example, the fact that the lamellar spacings for many smectic A phases are considerably shorter than the estimated all-trans molecular length and in some cases, the ratio of the lamellar spacing to the all-trans molecular length may be as low as 0.8. To account for such observations, the model of the smectic A phase is simply extended to allow for molecular fluctuations away from the layer normal or director. Figure 1.3.1.1 is a diagrammatic representation of the smectic A phase and it should be stressed that the layers are not well defined but are instead very diffuse.

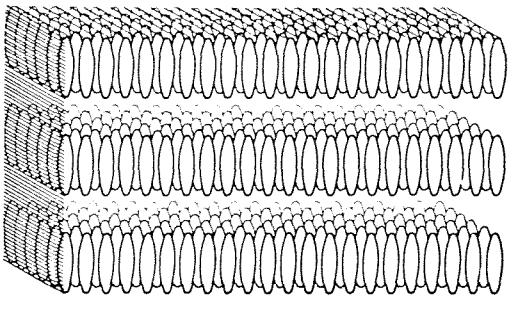

Figure 1.3.1.1 A diagrammatic representation of the molecular organisation in a smectic A phase.

Smectic A phases exhibited by compounds having strongly polar groups often have an additional ordering present which is based on a tendency to antiferroelectric ordering of molecules [8]. The known structures are termed S_{A_1}, S_{A_2}, S_{A_d} and $S_{\tilde{A}}$ and are illustrated in figure 1.3.1.2. S_{A_1} is a conventional smectic A phase with completely random head-to-

tail disorder and S_{A_2} has a bilayered structure with antiferroelectric ordering of the molecules [9]. Transitions between S_{A_1} and S_{A_2} phases have been observed with the S_{A_2} modification normally being the higher temperature phase. The S_{A_d} phase has an interdigitated bilayer structure with partial molecular association. It should be noted that it is possible to have smectic A phases that are composed of regions having differing structural types, for example a mixture of S_{A_2} and S_{A_d} [10], and such phases are termed incommensurate. The smectic A antiphase, denoted $S_{\tilde{A}}$ [10], is thought to possess an S_{A_2} type structure but there is modulated antiferroelectric ordering present within the layers. This is illustrated in figures 1.3.1.2(a) and 1.3.1.2(b). In figure 1.3.1.2(a), a bilayer structure is evident by looking along X, following the modulation. However, by looking along the bilayer X in a plane orthogonal to the molecular axes at the maxima and minima of the modulation a structure similar to figure 1.3.1.2(b) can be seen.

The final smectic A phase modification to be discussed is one in which the ratio of the lamellar spacing to the estimated all-trans molecular length is much less than one and its structure involves the interleaving of differing parts of the molecule. This modification has been termed the intercalated smectic A phase [11] and is discussed more fully in Chapter 3.

1.3.2 The smectic C phase

The smectic C phase is simply the tilted analogue of the smectic A phase. Thus, the molecules are arranged in layers in which the lateral distribution of the molecular centres is essentially random and the molecules are able to rotate freely about their long axes. The smectic C phase differs from the smectic A phase in that the director is tilted with respect to the layer normals and there is a long range correlation of this tilt direction. It should be noted that there is more than one tilt angle at the molecular level; for example, there is a core tilt angle and a different alkyl chain tilt angle. These tilt angles in a smectic C phase vary with temperature and usually increase

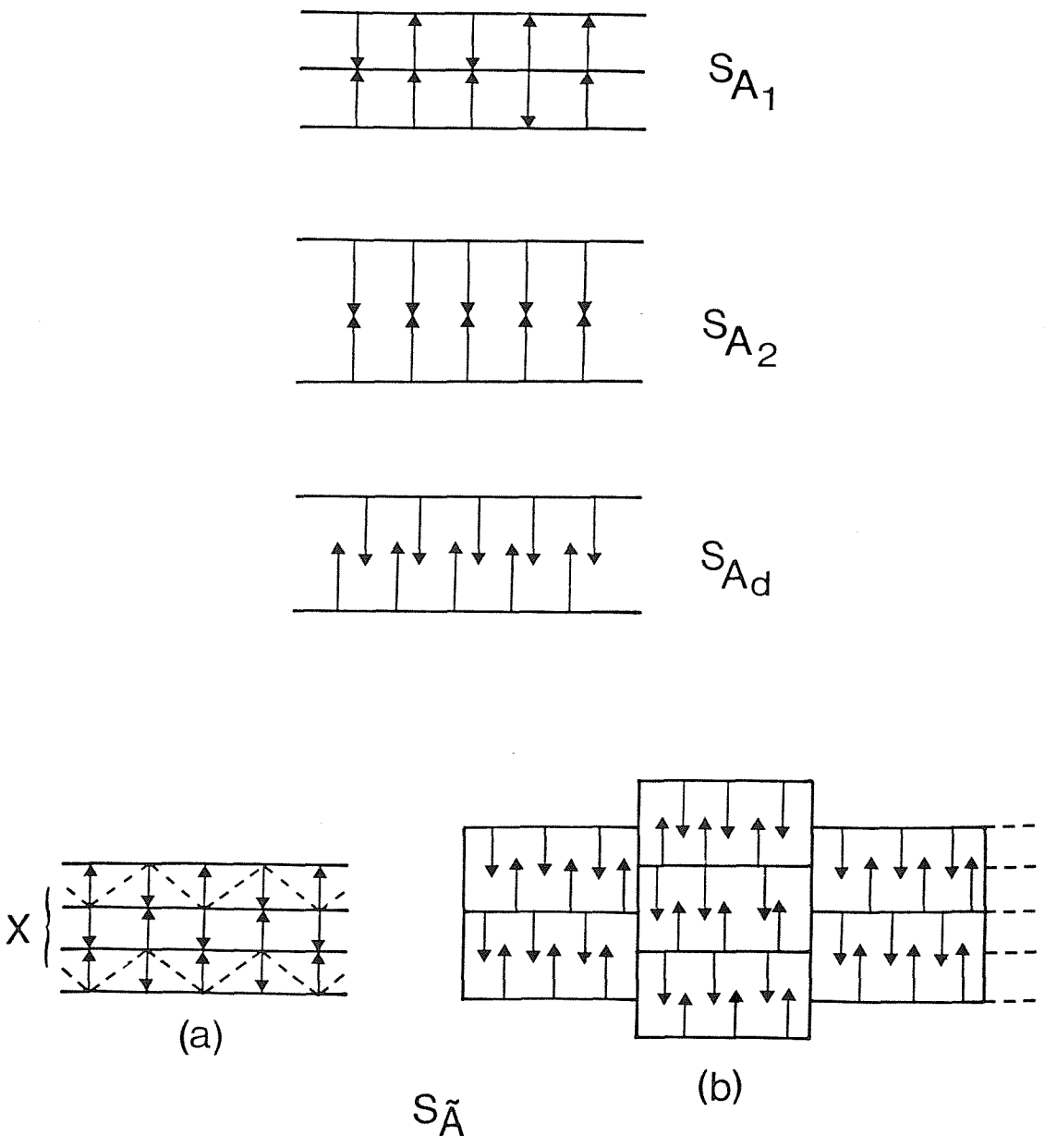

Figure 1.3.1.2 Schematic representations of smectic A phases exhibited by polar compounds; the arrows represent the molecules with the arrowhead depicting the terminal electronegative substituent.

with decreasing temperature [12]. This variation, however, is not so evident in a smectic C phase that has been produced by cooling a nematic phase. The smectic C phase is a biaxial phase and the smectic A-smectic C transition is second order in nature. Smectic C phases exhibited by polar compounds are the tilted analogues of the S_{A_1}, S_{A_2}, S_{A_d} and $S_{\tilde{A}}$ phases illustrated in figure 1.3.1.2 and are termed S_{C_1}, S_{C_2}, S_{C_d} and $S_{\tilde{C}}$ respectively.

If a compound consisting of chiral molecules forms a smectic C phase then the phase itself is optically active and is termed a chiral smectic C phase. The structure of this phase is essentially the same as the achiral smectic C phase except that the tilted directors form a helical distribution on passing from layer to layer.

1.3.3 The smectic B phase

Two very different modifications of the smectic B phase have been identified [13]; namely, the hexatic B phase and the crystal B phase. In both modifications, the director is orthogonal to the layer planes and the molecules rotate in cooperative manner about their long axes. The hexatic B phase is a true liquid crystal and its structure is based on weakly coupled ordered layers. Within the layers, the molecules are packed in a hexagonal manner with medium range positional order giving a correlation length which is an order of magnitude larger than in either the smectic A or C phases. There are no interlayer positional correlations in the hexatic B phase but three-dimensional long-range bond orientational ordering is present within the structure. In comparison, the crystal B phase possesses long-range layer correlations and also, positional long-range ordering within the layers as well as three-dimensional long-range bond orientational ordering [7]. Thus, the crystal B phase is uniaxial with true hexagonal symmetry associated with dynamic rotational disorder about the six-fold axis. Clearly, there are a number of possible packing arrangements of the layers in a crystal B phase and transitions between different packing modifications have been observed [13]. It should also be noted that transitions between the

hexatic B and crystal B phases have been observed [14]. The type of smectic B phase exhibited by a compound appears, not surprisingly, to be dependent upon its molecular structure. For example, if the central linkage in the aromatic core is of the Schiff's base type then a crystal B phase is observed whereas ester linked compounds normally exhibit hexatic B phases [15].

For smectic B phases exhibited by compounds composed of highly polar molecules we may expect to see the analogous stuctures to the S_{A_2}, S_{A_1} and $S_{\tilde{A}}$ phases and indeed, this is the case for CCH-3. The lamellar spacing of the smectic B phase exhibited by CCH-3 is twice its molecular length and this implies a bilayer similar to that of the S_{A_2} phase except that the the molecules are hexagonally close-packed within the layers [16]. Hence, this phase may be termed the S_{B_2} phase.

1.3.4 The smectic E phase

The structure of the smectic E phase is simply that of the crystal B phase in which free or co-operative motion of the molecules about their long axes is no longer possible resulting in a herringbone-type packing of the molecular cross-sectional areas within the layers, as illustrated in figure 1.3.4.1. Thus, the smectic E phase is a highly

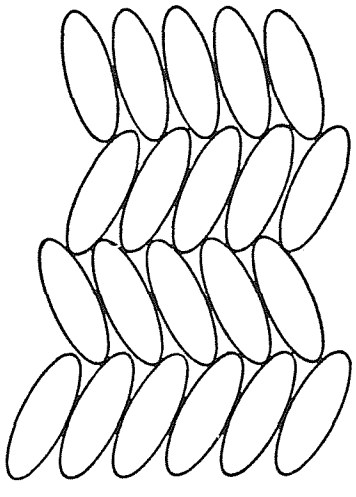

Figure 1.3.4.1 The herringbone packing of the molecules in a smectic E phase

ordered, biaxial orthogonal phase in which the molecules are in an orthorhombic array within the layers. There is both long-range positional ordering of the molecules within the layers and long-range layer corrrelations, as well as, three-dimensional long-range bond orientational ordering. Consequently, the smectic E phase should strictly be referred to as a crystal or a plastic crystal in which the molecules are disordered with respect to rotations of π about both their long and short molecular axes.

1.3.5 The smectic F and I phases

The smectic F and I phases are best considered together for structurally they are very similar. Both phases are composed of layers in which the molecules are packed in a pseudo-hexagonal manner and the director is tilted with respect to the normals to the layer planes. There is no long-range positional order of the molecular centres within the layers and no long-range correlation between layers. Both phases do possess, however, three-dimensional long-range bond orientational ordering and therefore, the smectic F and I phases may be considered to be the tilted analogues of the hexatic smectic B phase. The structural difference between the smectic F and I phases lies with the tilt direction of the director with respect to the quasi-hexagonal net. Clearly, there are two possible tilt directions of the director; towards an edge of the quasi-hexagon or towards its apex. In the smectic F phase the tilt direction of the director is towards an edge of the quasi-hexagon and in the smectic I phase it is towards an apex of the quasi-hexagon. This is represented schematically in figure 1.3.5.1. It should be noted that there is some debate concerning the in-plane correlation length in these two phases and it has been suggested that for the smectic I modification there is actually long-range ordering present within the layers [17]. The smectic I phase may, therefore, consist of stacks of two dimensionally ordered crystals whereas it is generally accepted that the smectic F phase is a tilted hexatic phase.

If a compound composed of chiral molecules exhibits either a smectic F

or I phase then the phase itself is optically active. The structures of the chiral smectic F and I phases are presumed to be analogous to that of the chiral smectic C phase but obviously, with the molecules packed in a pseudo-hexagonal manner within the layers.

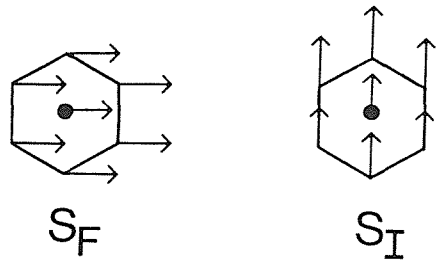

Figure 1.3.5.1 The tilt direction of the director in the smectic F and I phases.

1.3.6 The smectic G and J phases

The smectic G and J phases are the tilted analogues of the crystal B phase and so should be considered as the crystal analogues of the smectic F and I phases. Thus, in both the smectic G and J phases the molecular centres are pseudo-hexagonally packed within layers and the director is tilted with respect to the normal to the layer planes. There is long-range correlation of the molecular positions within the layers and also between the layers giving rise to a three-dimensionally ordered structure. The structural difference between the two phases rests with the direction of the tilt of the director with respect to the quasi-hexagonal net; in the crystal G phase, the director is tilted towards an edge of the quasi-hexagon whereas in the crystal J phase it is towards an apex of the quasi-hexagon.

If a pure compound possessing a chiral structure exhibits a smectic G or J phase then the phase is, surprisingly, achiral. Presumably, the crystal forces supress the helical arrangement of the tilt direction. Chiral smectic G phases have, however, been observed for mixtures in which it is believed the forces between the layers are weakened so permitting a helical structure to form.

1.3.7 The smectic H and K phases

The smectic H and K phases are the tilted analogues of the smectic E phase and thus, related to the smectic G and J phases by a loss of rotational freedom. The smectic H and K phases are, therefore, composed of layers in which the molecules are in a herringbone arrangement and the director is tilted with respect to the normal to the layer planes. There is both long-range positional order of the molecular centres within the layers and long-range correlations between the layers, as well as, three-dimensional long-range bond orientational order. The two phases have monoclinic symmetry and differ only in the tilt direction of the director with respect to the orthorhombic net; in the smectic H phase the director is tilted towards an edge of the net whereas in the smectic K phase the director is tilted towards an apex of the net. This is illustrated in figure 1.3.7.1. It should be stressed that the smectic H and K phases are crystals or plastic crystals which are disordered with respect to rotations of π about both the long and short molecular axes although, the time-scales of these motions are quite different.

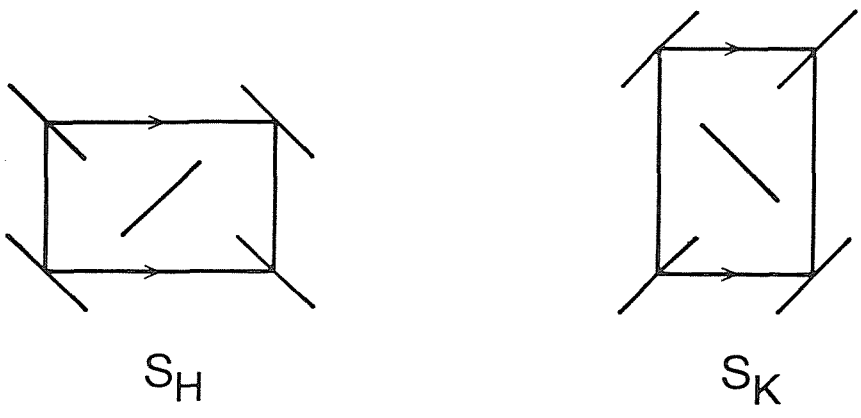

Figure 1.3.7.1 The tilt direction of the director in the smectic H and K phases.

1.4 Cubic phases

Cubic phases are exhibited by only a very small number of thermotropic liquid crystals and results from miscibility experiments suggest there to be at least two different structural modifications of the phase. The first of these to be observed is termed the D phase, fomerly the smectic D phase, is exhibited by two compounds of the homologous series, the 4'-n-alkoxy-3'-nitrobiphenyl-4-carboxylic acids [18]:

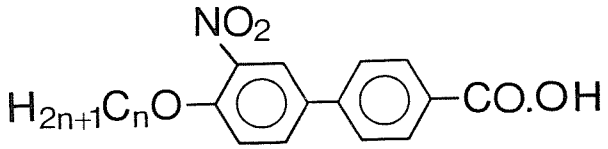

The D phase, and cubic phases in general, are easily identified for they are optically isotropic and very viscous but can not be mistaken for an isotropic liquid because it is sandwiched between two ordered phases. The cyano-substituted analogues of the nitro-acids, the 4'-n-alkoxy-3'-cyanobiphenyl-4-carboxylic acids, also exhibit a cubic phase and the cubic phases of all four compounds are continuously miscible over the entire composition range for all the possible binary mixtures [6]. Single-crystal diffraction experiments have shown the D phase to be a three-dimensional crystal with a primitive cubic structure and diffuse X-ray scattering reveals that locally molecules are packed with short range positional odering [19]. The structure giving rise to the cubic long-range ordering is thought to involve collections of molecules packed into quasi-spherical or rod-like aggregations which can pack together in a manner resulting in overall cubic symmetry.

The second type of cubic phase is exhibited by three members of the 1,2-bis-(4-n-alkoxybenzoyl)-hydrazines [20]:

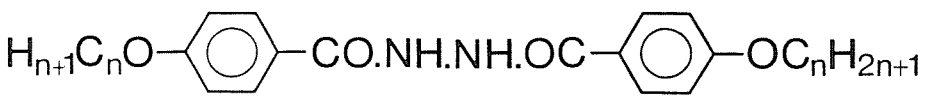

The cubic phase exhibited by these compounds is not miscible with the D phase and therefore, the same code letter can not be used to describe the two phases. The cubic phase of the hydrazine derivatives

also appears to have a primitive cubic space group.

Recently, Tinh et al [21] discovered a cubic phase exhibited by a biforked mesogen:

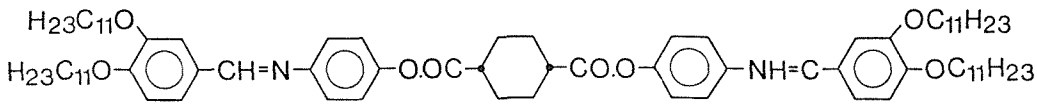

The miscibility of this cubic phase with either of the other two is currently not known.

1.5 Recent Developments

Malthete et al [22] have recently reported a new class of liquid crystals which they termed phasmids and are composed of molecules having a rod-like semi-rigid core terminating in two half-disc-shaped moieties, normally two trialkoxybenzoate groups. These compounds exhibit mesophases having structures intermediate between those of columnar and lamellar phases.

1.6 The characterisation of smectic phases

The unambiguous classification of a smectic phase can only be achieved by using a number of techniques including microscopy, miscibility, thermal analysis and x-ray diffraction. With the exception of miscibility, each of thse methods has been used throughout this thesis to identify mesophases; it is probably true that the increased availability of both x-ray and neutron diffraction has and will continue to reduce the need to perform miscibility experiments.

1.6.1 Polarising microscopy

A nematic or smectic phase when viewed under a polarising microscope exhibits an optical texture which is characteristic of that phase and hence, polarising microscopy can be used as a method of phase identification. Optical textures can be divided into two types, natural or paramorphotic. A natural texture is one which is obtained when the smectic phase is formed on cooling either the nematic or isotropic phase. A paramorphotic texture is obtained when the smectic phase under observation is formed by cooling another smectic phase and consequently, the resulting texture inherits some of its features from its predecessor. A brief summary of the more commonly observed optical textures will be given and a detailed account of these can be found in the book "Smectic Liquid Crystals - Textures and Structures" [6].

1.6.1.1 The smectic A phase

The smectic A phase exhibits two natural textures; the focal-conic fan texure and the homeotropic or pseudoisotropic texture. The homeotropic texture appears optically isotropic and is observed if the director is perpendicular to the glass slide. The focal-conic fan texture develops on cooling either the isotropic or nematic phase in the form of batonnets which consist of growing focal-conic domains and these coalesce forming the texture. If this is not the case and the phase instead separates out in the form of streaks or droplets then this indicates that the sample is impure. If the smectic A phase forms part

of a phase sequence, then to aid the identification of tilted phases it is particularly important to achieve regions of homeotropic alignment because the pseudoisotropic texture is lost if the director tilts. Homeotropic alignment can be achieved in a number of ways including, the use of very clean glass slides, by the preparation of thin samples or by using slides that have been treated with surfactants. For the characterisation of subsequent orthogonal phases it is better to obtain regions of focal-conic fan texture.

1.6.1.2 The smectic C phase

The smectic C phase has two natural textures, the focal-conic fan texture and the schlieren texture, and in addition exhibits one paramorphotic texture, the focal-conic fan texture. The natural focal-conic fan texture is very rarely obtained. The far more common schlieren texture may be distinguished from the nematic schlieren texture in three ways. First, a schlieren texture has black bands occuring throughout which are often referred to as schlieren-brushes and which meet at point singularities. In a nematic schlieren texture there are two types of point singularities, one having two associated brushes and the other has four brushes; by comparison, only the latter type of point singularity is observed in the smectic C schlieren texture. Secondly, the nematic schlieren texture 'flashes' when subjected to mechanical stress whereas the smectic C schlieren texture does not. Finally, the smectic C schlieren texture does not exhibit the same degree of brownian motion as its nematic counterpart. There are two other types of the smectic C schlieren texture: the sanded schlieren texture in which the point singularities and the associated brushes are very small and blurred resulting in a sanded appearance, and the lined schlieren texture in which the domains between the schlieren become lined. The paramorphotic focal-conic fan texture is always obtained on cooling the smectic A focal-conic fan texture and is typically very broken and sanded resulting in a rather ill-defined appearance. By comparison, the natural focal-conic fan texture of the smectic C phase is much less broken than that exhibited paramorphotically.

1.6.1.3 The smectic B phase

The smectic B phase exhibits two natural textures, the mosaic and homeotropic textures, and one paramorphotically, the focal-conic fan texture. Obviously, the homeotropic texture may be obtained as a pararmorphotic texture as well as naturally. The natural mosaic texture separates from either the isotropic or nematic phases in the form of platelets, discs or oblong sheets and these are often surrounded by homeotropic regions. The mosaic texture is characterised by the presence of 'H'-shaped birefringent areas. In the paramorphotic focal-conic fan texture, the fans appear as smooth cones showing no blemishes or fissures. On cooling the focal-conic fan texture of the smectic A phase transition bars sometimes occur at the transition to a smectic B phase. These bars occur transitorily and are reversible. The focal-conic fan texture of an smectic A phase which has been obtained by reheating a smectic B phase shows blemishes. There is, also, a truncated version of the focal-conic fan texture which is typically oberved for Schiff's base compounds that exhibit crystal B phases. In this texture, the fans are slightly deformed; the edges are stepped and the apices are squared-off rather than pointed.

1.6.1.4 The smectic E phase

There are very few examples of an isotropic to smectic E transition and, hence it is difficult to comment on natural textures. There are basically three types of paramorphotic texture exhibited by the smectic E phase; the focal-conic fan texture, the platelet texture and the mosaic texture. In the focal-conic fan texture, the backs of the fans are crossed with concentric lines or arcs which are not transitory but instead remain throughout the temperature range of the phase. The lines of the arcs are typically very clear and the areas between the lines are unbroken. This texture is very characteristic of the smectic ϵ phase and is often referred to as the arced paramorphotic focal-conic fan texture. A similar texture is obtained for the smectic G phase obtained by cooling a smectic B phase but in this instance the arcs appear broken and so can be readily

distinguished from the arced texture of the smectic E phase. The platelet texture is formed on cooling the homeotropic texture of either a smectic A or B phase and often appears grey-blue to yellow in colour. The texture differs from a normal platelet texture in that the platelets appear to be transparent so that ghost-like images of platelets can be seen through platelets near to the surface. Finally, the mosaic texture consists of mosaic platelets that are crossed with parallel lines and is normally obtained on cooling the mosaic texture of a smectic B phase.

1.6.1.5 The smectic F and I phases

The smectic F and I phases exhibit very similar textures and are difficult to distinguish if viewed in isolation. There are very few examples of transitions from the isotropic phase directly to either the smectic F or I phases and so generalisations concerning natural textures are impossible. It is, however, a relatively simple task to categorise a phase as being either a smectic F or I as opposed to any other phase and this stems from a very characteristic paramorphotic mosaic-schlieren texture. If a homeotropically smectic A phase or the schlieren smectic C texture is cooled to form a smectic F or I phase, if the resulting texture is largely schlieren in form and difficult to focus, it is probably a smectic I phase. If, however, the resulting texture has a mosaic appearance then it is more likely to be a smectic F phase.

The paramorphotic focal-conic fan texture of the smectic F phase produced by cooling a smectic C focal-conic fan texture is very distinctive. The broken and sanded fans of the smectic C texture become well defined and elongated 'L'-shaped patterns appear across their backs. A similar texture is also obtained on cooling the focal-conic fan texture of the smectic A phase.

1.6.1.6 The smectic G phase

The smectic G phase is known to exhibit a natural mosaic texture and this separates from the preceeding phase as large rectangular lancets which coalesce to form a mosaic texture composed of oblong platelets. Essentially two types of paramorphotic focal conic-fan textures are exhibited by the smectic G phase; the patchwork or broken fan texture which has a chequered appearance and the arced, broken focal-conic fan texture and this has already been discussed in 1.6.1.4. There are a large number of paramorphotic mosaic textures exhibited by the smectic G phase and these are dependent on the preceeding phase. In general, however, the texture consists of large, rounded platelet areas and often highly coloured. An exception to this is provided by cooling a homeotropically aligned smectic B sample which yields a mosaic texture at the transition to a smectic G phase that consists of small, ill-defined platelets that are not particularly birefringent.

1.6.1.7 The smectic H phase

The smectic H phase has yet to be obtained directly on cooling either the isotropic or nematic phases and consequently, no natural textures for this phase have been observed. A number of paramorphotic textures have been observed, however, and these can be divided into two types; the fan and the mosaic textures. The paramorphotic fan textures alone are not particularly useful in assigning this phase and instead it is easier to identify using the mosaic textures. There are a number of different types of paramorphotic mosaic texture observed for the smectic H phase ranging from those consisting of small, well-defined platelets to those comprising large, cross-hatched areas.

1.6.2 Differential Scanning Calorimetry

Differential scanning calorimetry is a valuable method for the investigation of phase transitions because it yields quantitative results from which conclusions may be drawn concerning the nature of the phases participating in the transition. The transition temperature and the enthalpy change associated with the transition are easily measured using differential scanning calorimetry. In addition, for single component systems the technique provides a fast non-destructive means of determining sample purity.

A differential scanning calorimeter consists of an average temperature circuit which measures and controls the temperature of the sample and reference holders, conforming to a predetermined time-temperature program. Simultaneously, a temperature difference circuit compares the temperature of the sample and reference holders and adjusts the heater of each so that their temperatures remain equal. When the sample undergoes a thermal transition there exists a temperature difference between the holders and thus, to maintain the same temperature in each pan the two heaters are supplied with a different power. This power difference is plotted as a function of the temperature of the holders and the area under the resulting curve is proportional to the enthalpy of transition for the sample. Therefore, to obtain the actual enthalpy value the calorimeter must be calibrated. For samples studied in this thesis, this calibration was performed using indium as the standard and the enthalpy of fusion of this was taken to be 28.47 $kJmol^{-1}$.

The transition temperature of a first order transition may be found by extrapolating the leading edge of the peak to the point at which it crosses the baseline. If the transition is broad, for example multiple melting transitions, then the temperature of the peak maximum is often quoted as being the transition temperature. In a second order transition the enthalpy change is zero and hence, no peak is observed. There is a change in the specific heat capacity, however, and this results in a step in the baseline. The temperature at which such a transition occurs is rather arbitrarily assigned as being the temperature at which the step reaches half-height. This is not

universally accepted and other points are often selected as representing the transition temperature. For example, the temperature of the onset of the step is sometimes referred to as being the transition temperature.

The determination of sample purity by differential scanning calorimetry uses the van't Hoff equation:

$$T_S = T_O - \frac{RT_O X}{\Delta H_f} \cdot \frac{1}{F}$$

where:

T_S = sample temperature;
T_O = melting point of the pure compound;
R = gas constant;
X = mole fraction impurity;
ΔH_f = the enthalpy of fusion for the pure compound;
F = fraction of total sample melted at T_S.

Theoretically, therefore, a plot of T_S against F^{-1} should yield a straight line with a gradient of $RT_OX(\Delta H_f)^{-1}$ and an intercept T_O. Experimentally, however, this line is usually curved concavely upwards and this is commonly attributed to undetected melting of the sample before the onset of the peak. This is corrected for by the addition of a small area to the curve before the start of the peak and then this area correction is varied until the T_S against F^{-1} plot is linear. If the initial plot of T_S against F^{-1} is linear or curved concavely downwards then the area correction is not required. The gradient and interecept, T_O, of the T_S against F^{-1} plot is calculated using a least squares fit to a straight line and the area, or corrected area, is used to determine ΔH_f. Finally, the van't Hoff equation may now be used to calculate the mole fraction impurity, X, using which a percentage purity value for the sample is obtained. Strictly, the van't Hoff isotherm is applicable to crystal-isotropic transitions only but in addition, it is assumed to hold for nematic-isotropic and smectic A-isotropic transitions.

1.6.3 X-ray Diffraction

X-ray diffraction is a very complex and powerful technique which can give the molecular architecture of a phase. In this thesis, however, X-ray diffraction is used solely as means to measure the thickness of smectic layers and, in consequence, the technique need only to be understood at a relatively simple level. Diffraction arises as a result of the interference between waves; if the wave amplitudes are in-phase then the waves augment each other and this is termed constructive interference whereas if the wave amplitudes are out-of-phase they cancel and this is destructive interference. The relative phases of waves originating from a common source depends on their path lengths. Figure 1.6.3.1 illustrates the reflection of X-rays from a stack of lattice planes in which d is the layer spacing and θ is the angle of incidence of the X-rays.

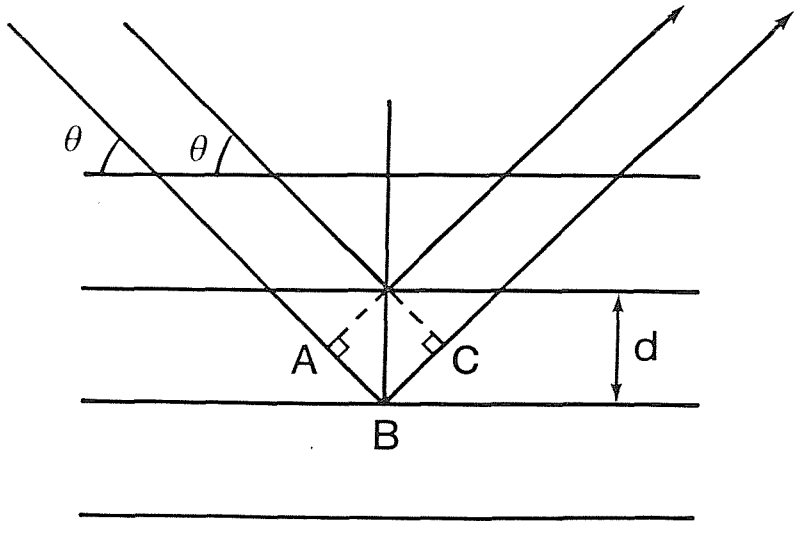

Figure 1.6.3.1 The reflection of X-rays from a stack of lattice planes.

The path-length difference between the rays shown in figure 1.6.3.1 is simply (AB+BC). Simple trigonometry then gives AB and BC to be the same and equal to $d\sin\theta$. Thus, the rays from adjacent layers and hence, from all layers, are in phase when the path-length difference,

$2d\sin\theta$, represents an integral number of wavelengths. For constructive interference to occur the wave amplitudes must be in-phase and therefore, bright reflections should be observed if:

$$n\lambda = 2d\sin\theta$$

and this condition is referred to as Bragg's law. The wavelength of the X-rays is known and the experiment measures 2θ. If we assume the first bright reflection to be the first order, that is n=1 in the Bragg condition, then it is a simple matter to calculate the layer spacing, d. It should be noted, however, that systematic absences of reflections may result in the first reflection not corresponding to n=1.

In a powder sample for example, an unorientated smectic phase, the layer stacks can occur at all orientations in space and this results in diffraction bands rather than spots as are observed for an orientated sample. The narrow angle band contains information concerning the layer spacing and the wide angle scattering arises as a consequence of nearest neighbour separations.

1.7 Structure-property relationships in low molar mass liquid crystals

The vast majority of low molar mass liquid crystals are composed of molecules having a semi-rigid core attached to which are one or two terminal alkyl chains. In essence, the rigid core enhances the liquid crystal-isotropic transition temperature and often comprises phenylene rings that are either connected directly or joined through a linking unit:

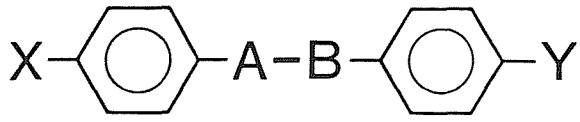

The linking unit, A-B, normally contains multiple bonds about which rotation is restricted thus preserving the rigidity and elongation of the core. In addition, multiple bonds increase the degree of conjugation present in the core and hence, enhance the polarisibility anisotropy of the molecule which, in turn, serves to increase the dispersion forces between the molecules. Figure 1.7.1 shows the effect of extending the core upon the nematic-isotropic transition temperature.

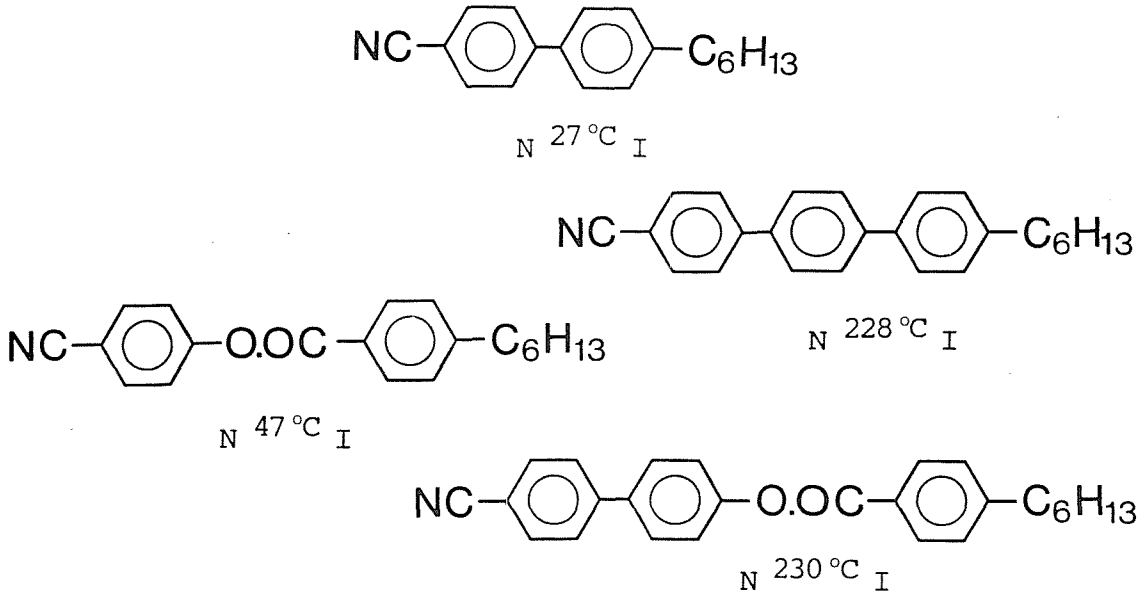

Figure 1.7.1 The effect of varying the core structure on nematic-isotropic transition temperatures [23,24,25].

Gray [26] has constructed an average order of efficiency for central groups, A-B, sited between two phenyl rings in increasing the nematic-isotropic transition temperature:

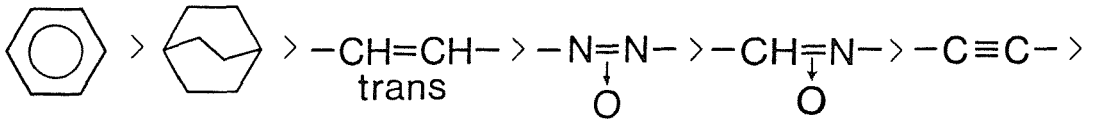

$$-N{=}N- > -CH{=}N- > -CO.O- > \text{none.}$$

In the light of the arguments offered involving conjugation the inclusion of the bicyclooctane ring in such a high position in the order is surprising but presumably this group preserves both the linearity and rigidity of the core; this example shows the importance molecular shape has in governing the liquid-crystalline properties of a compound. Indeed, if the terminal phenyl ring of a core is exchanged for either a bicyclooctyl ring or a cyclohexyl group then often increased nematic-isotropic transition temperatures are observed. For example:

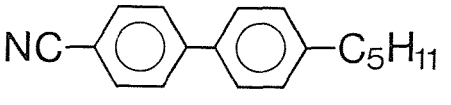

N 35 °C I [23]

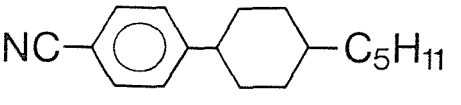

N 55 °C I [27]

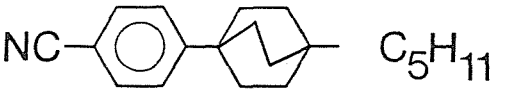

N 100 °C I [28]

It should be noted that heteroatomic rings, such as pyrimidine [29], have also been incorporated into the core structure.

Attached to the semi-rigid core are two terminal substituents of which one is normally an alkyl chain. Gray [26] has also constructed an average order of terminal group efficiency in enhancing the nematic-isotropic transition temperature:

$$Ph > NHCOCH_3 > CN > OCH_3 > NO_2 > Cl > Br > N(CH_3)_2 > CH_3 > F > H.$$

This ordering of different substituents can be rationalised in terms

of the substituent's polarisability and ability to interact with the conjugated system as well as its effect on the shape anisotropy of the molecule. It should be stressed that a substituent which is high in the order of promoting nematic thermal stability may be low in the order of enhancing smectic behaviour and in some cases substituents suppress smectic stability compared with the unsubstituted compounds [30].

The terminal substituents that have received greatest attention are alkyl and alkoxy chains. A great many homologous series have been characterised and the nematic-isotropic transition temperatures of a given series are found to alternate in a regular manner although as the length of the core is increased this alternation attenuates [31]. The higher transition temperatures are for compounds having an even number of carbon atoms in alkoxy chain or an odd number in an alkyl chain; it should be emphasised that it is the total number of atoms, excluding hydrogen atoms, in the chain that is important such that the oxygen atom in an alkoxy chain is equivalent to a carbon atom in an alkyl chain. The nematic-isotropic transition temperatures of a series having an alkoxy chain are some 30 °C to 40 °C greater than the analogous alkyl substituted compounds [26] and this obtains, in part, because the oxygen atom enhances the polarisabilty anisotropy of the core and thus, increases the dispersion forces between the molecules. The consequence of this alternation in the transition temperatures is that the nematic-isotropic transition temperatures of a given series lie on two smooth curves. Generally, if the nematic-isotropic transition tempertures are high then the curves fall whereas if they are low then the curves rise. The cross-over in behaviour occurs in the region of 100 °C in which the curves tend to be rather flat. The alternation in the transition temperatures can be rationalised in terms of the shape anistropy of the molecules and the change in the conformational distribution of the alkyl chain at the nematic-isotropic transition. An alkyl chain containing an odd number of carbon atoms can adopt more conformations for which the shape anisotropy of the molecule is enhanced than an alkyl chain consisting of an even number of carbon atoms. Furthermore, the nematic environment favours these elongated conformers and thus, there is a

greater change in the conformational distribution of an alkyl chain containing an odd number of carbon atoms than one containing an even number at the nematic-isotropic transition. It is this greater conformational contribution to the entropy change associated with the nematic-isotropic transition that results in a higher transition temperature for the even length alkyl chains. This explanation, however, only explains nematic-isotropic transition temperatures that rise as the length of the alkyl chain is increased. In order to rationalise falling transition temperatures with increasing chain length it is necessary to consider the alkyl chain as simply diluting the core-core interactions.

Increasing the length of terminal alkyl or alkoxy chains promotes smectic relative to nematic behaviour and eventually, nematic properties are extinguished. Figure 1.7.2 shows the dependence of the transition temperatures upon the length of the terminal alkyl chain for the 4-cyano-4'-n-alkylbiphenyls and both the alternation in the nematic-isotropic transition temperatures and the emergence of smectic behaviour upon increasing the chain length are clearly evident.

The effect of laterally substituting the core has been investigated [26] and this is discussed in Chapter 6. Briefly, however, the situation until recently was that generally the nematic-isotropic transition temperature was known to fall in proportion to the size of the substituent irrespective of its polarisability or polarity [26]; exceptions to this general observation are described in Chapter 6. The effect of lateral substituents upon the thermal stabilty of smectic phases is more complicated. For example, both the polarity and the size of the substituent are known to be important in determining smectic C phase stability so that although methyl and chloro substituents have approximately the same effect on nematic thermal stability, the methyl group reduces the thermal stability of the smectic C phase more than a chloro substituent [33].

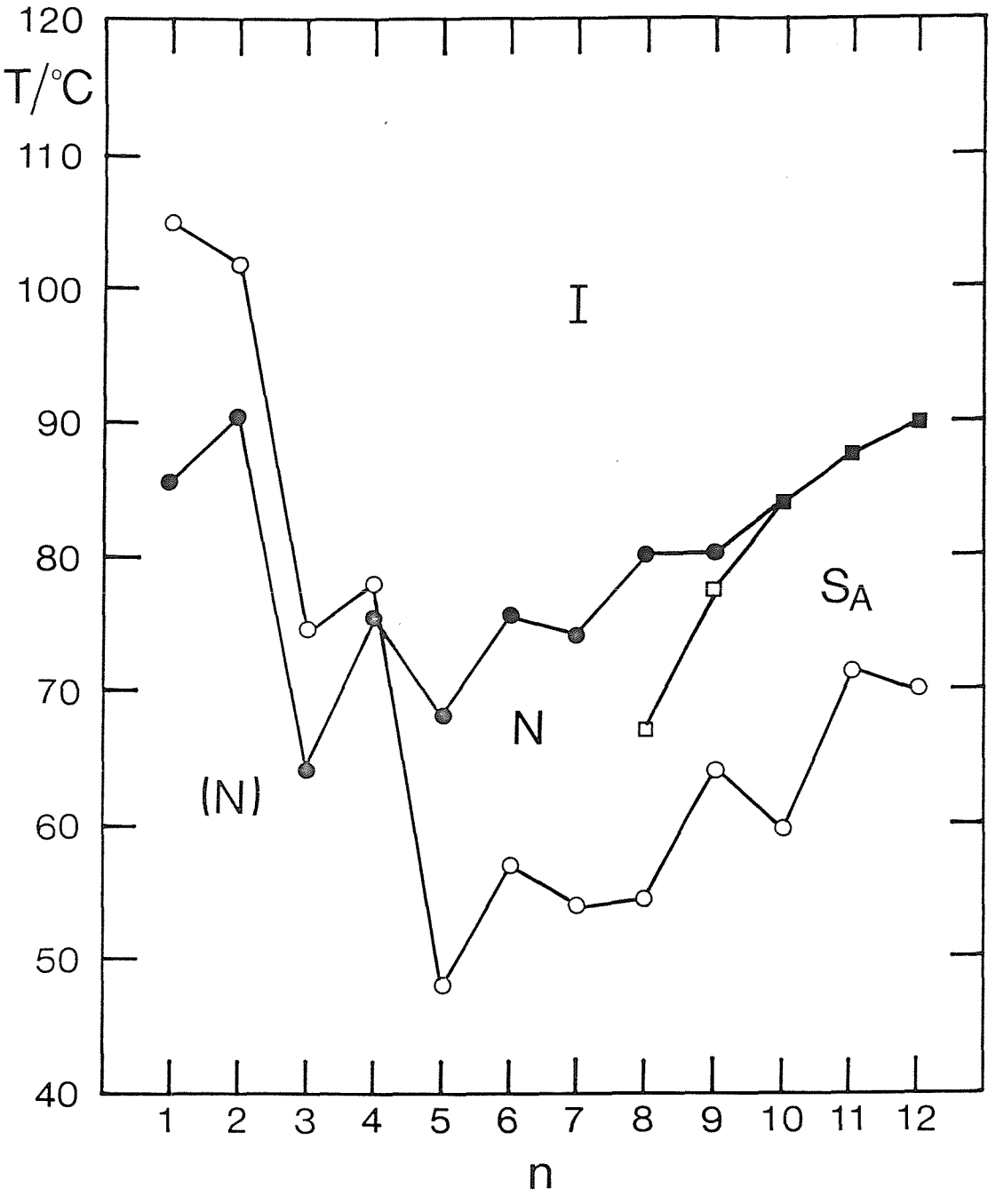

Figure 1.7.2 The dependence of the transition temperatures on the number of carbon atoms in the alkoxy chain for the 4-cyano-4-n-alkoxy-biphenyls; o denote the melting points, ● represent the nematic-isotropic transitions, ■ the smectic A-isotropic transitions and □ the smectic A-nematic transitions. Monotropic phases are marked in parentheses.

1.8 Structure property-relationships in thermotropic polymeric liquid crystals.

There are two conceivable ways in which low molar mass mesogenic moieties may be incorporated into a polymeric system; first, the mesogenic groups can form part of the polymer backbone or secondly, they may be attached as pendants linked via a flexible spacer to the polymer backbone. The former class of polymers are termed main-chain liquid-crystalline polymers and the latter class are known as side-chain liquid-crystalline polymers. Recently, these classes have been merged to produce combined liquid-crystalline polymers in which mesogenic groups are present both in the backbone and as pendants [34]. These three polymeric types are represented schematically in figure 1.8.1.

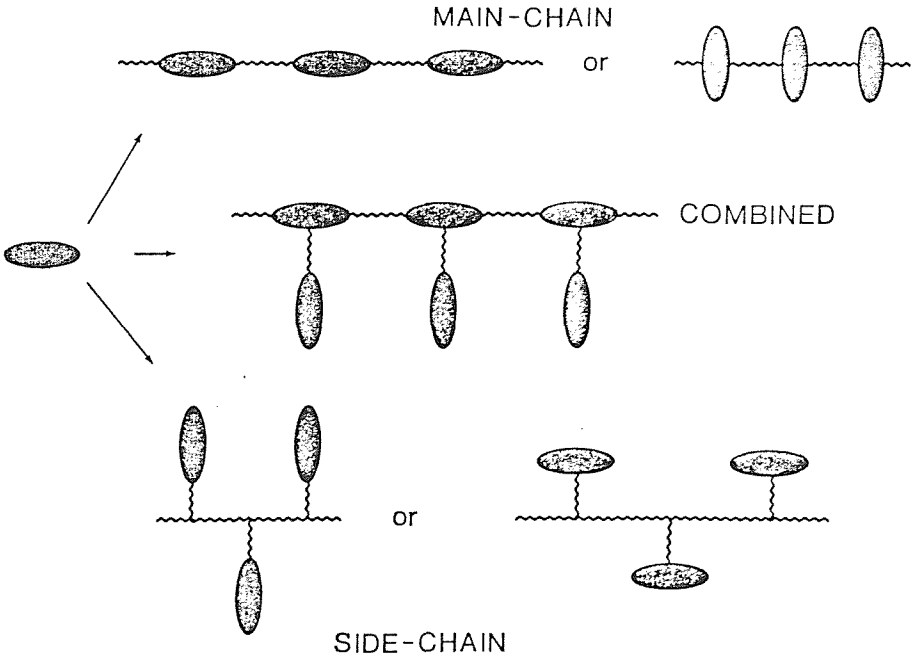

Figure 1.8.1 A schematic representation of the molecular structures of liquid-crystalline polymers; the ellipsoid represents the mesogenic group.

Side-chain polymers although of great commercial and academic interest will not be dicussed further. Main-chain polymers can essentially be sub-divided into two groups; rigid polymers and semi-flexible polymers. In a rigid main-chain polymer the mesogenic moities are directly connected forming a rigid, rod-like polymer and probably the best known example of this rigid polymeric structure is the polyamide referred to commercially as kevlar:

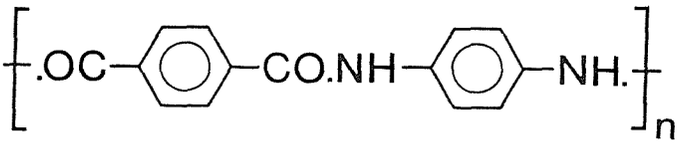

Kevlar, like the majority of rigid main-chain polymers, does not exhibit liquid-crystallinity because its decomposition temperature lies below its melting point. However, kevlar is soluble in concentrated sulphuric acid and in solution forms a nematic phase which may be processed by fibre spinning. This type of processing is typical for rigid main-chain polymers but obviously poses many difficulties. In consequence, chemists have attempted to reduce the melting points of these materials and have used essentially two differing strategies. First, the axial ratio of the backbone may be reduced by the introduction of rigid but non-linear groups and, by varying the numbers of such groups the melting point of the polymer can be tailored to lie below the materials decomposition temperature resulting in the observation of liquid-crystalline behaviour. For example, 2,6-dihydroxynapthalene has been used as rigid, non-linear group [35]:

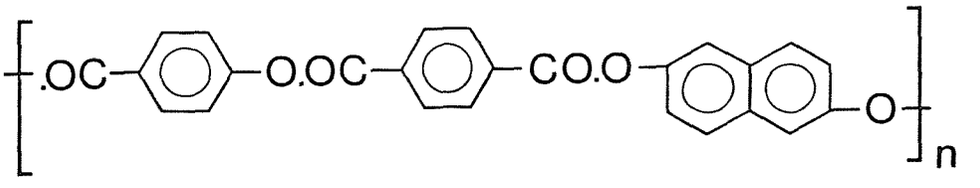

The second strategy has been to attach lateral alkyl chains to the mesogenic moieties in the backbone and these act as a sheath round the backbone so reducing intermolecular interactions. This serves to reduce the melting points of such materials and as a result liquid-crystalline phases can be observed [37].

The second class of main-chain liquid-crystalline polymers, the semi-flexible main-chain polymers, are composed of mesogenic groups separated by flexible spacers such as alkyl chains:

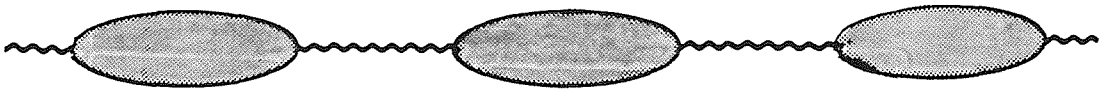

The introduction of flexible spacers into the polymer backbone reduces the transition temperatures so that mesogenic behaviour may be observed. The properties of semi-flexible main-chain polymers are dependent upon the degree of polymerisation; the chemical nature, length and parity of the flexible spacer; the structure of the mesogenic group. There is evidence to suggest that both the liquid crystal-isotropic transition temperature and the entropy change associated with the transition remain essentially constant providing there are at least ten repeating units in the backbone [37].

The liquid crystal-isotropic transition temperature of a semi-flexible main-chain polymer depends critically upon both the length and parity of the flexible spacer. Thus, the transition temperatures of a series of polymers in which only the length of the flexible spacer is varied exhibit a pronounced odd-even effect. Figure 1.8.2 gives the dependence of the nematic-isotropic transition temperature upon the length of the flexible spacer for the α,ω-[4,4'-(2,2'-dimethyl-azoxyphenyl)]alkandioates [38].

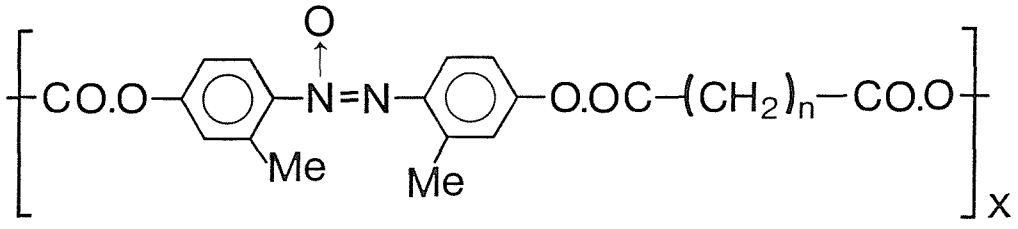

Figure 1.8.3 shows that there is also a pronounced alternation in the entropy change associated with the nematic-isotropic transition upon varying the length of the spacer. It should be noted that the alternation in the transition temperatures attenuates with increasing length whereas the alternation in the entropy change does not. The behaviour illustrated in figures 1.8.2 and 1.8.3 has often been explained by considering the all-trans conformation of the spacer [39]. In such an arrrangement, the mesogenic moieties are colinear for

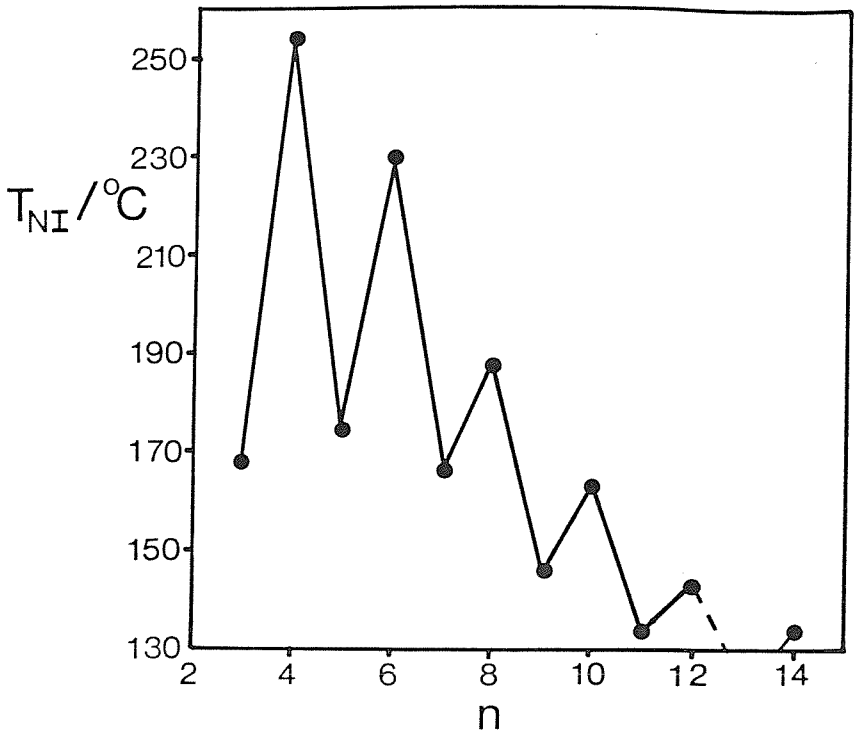

Figure 1.8.2 The dependence of the nematic-isotropic transition temperatures on the number of methylene groups in the flexible spacer for the poly α,ω-[4,4'-(2,2'-dimethylazoxyphenyl)]alkandioates [38].

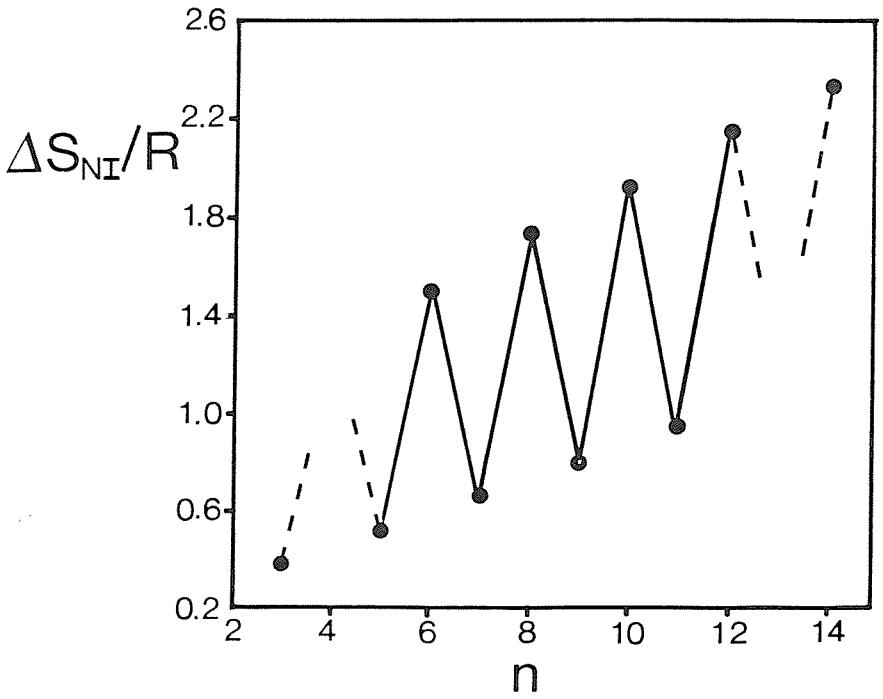

Figure 1.8.3 The dependence of the nematic-isotropic entropy of transition on the number of methylene groups in the flexible spacer for the poly α,ω-[4,4'-(2,2'-dimethylazoxyphenyl)]alkandioates [38].

even length spacers but are not for odd length spacers and this is considered to reduce the thermal stability of the mesophase. This argument is somewhat simplistic and is discussed elsewhere in this thesis. It should be noted that increasing the length of the flexible spacer promotes smectic behaviour. The influence of the chemical nature of the spacer upon the properties of the polymer is discussed in Chapter 4.

The effects of the chemical structure of the mesogenic moiety upon the liquid-crystalline transition temperatures of a semi-flexible main-chain polymer are comparable in many ways to those discussed in the section on low molar mass liquid crystals. For example, increasing the length and rigidity of the mesogenic group enhances mesophase thermal stability whereas lateral substituents reduce the transition temperatures [40].

1.9 Dimeric Liquid Crystals

We have already seen that the vast majority of low molar mass liquid crystals are composed of molecules with a single semi-rigid core attached to which are one or two flexible alkyl chains. In essence the semi-rigid core enhances the liquid crystal-isotropic transition temperature while the alkyl chains reduce the freezing point. It has often been argued that the introduction of a flexible alkyl chain linking two mesogenic groups would result in a dramatic decrease in the thermal stability of the mesophase or indeed, its destruction. In the preceeding section, however, we saw that semi-flexible main chain polymers in which mesogenic groups and flexible spacers alternate along the polymer backbone are liquid-crystalline and this discovery prompted the synthesis of low molar mass analogues in which just two semi-rigid units are linked through an alkyl spacer [41]:

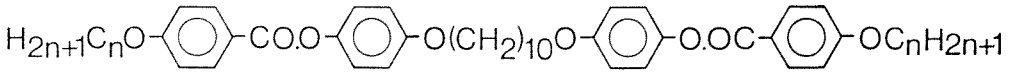

these diesters are indeed nematogens and have higher nematic-isotropic transition temperatures than the comparable mesogens containing a single semi-rigid core [42]:

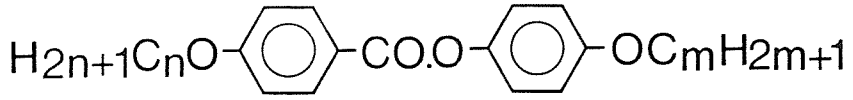

It may be argued that the properties of the diesters should actually be compared with those of the diester without the flexible spacer [43]:

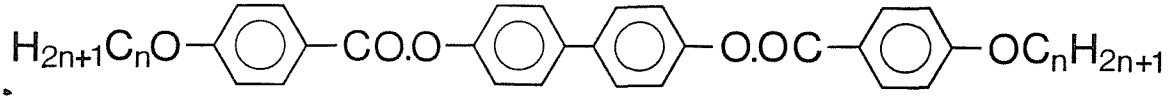

The introduction of the flexible spacer results in an average decrease in the nematic-isotropic transition temperatures of these compounds by about 180 °C and presumably reflects the increased flexibilty and decreased linearity on introducing the decamethylene

spacer. This new class of low molar mass liquid crystals possessing a flexible core has been termed dimeric liquid crystals; the analogous monomers are the compounds having the same mesogenic group as the dimer. Dimers are not compared to the corresponding compounds without the flexible core simply because such compounds generally have not been prepared. The diesters [41] actually represent the rediscovery of dimers, for fifty years earlier Vorlander [44] reported the transition temperatures of the α,ω-bis(4-alkoxyphenyl-4'-azophenyl)alkanedioates but these compounds seem to have been overlooked.

A characteristic feature of semi-flexible main-chain polymers is that their transitional properties depend strongly upon both the length and parity of the alkyl spacer. In order to investigate whether similar behaviour is observed for compounds containing just two mesogenic groups linked via a flexible spacer, Emsley et al [45] synthesised the α,ω-bis(4-cyanobiphenyl-4'-oxy)alkanes (BCBO-n);

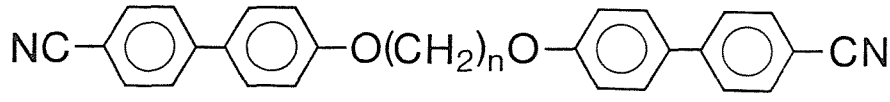

Figures 1.9.1 and 1.9.2 illustrate that both the transition temperatures and the entropy change associated with the nematic-isotropic transition of the BCBO-n's do indeed exhibit a pronounced alternation upon varying the length of the spacer. In addition, the alternation in the transition temperatures attenuates on increasing the spacer length whereas that of the entropy change does not and this behaviour is strongly reminiscent of that of semi-flexible main-chain polymers described in the preceeding section. Therefore, certain properties of dimeric liquid crystals appear to be analogous to those of semi-flexible main-chain polymers and the root of this similarity is discussed in detail elsewhere in this Thesis.

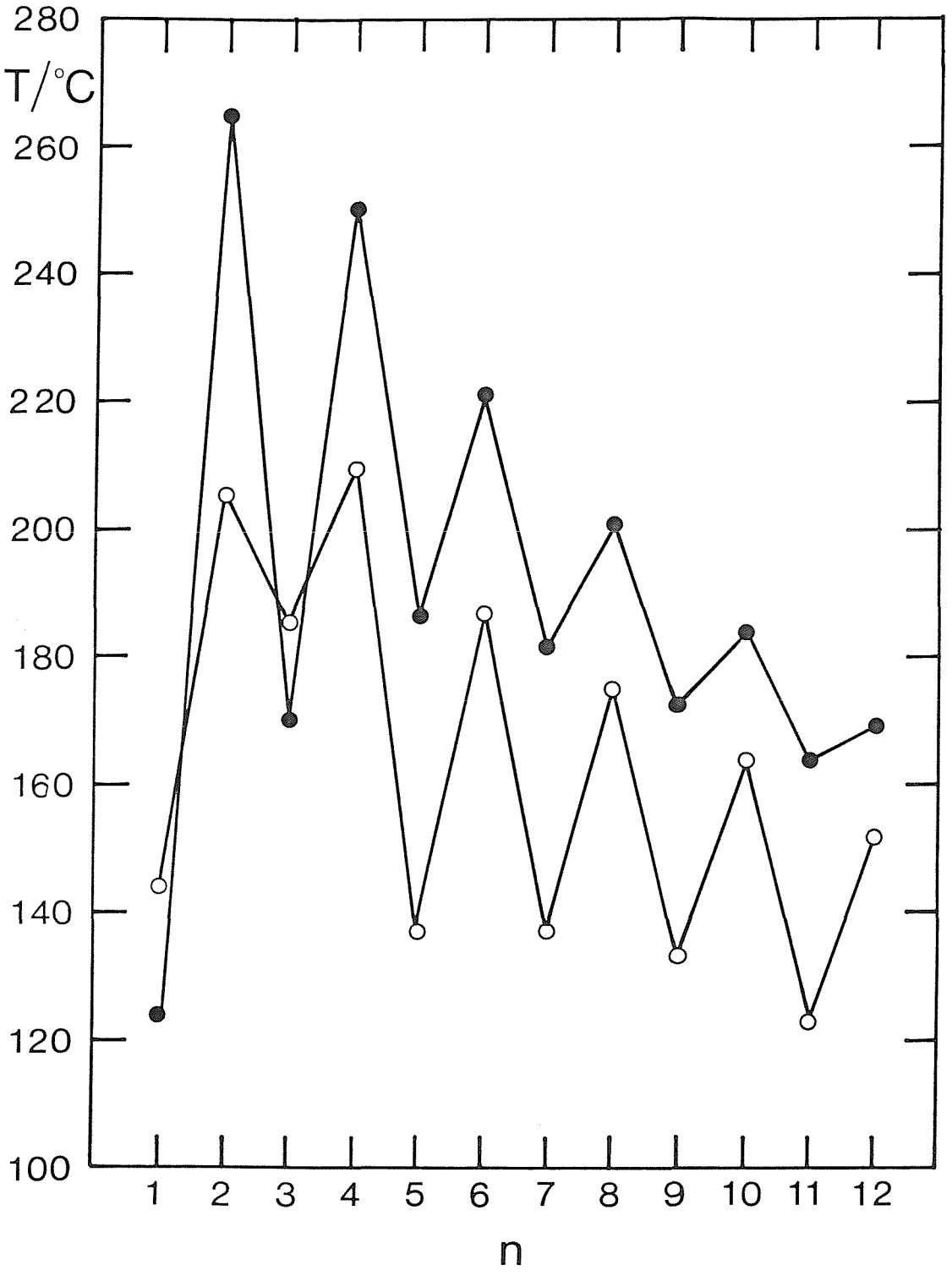

Figure 1.9.1 The dependence of the transition teperatures on the number of methylene groups in the flexible core for the α,ω-bis(4-cyanobiphenyl-4'-oxy)alkanes; the melting point is denoted by o and ● indicates the nematic-isotropic transition.

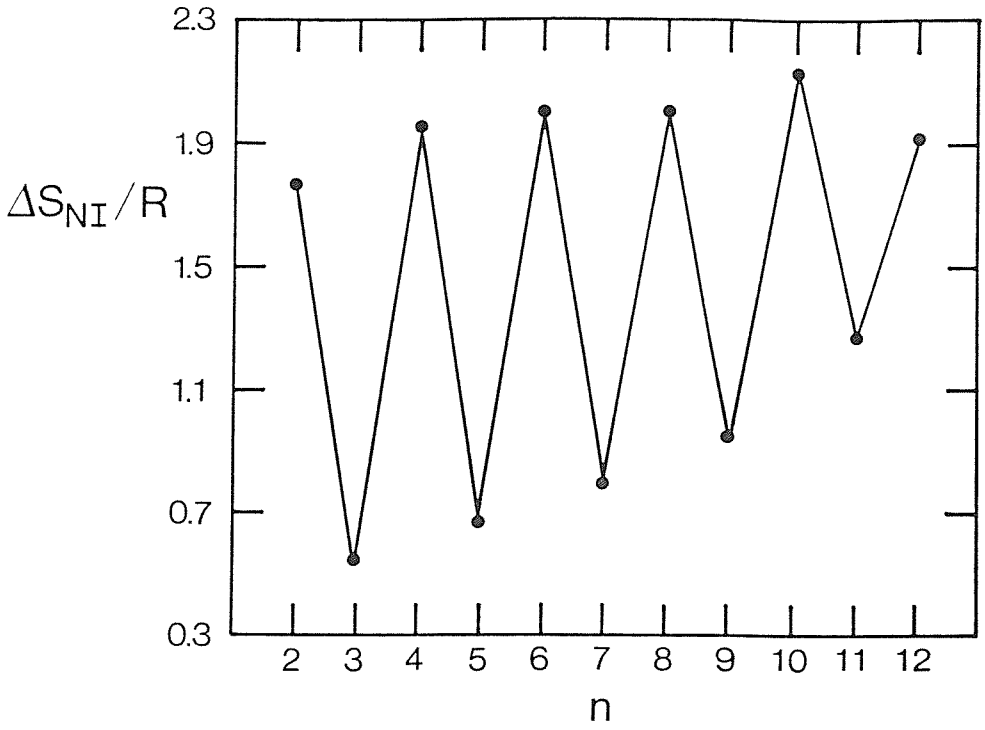

Figure 1.9.2 The dependence of the nematic-isotropic entropy of transition on the number of methylene groups in the flexible core for the α,ω-bis(4-cyanobiphenyl-4'-oxy)alkanes.

Jin et al [46] investigated the effect of terminal substituents upon the properties of dimeric liquid crystals by synthesising the 1,10-bis[4-(p-substitutedphenyloxycarboxy)phenyloxy]decanes:

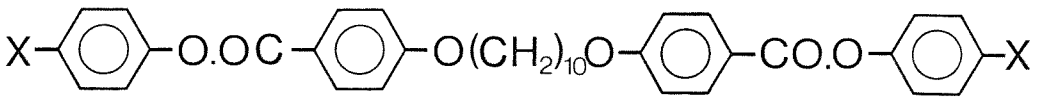

These compounds exhibit nematic behaviour for a range of substituents, X, including methyl, chloro, cyano and nitro groups and the effect of the substituents upon the thermal stability of the nematic phase was found to be in accord with the behaviour of analogous nematogens with a single semi-rigid core.

Although a large number of dimers have been reported in recent years there is still a paucity of information on such compounds when compared to the vast literature concerning monomeric and polymeric liquid crystals. Thus, the majority of this thesis is concerned with investigating the properties of dimeric liquid crystals and their relationship to molecular structure. The great interest in this class

of mesogen obtains primarily for three reasons: first, dimers serve as useful models of semi-flexible main-chain liquid-crystalline polymers; second, they have application potential; finally, the molecular structure of dimers and their properties are very different to those of conventional low molar mass mesogens and so are inherently interesting.

The need for model compounds in order to enhance our understanding of main-chain polymers stems, in part, from the difficulty in reproducing behaviour in different polymeric samples and also, from the sheer complexity of a polymeric system. The problem of reproducing the transitional properties of a polymer arises for several reasons including the apparently simple but experimentally very difficult task of removing 'low' molar mass oligomeric materials from the final product and such oligomers can have a pronounced effect on, for example, the transition temperatures of the polymer. In comparison, dimeric compounds can be obtained in a pure form and thus, their transitional properties are reproducible. Therefore, structure-property relationships are more easily established for dimers than polymers but may be applicable to both sets of materials. The second role of dimers is to serve as models on which theories may be tested. The sheer complexity of a polymeric system effectively prevents the development of a molecular theory to describe its properties but such a theory can be developed for dimers and an example is described in the final section of this Introduction.

The application potential of dimeric liquid crystals lies largely with the development of materials for display devices and at the root of this potential is the high orientational ordering of dimers possessing even length spacers in comparison with that of conventional monomeric mesogens. For example, the contrast ratio of a guest-host display device is dependent on the extent to which the dye is ordered by the liquid crystal host. Thus, the incorporation of an even membered dimer would result in a greater alignment of the dye and hence, an improved contrast ratio. In addition, the increased order also enhances the anisotropy in the dielectric permittivity and this would tend to reduce the threshold voltage. It should be noted, however, that

material parameters such as viscosities and elastic constants have not been measured for dimers and so it is not possible to assess their effect on the display's performance.

A second type of display, the ferroelectric smectic C liquid crystal display, is poised to revolutionalise the display industry for it possesses a unique combination of both fast response times and bistability. A ferroelectric smectic C phase has essentially the same structure as a conventional smectic C phase but is composed of molecules possessing a chiral centre and a transverse dipole moment. The molecular chirality results in a preferred tilt direction and so all the transverse dipoles lie in a single direction orthogonal to the tilt direction. The strength of the resulting dipole moment is measured by the spontaneous polarisation (P_S). This is a simple picture of the ferroelectric smectic C phase and in reality the molecules rotate freely about their long axes and the tilt direction is an energetically preferred direction. It should also be noted that the chiral interactions across the layer and the reduced symmetry of the phase result in a twisting of the tilt direction through successive layers giving a helical structure in which the dipole moment averages to zero. The ferroelectric display, however, uses very thin films of the liquid crystal and surface forces are sufficient to unwind the helical structure. The response time, τ, of a ferroelectric display is related to the spontaneous polarisation, P_S, the rotational viscosity, η, of the liquid crystal and to the applied field, E, by [47]:

$$\tau = \frac{\eta}{P_S E} \quad .$$

The device engineer requires, therefore, materials having high P_S values in order to fabricate displays operating at low voltages. The spontaneous polarisation of a conventional monomeric liquid crystal is considerably smaller than would be predicted and this is thought to result from weak coupling of both the molecular motion to the biaxial environment of a tilted phase and of the chiral group to the transverse dipole moment. To obtain high values of the spontaneous

polarisation, therefore, the liquid crystal should possess a high degree of orientational order and the chiral centre should be strongly coupled to both the core of the molecule and the transverse dipole moment. These conditions are satisfied in an even membered dimer in which the chiral centre is built into the flexible core and thus, such a compound should possess a higher spontaneous polarisation than if the same group was in a terminal alkyl chain. If other molecular parameters such as the pitch length of the smectic phase and the viscosity result in chiral dimers being unsuitable as a major component in display devices then it is conceivable that they may be incorporated as dopants.

A third area of the application potential of dimeric liquid crystals was described in a recent patent [48] and involves the use of phenylcyclohexyldicarboxylates [49]:

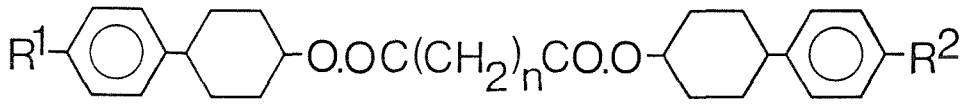

as additives in liquid crystal mixtures to improve the elastic properties of nematic mixtures in display devices.

1.10 A theoretical description of dimeric liquid crystals

We have already seen that the liquid-crystalline properties of dimeric liquid crystals are in many ways analogous to those of semi-flexible main-chain polymers. In particular, the liquid-crystalline properties of the two classes of material are found to depend critically on both the length and parity of the flexible alkyl spacers. Therefore, a molecular theory of such systems has to allow specifically for the effects of the spacer. Such a theory is clearly easier to develop for dimeric compounds rather than complex polymeric materials but should enable us to understand the liquid-crystalline behaviour of both sets of mesogens. Here we present a purely qualitative theoretical description of nematic liquid crystals formed from flexible molecules; a mathematical account of this theory can be found elsewhere [50].

The first stage of any molecular theory for flexible molecules is to describe the conformational states available and to proceed to determine their relative weights. This problem is tackled using Flory's rotameric state model [51] which allows only three conformations to be adopted; namely, a trans and two gauche conformers. Thus, all other internal modes which contribute to the mesogens non-rigidity have been ignored except for rotations about C-O and C-C bonds in the alkoxy chain. The conformation of the chain is then described by the number and locations of the gauche linkages.

The second stage in the development of the theory requires the form of the potential of mean torque. Molecules in a nematic phase tend to align with their long axes parallel to a preferred direction known as the director. However, the molecules actually fluctuate about this direction and the magnitude of such fluctuations are governed by the energy of the molecule as it changes its orientation with respect to the director. This orientational energy, or as it is known the potential of mean torque, results from the interactions of a molecule with its nearest neighbours which may be thought of as providing a molecular field. The strength of this field depends on many factors including molecular packing and the orientational order in the system. The form of the potential of mean torque can be used to determine the

probability of finding a molecule at a particular angle to the director from the appropriate Boltzmann factor. This probability distribution may then be used to determine the average of any function of the molecular orientation which has been chosen to define the orientational order parameter. The extent of the molecular fluctuations with respect to the director is reflected by the orientational order parameters; for cylindrically symmetric particles these are chosen to be unity in a perfectly ordered crystal and zero in an isotropic liquid. In a nematic phase the order parameters are intermediate between these two extremes.

For a cylindrically symmetric particle, the orientational energy is determined solely by the angle between the director and the molecular symmetry axis. For a biaxial molecule, however, the potential of mean torque resulting from the molecular field depends on the spherical polar angles made by the director in a frame set in the molecule. The singlet orientational distribution function may be calculated using the potential of mean torque and in turn the orientational order parameters for the conformer can be evaluated from the distribution function. These, however, cannot be compared with those determined from N.M.R. experiments because the rate of exchange between conformers is fast on the N.M.R. time scale and thus, weighted order parameters over all conformers are measured. Thus, we need to calculate the order parameters for each conformer and they are also needed in order to obtain, for example, transition temperatures. This, however, would introduce too many arbitrary variables into the theory if the orientational distribution functions were unrelated. This problem is avoided by assuming the strength of the molecular field is composed of a limited number of segmental interactions. The simplest choice of such segments is the aromatic core with a strength parameter X_a and C-C segments with their parameter X_c; these segments are assumed to be cylindrically symmetric. It has been assumed that C-H bonds do not contribute to the molecular field and that the C-O and C-C bonds in the chain are identical. The order parameters of each conformation may now be determined using X_a and X_c. To obtain the conformational average, the difference in energy between a trans and gauche linkage, E_{tg}, is required and this value is available from

independent experiments. Therefore, by varying X_a and X_c and using typical values of E_{tg}, it has proved possible to fit the order parameter profile for the alkoxy chain in 6OCB; strictly, this method provides a means of obtaining numerical values for parameters included in the theory. This suggests the assumptions made in developing the theory are reasonable. In addition, the theory may be used to determine the degree to which the anisotropc environment of the nematic phase discriminates between conformers. The results for 6OCB reveal a significant change in the statistical weights of conformers on going from the isotropic to the nematic phase in which the more elongated conformers are favoured.

The final stage in the theory is to calculate the free energy of the system and using this the other thermodynamic properties may be evaluated. The molecular field approximation is extremely useful in this task because the statistical mechanical calculation of the free energy via the configurational partition function is straightforward for a set of non-interacting particles. Therefore, the use of a molecular field acting on a single molecule instead of having many molecular interactions simplifies the problem enormously. The molecular field strength parameters are dependent on orientational order and hence, will vary with temperature. This is accounted for by assuming that the strength parameters are linear in the second rank orientational order parameters in the chain and core segments. The contribution of each order parameter to a particular molecular field strength parameter introduces a variable into the theory. Thus, for X_a a core-core interaction parameter is required as well as a core-chain parameter in order to relate the strength parameter to the core order parameter and the chain order parameter respectively. Similarly, for X_c a chain-chain interaction parameter is required as well as the same core-chain parameter. The core-core interaction parameter is obviously expected to be larger than the chain-chain parameter and for convenience the core-chain parameter is assumed to be the geometric mean of the other two. The ratio of the core-core and chain-chain interaction parameters may be obtained by fitting the theoretical order parameter profile of an alkyl chain with that observed experimentally. The remaining unknown can then be used to scale the

calculated transition temperatures. For the α,ω-bis(4-cyanobiphenyl-4'-oxy)alkanes the agreement between the calculated and experimental nematic to isotropic transition temperatures is very good and theory correctly predicts the pronounced alternation as the parity of the spacer is varied as well as the attenuation of this effect on increasing the spacer length. The calculation of the free energy also allows the entropies of transition to be evaluated and again these are in excellent agreement with those measured experimentally; the theory predicts correctly the large alternation as the parity of the spacer is varied as well as the absence of attenuation as the length of the spacer is increased. Finally, the core order parameter is determined as part of the calculation of the free energy and its value at the nematic-isotropic transition is predicted to be strongly dependent on the parity of the spacer with the even members having far higher values; this has subsequently been confirmed experimentally [52].

This relatively simple molecular theory for liquid crystals composed of flexible molecules predicts both the dependence of the nematic-iostropic transition temperatures and the entropy change associated with the transition in a semi-quantitative manner. The theory, therefore, appears to be a useful tool with which to understand the behaviour of low molar mass dimeric liquid crystals and possibly even the analogous characteristics of semi-flexible main-chain liquid-crystalline polymers.

1.11 References

[1] Dewar, M.J.S., 1967, An Introduction to Modern Chemistry, Athlone Press.

[2] Reinitzer, F., 1888, Mh. Chem., 9, 421.

[3] Lehmann, O., 1900, Vernhandl. d. Deutschen Phys. Ges., Sitzung v. 16.3, 12.

[4] Demus, D., Demus, H., and Zaschke, H., 1974, Flussige Kristalle in Tabellen, VEB Deutscher Verlag fur Grundstoffindustrie.

[5] Demus, D., and Zaschke, H., 1984, Flussige Kristalle in Tabellen, 2, VEB Deutscher Verlag fur Grundstoffindustrie.

[6] Gray, G.W., and Goodby, J.W., 1984, Smectic Liquid Crystals, Leonard Hill.

[7] Leadbetter, A.J., 1987, Thermotropic Liquid Crystals, edited by G.W. Gray, Wiley, Chap. 1.

[8] Tinh, N., 1983, J. Chim. Phys., 80, 83.

[9] Hardouin, F., Levelut, A.M., Benattar, J.J., and Sigaud, G., 1980, Solid State Comm., 33, 337.

[10] Ratna, B.R., Shashidhar, R., and Raja, V.N., 1985, Phys. Rev. Lett., 55, 1476.

[11] Diele, S., Weissflog, W., Pelz, G., Manke, H., and Demus, D., 1986, Liq. Cryst., 1, 101.

[12] Doucet, J., Levelut, A.M., and Lambert, M., 1973, Mol. Cryst. Liq. Cryst., 24, 317.

[13] Leadbetter, A.J., Frost, J.C., and Mazid, M.A., 1979, J. Phys. (Paris) Lett., 40, 325.

[14] Goodby, J.W. 1981, Mol. Cryst. Liq. Cryst. Lett., 72, 95.

[15] Goodby, J.W., 1984, Liquid Crystals and Ordered Fluids, edited by A.C. Griffin and J.F. Johnson, 4, 175.

[16] Brownsey, G.J., and Leadbetter, A.J., 1981, J. Phys. (Paris) Lett., 39, 399.

[17] Benattar, J.J., Moussa, F., and Lambert, M., 1980, J. Phys. (Paris), 41, 1371.

[18] Gray, G.W., Jones, B., and Marson, F., 1957, J. Chem. Soc., 393.

[19] Etherington, G.E., Leadbetter, A.J., Wang, X.J., Gray, G.W., and Tajbakhsh, A.R., 1986, Liq. Cryst., 1, 209.

[20] Demus, D., Gloza, A., Hartung, H., Rapthel, I., and Wiegeleben, A., 1981, Cryst. Res. Techn., 16, 1445.

[21] Tinh, N.H., Destrade, C., Levelut, A.M., and Malthete, J., 1986, J. Phys. (Paris), 47, 553.

[22] Malthete, J., Levelut, A.M., and Tinh, N.H., 1985, J. Phys. (Paris) Lett., 46, 875.

[23] Gray, G.W., 1975, J. Phys. (Paris), 36, 337.

[24] Ivashchenko, A.V., Titov, V.V., and Koshev, E.I., 1976, Mol. Cryst. Liq. Cryst., 33, 195.

[25] Coates, D., and Gray, G.W., 1976, Mol. Cryst. Liq. Cryst., 37, 249.

[26] Gray, G.W., 1979, The Molecular Physics of Liquid Crystals, edited by G.R. Luckhurst and G.W. Gray, Academic Press, Chap 1.

[27] Eidenschink, R., Erdmann, D., Krause, J., and Pohl, L., 1977, Angew. Chem., 89, 103.

[28] Gray, G.W., and Kelly, S.M., 1981, J. Chem. Soc. Perkin Trans. 2, 26.

[29] Wiegelben, A., Richter, L., Deresch, J., and Demus, D., 1980, Mol. Cryst. Liq. Cryst., 59, 329.

[30] Gray, G.W., 1979, The Molecular Physics of Liquid Crystals, edited by G.R. Luckhurst and G.W. Gray, Academic Press, Chap 12.

[31] Toyne, K.J., 1987, Thermotropic Liquid Crystals, edited by G.W. Gray, Wiley, Chap. 2.

[32] Gray, G.W., and Moseley, A., 1976, J. Chem. Soc. Perkin Trans. 2, 97.

[33] Gray, G.W., 1974, Liquid Crystals and Plastic Crystals 1, edited by G.W. Gray and P.A. Winsor, Ellis Horwood, Chap. 4.1.

[34] Reck, B., and Ringsdorf, H., 1986, Makromol. Chem. Rapid Commun., 7, 389.

[35] Irwin, R.S., 1980, U.S. Pat., 4, 188, 476.

[36] Gray, D.G., 1985, Polymeric Liquid Crystals, edited by A. Blumstein, Plenum Press, Chap. 369.

[37] Blumstein, A., 1985, Polym. J., 17, 277.

[38] Blumstein, A., and Thomas, O., 1982, Macromol., 15, 1264.

[39] Finkelmann, H., Thermotropic Liquid Crystals, edited by G.W. Gray, Wiley, Chap. 6.

[40] Lenz, R.W., 1985, Faraday Discuss. Chem. Soc., 79, 21.

[41] Griffin, A.C., and Britt, T.R., 1981, J. Am. Chem. Soc., 103, 4957.

[42] Neubert, M.E., Carlino, L.T., Fishel, D.L., and D'Sidocky, R.M., 1980, Mol. Cryst. Liq. Cryst., 59, 253.

[43] Karamysheva, L.A., Kovshev, E.I., and Titov, V.V., 1976, Zh. Org. Khim., 12, 1508.

[44] Vorlander, D., 1927, Z. Phys. Chem., 126, 449.

[45] Emsley, J.W., Luckhurst, G.R., Shilstone, G.N., and Sage, I., 1984, Mol. Cryst. Liq. Cryst. Lett., 102, 223.

[46] Jin, J.I., Chung, J.S., Kang, J.S., and Lenz, R.W., 1982, Mol. Cryst. Liq. Cryst. Lett., 82, 261.

[47] Coates, D., 1987, Thermotropic Liquid Crystals, edited by G.W. Gray, Wiley, Chap. 4.

[48] Giroud, A.M., 1987, Fr. Demande, FR 2587996.

[49] Gauthier, M.M., and Giroud-Godquin, A.M., 1986, Mol. Cryst. Liq. Cryst. Lett., 3, 139.

[50] Luckhurst, G.R., 1985, Recent Advances in Liquid Crystalline Polymers, edited by L.L. Chapoy, Elsvier Applied Science, Chap. 7.

[51] Flory, P.J., 1969, Statistical Mechanics of Chain Molecules, Interscience.

[52] Emsley, J.W., Luckhurst, G.R., and Shilstone, G.N., 1984, Molec. Phys., 53,1023.

CHAPTER 2: THE PREPARATION AND PROPERTIES OF THE α,ω-BIS(4-ALKYLANILINEBENZYLIDINE-4'-OXY)ALKANES

2.1 Introduction

The recent rediscovery of dimeric liquid crystals [1], some fifty years after the first observation of such materials [2], has generated great interest and many series of dimers have since been reported [3]. Curiously, of all these very few have exhibited any smectic behaviour. Indeed, it has been suggested that smectic tendencies of the monomeric analogues are lost when they couple to form the dimer [1]. There is no apparent reason for this to be true because smectic behaviour is thought to be a consequence of molecular inhomogeniety. Clearly, molecular inhomogeniety is a property inherent to dimeric materials for there are 'core-like' segments and alkyl chain regions and thus, there should be a disparity in the strengths of the various interactions between such areas; these regions should, therefore, separate so forming a smectic arrangement. The aim, therefore, was to synthesise a series of smectogenic dimeric mesogens and then proceed to investigate, for example, the influence of the flexible core upon smectic phase stability. The problem was to design a molecule in which we could readily vary the terminal alkyl chains and the flexible spacer independently of each other. These requirements are satisfied by the α,ω-bis(4-alkylanilinebenzylidine-4'-oxy)alkanes:

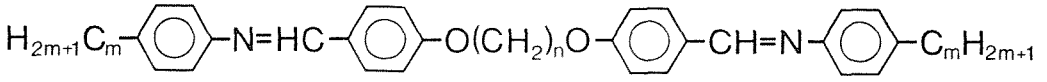

The monomeric analogues of these dimers are the N-(4-n-alkoxy-benzylidine)-4'-n-alkylanilines:

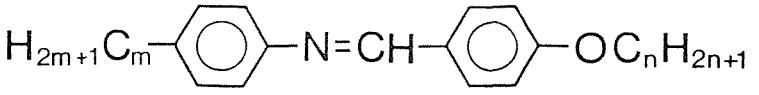

and are more commonly referred to as the nO.m's where n represents the length of the alkoxy chain and m that of the alkyl chain [4,5]. The

nO.m's have been extensively studied for they exhibit a high degree of smectic polymorphism [6]. In order to emphasise the monomer-dimer relationship between the nO.m's and the α,ω-bis(4-alkylaniline-benzylidine-4'-oxy)alkanes, the mnemonic used to describe the dimers is m.OnO.m; m represents the length of the terminal alkyl chains and n that of the flexible alkyl spacer. For example, 8.O5O.8, simply and unambiguously represents:

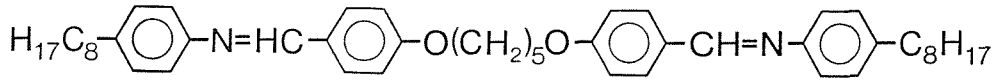

The dimeric m.OnO.m's do indeed exhibit a high degree of smectic polymorphism. In this Chapter, six series of this family will be discussed in detail and also, unpublished material [7] describing a further five series will be mentioned briefly. It should be noted that two members, 0.O1OO.0 and 1.O1OO.1, have previously been reported [8].

2.2 Experimental

The reaction scheme for the preparation of the m.OnO.m's essentially involves two steps:

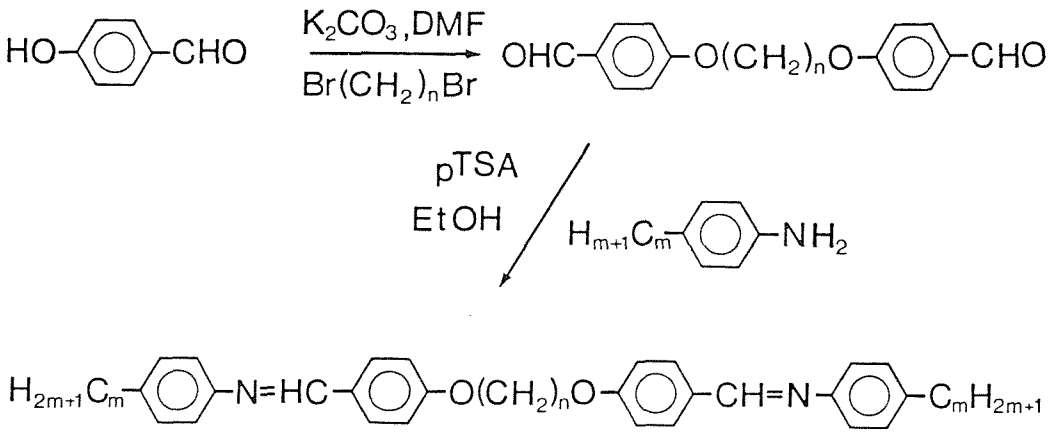

α,ω-bis(4-formylphenyl-4'-oxy)alkanes

A mixture of 4-hydroxybenzaldehyde (0.053mol, 6.5g), an α,ω-dibromoalkane (0.025mol) and anhydrous potassium carbonate (0.063mol, 8.7g) in N,N-dimethylformamide (25ml) was refluxed with stirring for three hours. The reaction mixture was allowed to cool and then added to water (300ml). The resulting precipitate was filtered off, washed thoroughly with water, dried and then recrystallised twice from ethanol. We found that in the preparation of the eleventh and twelfth homologues the reaction solvent had to be changed from N,N-dimethylformamide to ethanol to prevent a polymerisation reaction occurring. All the yields were in excess of 65% and the melting points, listed in table 2.2.1, agree closely with literature values [9]. Characterisation of the products was performed using ^{1}H-N.M.R. and I.R. spectroscopy.

Spectra

1,5-bis(4-formylphenyl-4'-oxy)pentane:

^{1}H-N.M.R.: δ ($CDCl_3$) 1.6-2.2 (m, 3H), 4.1 (t, 2H), 6.9 (d, 2H), 7.8 (d, 2H), 9.9 (s, 1H) ppm;

I.R.: ν 1690cm^{-1}.

n	T_{CI} / °C
3	132-133
4	104-106
5	80-82
6	109-111
7	63-65
8	85-87
9	88-89
10	79-81
11	85-86
12	72-73

Table 2.2.1 The melting points of the α,ω-bis(4-formylphenyl-4'-oxy)alkanes.

4-n-alkylanilines

The 4-n-alkylanilines used were available commercially from the Aldrich Chemical Company with the exception of pentylaniline and these were redistilled before use. 4-n-pentylaniline was prepared using a reaction scheme consisting of three steps;

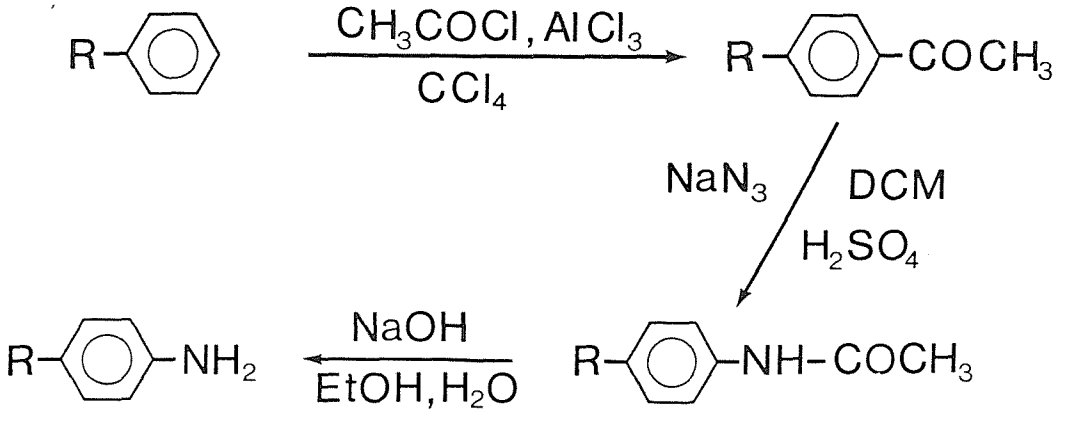

The experimental details for these reactions are described in detail elsewhere [10].

α,ω-bis(4-alkylanilinebenzylidine-4'-oxy)alkanes

To a stirred solution of an α,ω-bis(4-formylphenyl-4'-oxy)alkane (0.004mol) and a few crystals of p-toluene sulphonic acid in hot ethanol was added a 4-n-alkylaniline (0.0084mol). The mixture was allowed to stir at room temperature for four hours. The resulting white precipitate was filtered off, washed thoroughly with cold ethanol and dried. In general, all the m.OnO.m's were recrystallised twice from ethyl acetate; the exceptions being even membered materials with terminal chains of length 0, 1 and 2 for which toluene was used as the recrystallisation solvent. All yields were in excess of 70%. Structural characterisation of the products was performed using ^{1}H-N.M.R. and I.R. spectroscopy.

Spectra

4.O4O.4:

^{1}H-N.M.R.; δ ($CDCl_3$) 0.9 (t,3H), 1.2-1.7 (m,4H), 2.0 (t,2H), 2.6 (t,2H), 4.1 (t,2H), 6.9 (d,2H), 7.1 (d,2H), 7.2 (d,2H), 7.8 (d,2H), 8.4 (s,1H) ppm;

I.R.: ν 1630cm^{-1}.

Thermal characterisation of the m.OnO.m's

The thermal behaviour of the m.OnO.m's was investigated using a Perkin-Elmer DSC-2C differential scanning calorimeter calibrated using indium as the standard. The optical textures of the mesophases formed were studied using a Nikon polarising microscope equipped with a Linkam hot stage. Selected examples of the smectic phases were studied further using X-ray diffraction with a Guinier camera fitted with a bent quartz monochromator (R. Huber, F.R. Germany) using $CuK_{\alpha 1}$ radiation (λ=1.5405 A).

2.3 Results and Discussion

0.OnO.0 series

The transitional properties of the 0.OnO.0 series are given in table 2.3.1; 0.O4O.0 is the only liquid-crystalline compound, exhibiting a monotropic nematic phase. Throughout this Chapter nematic phases were assigned as such on the basis of the schlieren texture observed when viewed under the optical microscope; a typical nematic schlieren texture is shown in plate 2.3.1. In addition, the phase was very mobile and 'flashed' when subjected to mechanical stress. It is interesting to note that the melting points of the 0.OnO.0 series show a large odd-even effect with those homologues possessing even length spacers having the higher values; this is shown in figure 2.3.1. Such behaviour was thought to be a general phenomenon for all dimeric materials [11] but this will be demonstrated to be incorrect.

n	C-I/ °C	N-I/ °C	ΔH_{C-I}/kJmol^{-1}	ΔS_{C-I}/R
3	133	-	69.9	20.8
4	188.5	(116)	47.6	12.4
5	114.5	-	43.5	13.5
6	166	-	66.0	18.1
7	106.5	-	46.2	14.7
8	159.5	-	79.5	22.1
9	102	-	48.7	15.6
[1]10	153.5	-	80.9	22.8
11	116.5	-	62.1	19.2
12	150	-	91.6	26.1

Table 2.3.1 The transition temperatures, enthalpies and entropies of transition for the 0.OnO.0 series; () denotes a monotropic transition. The uncertainties in the transition temperatures are ±1 °C and in the thermodynamic data ±10%.

[1] Lit. value: 153 °C [8].

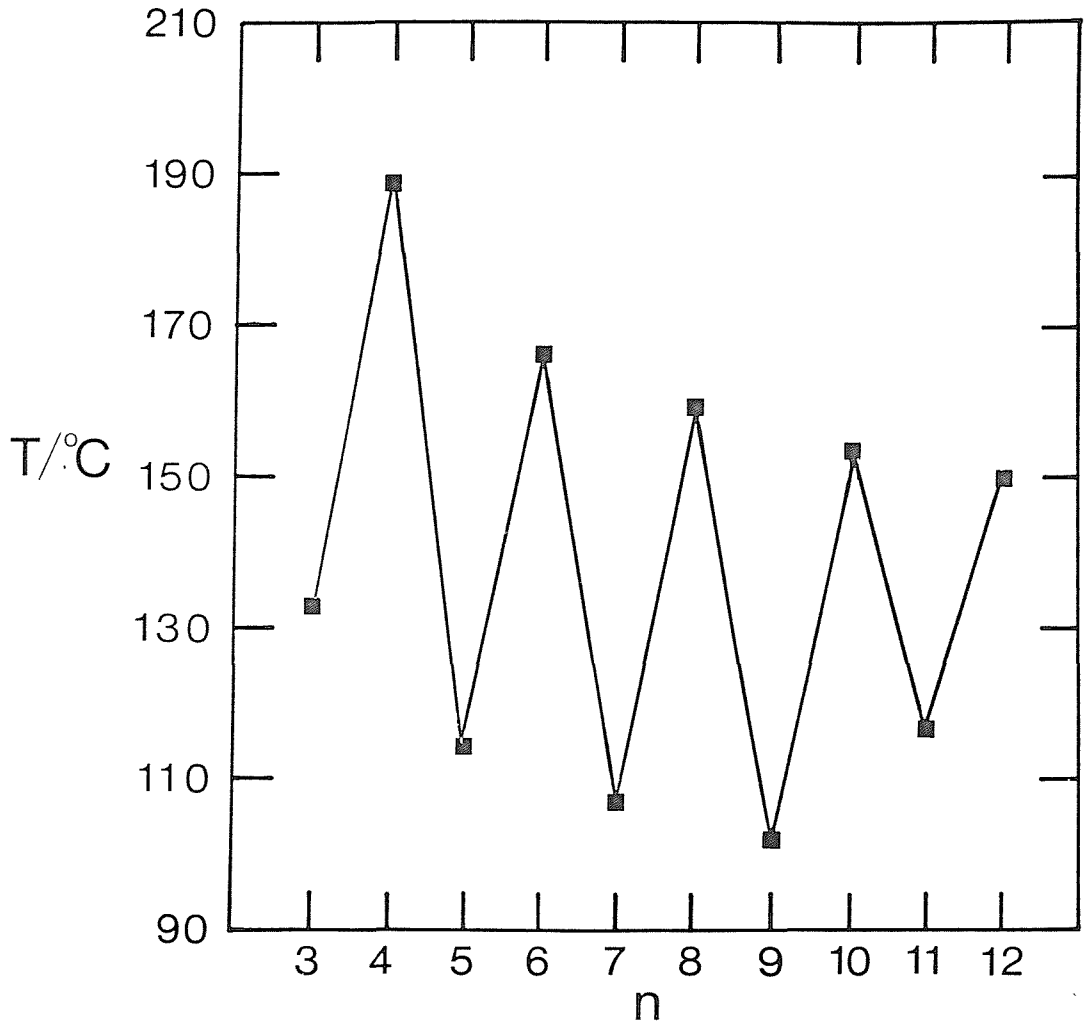

Figure 2.3.1 The dependence of the melting points for the 0.OnO.0 series on the number of methylene groups, n, in the flexible spacer.

1.On0.1 series

The transitional properties of the 1.On0.1 series are given in table 2.3.2; all ten members of the series are nematogenic, the compounds with spacer lengths of 3, 5, 10 and 12 being monotropic. The dependence of the transition temperatures upon the length of the flexible core is shown in figure 2.3.2. Both the melting points and nematic-isotropic transitions show a pronounced odd-even effect with the compounds possessing an even length spacer having the higher values. The alternation in the nematic-isotropic transition temperatures clearly attenuates with increasing core length whereas the alternation in the melting points remains constant.

Figure 2.3.3 illustrates the dependence of the entropy associated with the nematic-isotropic transition upon the length of the flexible alkyl spacer for the 1.On0.1 series and a dramatic odd-even effect is revealed. The entropies of the even members of the series are in most instances several times larger than those of the odd members. Also, it should be noted that the values for the even members are much larger than those of the monomeric analogues. For example, the value of $\Delta S/R$ for 1.0120.1 is 2.37 whereas 60.1 has a value of just 0.36 [12]. The alternation in the entropies associated with the nematic-isotropic transition for this series does not attenuate with increasing core length but instead the underlying trend for both even and odd membered materials is an increasing one.

n	†C-I/°C C-N/°C	N-I/°C	$\Delta H_{C\_}$/kJmol^{-1} ΔH_{N-I}/kJmol^{-1}		$\Delta S_{C\_}$/R ΔS_{N-I}/R	
3	†162.5	(98)	43.9	-	12.1	-
4	192.5	229	42.7	6.93	11.1	1.66
5	†147.5	(143.5)	53.7	1.31	15.4	0.38
6	177	200.5	54.8	7.22	14.6	1.84
7	136	147	54.4	2.24	16.0	0.65
8	170.5	182	68.1	7.77	18.5	2.06
9	137	143.5	56.7	2.80	16.6	0.81
[1]10	†166.5	(166)	79.6	7.93	21.8	2.18
11	129.5	143	58.8	3.86	17.6	1.12
12	†162	(154.5)	92.0	8.41	25.5	2.37

Table 2.3.2 The transition temperatures, enthalpies and entropies of transition of the 1.OnO.1 series; ( ) denotes a monotropic transition. The uncertainties in the temperatures are ±1 °C and in the thermodynamic data are ±10%.

[1] Lit. values, C-I 164 °C; N-I 161 °C [8].

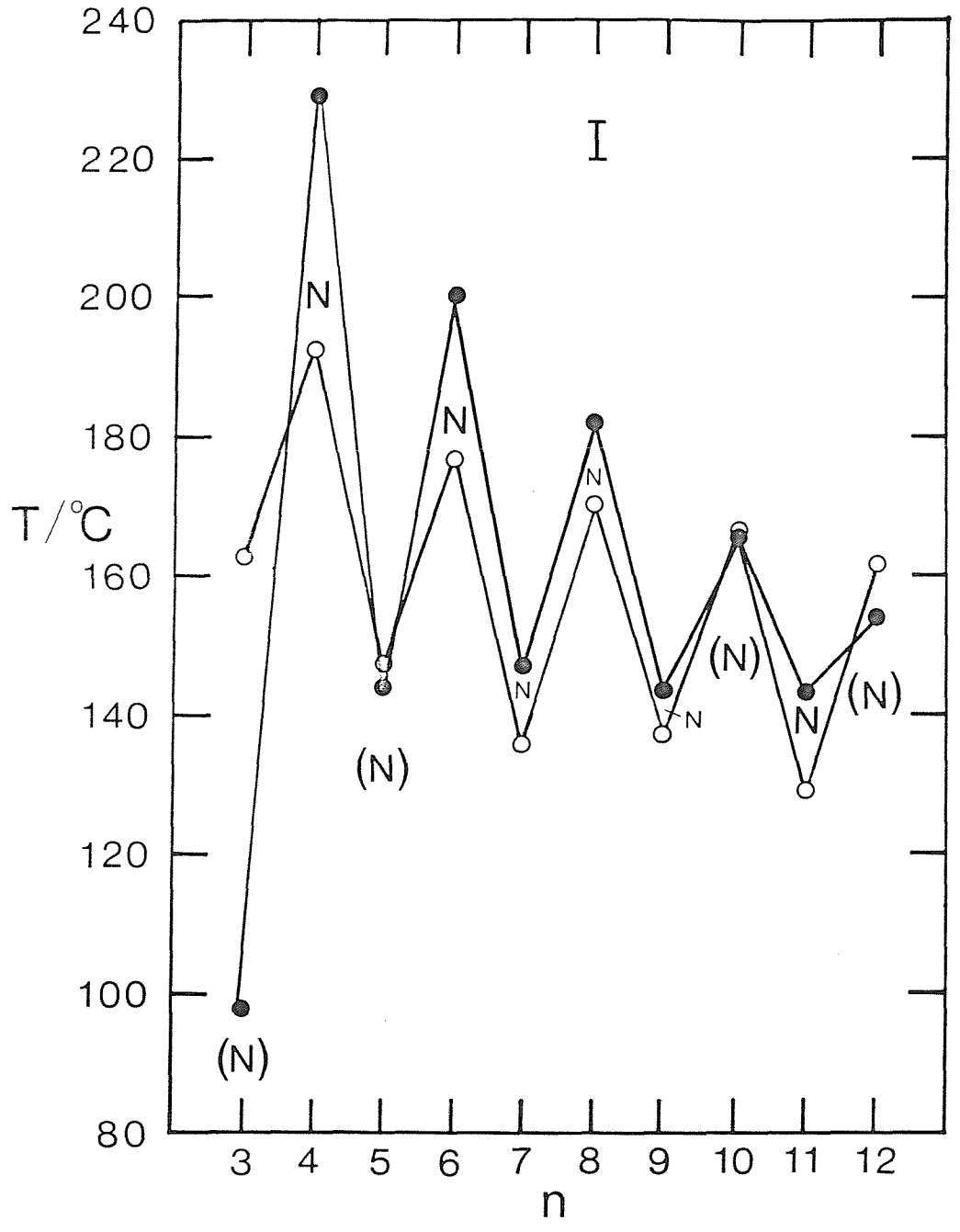

Figure 2.3.2 The dependence of the melting points (o) and the nematic-isotropic transition temperatures (●) upon the length of the flexible spacer for the 1.OnO.1 series.

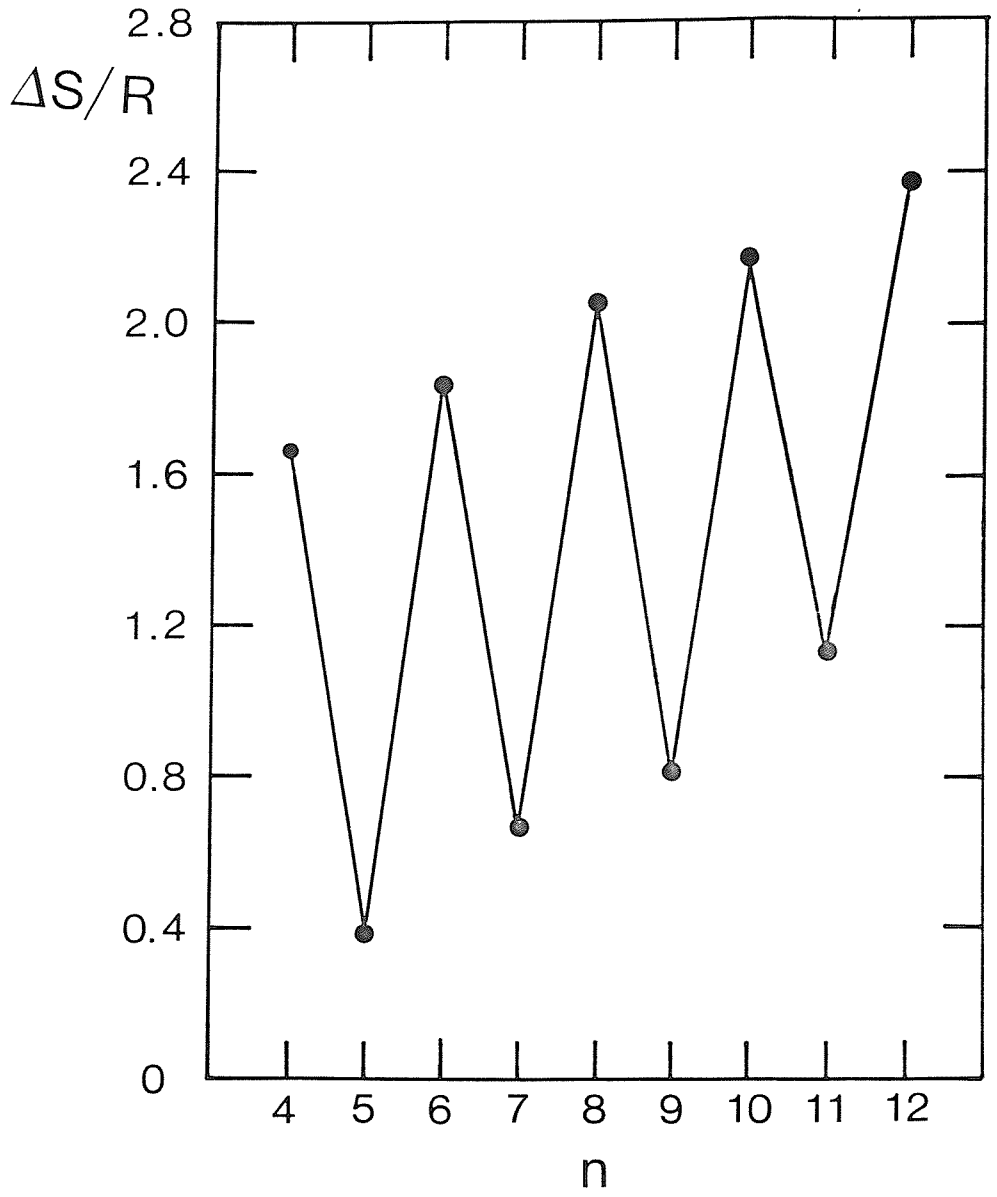

Figure 2.3.3 The dependence of the entropy associated with the nematic-isotropic transition upon the length of the flexible spacer for the 1.OnO.1 series.

2.OnO.2 series

The transitional properties of the 2.OnO.2 series are given in table 2.3.3; all the members of the series are nematogenic with the compounds of spacer length 3, 5, and 12 being monotropic. The properties of this series are very similar to those of the 1.OnO.1 series and this is partly shown in figure 2.3.4 which reveals that both the melting points and the nematic-isotropic transition temperatures show a pronounced odd-even effect on varying the length of the flexible spacer with the even members having the higher values. Again, the alternation in the nematic-isotropic transition temperature attenuates with increasing spacer length whereas there is no such attenuation in the melting point alternation.

Figure 2.3.5 shows that the 2.OnO.2 series also exhibits a very dramatic odd-even effect in the entropies associated with the nematic-isotropic transition, again the even members having the higher values. Also shown in figure 2.3.5 are the entropy changes for 40.2, 50.2, 60.2 and 8.02 and these clearly demonstrate that the entropy of transition is far larger for even membered dimers than for either odd membered dimers or the monomeric analogues. Again, the underlying trend in the entropies is an increasing one with increasing spacer length and without attenuation. It may be argued that there is an attenuation in a relative sense since the values of $\Delta S/R$ increase with increasing n but the difference in $\Delta S/R$ between the n and (n+1) homologues appears to be approximately constant for a given series.

n	^{1}C-I/ °C C-N/ °C	N-I/ °C	ΔH_{C-}/kJmol^{-1} ΔH_{N-I}/kJmol^{-1}		ΔS_{C-}/R	ΔS_{N-I}/R
3	^{1}152.5	(87)	43.7	-	12.4	-
4	207.5	215	41.0	5.87	10.3	1.45
5	^{1}128	(125.5)	44.2	1.04	13.3	0.32
6	159.5	186	45.1	5.78	12.6	1.52
7	116	131	44.5	1.53	14.1	0.46
8	153.5	167	57.1	6.60	16.1	1.81
9	112	129.5	52.5	2.13	16.4	0.64
10	150.5	154	67.5	6.70	19.2	1.89
11	112	128	57.0	2.86	17.8	0.86
12	^{1}149.5	(144.5)	81.9	6.94	23.4	2.00

Table 2.3.3 The transition temperatures, enthalpies and entropies of transition of the 2.OnO.2 series; ( ) denotes a monotropic transition. The uncertainties in the temperatures are ±1 °C and in the thermodynamic data are ±10%.

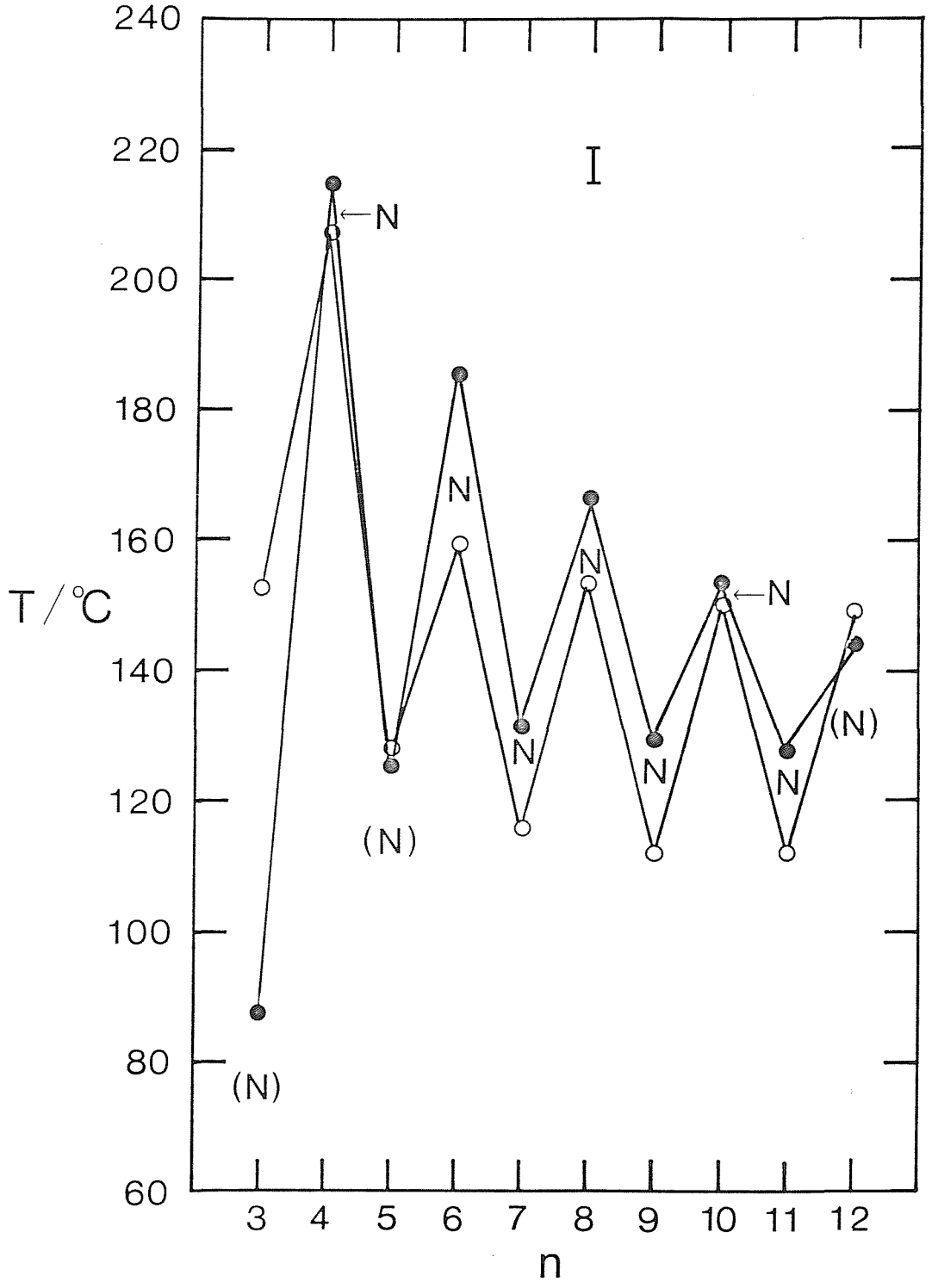

Figure 2.3.4 The dependence of the melting points (o) and the nematic-isotropic transition temperatures (●) upon the length of the flexible spacer for the 2.OnO.2 series.

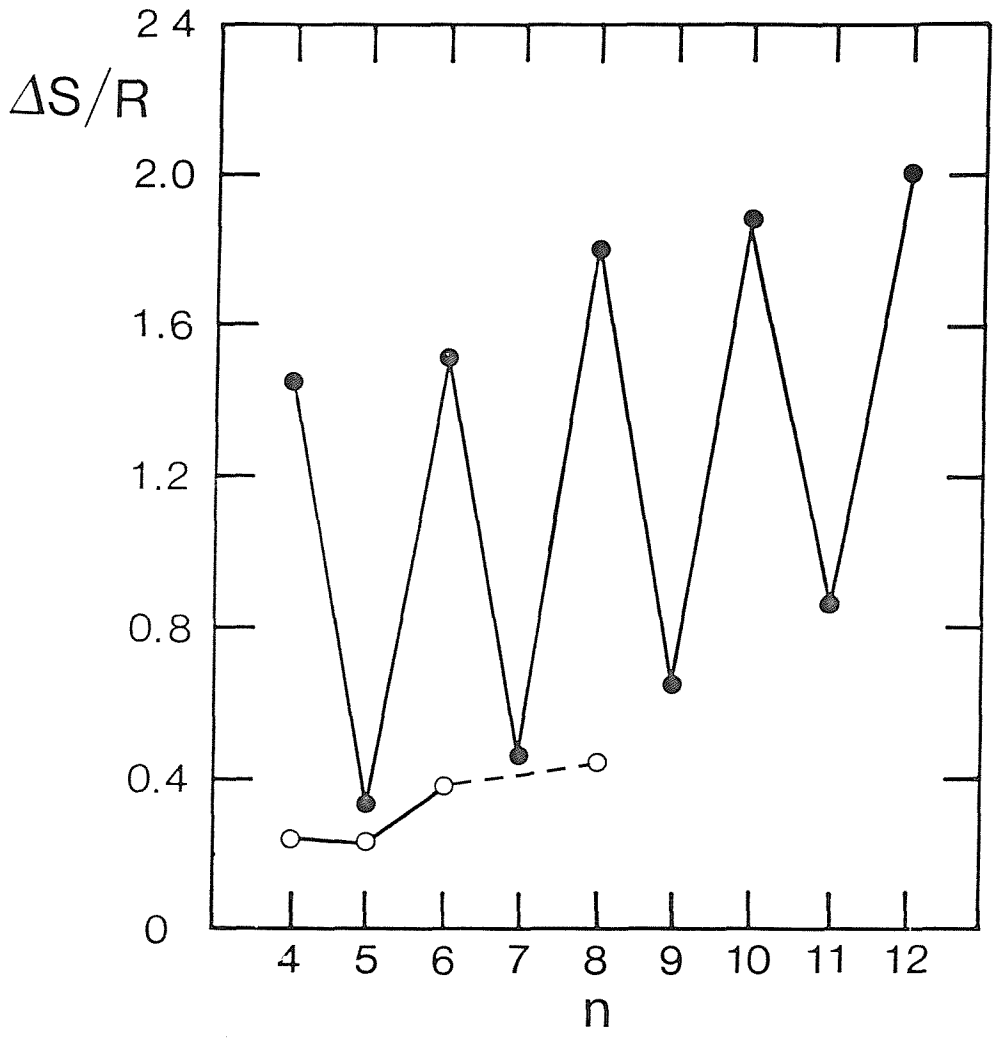

Figure 2.3.5 The dependence of the entropy (●) associated with the nematic-isotropic transition upon the length of the flexible spacer for the 2.OnO.2 series. The open circles denote the entropies for the nO.2's where n is the number of methylene units in the alkoxy chain [12].

The two series, 1.OnO.1 and 2.OnO.2, serve as excellent examples of dimeric liquid crystals; their properties are very typical indeed. First, the nematic-isotropic transition temperatures show a very pronounced odd-even effect on varying the length of the spacer and this attenuates on increasing core length. Secondly, the entropies associated with the nematic-isotropic transition show an equally dramatic odd-even dependence on the length of the flexible core which does not attenuate on increasing spacer length. The similarity of this behaviour to that observed for semi-flexible main-chain polymers should be noted. A somewhat simplistic explanation has been offered by many authors to explain these observations [8] which assumes the spacer exists in an all-trans conformation in the nematic phase. Thus, for even membered spacers the two mesogenic moieties are almost collinear as shown in figure 2.3.6(a) whereas for odd membered spacers they are no longer collinear and instead form an angle of about 108°, see figure 2.3.6(b).

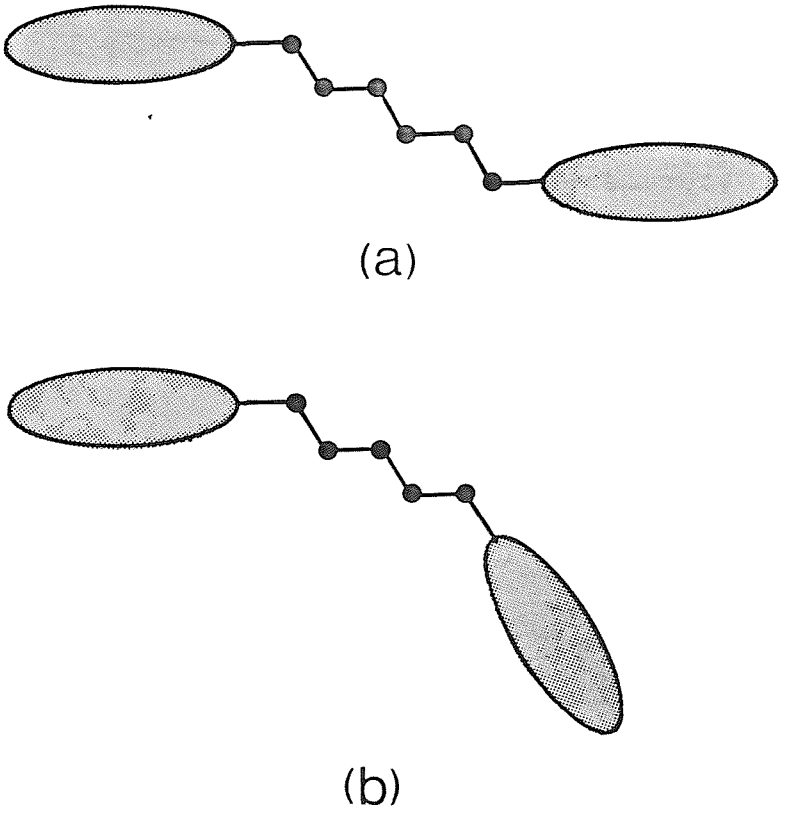

Figure 2.3.6 Schematic representations of (a) an even and (b) an odd membered dimer in which the spacers are in all-trans conformations.

It is, however, rather naive to consider only a single conformation of the flexible core and a more realistic explanation relies on the fact that there is a greater number of conformations for the even spacer which preserve the collinearity of the two rigid units than there is for the odd spacer. This is not immediately obvious and figure 2.3.7 is a diagrammatic representation of the effect of introducing a single gauche defect into the spacer and then systematically moving it along the chain. Clearly, for the even spacer there are two positions in which a gauche defect preserves the collinearity of the two rigid units but there are no positions in the odd spacer in which the gauche defect can increase the linearity of the molecule. Also, elongated conformers are more favoured in the nematic environment and hence, there is a greater conformational entropy change for even members than for odd members at the nematic-isotropic transition.

4.OnO.4 series

On increasing the length of the terminal alkyl chains the smectic tendencies of the molecule are predicted to increase and indeed this is observed. The transitional properties of the 4.OnO.4 series are listed in table 2.3.4; smectic properties are observed for 4.O3O.4, 4.O4O.4, 4.O5O.4 and 4.O6O.4. 4.O3O.4 is the only monotropic material; all the remaining members being enantiotropic mesogens. The smectic phases exhibited by 4.O3O.4, 4.O5O.4 and 4.O6O.4 and the higher temperature smectic phase of 4.O4O.4, all exhibit identical optical textures when viewed under a polarising microscope; namely, areas of focal-conic fan texture and homeotropic regions. This is shown in plate 2.3.2 for 4.O4O.4. In addition, X-ray diffraction studies of 4.O4O.4 revealed that the higher temperature mesophase has a lamellar spacing of 38.7 Å which is approximately equal to the estimated all-trans molecular length of 40 Å. Also, the lamellar spacing in the smectic phase of 4.O5O.4 was measured to be 38.6 Å as opposed to the estimated all-trans molecular length of 39.9 Å. These layer spacings imply that the director is orthogonal to the layer planes. Both compounds have a diffuse outer ring in their X-ray diffraction pattern which is characteristic of a liquid-like arrangement of molecules

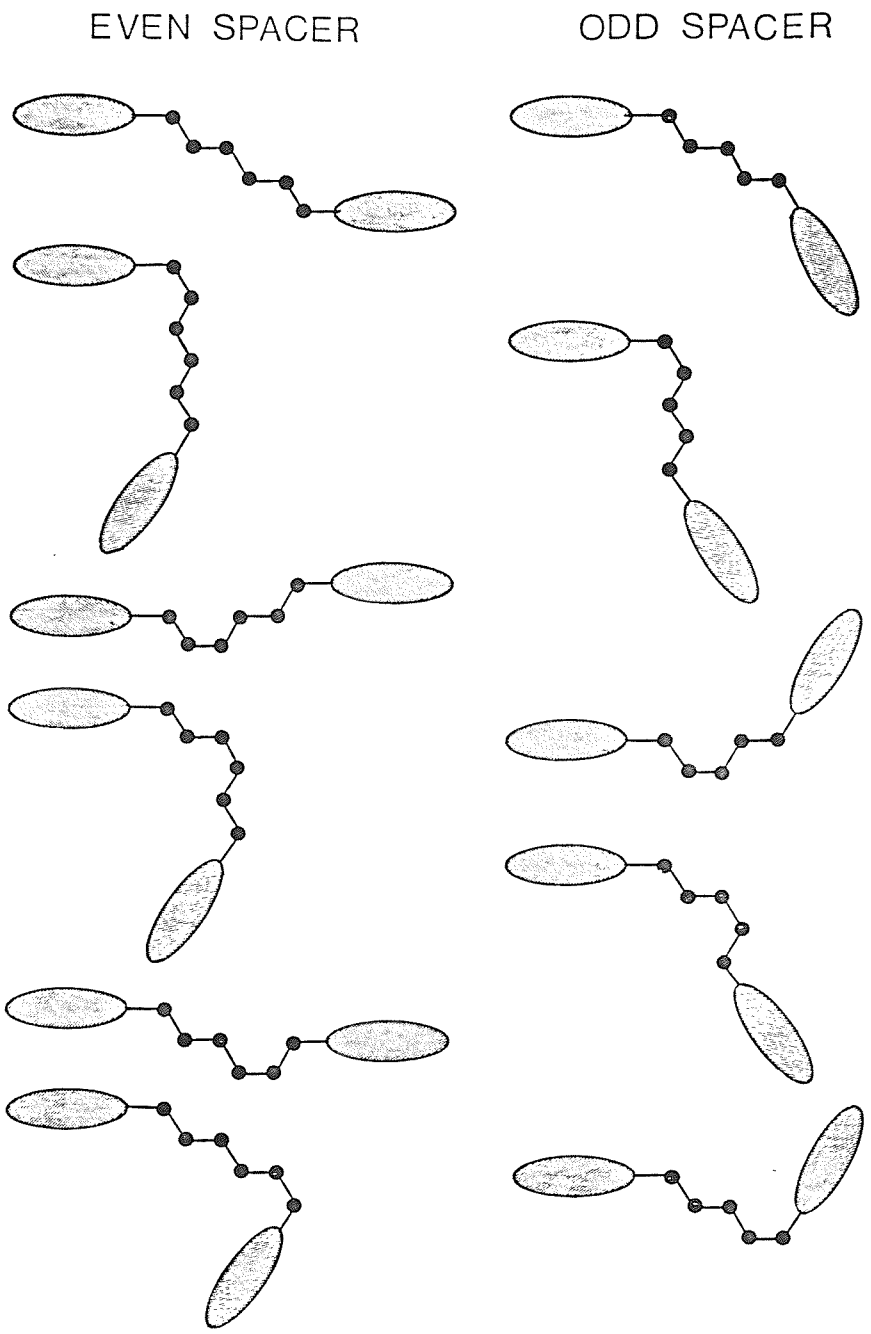

Figure 2.3.7 A diagrammatic representation in two-dimensions of introducing a single gauche defect into the alkyl core of a dimeric liquid crystal.

n	C-/ °C	S_A-N/ °C	N-I/ °C	ΔH_{S_A-N}/kJmol^{-1}	ΔH_{N-I}/kJmol^{-1}	$\Delta S_{S_A-N}/R$	$\Delta S_{N-I}/R$
				ΔH_{C-}/kJmol^{-1}	$\Delta S_{C-}/R$		
	[1]C-I/ °C	[2]S_B-S_A/ °C	[3]S_A-I/ °C	[1]$\Delta H_{S_B-S_A}$/kJmol^{-1}	[2]ΔH_{S_A-I}/kJmol^{-1}	[1]$\Delta S_{S_A-S_B}/R$	[2]$\Delta S_{S_A-I}/R$
3	[1]141	-	[3](114)	39.0	-	-	11.3	-	-
4	145	[2]150	[3]212	32.0	[1]5.19	[2]11.6	9.22	[1]1.48	[2]2.88
5	112	(107)	122	26.0	0.63	1.20	8.14	0.20	0.37
6	139.5	166	182	43.4	0.64	6.73	12.7	0.18	1.78
7	110	-	130	44.6	-	2.08	14.1	-	0.62
8	136.5	-	164	54.3	-	7.27	16.0	-	2.00
9	108	-	124	45.0	-	2.16	14.2	-	0.66
10	135	-	149	60.2	-	7.15	17.9	-	2.04
11	104	-	127	47.4	-	2.59	15.2	-	0.78
12	134.5	-	138.5	59.2	-	7.21	17.5	-	2.11

Table 2.3.4 The transition temperatures, enthalpies and entropies of transition for the 4.OnO.4 series; () denotes a monotropic transition. The uncertainties in the temperatures are ±1 °C and in the thermodynamic data are ±10%.

within the layers. Therefore, the mesophase was identified as a smectic A phase. This assignment has not been confirmed by miscibility studies and it is unclear whether such investigations would be useful because there are no standard dimeric smectic A compounds and hence, monomeric compounds would have to be used. However, the introduction of a monomer into the dimer may disrupt the packing of the dimeric molecules and hence, yield misleading results.

On cooling the smectic A phase of 4.O4O.4 to obtain the lower temperature mesophase, bars were observed across the backs of the focal-conic fans and these were transitory in nature, occuring reversibly. This sequence is shown in plates 2.3.2, 2.3.3 and 2.3.4; it is very characteristic of a smectic A to smectic B transition [13]. It should also be noted that the homeotropic regions remain unchanged implying that the orthogonal alignment of the director is maintained. The diffraction pattern for the lower temperature mesophase has a sharp outer band implying the presence of a least medium range order within the layers. Thus, this phase is considered to be a smectic B. The focal-conic fan texture of the smectic A phase formed on heating the smectic B phase shows blemishes, see plate 2.3.5, and again, this is characteristic of a smectic A to B transition.

The dependence of the transition temperatures upon the spacer length is given in figure 2.3.8. The liquid crystal-isotropic transition temperatures again show a very pronounced odd-even effect as do the melting points. It is interesting to note that as the alkyl spacer length is increased the smectic tendencies of the compound decreases. This opposes the general observation that increasing alkyl chain length promotes smectic phase behaviour [14]. This will be rationalised later. Figure 2.3.9 shows the very dramatic alternation in the entropy change associated with the liquid crystal-isotropic transition for the 4.OnO.4 series. The value of $\Delta S/R$ for 4.O4O.4 is by far the largest because this is a smectic A-isotropic transition. Again, the underlying trend for the remaining members is an increasing one for both odd and even spacer lengths.

It has often been observed that smectic tendencies of monomers are

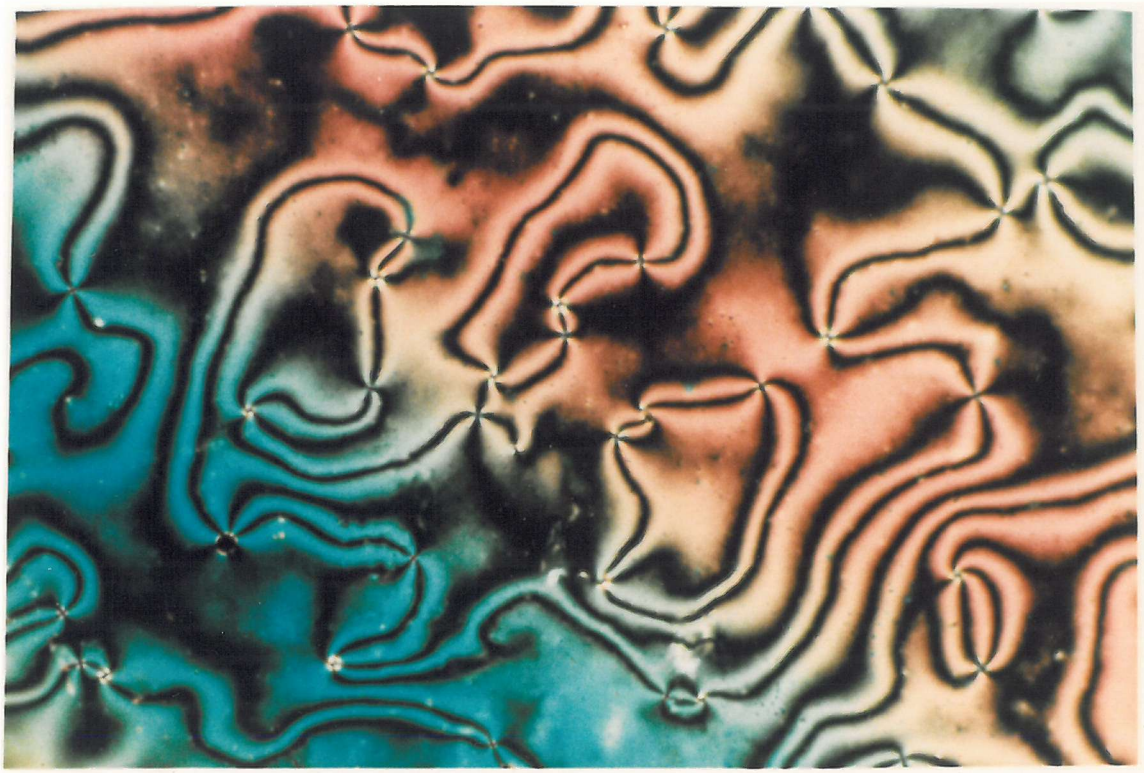

Plate 2.3.1 The schlieren texture of the nematic phase of 1.040.1 (T=220 °C).

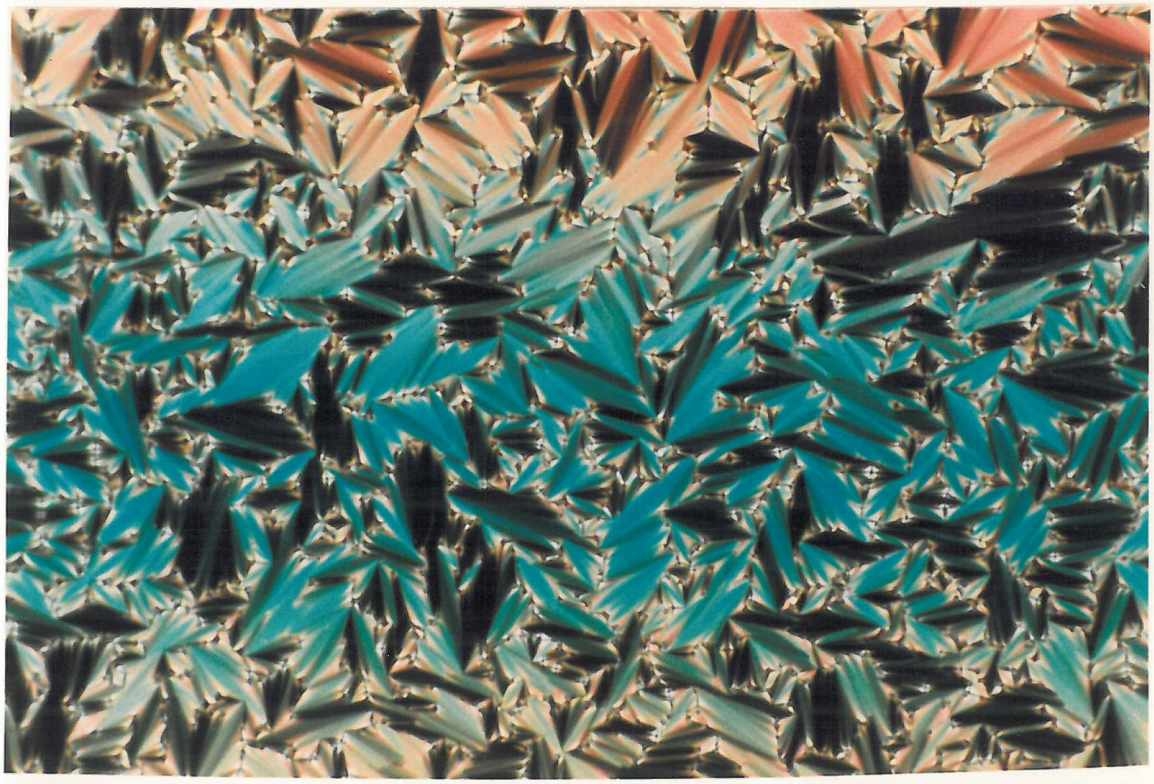

Plate 2.3.2 The focal-conic fan texture of the smectic A phase of 4.040.4 (T=155 °C).

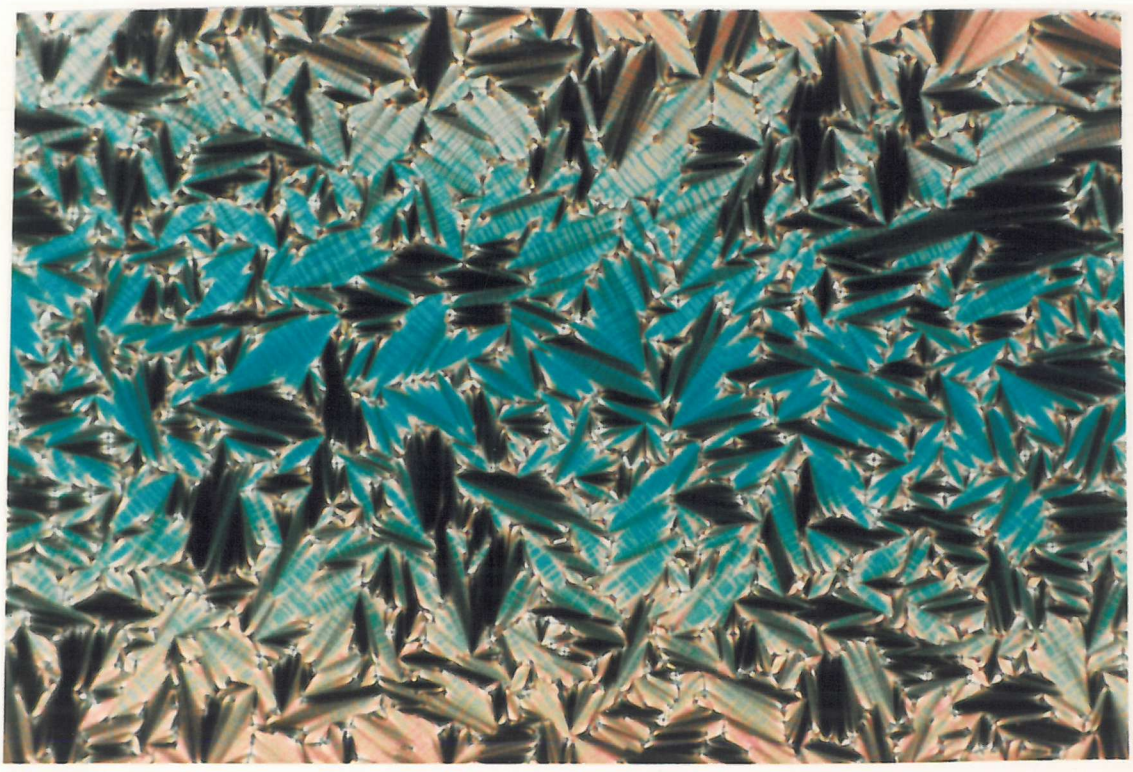

Plate 2.3.3 The transition from the focal-conic fan texture of the smectic A phase to the paramorphotic focal-conic fan texture of the smectic B phase for 4.O4O.4 (T=150 °C).

Plate 2.3.4 The paramorphotic focal-conic fan texture of the smectic B phase formed on cooling the focal-conic fan texture of the smectic A phase of 4.O4O.4 (T=140 °C).

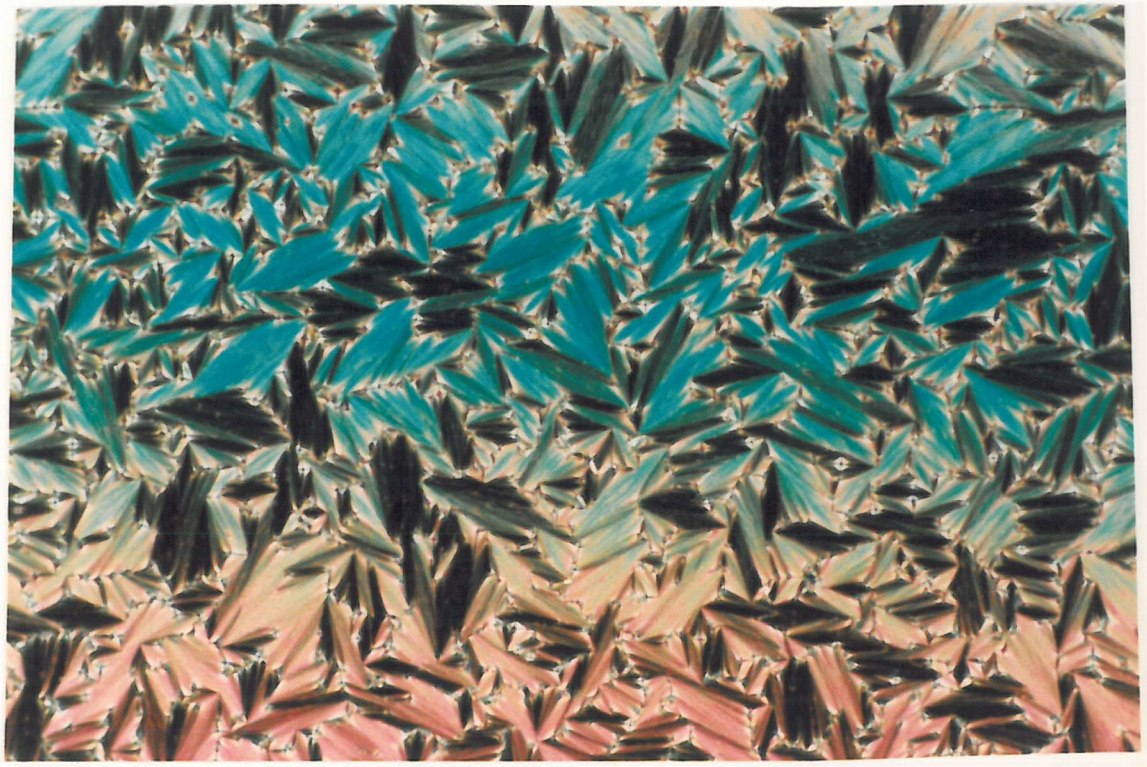

Plate 2.3.5 The focal-conic fan texture of the smectic A phase formed on heating the smectic B phase of 4.040.4 (T=155 °C).

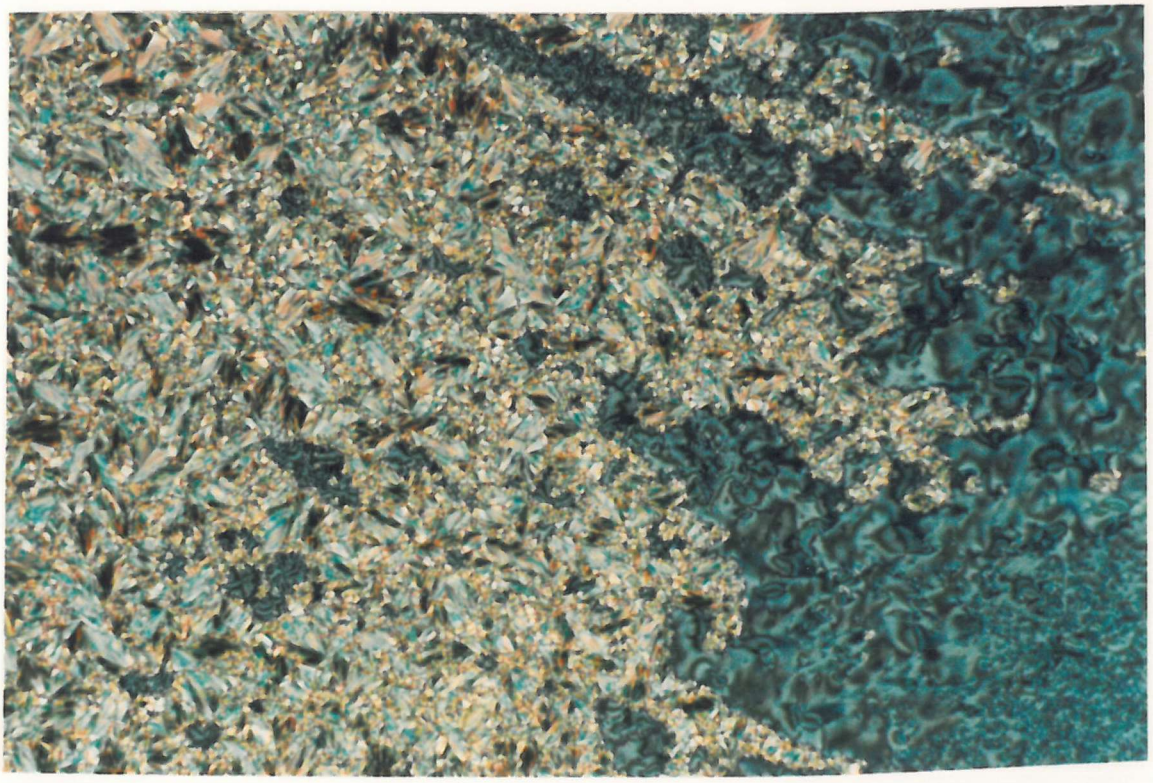

Plate 2.3.6 The paramorphotic focal-conic fan texture and the schlieren texture of the smectic C phase formed on cooling the smectic A phase of 8.040.8 (T=175 °C).

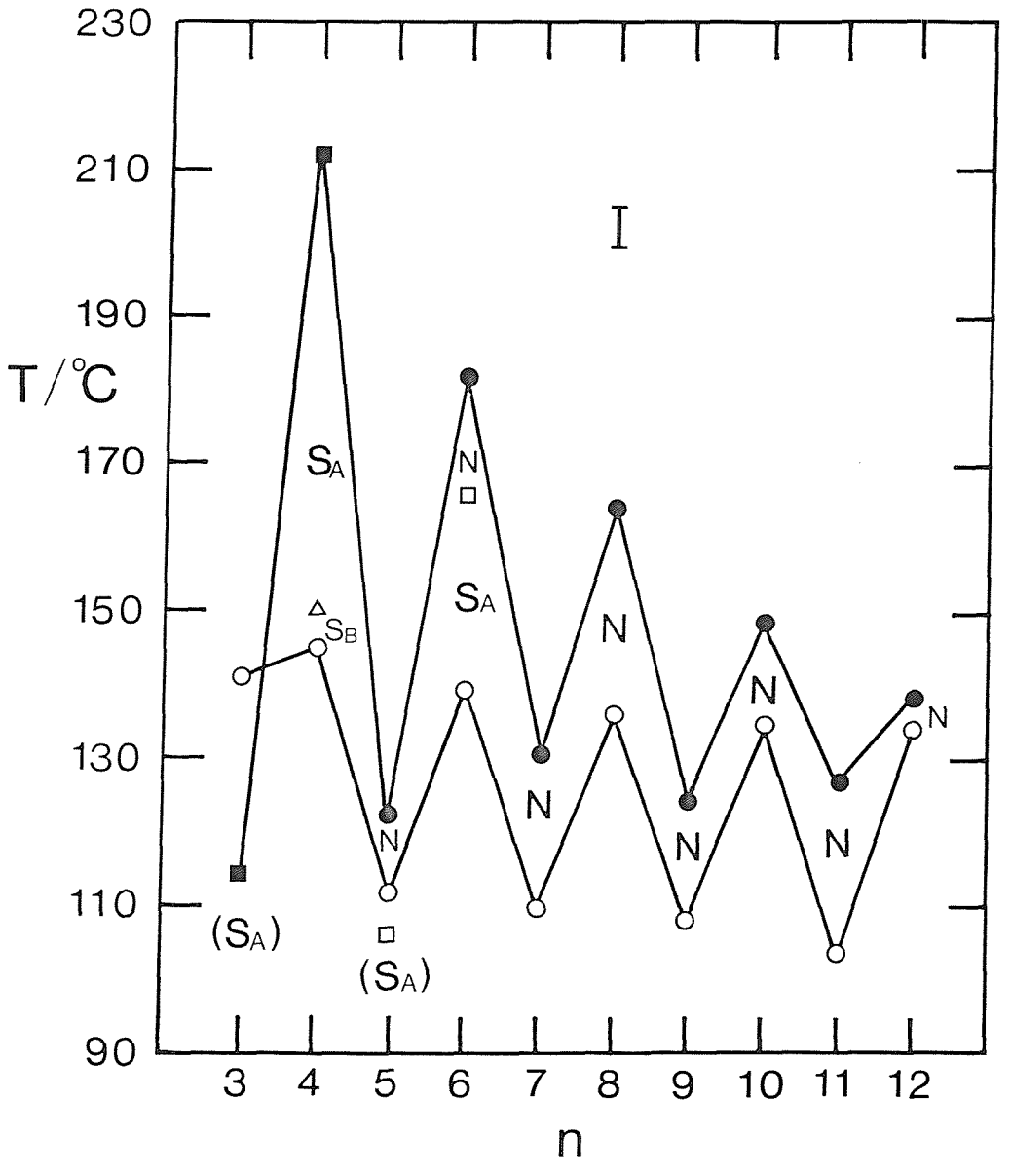

Figure 2.3.8 The dependence of the transition temperatures upon the number of methylene groups in the alkyl core for the 4.OnO.4 series. The melting point is denoted by ○ , ● indicates the nematic-isotropic transition, □ the smectic A-nematic transition, △ the smectic B-smectic A transition and ■ the smectic A-isotropic transition. Monotropic phases are marked in parentheses.

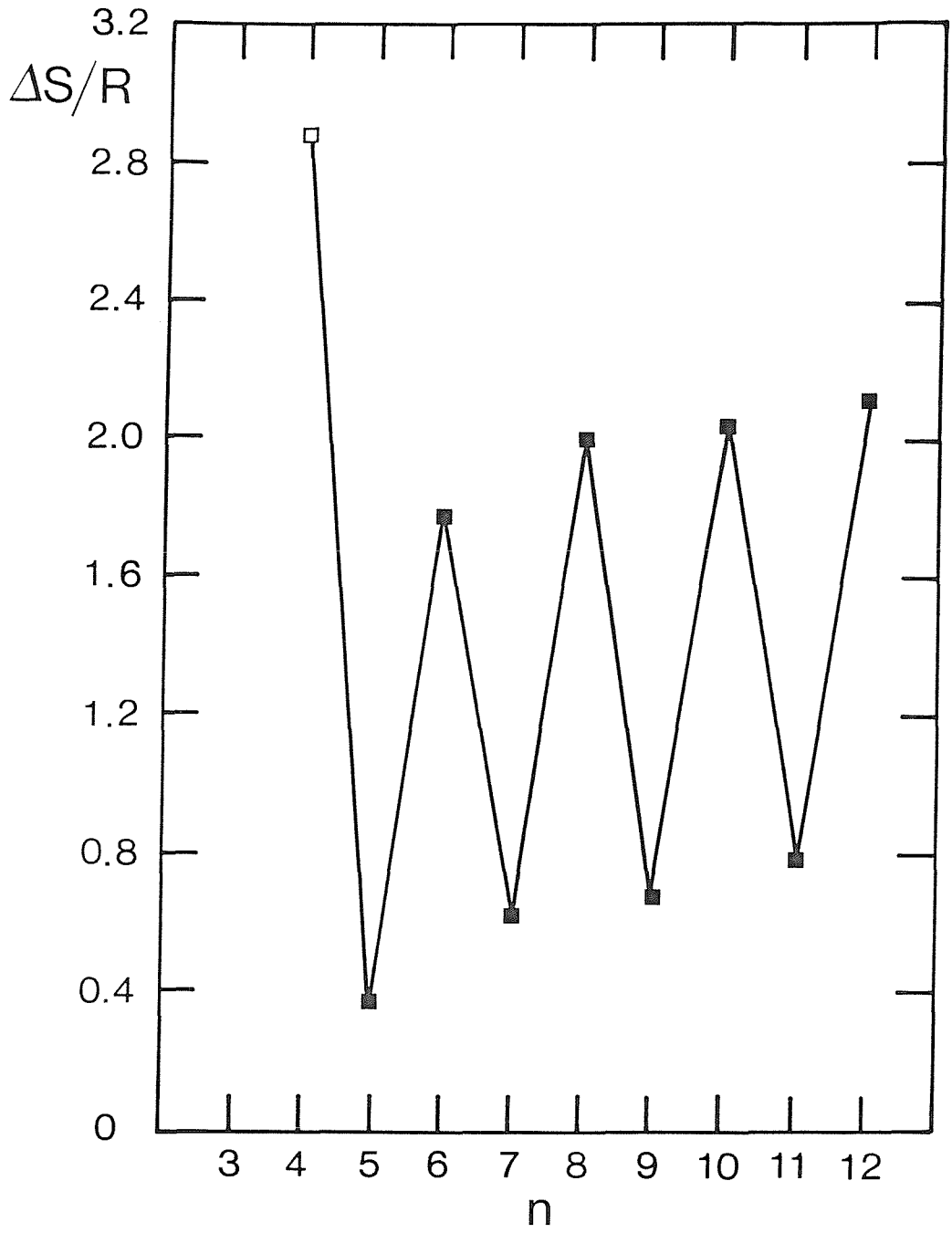

Figure 2.3.9 The dependence of the entropy change associated with the liquid crystal-isotropic transition on the number of methylene groups in the alkyl core for the 4.OnO.4 series. ■ indicates a nematic-isotropic transition and □ denotes a smectic A-isotropic transition.

lost when coupled to form the dimer [1]. If, however, we consider the monomeric analogue of 4.O4O.4 to be 20.4 then quite the opposite is true. 20.4 is purely nematic [6] whereas 4.O4O.4 exhibits both smectic B and A phases. Thus, this is an example in which coupling the monomer has led to enhanced smectic tendencies. It should be stressed that this is not a general result for the m.OnO.m's. For example, 60.4 has a complicated smectic phase sequence [6] whereas 4.O12O.4 is purely nematic. Using examples from other series these observations will be extended and rationalised later.

5.OnO.5 series

Increasing the length of the terminal alkyl chains further we would expect to see the compounds exhibiting increasingly smectic tendencies and this is indeed the case. Table 2.3.5 lists the transitional properties of the 5.OnO.5 series and now, all members up to and including eight methylene units in the spacer exhibit smectic behaviour. The smectic phase assignments were made using identical arguments to those described for the 4.OnO.4 series. Figure 2.3.10 shows the dependence of the transition temperatures upon the length of the alkyl spacer. All the members of the series exhibit enantiotropic mesophases with the exception of 5.O3O.5 which forms a monotropic smectic A phase. Again, the melting points show a pronounced alternation with the single exception of 5.O3O.5 whose melting point is slightly higher than that of 5.O4O.5. The liquid crystal-isotropic transition temperatures show the now familiar large odd-even effect which attenuates with increasing spacer length. The dependence of the entropy associated with the liquid crystal-isotropic transition is given in figure 2.3.11; again a dramatic alternation is apparent with an underlying increase for both odd and even spacer lengths.

n	C-/ °C	S_B-S_A/ °C	S_A-N/ °C	N-I/ °C	ΔH_{C-}/kJmol^{-1}	$\Delta H_{S_B-S_A}$/kJmol^{-1}	ΔH_{S_A-N}/kJmol^{-1}	ΔH_{N-I}/kJmol^{-1}	ΔS_{C-}/R	$\Delta S_{S_A-S_B}$/R	ΔS_{S_A-N}/R	ΔS_{N-I}/R
	[1]C-I/ °C			[2]S_A-I/ °C			[1]ΔH_{S_A-I}/kJmol^{-1}				[2]ΔS_{S_A-I}/R	
3	[1]137.5	-	-	[2](131)	37.1	-	-	[1]5.80	10.9	-	-	[2]1.73
4	133	162	-	[2]218	31.0	6.22	-	[1]16.0	9.22	1.72	-	[2]3.92
5	113	-	-	[2]133.5	28.8	-	-	[1]4.89	9.09	-	-	[2]1.47
6	133.5	(129)	182.5	184.5	43.9	2.17	1.85	9.21	13.1	0.65	0.49	2.42
7	115	-	119	135	45.7	-	0.48	2.68	14.2	-	0.15	0.79
8	131	-	146	167	53.4	-	0.33	9.38	15.9	-	0.10	2.57
9	103	-	-	131	51.6	-	-	3.67	16.5	-	-	1.09
10	131	-	-	151	65.7	-	-	9.58	19.6	-	-	2.72
11	106	-	-	129	59.4	-	-	3.70	18.9	-	-	1.11
12	131.5	-	-	140.5	63.5	-	-	9.52	18.9	-	-	2.77

Table 2.3.5 The transition temperatures, enthalpies and entropies of transition for the 5.OnO.5 series; () denotes a monotropic transition. The uncertainties in the temperatures are ±1 °C and in the thermodynamic data are ±10%.

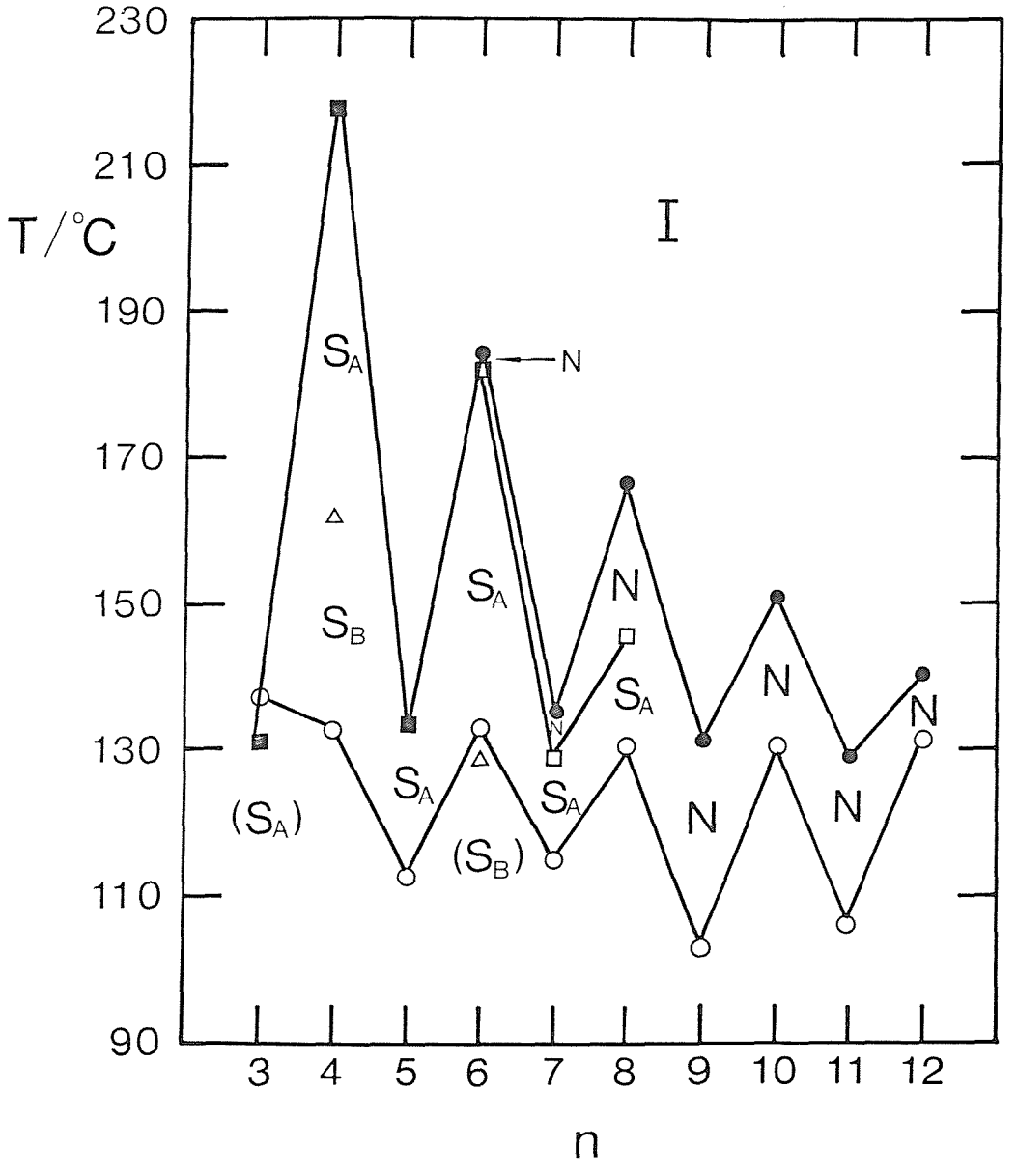

Figure 2.3.10 The dependence of the transition temperatures upon the number of methylene groups in the flexible alkyl core for the 5.OnO.5 series. The melting point is denoted by o , △ indicates the smectic A-smectic B transition, □ the smectic A-nematic transition, ■ the smectic A-isotropic transition and ● the nematic-isotropic transition. Monotropic phases are marked in parentheses.

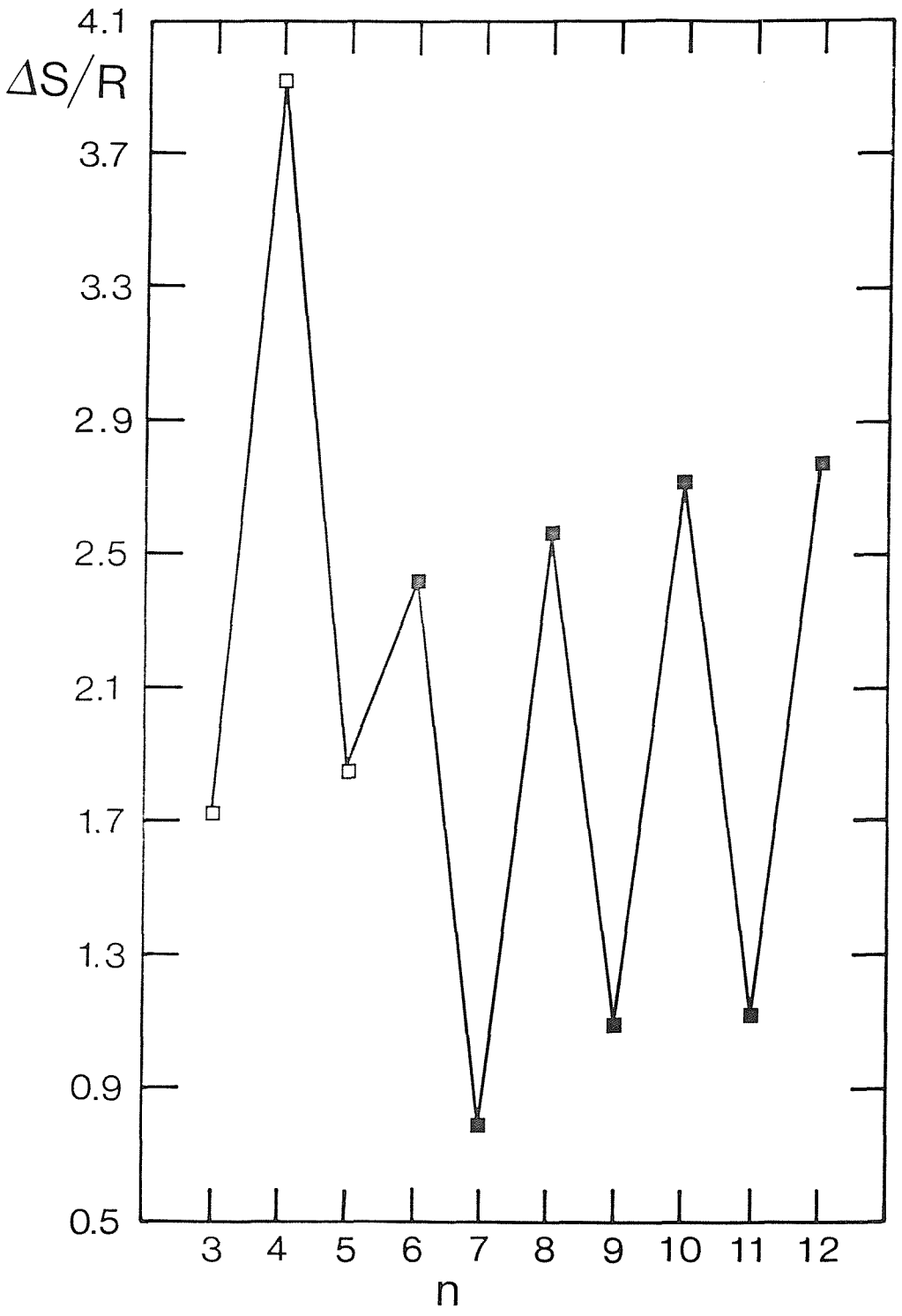

Figure 2.3.11 The dependence of the entropy change associated with the liquid crystal-isotropic transition on the number of methylene groups in the alkyl core for the 5.OnO.5 series. □ indicates a smectic A-isotropic transition while ■ denotes a nematic-isotropic transition.

8.On0.8 series

On increasing the terminal chain lengths to eight methylene units giving the 8.On0.8 series only one homologue, 8.0110.8, possesses nematic properties. The transitional properties for this series are listed in table 2.3.6; all ten members exhibit enantiotropic mesophases. The smectic A phases were assigned on the basis of both focal-conic fan and homeotropic textures being observed using polarising microscopy. On cooling the smectic A phase of 8.040.8 and 8.060.8, the homeotropic regions adopted schlieren textures and the backs of the fans became sanded and broken, appearing to have a shimmering texture, an effect caused by director fluctuations [13]. This texture is shown in plate 2.3.6 and is very typical of a smectic C phase [13]. On cooling the smectic C phase of 8.040.8 and 8.060.8 a mosaic-schlieren texture develops from the areas of schlieren texture. The fans in the smectic C phase are somewhat sanded and broken, see plate 2.3.6, and on cooling, the sanding disappeared and the breaks became well-defined, transforming into black patches; this is very characteristic of a smectic C to F transition. On cooling the smectic A phase of 8.080.8, the homeotropic regions develop into areas of blue-grey mosaic texture and the focal-conic fans develop lines across their backs. These textures are shown in plates 2.37 and 2.38 and are indicative of a smectic A to F transition.

On cooling the smectic A phases of 8.050.8, 8.070.8, 8.090.8, 8.0100.8 and 8.0110.8, the focal-conic fan texture becomes broken while a mosaic texture composed of poorly coloured elongated platelets is obtained from homeotropic areas. The phase is very viscous but can be sheared. The texture is shown in plate 2.3.9 and is indicative of a smectic G phase. On cooling the isotropic phase of 8.0120.8 a mosaic texture forms via dentritic growth of elongated platelets producing the texture shown in plate 2.3.10. The phase though very viscous can be sheared. The phase is thus identified as being a smectic G. We should stress that all these phase assignments have been made on the basis of both their optical textures and X-ray diffraction experiments on powder samples [7]. However, the phases identified as smectic F and G may actually be smectic I and J respectively. In order to

n	$^{1}C-$/°C	S_F-S_C/°C $^{1}S_G-S_A$/°C $^{2}S_F-S_A$/°C	S_C-S_A/°C $^{1}S_A-N$/°C	S_A-I/°C $^{2}N-I$/°C $^{3}S_G-I$/°C	ΔH_{C-}/kJmol^{-1} ΔH_{S-S}/kJmol^{-1}	ΔH_{S_A-I}/kJmol^{-1} $^{2}\Delta H_{N-I}$/kJmol^{-1} $^{3}\Delta H_{S_G-I}$/kJmol^{-1}	$\Delta S_{C-}/R$	$\Delta S_{S-S}/R$	$\Delta S_{S_A-I}/R$ $^{2}\Delta S_{N-I}/R$ $^{3}\Delta S_{S_G-I}/R$
3	^{1}127	-	-	142	30.2 -	9.02	9.09	-	2.61
4	106	168.5	186	211	51.3 7.30	18.6	16.3	2.00	4.61
5	103	^{1}104	-	143	29.5 9.04	9.84	9.42	2.93	2.85
6	112	145	146	181	34.8 8.95	18.0	10.9	2.59	4.77
7	116	^{1}101.5	-	134	49.9 10.6	9.75	15.4	3.42	2.88
8	128	^{2}136	-	157	44.7 9.33	18.0	13.4	2.74	5.04
9	109.5	^{1}(106)	-	122	53.0 14.1	9.81	16.7	4.48	2.99
10	123	^{1}133	-	140.5	43.2 16.3	18.1	13.1	4.83	5.25
11	99	^{1}117	^{1}119	^{2}123	35.1 24.2	^{2}3.41	11.3	7.48	^{2}1.04
12	124	-	-	^{3}129	47.2 -	^{3}32.7	14.3	-	^{3}9.78

Table 2.3.6 The transition temperatures, enthalpies and entropies of transition for the 8.OnO.8 series; () denotes a monotropic transition. The uncertainties in the temperatures are ±1 °C and in the thermodynamic data are ±10%.

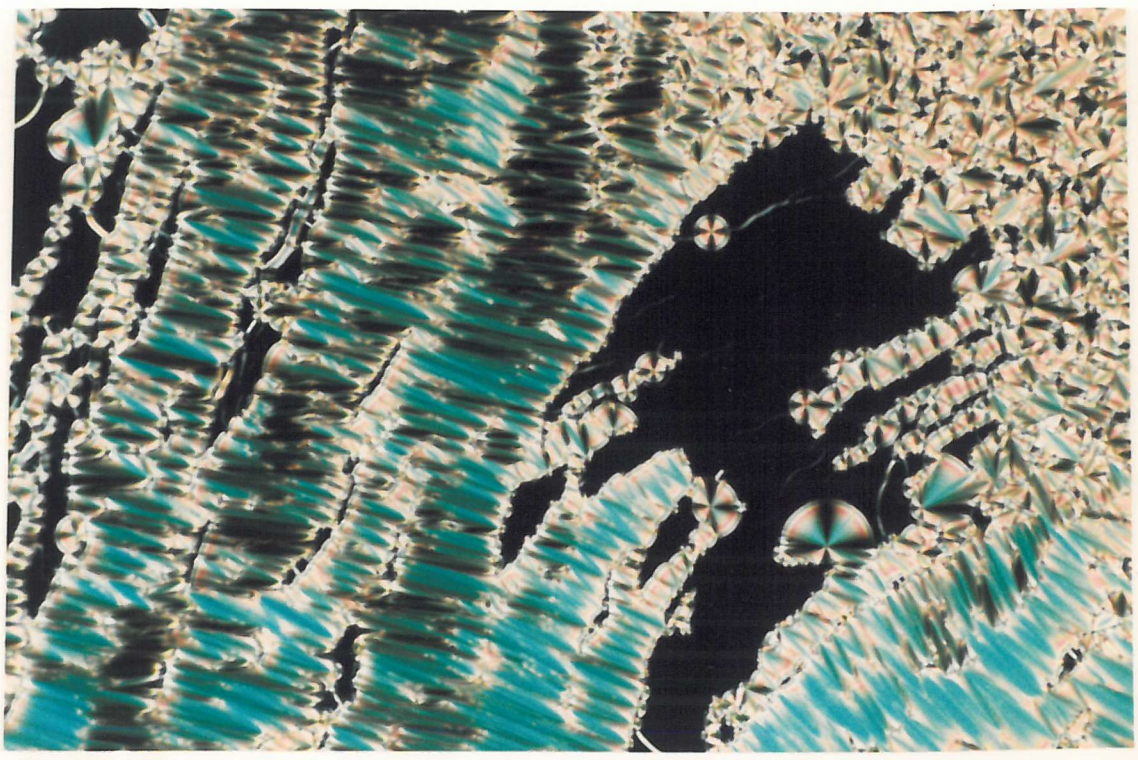

Plate 2.3.7 The focal-conic fan and homeotropic textures of the smectic A phase of 8.O8O.8 (T=145 °C).

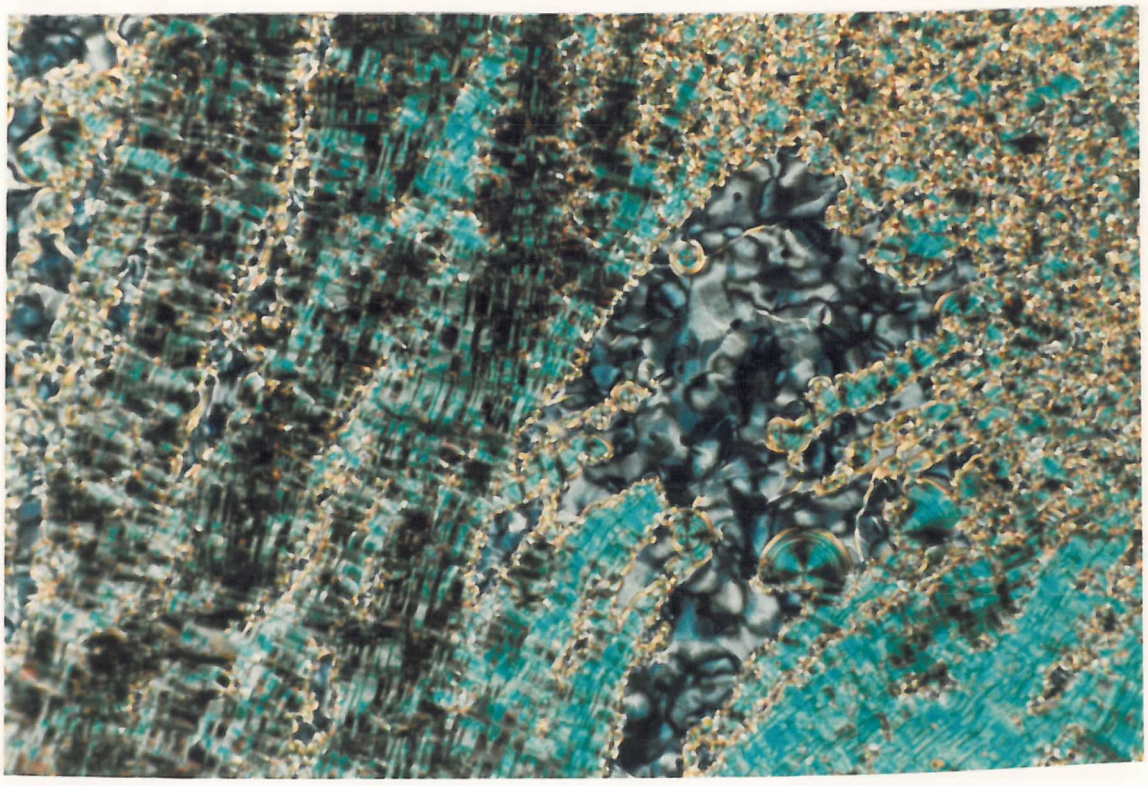

Plate 2.3.8 The paramorphotic focal-conic fan texture and the mosaic texture of the smectic F phase formed on cooling the smectic A phase of 8.O8O.8 (T=129 °C).

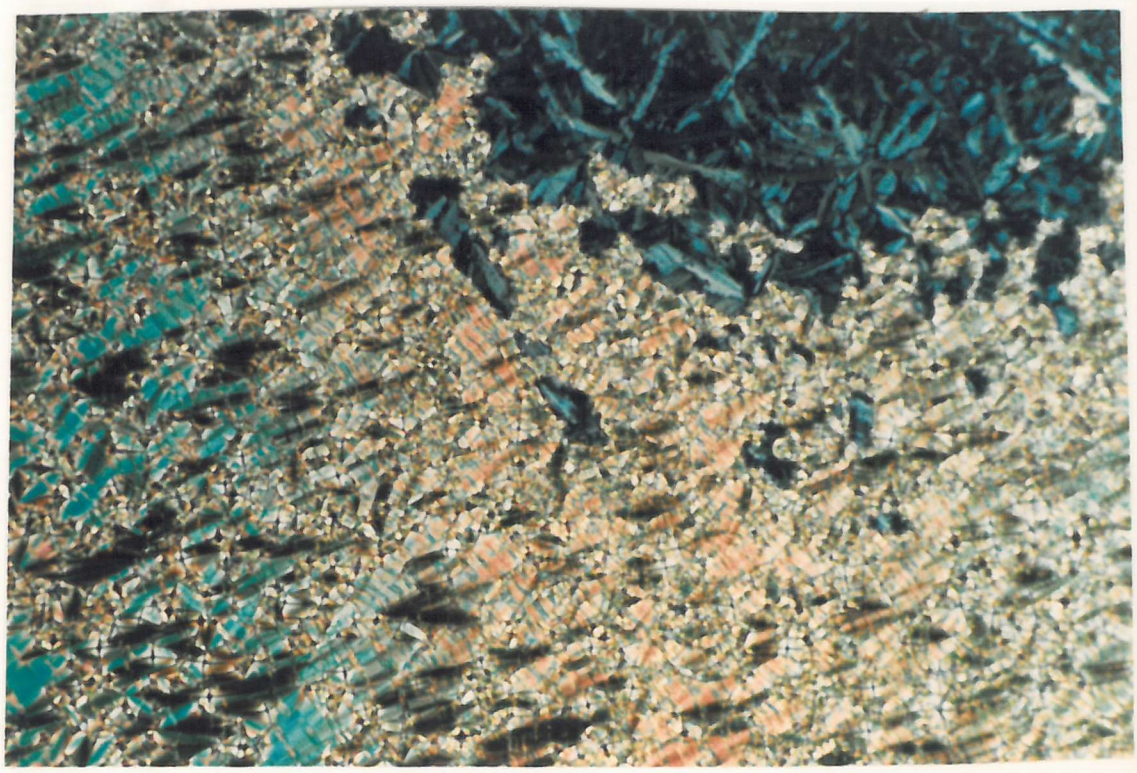

Plate 2.3.9 The paramorphotic focal-conic fan texture and the mosaic texture of the smectic G phase formed on cooling the smectic A phase of 8.090.8 (T=104 °C).

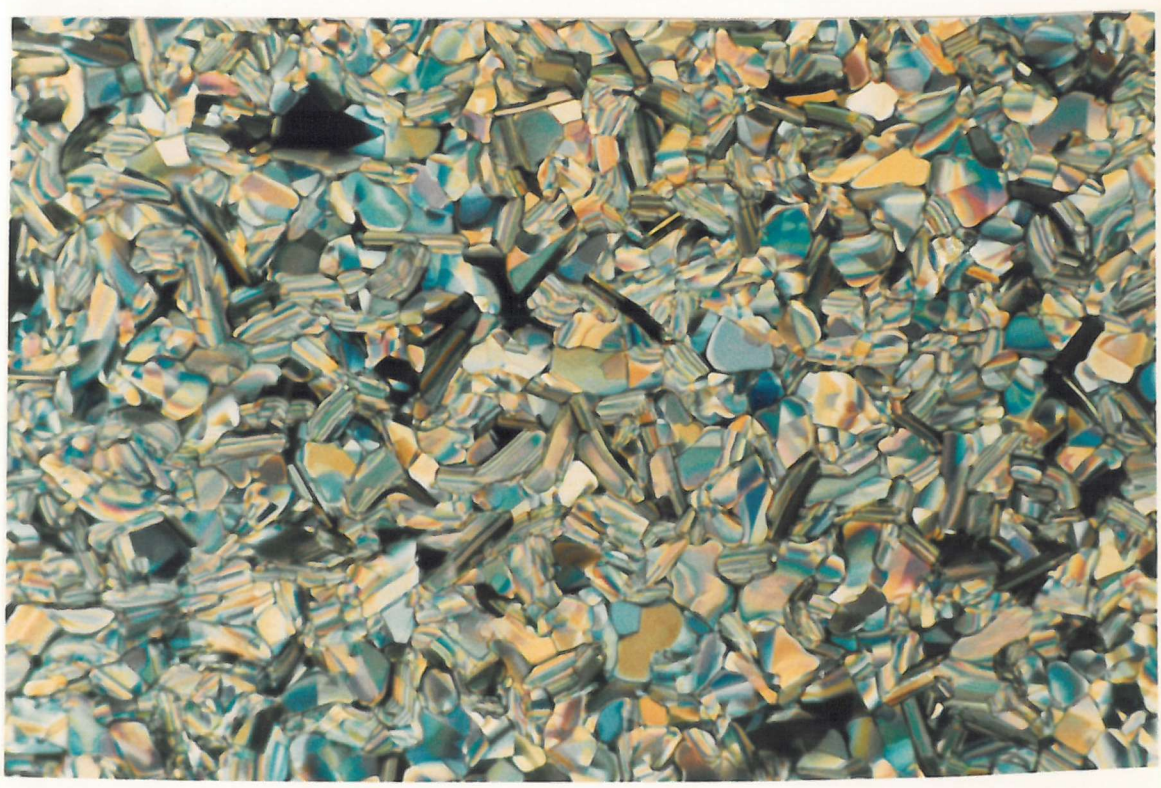

Plate 2.3.10 The natural mosaic texture of the smectic G phase formed on cooling the isotropic liquid of 8.0120.8 (T=125 °C).

assign these phases unambiguously requires X-ray diffraction patterns of aligned samples.

Figure 2.3.12 illustrates the dependence of the transition temperatures upon the length of the flexible spacer for the 8.OnO.8 series. The melting points behave irregularly for spacer lengths of less than seven methylene units contradicting the view that the alternation in melting points for a homologous series of dimeric liquid crystals is a general phenomenon [11]. The liquid crystal-isotropic transition temperatures of the 8.OnO.8 series show the now familiar large odd-even effect, attenuating with increasing spacer length. The smectic-smectic transition temperatures behave similarly and quite unlike those of the nO.8 series [6]. For early members of the nO.8 series only nematic behaviour is observed, higher homologues showing a combination of smectic and nematic properties and after the sixth homologue purely smectic behaviour is exhibited [6]. The dimeric analogues, the 8.OnO.8 series, behave in the opposite sense, purely smectic for shorter lengths with nematic properties emerging with increasing spacer length. Thus, it appears that providing the alkoxy chain length (n) is less than that of the alkyl chain (m) in an nO.m material then coupling to form the dimeric analogue, m.OnO.m, leads to enhanced smectic tendencies. If, however, the reverse is true, m being less than n, then coupling the monomer results in enhanced nematic properties. This will be rationalised later.

Figure 2.3.13 gives the dependence of the entropy change associated with the smectic A-nematic transition on the length of the alkyl spacer for the 8.OnO.8 series. This transition is exhibited by the members having spacer lengths between two [7] and ten. The observed behaviour is very similar to that of the entropies associated with the nematic-isotropic transition for the 4.OnO.4 and 5.OnO.5 series namely; the values exhibit a very pronounced alternation with spacer length which does not attenuate with increasing core length. Also, the underlying trend for both odd and even spacer lengths is that the entropy change associated with the transition increases with increasing core length. Again, as with the entropies associated with nematic-isotropic transitions for the 4.OnO.4 and 5.OnO.5 series, the

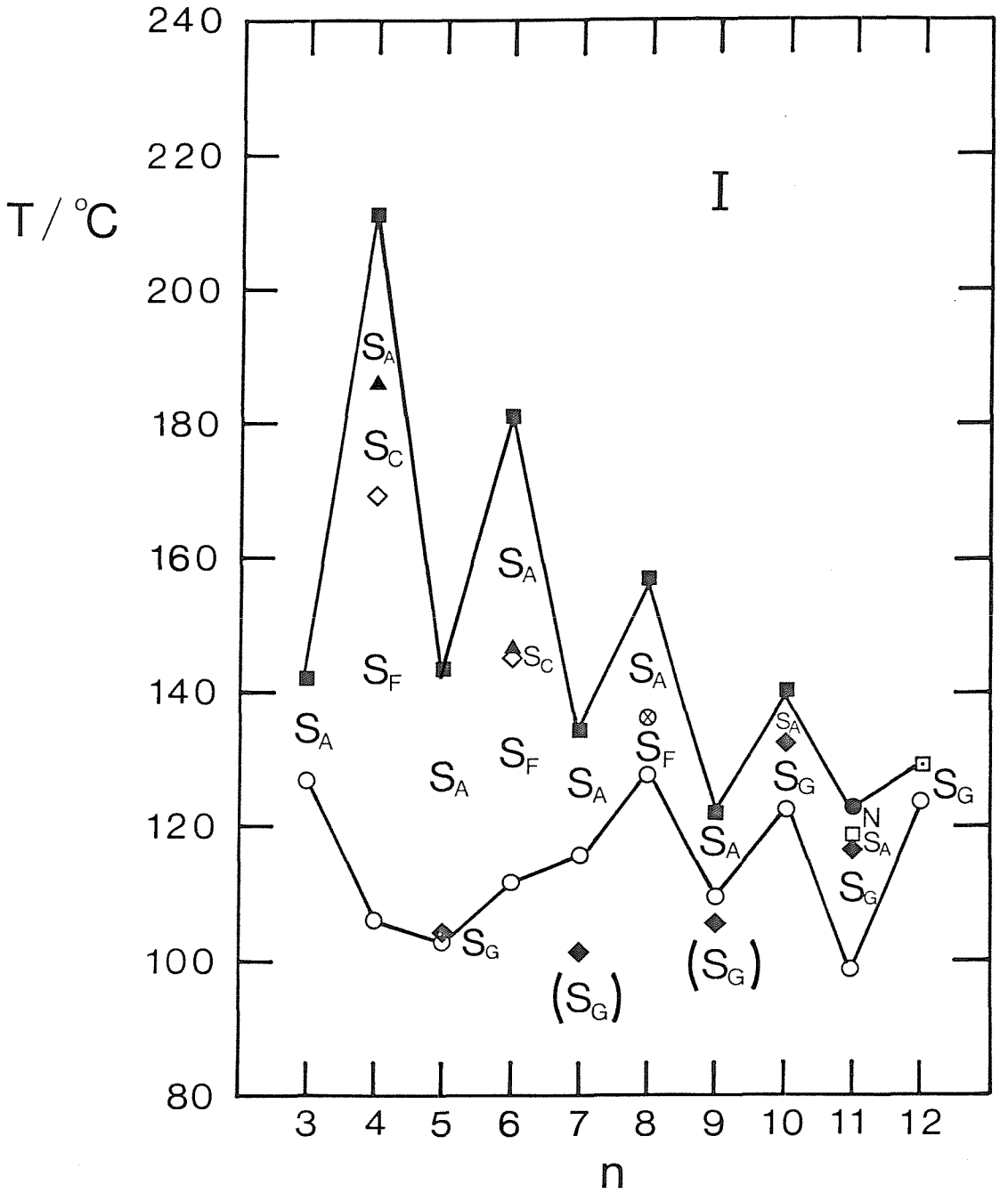

Figure 2.3.12 The dependence of the transition temperatures upon the number of methylene groups in the flexible alkyl core for the 8.On0.8 series. The melting point is denoted by ○ , ◇ indicates the smectic F-smectic C transition, ▲ the smectic C-smectic A transition, ■ the smectic A-isotropic transition, ◆ smectic G-smectic A transition, ⊗ smectic F-smectic A transition, □ the smectic A-nematic transition, ⊡ the smectic G-isotropic transition and ● the nematic-isotropic transition. Monotropic phases are marked in parentheses.

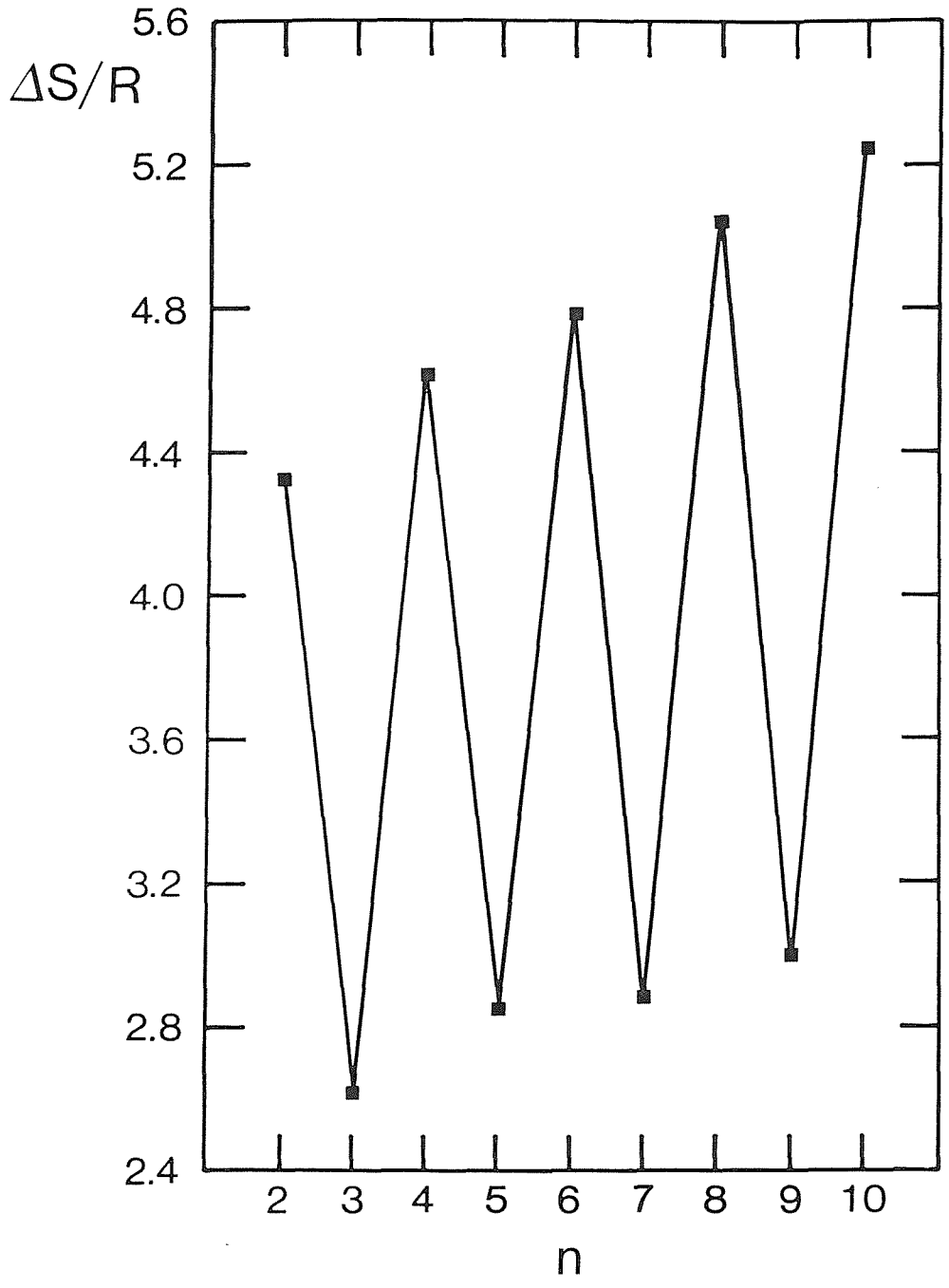

Figure 2.3.13 The dependence of the entropy change associated with the smectic A-isotropic transition on the number of methylene groups in the alkyl core for the 8.OnO.8 series.

values of ΔS/R are much higher for even membered dimers than for either odd membered dimers or the monomeric analogues. For comparison, the smectic A-isotropic transition of 70.8 has an associated ΔS/R of 1.98 [12] which is less than half the value of an even membered dimer.

Thus far, the discussion has been limited to varying the spacer length (n) while holding the terminal chain lengths (m) constant. We shall now consider the reverse, holding n constant while varying m. Figure 2.3.14 shows the dependence of the liquid crystal-isotropic transition temperature on the length of the terminal alkyl chains for m.OnO.m series with even spacer lengths. It is immediately apparent that the curves do not intersect each other and this emphasises the point that in any given m.OnO.m series the liquid crystal-isotropic transition temperatures for even values of n always lie on a decreasing curve with increasing m. Two quite distinct types of behaviour are evident in figure 2.3.14. For spacer lengths of two and four the transition temperatures alternate with increasing m up to m=5 and then decrease with little or no alternation. This suggests that the core is largely conformationally locked or semi-rigid and increasing the terminal alkyl chain lengths serves merely to dilute the core-core interactions. The longer spacer lengths show the same early odd-even effect but then pass through a minimum before increasing with alternation on increasing m. This implies the terminal chains may now play a more important role in determining molecular shape and hence, also molecular interactions. Thus, the core is considered to have greater flexibility and the terminal chains adopt conformations which act to preserve the linearity of the molecule. This effect appears to be dampened with increasing m.

Figure 2.3.15 shows the dependence of the liquid crystal-isotropic transition temperature upon the length of the terminal alkyl chains for m.OnO.m series with odd spacer lengths. This shows a very different behaviour to that seen in figure 2.3.14 for even spacer lengths. The five curves show many intersections of each other and reflects that in a given m.OnO.m series on holding m constant and varying n the transition temperatures of the odd members never fall on a smooth increasing or decreasing curve but instead pass through a

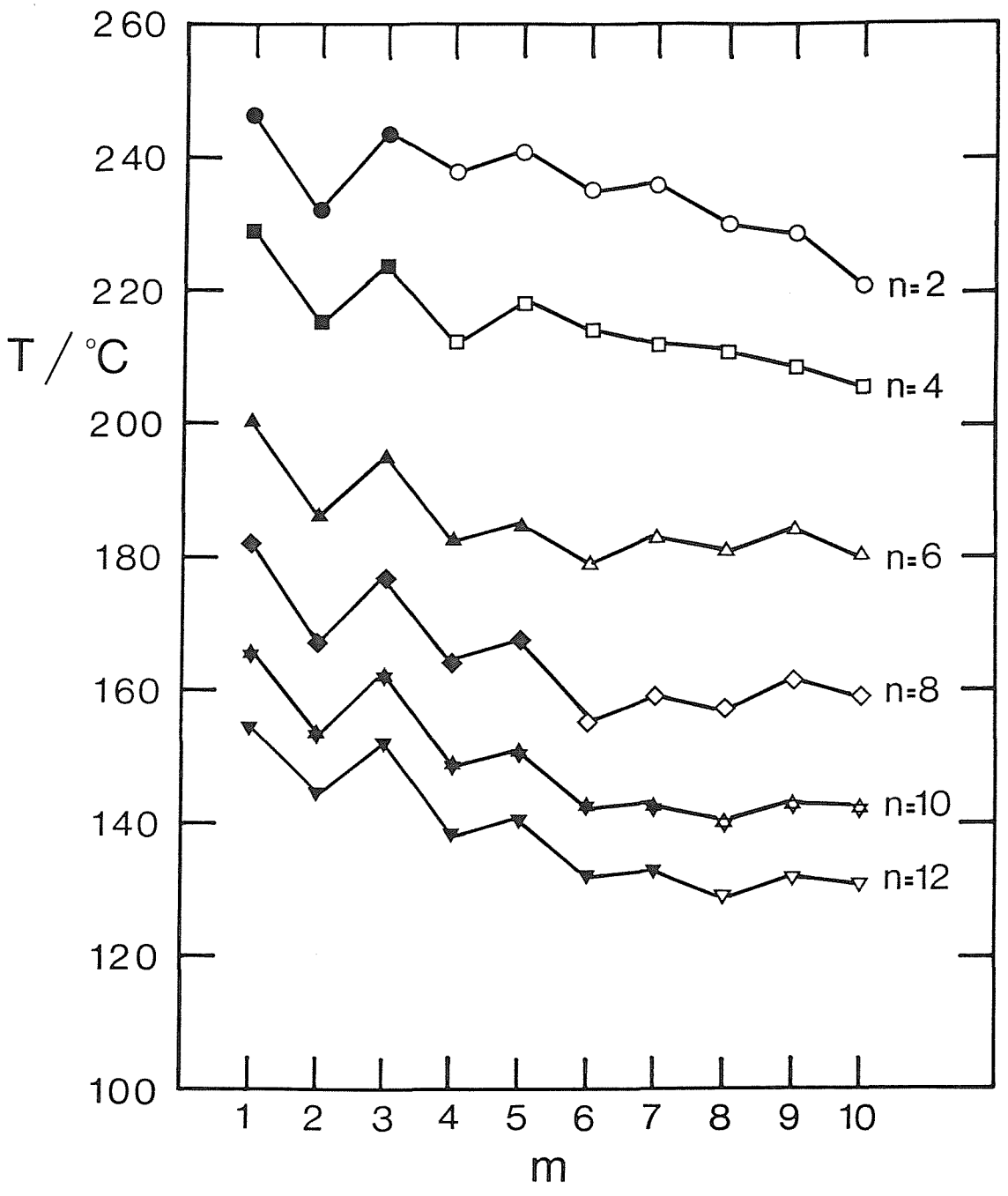

Figure 2.3.14 The dependence of the liquid crystal-isotropic transition temperature on the length of the terminal alkyl chains for m.OnO.m series having an even number of methylene units in the alkyl core. ■ indicates a nematic-isotropic transition and □ denotes a smectic-isotropic transition.

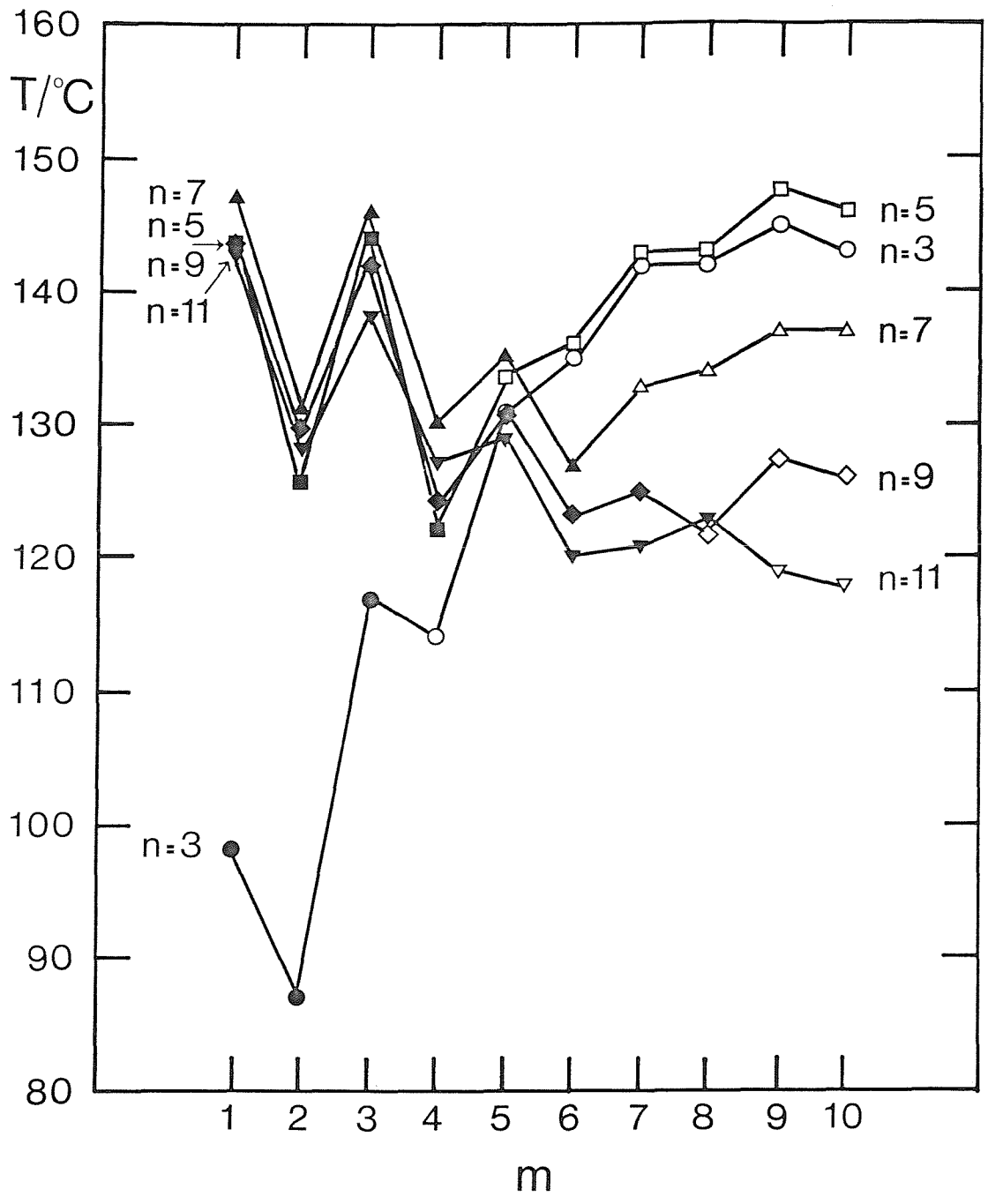

Figure 2.3.15 The dependence of the liquid crystal-isotropic transition temperature on the length of the terminal alkyl chains for m.OnO.m series having an odd number of methylene units in the alkyl core. Filled symbols indicate a nematic-isotropic transition and open symbols denote a smectic-isotropic transition.

maxima. This is evident in figures 2.3.2, 2.3.4, 2.3.8, 2.3.10 and 2.3.12. The m.O3O.m series behaves quite differently to the others for small values of m, by exhibiting a steeply rising liquid crystal-isotropic transition temperature curve which levels off with increasing m. This is similar to the behaviour seen in monomeric materials possessing low transition temperatures [15]. The complex behaviour illustrated in figure 2.3.15 cannot be rationalised simply in terms of the conformational distribution of the spacer alone and it appears that the terminal chains play a more important role in determining the properties of dimers possessing odd length spacers than in those with even length cores. This arises, in part, because the core is not so dominant in determining the transition temperature of an odd-membered compound.

Figure 2.3.16 shows the dependence of $\Delta S/R$ at the liquid crystal-isotropic transition on varying m while holding n constant. It is immediately apparent that the m.O4O.m series exhibits consistently higher values of $\Delta S/R$ than the m.O5O.m series. It is, however, difficult to compare the values, for in many cases they represent different transitions. Figure 2.3.17 ilustrates the dependence of $\Delta S/R$ at the nematic-isotropic transition upon m for both the m.O11O.m and m.O12O.m series. As would be predicted, the curve for the m.O12O.m series lies above that of the m.O11O.m series. Both curves show an odd-even effect and behave very similarly, the spacing between the curves being approximately constant as m is increased. It is tempting to suggest that the average difference in $\Delta S/R$ between the corresponding members of the two series of 1.31 is a direct measure of the difference in the change in the conformational distribution of the alkyl spacer at the nematic-isotropic transition between the eleven and twelve membered spacers. This assumes, however, that the conformational change of the terminal alkyl chains is constant for both even and odd membered spacers at the mematic-isotropic transition which is unreasonable.

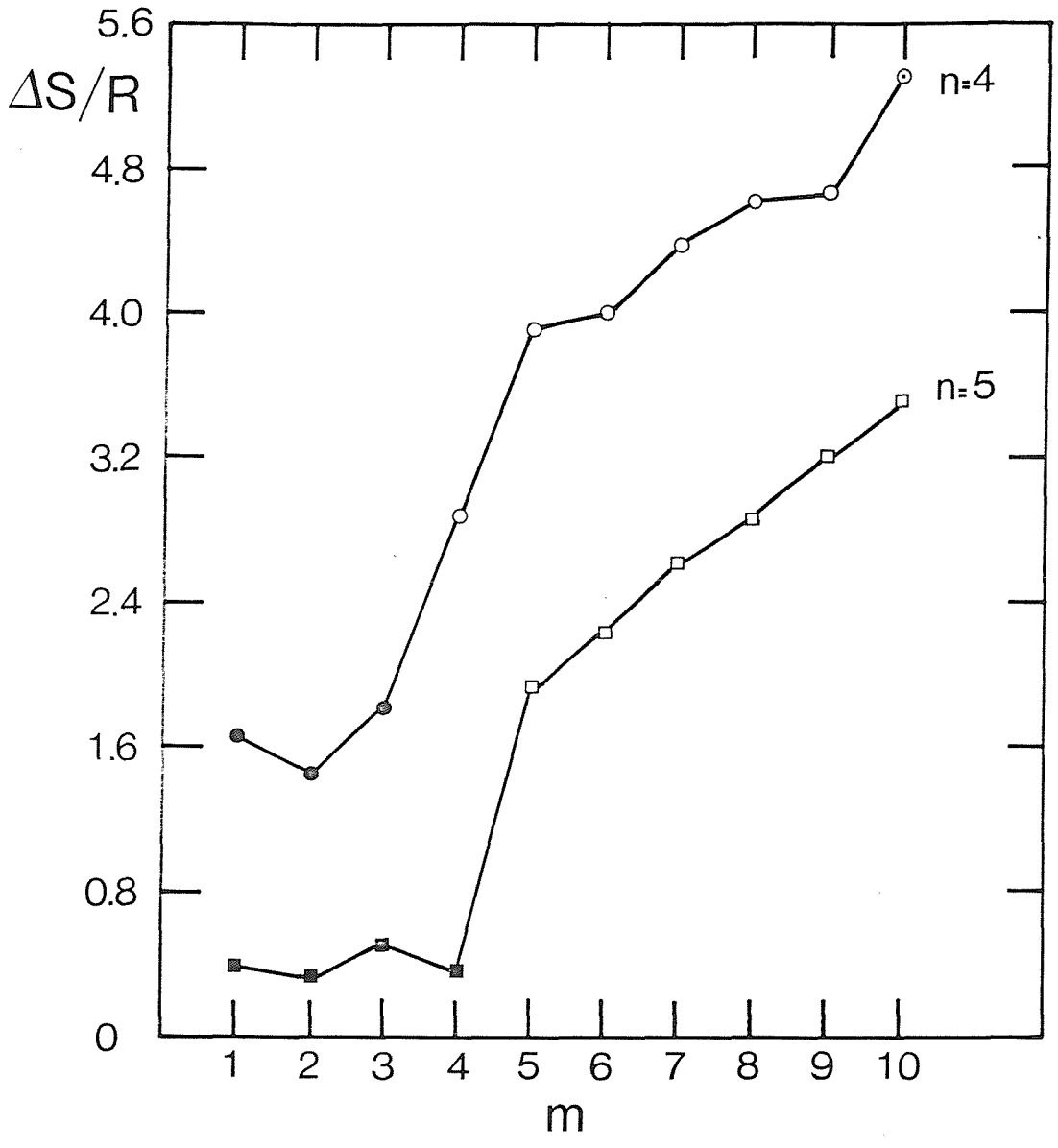

Figure 2.3.16 The dependence of the entropy change associated with the liquid crystal-isotropic transition on the length of the terminal alkyl chains for the m.040.m and m.050.m series. Filled symbols denote nematic-isotropic transitions; open symbols indicate a smectic A-isotropic transitions and ⊙ represents a smectic C-isotropic transition.

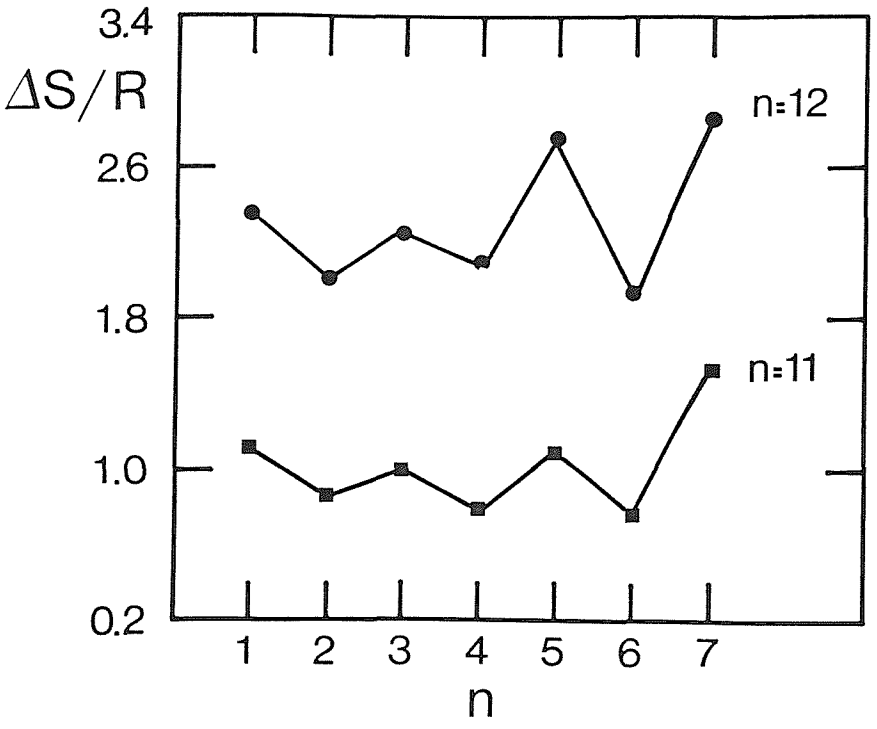

Figure 2.3.17 The dependence of the entropy change associated with the nematic-isotropic transition on m for the m.0110.m and m.0120.m series.

We now consider individual series in which the spacer length, n, is fixed and the terminal chain length, m, is varied, in more detail in order to examine further the influence of the alkyl core upon smectic phase formation. For this purpose we have chosen three series; one with a short spacer, m.030.m, a medium length spacer, m.080.m and finally a long spacer, m.0120.m. Thus, figure 2.3.18 shows the dependence of the transition temperatures on the length of the terminal alkyl chains for the m.030.m series. The early members of the series are purely nematic, at 4.030.4 nematic properties are extinguished leaving the remaining members purely smectic. This increase in smectic properties on increasing the length of terminal chains is to be expected and is a quite general result in monomeric systems [14]. Such behaviour is also observed for the m.080.m series and is illustrated in figure 2.3.18; the first four members are purely nematic, smectic characteristics are first observed for 8.050.8, nematic properties are extinguished at 8.060.8 and the remaining members are purely smectic. Similar behaviour is also seen for the

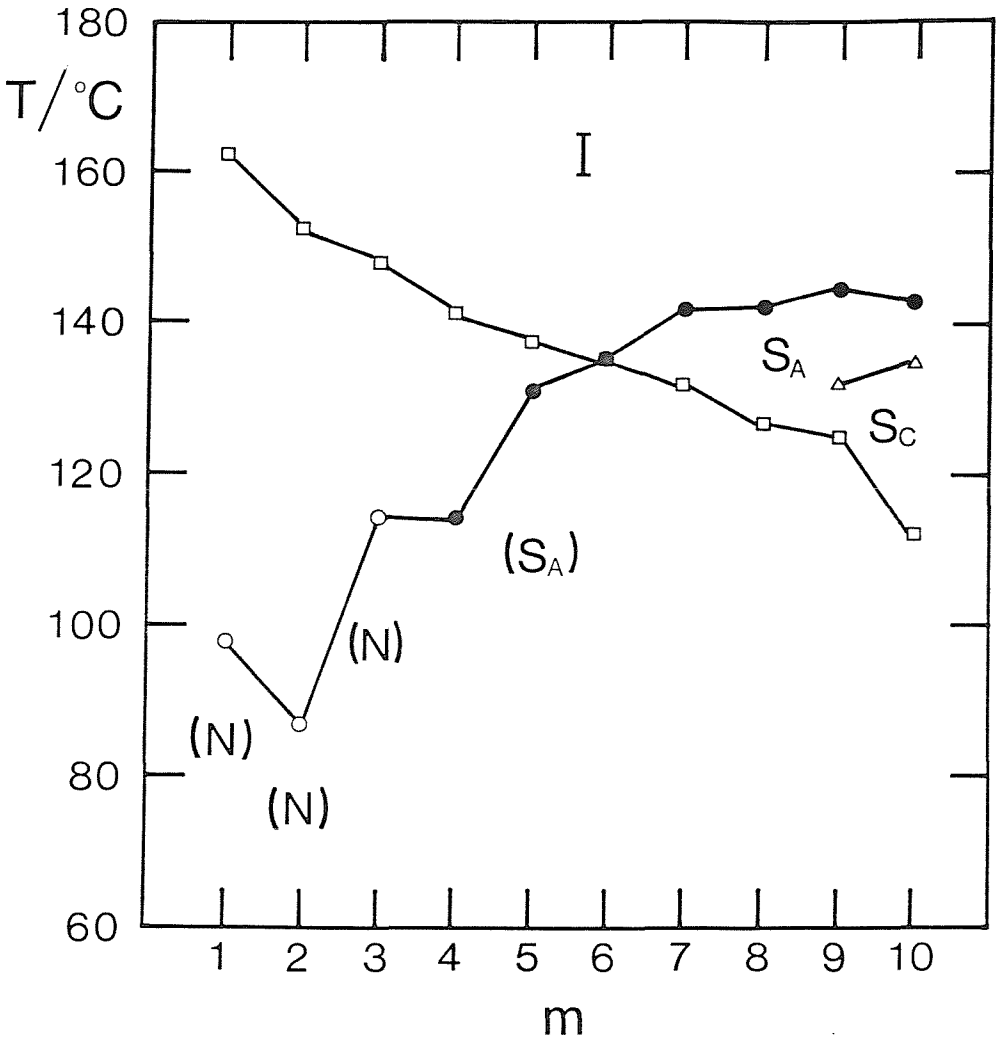

Figure 2.3.18 The dependence of the transition temperatures on the length of the terminal alkyl chains for the m.O3O.m series. The melting point is denoted by □ , o indicates the nematic-isotropic transition, ● the smectic A-isotropic transition and △ the smectic C-smectic A transition. Monotropic phases are marked in parentheses.

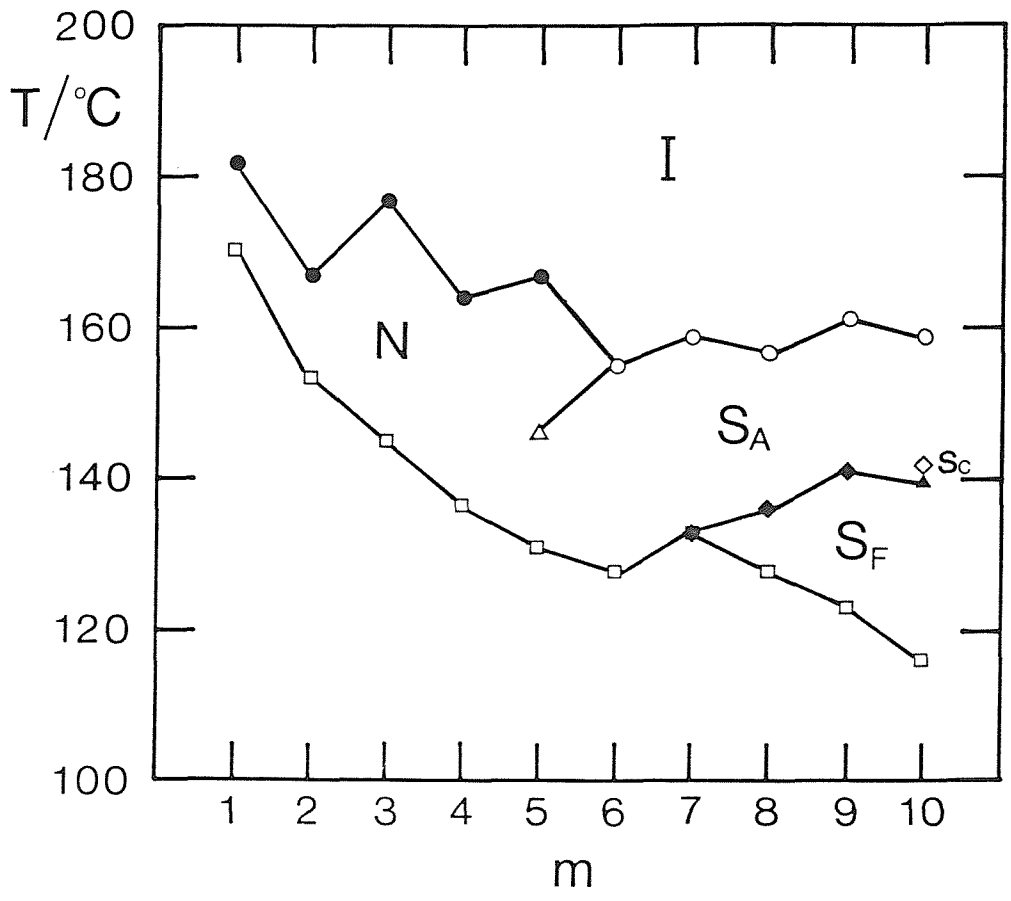

Figure 2.3.19 The dependence of the transition temperatures on the length of the terminal alkyl chains for the m.O8O.m series. The melting point is denoted by □ , ● indicates the nematic-isotropic transition, △ the smectic A-nematic transition, o the smectic A-isotropic transition, ◆ the smectic F-smectic A transition, ▲ the smectic F-smectic C transition and ◇ the smectic C-smectic A transition.

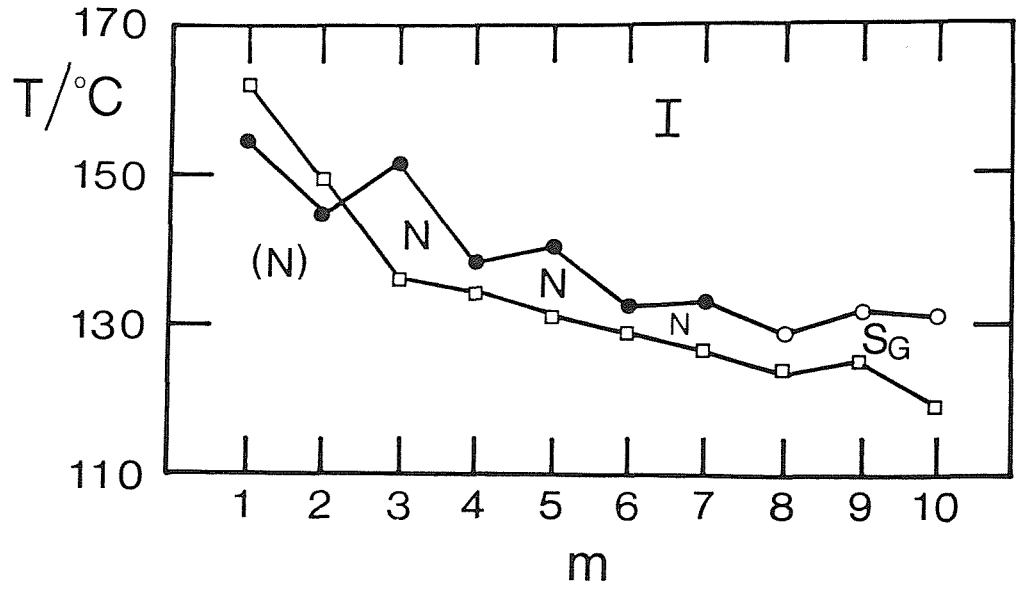

Figure 2.3.20 The dependence of the transition temperatures on the length of the terminal alkyl chains for the m.O12O.m series. The melting point is denoted by □ , ● indicates the nematic-isotropic transition and ○ the smectic G-isotropic transition. Monotropic phases are marked in parentheses.

m.O12O.m series and is shown in figure 2.3.20; the first seven members of this series are purely nematic and the remaining purely smectic. A relationship between the ratio of lengths of the terminal chains to that of the spacer has started to appear; namely, if a dimer is to exhibit smectic properties then the terminal chain length must be greater than half the spacer length. Although this rule has only been shown to be true for a limited number of compounds, it has been tested by the characterisation of over one hundred and forty members of the m.OnO.m family [7] and an exception to it has yet to be found. This observation can be rationalised simplistically in either energetic or entropic terms. If we assume that the mean of the rigid unit-rigid unit and chain-chain interactions is greater than the mixed interaction then, for terminal chain lengths greater than half of the spacer length, the molecular arrangement must be lamellar to conserve the more favourable Schiff's base-Schiff's base interactions. This is sketched in figure 2.3.21(a). If, however, the terminal chain length is much less than that of the spacer, the molecular arrangement is no

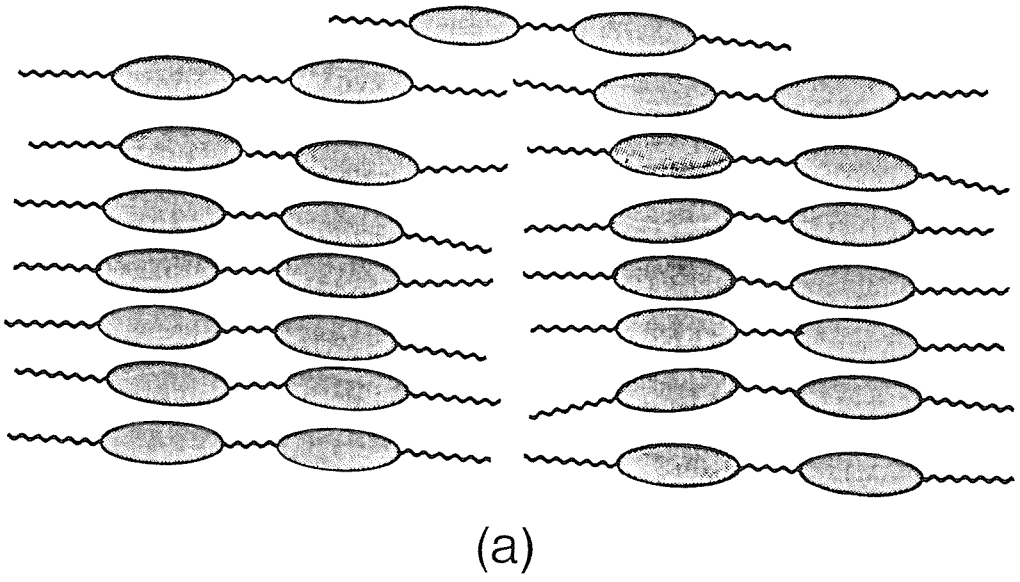

(a)

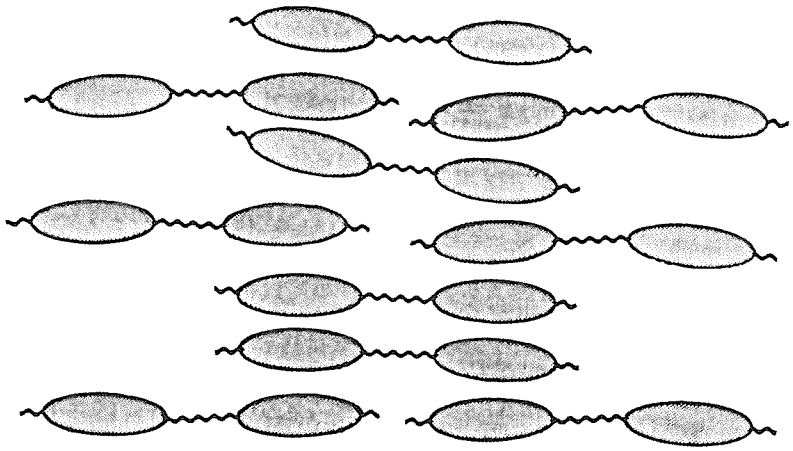

(b)

Figure 2.3.21 A diagrammatic representation of intermolecular packing for m.OnO.m compounds in which (a) m > n and (b) m < n.

longer required to be lamellar for the conservation of the energetically favoured rigid unit-rigid unit interactions; this is shown in figure 2.3.21(b). Alternatively, if we consider that for a given terminal chain length smectic properties diminish with increasing spacer length then it would appear that increasing the length of the flexible alkyl core serves merely to increase core-core interactions so diluting the influence of the smectic promoting terminal chains. This effect of increasing core size diminishing smectic tendencies is well documented in monomeric materials [15]. There appears, however, to be an inconsistency in this argument. If we consider that the core is not composed of three independent segments but rather is a single entity and that increasing the core size promotes nematic behaviour as a result of increasing core-core interactions, is it not, also, reasonable to assume that transition temperatures should also increase rather than decrease? This is readily explained by remembering that this simple explanation has made no allowance for the increase in spacer flexibility which acts to reduce the liquid crystal-isotropic transition temperature.

It is tempting to believe that this simple emperical rule for deciding the nematic/smectic characteristics of a dimeric liquid crystal should hold for all such molecular archetictures but this, of course, would be naive. To illustrate this, table 2.3.7 lists the mesophases formed by the α,ω-bis-[p-(4-alkoxy phenoxycarbonyl)phenoxy]-alkanes;

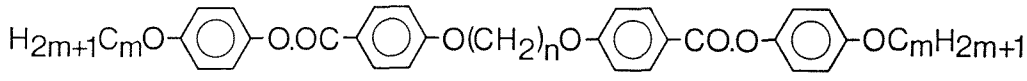

as a function of the length of the flexible spacer, n, and that of the terminal alkoxy chains, m [16]. All these esters either exhibit purely nematic or purely smectic A behaviour. The materials with six methylene units in the spacer behave as would be predicted; for low values of m nematic properties are observed, which are extinguished at m=5 in favour of smectic A behaviour. The compounds with a pentamethylene spacer are all exclusively smectic and again, this is in accord with our observations for the m.OnO.m's. It is, however, the compounds having a decamethylene spacer that exhibit phase behaviour

m	n=5	n=6	n=10
1	A	N	A
2	A	N	A
3	A	N	A
4	A	N	N
5	A	A	N
6	A	A	N
7	A	A	N

Table 2.3.7 The phase behaviour of the α,ω-bis-[p-(4-alkoxyphenoxycarbonyl)phenoxy]-alkanes; N denotes nematic and A smectic A [16].

that is hard to understand. For short terminal chain lengths, the materials are smectic but on increasing m nematic properties appear. Such behaviour opposes the very general observation that smectic properties increase with increasing terminal chain length [14]. The authors offer no explanation for this unusual trend [16]. The entropy changes associated with the liquid crystal-isotropic transition for these dimeric esters are given in table 2.3.8 and a comparison of these with the values for the analogous m.OnO.m compounds, presented in table 2.3.9 reveals several fundamental differences:

(1) the entropies of the esters show little variation on varying m whereas those of the m.OnO.m's show a definite dependence on m. This implies that the change in the conformational distribution of the terminal alkyl chains at the liquid crystal-isotropic transition makes a significant contribution to $\Delta S/R$ for the m.OnO.m's but not for the esters. Alternatively, increasing the terminal chain length increases the orientational ordering of the molecules for the m.OnO.m's but not for the esters.

m	n=5	n=6	n=10
1	1.1 (A)	1.3 (N)	1.6 (A)
2	1.2 (A)	1.4 (N)	1.7 (A)
3	1.1 (A)	1.2 (N)	1.4 (A)
4	1.2 (A)	1.4 (N)	1.7 (N)
5	1.0 (A)	1.2 (A)	1.3 (N)
6	1.1 (A)	1.3 (A)	1.6 (N)
7	0.9 (A)	1.2 (A)	1.3 (N)

Table 2.3.8 The entropy change, $\Delta S/R$, associated with the liquid crystal-isotropic transition for the α,ω-bis-[p-(4-alkoxy-phenoxycarbonyl)phenoxy]-alkanes [16]; N denotes a nematic-isotropic transition and A indicates a smectic A-isotropic transition.

m	n=5	n=6	n=10
2	0.32 (N)	1.52 (N)	1.89 (N)
3	0.50 (N)	1.82 (N)	2.18 (N)
4	0.37 (N)	1.78 (N)	2.04 (N)
5	1.47 (A)	2.42 (N)	2.72 (N)
6	2.21 (A)	3.81 (A)	2.28 (N)
7	2.62 (A)	4.63 (A)	2.50 (N)
8	2.85 (A)	4.77 (A)	5.25 (A)

Table 2.3.9 The entropy change, $\Delta S/R$, associated with the liquid crystal-isotropic transition for the m.OnO.m's; N denotes a nematic-isotropic transition and A indicates a smectic A-isotropic transition.

(2) The differences in $\Delta S/R$ between odd and even length spacers are large for the m.OnO.m's but very small for the esters. This suggests that the change in the conformational distribution of the spacer at the liquid crystal-isotropic transition is very similar for odd and even membered spacers in the esters but very different in the m.OnO.m's. Alternatively, the orientational ordering at the transition is very similar for even and odd length spacers in the esters but very different in the m.OnO.m's.

(3) For the esters $\Delta S/R$ is of similar magnitude for both nematic-isotropic and smectic A-isotropic transitions whereas for the m.OnO.m's, the smectic-isotropic transition for any given n is much larger than a nematic-isotropic transition in the same series. This implies that the orientational ordering in the two phases is similar for the esters and very different for the m.OnO.m's.

(4) The esters with a decamethylene spacer always possess the highest $\Delta S/R$ for a given m irrespective of whether a nematic-isotropic transition is being compared to a smectic-isotropic transition. For the m.OnO.m's this is true providing only like transitions are compared.

These differences coupled with the inversion of smectic/nematic behaviour in the esters with a decamethylene spacer are indeed difficult to understand. It appears likely, however, that the phase identification is in error for the diesters containing a decamethylene spacer and instead the nematic phase is actually a smectic C. The low values of the entropy changes are puzzling and the synthesis and characterisation of a greater number of the dimeric esters may clarify the situation.

Finally, it is interesting to note that increasing the length of the spacer in a semi-rigid main-chain polymer promotes smectic behaviour [17] whereas the reverse is true for the m.OnO.m compounds for which short spacers promote smectic tendencies. The relevance of this is not clear.

2.4 Conclusions

The primary aim of this Chapter has been fulfilled in that we have prepared and characterised several series of the m.OnO.m's, a new family of thermotropic mesogens and the first dimeric liquid crystals to exhibit extensive smectic polymorphism. These series are, therefore, valuable for physical studies of the structures of smectic phases and also, of phase transitions. The transitional properties of these dimers are found to depend strongly on the length and parity of the alkyl spacer. Furthermore, the smectic tendencies of any given m.OnO.m is critically dependent on the ratio of the length of the alkyl spacer, n, to that of the terminal chains, m. If n is larger than m then no smectic properties are observed but as m increases smectic phases appear and nematic properties are eventually extinguished. We have rationalised this observation by either considering the core to be three individual segments, two mesogenic moieties linked via a flexible spacer, or as one large semi- rigid core. Further speculation awaits the results of model calculations which allow for the flexible nature of the alkyl core as well as deuterium N.M.R. experiments using dimers having deuteriated spacers.

2.5 References

[1] Griffin, A.C., and Britt, T.R., 1981, J. Am. Chem. Soc., 103, 4957.

[2] Vorlander, D., 1927, Z. Phys. Chem., 126, 449.

[3] See, for example, Emsley, J.W., Luckhurst, G.R., Shilstone, G.N., and Sage, I., 1984, Mol. Cryst. Liq. Cryst. Letts, 102, 223.

[4] Smith, G.W., Gardlund, Z., and Curtis, R.J., 1973, Mol. Cryst. Liq. Cryst., 19, 327.

[5] Smith, G.W., and Gardlund, Z., 1973, J. Chem. Phys., 59, 3214.

[6] See, for example, Goodby, J.W., Gray, G.W., Leadbetter, A.J., and Mazid, M.A., 1980, Liquid Crystals of One- and Two-Dimensional Order, Springer Series in Chem. Phys. 11, edited by W. Helfrich and G. Heppke, Springer-Verlag.

[7] Date, R.W., unpublished results.

[8] Jin, J.I., and Park, J.H., 1984, Mol. Cryst. Liq. Cryst., 110, 293.

[9] Donahoe, H.B., Benjamin, L.E., Fennoy, L.V., and Greiff, D., 1960, J. Org. Chem., 26, 474.

[10] Keller, P., and Liebert, L., 1978, Solid State Phys. Suppl., 14, 19.

[11] Jin, J.I., 1983, Polymer Preprints (Japan), 32, 935.

[12] Wiegeleben, A., Richter, L., Deresch, J., and Demus, D., 1980, Mol. Cryst. Liq. Cryst., 59, 329.

[13] Gray, G.W., and Goodby, J.W., 1984, Smectic Liquid Crystals-Textures and Structures, Leonard Hill.

[14] Gray, G.W., 1979, The Molecular Physics of Liquid Crystals, edited by G.R. Luckhurst and G.W. Gray, Academic Press, Chap. 12.

[15] Gray, G.W., in [14], Chap. 1.

[16] Jin, J.I., Oh, H.T., and Park, J.H., 1986, J. Chem. Soc. Perkin Trans. 2, 343.

[17] Finkelmann, H, 1987, Thermotropic Liquid Crystals, edited by G.W. Gray, Wiley, Chap. 6.

CHAPTER 3 ASYMMETRIC DIMERIC LIQUID CRYSTALS; THE PREPARATION AND PROPERTIES OF THE α-(4-CYANOBIPHENYL-4'-OXY)-ω-(4-ALKYLANILINEBENZYLIDENE-4'-OXY)ALKANES

3.1 Introduction

The study of solutes dissolved in liquid crystal solvents is actively pursued in both academic and industrial environments. Commercially such research is of great importance because, for example, dye coloured displays incorporate pleochroic dyes dissolved in a liquid crystal solvent and the contrast ratio of such devices depends on the orientational ordering of the dye molecule. Fundamentally, the study of solutes in liquid crystal solvents provides a means of testing the validity of quantitative molecular theories because the solute can be chosen to be rigid and symmetric thus approaching the type of particle for which theoretical calculations are possible. Despite such intensive research, however, the interactions that result in the ordering of the solute molecule are still poorly understood. Many ordering mechanisms have been postulated including interactions with the liquid crystal through dispersion forces [1,2] and steric factors [3] but these do not fully explain experimental observations; for example, the negative order parameters observed for molecular hydrogen [4]. In this particular case, the important ordering mechanism was shown to be the interaction of the solute's molecular quadrupole moment with the mean electric field gradient present in the liquid crystal environment [5]. The average electric field gradient in a liquid crystal can either be positive or negative and thus, it is reasonable to assume that by mixing appropriate mesogens one could obtain a mixture for which the average electric field gradient was zero. This has been demonstrated by Barker et al [5] for a mixture of Merck ZLI 1132 and EBBA containing 55 weight percent of ZLI 1132; in this mixture the ordering of molecular hydrogen falls to approximately 10% of that observed in either of the two component liquid crystals. This suggests the interaction between the molecular quadrupole moment and the mean external field gradient may be the dominant ordering mechanism but it is not solely responsible for the ordering of molecular hydrogen in liquid crystals. It should be noted that the

shape anisotropy of molecular hydrogen is very small and thus, steric considerations are not expected to be important. In order to test the importance of this ordering mechanism involving the molecular quadrupole moment for larger solutes, Sachdev [6] investigated the orientational ordering of para-xylene in two equimolar mixtures, ZLI 1132 and EBBA, and PCH7 and EBBA. The experiments clearly showed that the quadrupole moment-electric field gradient interaction is not a dominant mechanism in the ordering of para-xylene and this is probably because steric factors are much more important since the shape anisotropy of para-xylene is far greater than that of molecular hydrogen. The experiments did, however, reveal some curious behaviour. In particular, the values of $(S_{XX} - S_{YY})$ for the solute were the average of those measured in the single components whereas S_{ZZ} measured in the mixture lies below those recorded in the individual liquid crystals.

This work prompted the question what solvent properties would be possessed by a dimeric liquid crystal comprised of two monomers having electric field gradients of opposing sign. This molecular architecture is a novel design concept so we decided to prepare several closely related homologous series of such molecules in order to elucidate structure - property relationships and to study solute ordering in these dimers. To distinguish this new class of mesogen from conventional dimers possessing two identical mesogenic groups we have termed them asymmetric dimers and describe the conventional dimer as being symmetric. The synthetic problem, therefore, was to design a molecule in which different mesogenic moieties are linked through an alkyl spacer. We chose to prepare the α-(4-cyanobiphenyl-4'-oxy)-ω-(4-alkylanilinebenzylidene-4'-oxy)alkanes :

This particular series was chosen for several reasons. First, the corresponding symmetric dimers, the α,ω-bis(4-cyanobiphenyl-4'-oxy)alkanes (BCBO-n) [7]:

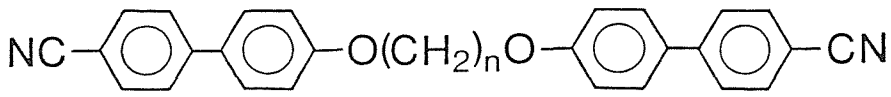

and the α,ω-bis(4-alkylanilinebenzylidene-4'-oxy)alkanes (m.OnO.m) [8]:

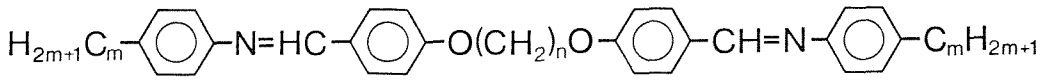

have been prepared and certain of their properties determined. Secondly, the analogous monomeric species, the 4-n-alkoxy-4'-cyanobiphenyls (nOCB):

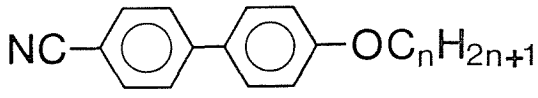

and the N-(4-n-alkoxybenzylidene)-4'-n-alkylanilines (nO.m):

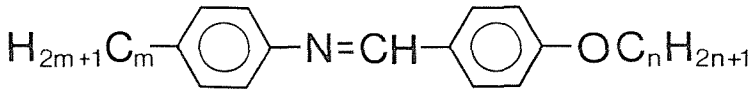

have also been thoroughly investigated. Thirdly, the properties of these monomers are known to be qualitatively different [5,9] and their binary mixtures exhibit unusual phase behaviour [10,11,12]. Finally, it is easy to vary the length of both the flexible spacer and the terminal chain independently although the synthetic route used limited the values of n to 3, 4, 5 or 6. This restriction arises simply because only a limited number of α-chloro-ω-iodoalkanes are available commercially.

The mnemonic used for this family of asymmetric dimers is CB.OnO.m so that, for example, CB.O6O.4 simply and unambiguously represents:

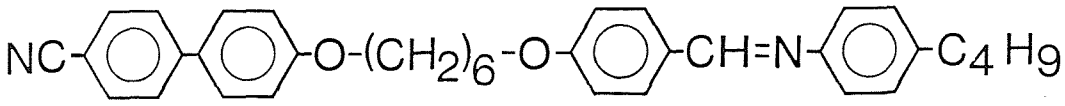

In this chapter the transitional properties of four series of CB.OnO.m's are presented and we compare these to those of the corresponding symmetric dimers, and equimolar mixtures of them, as well as equimolar mixtures of the analogous monomeric compounds.

3.2 Experimental

The synthetic route for the preparation of the CB.OnO.m's essentially involves three steps:

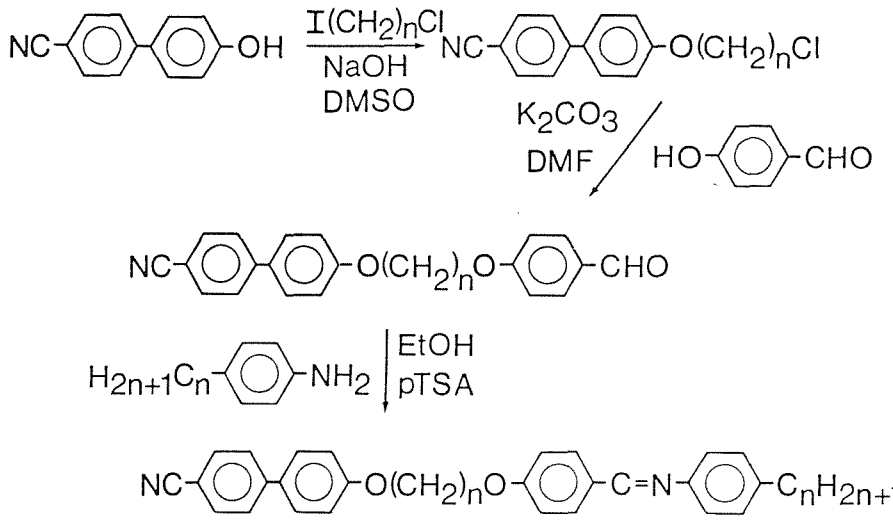

The reactions yielding the α-chloro-ω-(4-cyanobiphenyl-4'-oxy)alkanes and the α-(4-cyanobiphenyl-4'-oxy)-ω-(4-formylphenyl-4'-oxy)alkanes are described fully in Chapter 5.

4-n-alkylanilines

The 4-n-alkylanilines available commercially were distilled prior to use and the remaining were prepared using standard procedures [13] outlined in Chapter 2.

α-(4-cyanobiphenyl-4'-oxy)-ω-(4-alkylanilinebenzylidene-4'-oxy)alkanes

A 4-n-alkylaniline (2.75 mmol) was added to a stirred solution of an α-(4-cyanobiphenyl-4'-oxy)-ω-(4-formylphenyl-4'-oxy)alkane (2.5 mmol) and a few crystals of p-toluenesulphonic acid in hot ethanol. The reaction mixture was alllowed to cool and stirred at room temperature for three hours. The resulting white precipitate was filtered off,

washed with cold ethanol and dried. Compounds possessing an even number of carbon atoms in their spacer were recrystallised from ethyl acetate with the sole exception of CB.040.1 which required toluene. The CB.030.m and CB.050.m series were recrystallised from ethyl acetate with the exception of those possessing a long terminal chain (m=7,8,9 or 10) which were recrystallised from absolute ethanol. All the compounds were recrystallised at least twice. The poorer solubility of compounds having an even membered spacer presumably reflects their higher transition temperatures as compared with compounds having an odd membered spacer. The yields of all these reactions were in the range 70% to 80%. The structural characterisation of the final products was performed using ^{1}H-N.M.R. and I.R. spectroscopy.

Spectra

CB.050.4;

^{1}H-N.M.R.; δ ($CDCl_3$) 0.9 (t,3H), 1.4-2.1 (m,10H), 2.6 (t,2H), 4.0 (t,4H), 6.7-7.9 (m,16H), 8.3 (s,1H) ppm;

I.R.; ν 1620, 2220 cm^{-1}.

Thermal characterisation of the CB.OnO.m's

The thermal properties of the CB.OnO.m's were characterised using a Perkin-Elmer DSC-2C differential scanning calorimeter in conjunction with a Nikon polarising microscope equipped with a Linkam hot-stage. Selected examples of the smectic phases were studied further by X-ray diffraction with a Guinier camera fitted with a bent quartz monochromator (R. Huber, F.R. Germany) using $CuK_{\alpha 1}$ radiation (λ=0.15405nm).

3.3 Results and Discussion

CB.030.m series

The transitional properties of the CB.030.m series are presented in table 3.3.1. All eleven members of this series exhibit liquid-crystalline behaviour although the first five homologues are monotropic. The nematic phases were assigned from their schlieren optical texture combined with the high mobility of the phase which 'flashed' when subjected to mechanical stress. The nematic phase of the heptyl, octyl and nonyl homologues changed on cooling to give regions of homeotropic and focal-conic fan texture and therefore, the lower temperature phase is assigned as a smectic A. On cooling the isotropic liquid of the decyl homologue regions of focal-conic fan and homeotropic texture developed and thus, the phase is assigned as a smectic A. On lowering the temperature of the smectic A phase of the octyl, nonyl and decyl homologues, the regions of focal-conic fan texture became somewhat broken and sanded, while the homeotropic regions produced a schlieren texture. In consequence, this new phase is assigned as a smectic C. The lower temperature phases of the propyl, butyl, pentyl and hexyl homologues have yet to be identified positively. On cooling the nematic phase of these compounds a rather poorly defined focal-conic fan texture developed but rapid crystallisation of the sample prevents further study.

The dependence of the transition temperatures upon the length of the terminal alkyl chain, m, for the CB.030.m series is shown in figure 3.3.1. The nematic-isotropic transition temperature increases markedly on going from CB.030.0 to CB.030.1 although it is not apparent why the addition of a single methyl group should have such a large relative effect on T_{NI}. Subsequent increases in the length of the alkyl chain cause the nematic-isotropic transition temperature to fall with a small alternation between odd and even members of the series in a manner comparable to that observed for conventional monomeric nematics having high transition temperatures [14]. The melting points of this series generally decrease with increasing chain length. The smectic-nematic transition temperatures initially fall before rising as m is

m	C-/°C *C-I/°C	S_C-S_A/°C	S-N/°C *S_A-N/°C	N-I/°C *S_A-I/°C	ΔH_{C-}/kJmol^{-1} ΔH_{S-N}/kJmol^{-1}	ΔH_{N-I}/kJmol^{-1} *ΔH_{S_A-I}/kJmol^{-1}	ΔS_{C-}/R	ΔS_{S-N}/R	ΔS_{N-I}/R *ΔS_{S_A-I}/R
0	*145	-	-	(60.5)	44.9 -	-	13.0	-	-
1	*155.5	-	-	(140)	51.4 -	0.81	14.5	-	0.24
2	*144.5	-	-	(128)	45.0 -	0.66	13.0	-	0.20
3	*143	-	(57)	131	35.3 0.24	0.68	10.2	0.09	0.20
4	120	-	(54.5)	119.5	36.0 -	0.59	11.0	-	0.18
5	117	-	(53)	124	36.7 0.04	0.90	11.3	0.01	0.27
6	111.5	-	(45)	114.5	35.5 -	0.70	11.1	-	0.22
7	106.5	-	*(59)	116	40.5 0.21	0.87	12.9	0.08	0.27
8	91	(70)	*(89.5)	113.5	31.7 -	0.65	10.5	-	0.20
9	96.5	(79)	*107.5	114	34.0 0.38	0.89	11.1	0.12	0.28
10	94	(85.5)	-	*113	36.3 -	*2.83	11.9	-	*0.88

Table 3.3.1 The transition temperatures, enthalpies and entropies of transition for the CB.030.m series; () denotes a monotropic transition. The uncertainties in the temperatures are ±1 °C and in the thermodynamic data are ±10%.

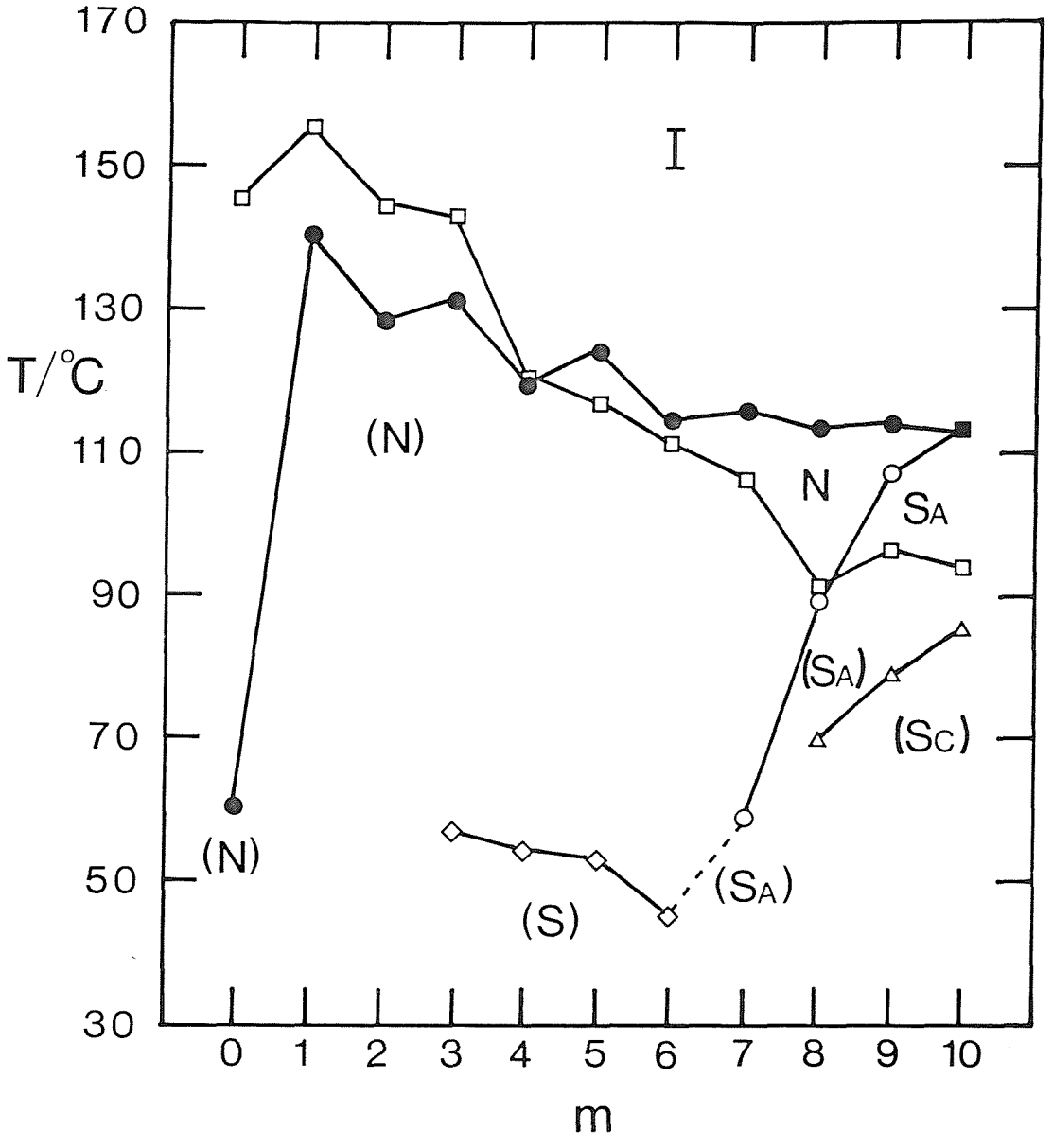

Figure 3.3.1 The dependence of the transition temperatures on the length of the terminal alkyl chain for the CB.O3O.m series. The melting point is denoted by □ , ● indicates the nematic-isotropic transition, ■ the smectic A-isotropic transition, O the smectic A-nematic transition, △ the smectic C-smectic A transition and ◇ the smectic-nematic transition. Monotropic phases are marked in parentheses.

increased although it should be noted that differences between T_{SN} for the propyl, butyl and pentyl homologues are small.

CB.040.m series

The transitional properties of the CB.040.m series are listed in table 3.3.2; all eleven homologues are enantiotropic mesogens. The phase assignments were made using identical arguments to those described for the CB.030.m series. Figure 3.3.2 shows the dependence of the transition temperatures upon the length of the terminal alkyl chain, m, for the CB.040.m series. The nematic-isotropic transition temperatures behave very similarly to those of the CB.030.m series. The smectic A-nematic transition temperatures show a very unusual dependence on the length of the terminal alkyl chain. For conventional monomers the smectic A-nematic transition temperature simply increases with increasing chain length [14]. This increase is observed for the first three members of the series but on going from CB.040.2 to CB.040.3 there is a dramatic decrease in T_{S_AN} and a further drop in T_{S_AN} is found on passing to CB.040.4. This decrease presumably continues for no smectic phases are observed for CB.040.5, CB.040.6, and CB.040.7 although their nematic phases may be supercooled to temperatures in the region of 80 °C. The smectic A phase then reappears dramatically with the octyl homologue and the thermal stability of the smectic A phase increases for the last three homlogues. Indeed, the decyl homologue actually exhibits a smectic A-isotropic transition. This unusual dependence of the smectic A-nematic transition temperatures on the length of the terminal alkyl chain is to our knowledge unique to these compounds and we will attempt to rationalise it later. It should be noted that the smectic B-nematic transition temperatures of the CCH-n compounds [15] also decrease with increasing chain length for early members of the series but it is not known whether smectic properties subsequently reemerge at longer chain lengths.

m	C-/°C	S_C-S_A/°C	S_A-N/°C	N-I/°C *S_A-I/°C	ΔH_{C-}/kJmol^{-1}	ΔH_{N-I}/kJmol^{-1} *ΔH_{S_A-I}/kJmol^{-1}	ΔS_{C-}/R	ΔS_{N-I}/R *ΔS_{S_A-I}/R
0	178.5	-	(131)	197.5	44.1	6.59	11.8	1.69
1	191	-	(134)	245.5	39.3	7.69	10.2	1.78
2	172.5	-	(136.5)	234	37.4	7.13	10.1	1.69
3	150.5	-	(106)	234.5	34.7	7.75	9.86	1.84
4	149	-	(99)	224.5	38.0	6.95	10.8	1.68
5	126.5	-	-	222	37.6	7.54	11.3	1.83
6	116.5	-	-	214.5	25.5	6.72	7.89	1.66
7	120	-	-	212	23.9	7.29	7.32	1.81
8	121	-	(118)	205	27.3	6.63	10.4	1.67
9	125	(115)	168.5	203.5	29.9	7.46	9.04	1.88
10	110	133	-	*197	57.8	*9.98	18.2	*2.56

Table 3.3.2 The transition temperatures, enthalpies and entropies of transition for the CB.040.m series; () denotes a monotropic transition. The uncertainties in the temperatures are ±1°C and in the thermodynamic data are ±10%.

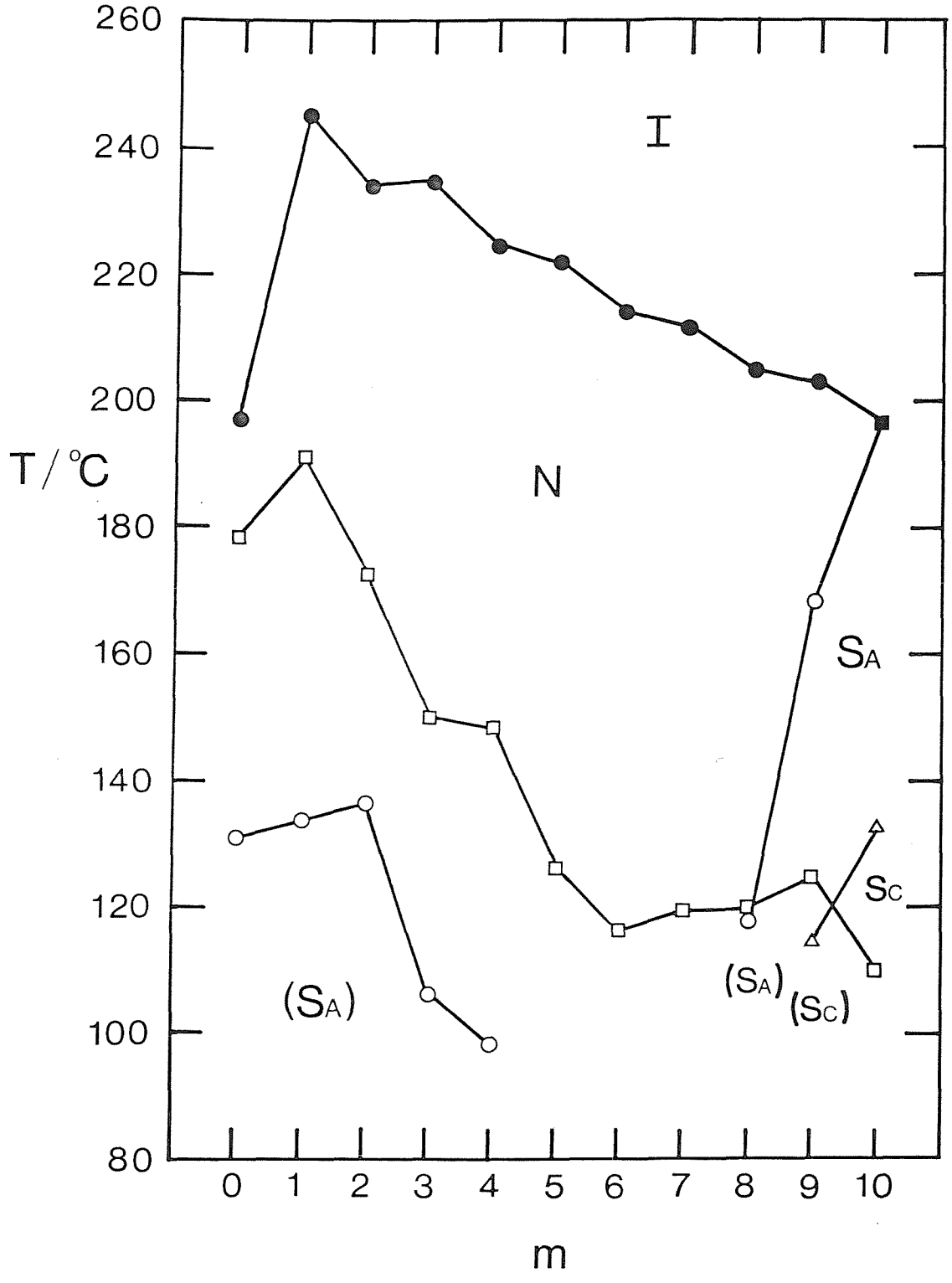

Figure 3.3.2 The dependence of the transition temperatures on the length of the terminal alkyl chain for the CB.040.m series. The melting point is denoted by □ , ● indicates the nematic-isotropic transtion, ■ the smectic A-isotropic transition, ○ the smectic A-nematic transition and △ the smectic-smectic transition. Monotropic phases are marked in parentheses.

CB.050.m series

The transitional properties for the CB.050.m series are listed in table 3.3.3; all eleven homologues are enantiotropic mesogens with the single exception of CB.050.0 which is monotropic. Again, the phase assignments were performed using the arguments offered for the CB.030.m series including the comments concerning the monotropic smectic phase that has yet to be identified. Figure 3.3.3 shows the dependence of the transition temperatures on the length of the terminal alkyl chain, m, for the CB.050.m series and the nematic-isotropic transition temperatures clearly behave very similarly to those of the CB.030.m and CB.040.m series. Again, the thermal stability of the smectic phase on increasing m is unusual because it decreases essentially without alternation from CB.050.1 to CB.050.8 and then rises for the nonyl and decyl homologues. The dependence of the smectic-nematic transition temperature upon m is much less dramatic for the CB.050.m series than it is for the CB.040.m series and this will be discussed later.

m	C-/°C *C-I/°C	S_C-S_A/°C	S-N/°C *S_A-N/°C	N-I/°C	ΔH_{C-}/kJmol^{-1} ΔH_{S-N}/kJmol^{-1}		ΔH_{N-I}/kJmol^{-1}	ΔS_{C-}/R	ΔS_{S-N}/R	ΔS_{N-I}/R
0	*128.5	-	-	(118.5)	33.4	-	1.23	10.0	-	0.38
1	115.5	-	(85.5)	168	32.4	-	1.70	10.0	-	0.46
2	107.5	-	(81.5)	163	34.3	-	1.70	10.9	-	0.47
3	107	-	(80)	164	34.4	-	1.94	10.9	-	0.53
4	99	-	(72.5)	154.5	30.8	-	1.57	9.96	-	0.44
5	102	-	(74)	155	31.5	-	1.89	10.1	-	0.53
6	99	-	(66.5)	146.5	32.7	-	1.64	10.6	-	0.47
7	106.5	-	(65.5)	143	39.6	-	1.74	12.6	-	0.50
8	103	-	(64)	137.5	35.0	-	1.54	11.2	-	0.45
9	103	-	(69.5)	139.5	36.6	0.14	1.90	11.7	0.05	0.55
10	101	(86.5)	*103	135.5	35.6	-	1.80	11.5	-	0.53

Table 3.3.3 The transition temperatures, enthalpies and entropies of transition for the CB.O5O.m series; () denotes a monotropic transition. The uncertainties in the temperatures are ±1°C and in the thermodynamic data are ±10%.

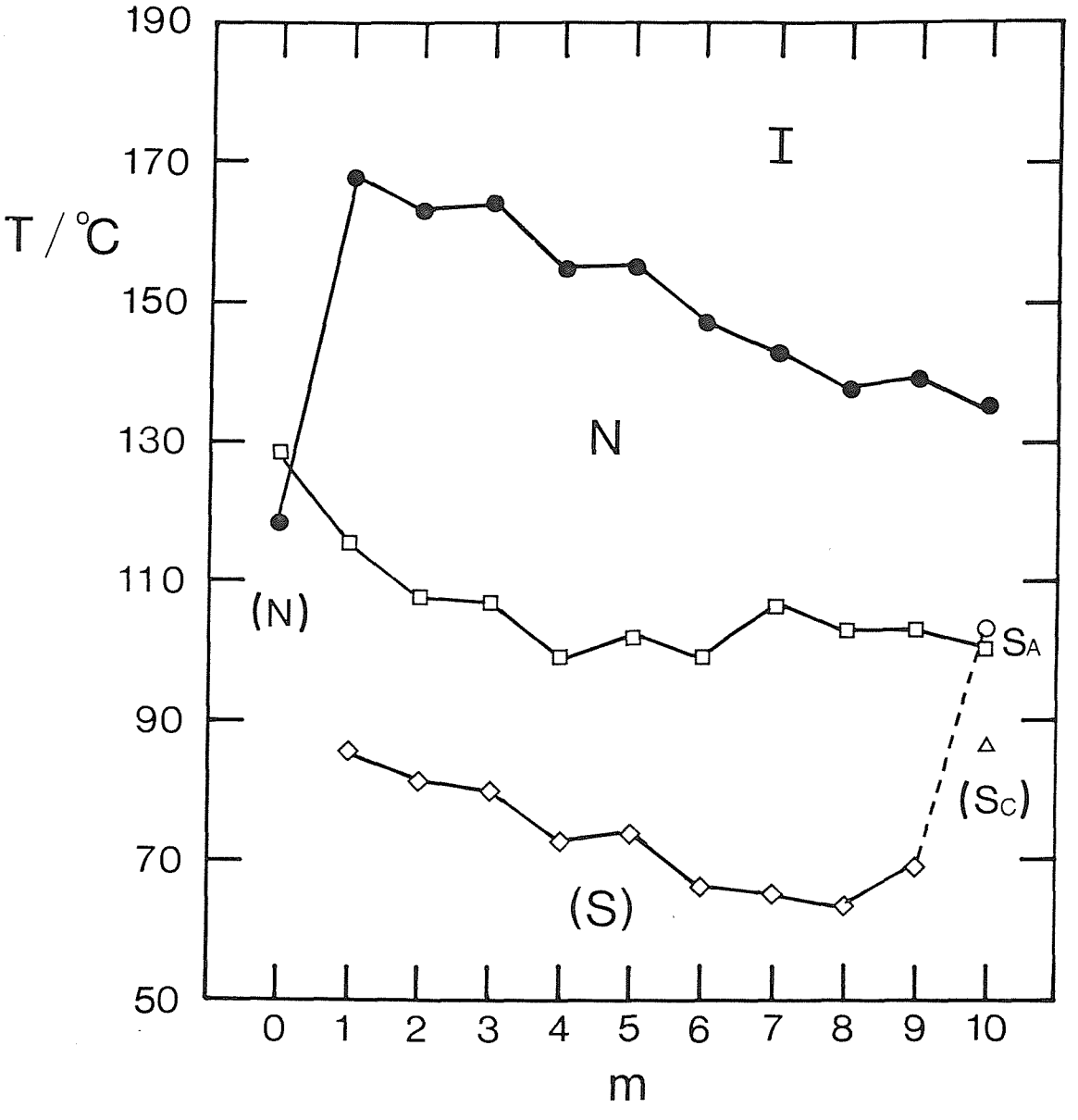

Figure 3.3.3 The dependence of the transition temperatures on the length of the terminal alkyl chain for the CB.O5O.m series. The melting point is denoted by □ , ● indicates the nematic-isotropic transition, ◇ the smectic-nematic transition, O the smectic A-nematic transition and △ the smectic C-smectic A transition. Monotropic phases are marked in parentheses.

CB.O6O.m series

The transitional properties of the CB.O6O.m series are given in table 3.3.4 and all eleven members are enantiotropic mesogens. The phase assignments were performed using the arguments detailed for the CB.O3O.m series. The lower temperature smectic phases of CB.O6O.3 and CB.O6O.5 have yet to be identified. On cooling the smectic A phase of CB.O6O.3, the focal-conic fans become crossed by lines that are not transitory in nature and large poorly defined platelets develop from the homeotropic regions; this suggests that the phase may be a smectic G. The lower temperature smectic phase of CB.O6O.5 displays similar textures but is harder to study for crystallisation occurs rapidly after the phase is formed.

Figure 3.3.4 shows the dependence of the transition temperatures on the length of the terminal alkyl chain for the CB.O6O.m series. The dependence of the nematic-isotropic transition temperatures upon m is very similar to that observed for the other three series. The smectic A-nematic transition temperatures again show a very unusual dependence on the length of the terminal alkyl chain. The value of T_{S_AN} increases for the first three members of the series but then is found to fall quite rapidly for the next four members. The rapid decrease presumably continues for no smectic phases are observed for the heptyl, octyl or nonyl homologues although their nematic phases may be supercooled to approximately 80 °C. The smectic A phase then reappears dramatically with CB.O6O.10 and this actually has the highest smectic A-nematic transition temperature of the CB.O6O.m series. We attempt to rationalise this novel behaviour later.

m	*S_C-S_A/°C		S_A-N/°C	N-I/°C	ΔH_{C-}/kJmol^{-1}	ΔH_{S_A-N}/kJmol^{-1}	ΔH_{N-I}/kJmol^{-1}	ΔS_{C-}/R	ΔS_{S-N}/R	ΔS_{N-I}/R
	C- /°C	S-S_A/°C								
0	161	-	(133)	174	31.5	-	7.00	8.73	-	1.88
1	151	-	(147.5)	216.5	32.5	1.05	7.35	9.25	0.30	1.81
2	142	-	152	207	20.5	1.26	6.59	5.94	0.36	1.65
3	106	(105)	140	210	29.7	0.53	7.58	9.43	0.15	1.89
4	111	-	142	202	31.0	1.02	6.70	9.70	0.30	1.70
5	113	(87)	(111.5)	199.5	33.4	-	7.70	10.4	-	1.96
6	115.5	-	(95)	192	36.1	-	7.09	11.2	-	1.84
7	116.5	-	-	189	36.6	-	7.66	11.3	-	2.00
8	119	-	-	184	32.2	-	6.84	9.90	-	1.80
9	118	-	-	181	35.0	-	7.92	10.8	-	2.10
10	119	*(103)	154.4	177	41.5	-	7.29	12.8	-	1.95

Table 3.3.4 The transition temperatures, enthalpies and entropies of transition for the CB.060.m series; () denotes a monotropic transition. The uncertainties in the temperatures are ±1°C and in the thermodynamic data are ±10%.

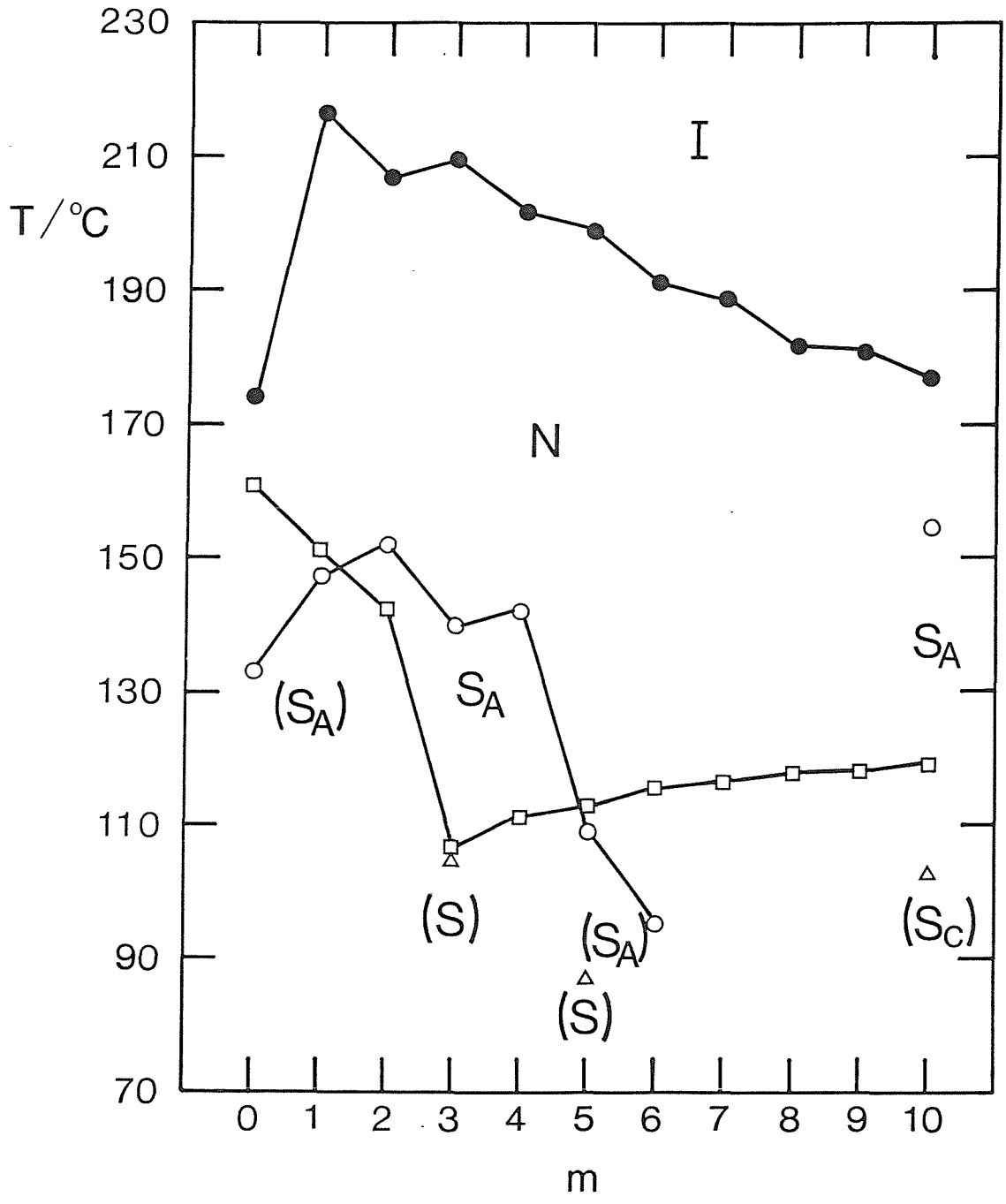

Figure 3.3.4 The dependence of the transition temperatures on the length of the terminal alkyl chain for the CB.O6O.m series. The melting point is denoted by □ , ● indicates the nematic-isotropic transition, O the smectic A-nematic transition, and △ the smectic-smectic transition. Monotropic phases are marked in parentheses.

Figure 3.3.5 compares the dependence of the liquid crystal-isotropic transition temperature on the length of the terminal alkyl chain for the four CB.OnO.m series. The four curves show no intersections, quite unlike the behaviour of the m.OnO.m's described in Chapter 2 and for any given value of m, CB.O4O.m has a higher transition temperature than CB.O6O.m which in turn has a higher T_{NI} than CB.O5O.m, with CB.O3O.m always possessing the lowest clearing temperature.

The dependence of the entropy change associated with the liquid crystal-isotropic transition upon the length of the terminal alkyl chain, m, is shown in figure 3.3.6 for all four series of CB.OnO.m compounds. The entropy change at the nematic-isotropic transition exhibits a small alternation on increasing m in all four series. This alternation is larger for the CB.O4O.m and CB.O6O.m series than it is for the CB.O3O.m and CB.O5O.m series and this is probably related to higher orientational order being observed for the compounds having even membered spacers. However, the most striking feature of figure 3.3.6 is that the two series possessing a spacer containing an even number of methylene units exhibit entropy changes over three times larger than those containing an odd length spacer. Also, the values of $\Delta S/R$ for the CB.O6O.m series are, with a single exception, consistently greater than those of the corresponding CB.O4O.m compounds. Similarly, the values of $\Delta S/R$ for the CB.O5O.m series are larger than those of the corresponding CB.O3O.m compound. This, of course, is not true for the CB.OnO.10 compounds because CB.O3O.10 and CB.O4O.10 both exhibit a smectic A-isotropic transition whereas CB.O5O.10 and CB.O6O.10 undergo nematic-isotropic transitions and thus, larger entropy changes would be anticipated for the former compounds. It is interesting to note, however, that the entropy change associated with the nematic-isotropic transition of CB.O6O.10 is more than twice that associated with the smectic A-isotropic transition of CB.O3O.10. This may imply that the contribution to $\Delta S/R$ from the change in the conformational distribution at the transition outweighs the contribution from the change in translational order at the transition.

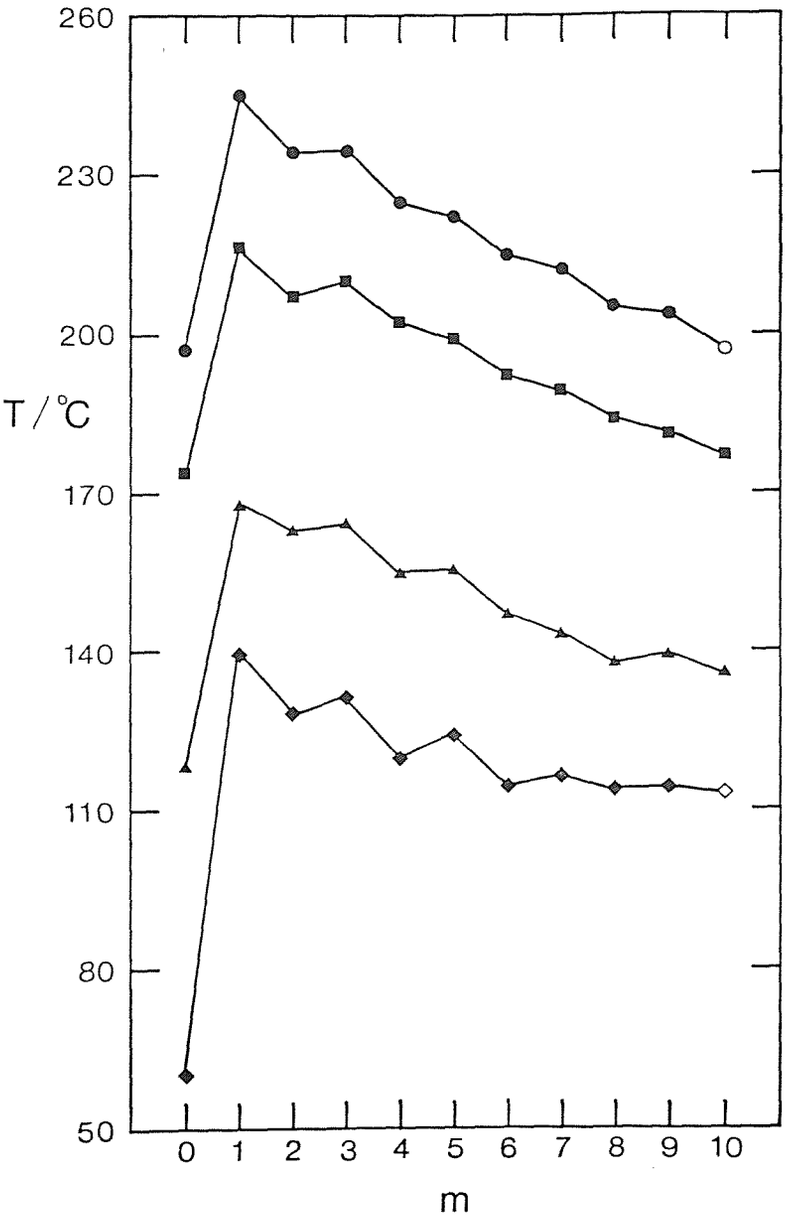

Figure 3.3.5 The dependence of the clearing temperatures on the length of the terminal alkyl chain for the CB.O3O.m (◆), the CB.O4O.m (●), the CB.O5O.m (▲) and the CB.O6O.m (■) series; filled symbols denote nematic-isotropic transitions and open symbols indicate smectic-nematic transitions.

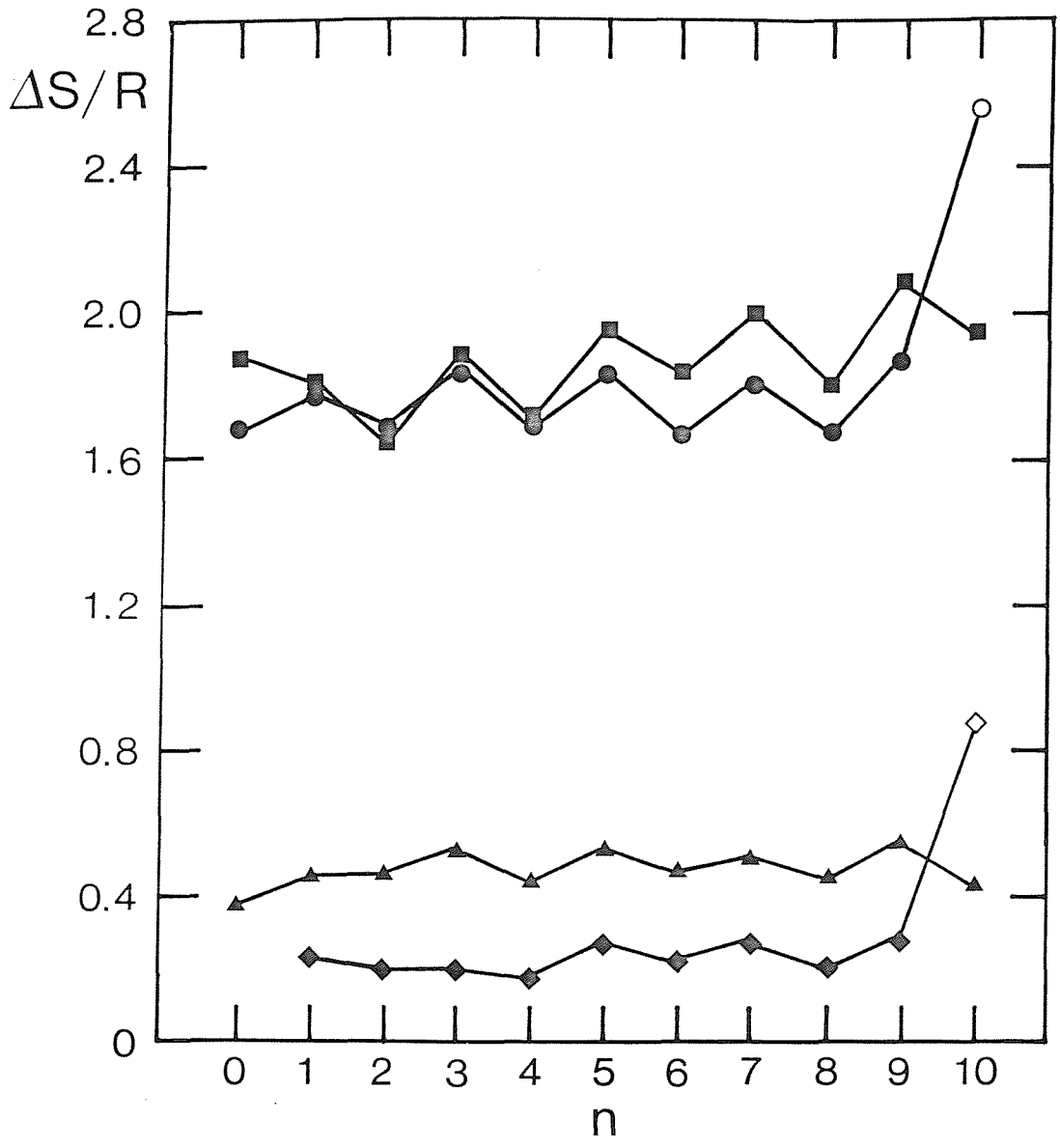

Figure 3.3.6 The dependence of the entropy change at the clearing temperatures on the length of the terminal alkyl chain for the CB.O3O.m (◆), the CB.O4O.m (●), the CB.O5O.m (▲) and the CB.O6O.m (■) series; filled symbols denote nematic-isotropic transitions and open symbols indicate smectic-nematic transitions.

Figures 3.3.7 through to 3.3.17 show the dependence of the transition temperatures upon varying the length of the flexible spacer, n, for the eleven CB.OnO.m series. The melting points of all eleven series exhibit an odd-even effect which is large for small values of m but attenuates with increasing m. The liquid crystal-isotropic transition temperatures of all the series display a very pronounced odd-even effect, reflecting the behaviour shown in figure 3.3.5. It is the dependence of the thermal stability of the smectic phases upon n for these asymmetric dimers, however, that distinguishes them from their symmetric dimer analogues. The CB.O6O.m series for m up to six exhibit smectic phases of greater thermal stability than the corresponding CB.O4O.m compounds and this is clearly illustrated in figures 3.3.7 to 3.3.13. This is reversed, however, when comparing CB.O6O.8, CB.O6O.9 and CB.O6O.10 with the analogous CB.O4O.m compounds and is shown in figures 3.3.15 to3.3.17. The latter observation holds true, without exception, for the m.OnO.m's described in Chapter 2 such that for even membered spacers increasing the spacer length decreases the thermal stability of the smectic phase. For the m.OnO.m's possessing odd length spacers the situation is somewhat more complicated.

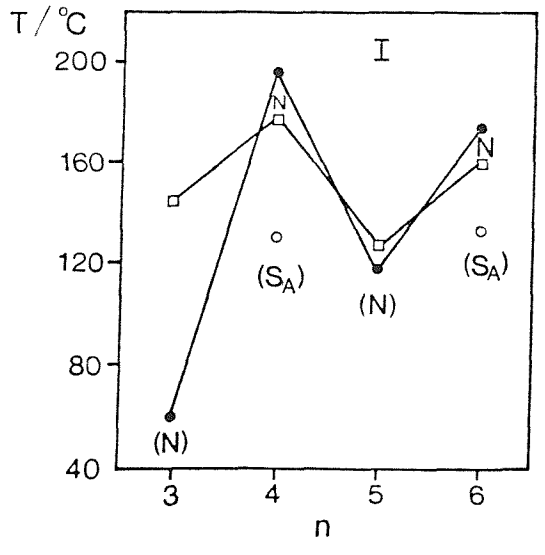

Figure 3.3.7 The dependence of the transition temperatures on the number of methylene units in the flexible alkyl core for the CB.OnO.O series. The melting point is denoted by □ , ● indicates the nematic-isotropic transition and o the smectic-nematic transition. Monotropic phases are marked in parentheses.

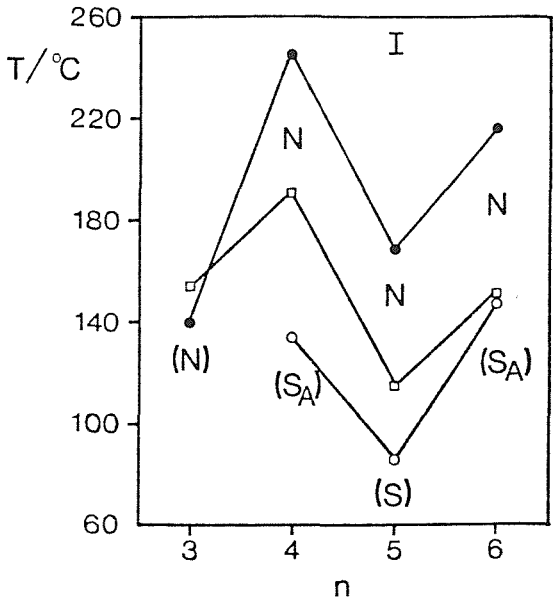

Figure 3.3.8 The dependence of the transition temperatures on the number of methylene units in the flexible alkyl core for the CB.OnO.1 series. The melting point is denoted by □ , ● indicates the nematic-isotropic transition and ○ the smectic-nematic transition. Monotropic phases are marked in parentheses.

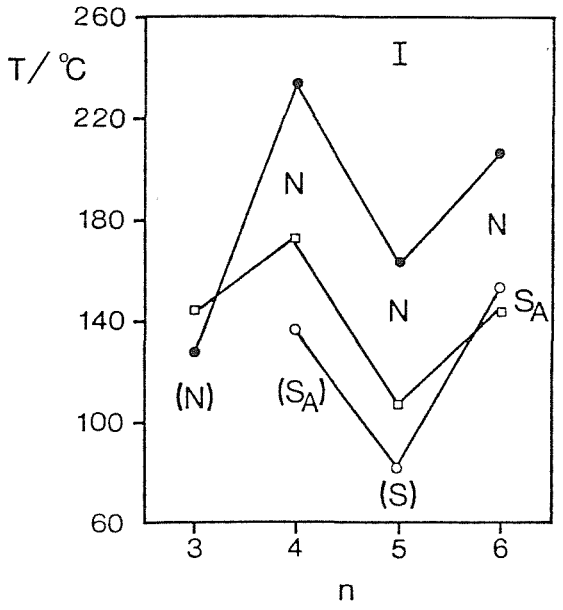

Figure 3.3.9 The dependence of the transition temperatures on the number of methylene units in the flexible alkyl core for the CB.OnO.2 series. The melting point is denoted by □ , ● indicates the nematic-isotropic transition and ○ the smectic-nematic transition. Monotropic phases are marked in parentheses.

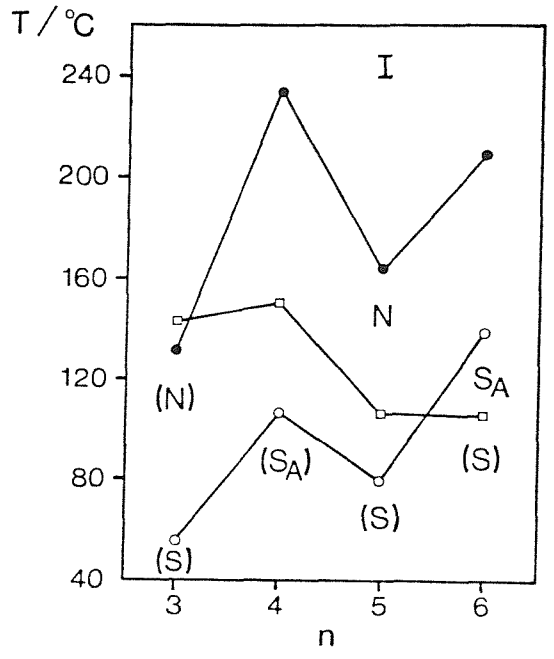

Figure 3.3.10 The dependence of the transition temperatures on the number of methylene units in the flexible alkyl core for the CB.OnO.3 series. The melting point is denoted by □ , ● indicates the nematic-isotropic transition and ○ the smectic-nematic transition. Monotropic phases are marked in parentheses.

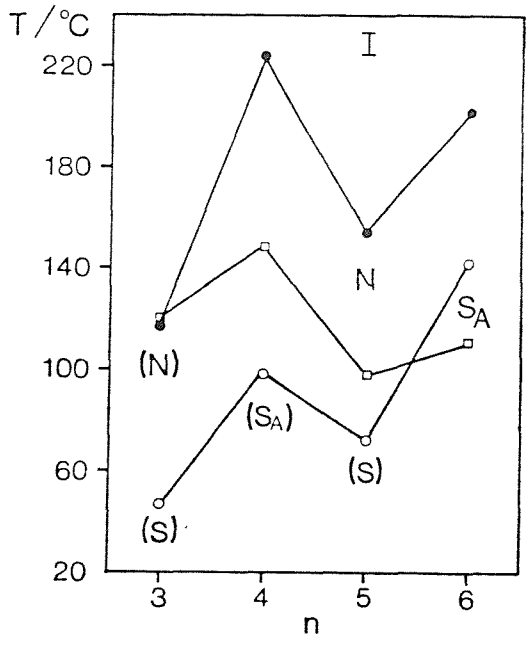

Figure 3.3.11 The dependence of the transition temperatures on the number of methylene units in the flexible alkyl core for the CB.OnO.4 series. The melting point is denoted by □ , ● indicates the nematic-isotropic transition and ○ the smectic-nematic transition. Monotropic phases are marked in parentheses.

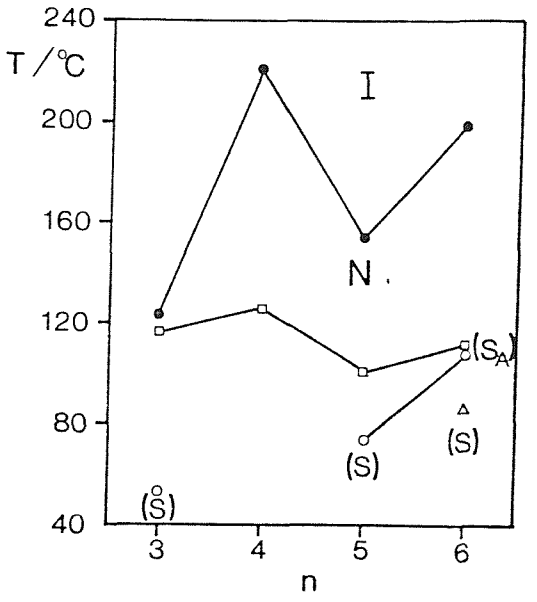

Figure 3.3.12 The dependence of the transition temperatures on the number of methylene units in the flexible alkyl core for the CB.OnO.5 series. The melting point is denoted by □ , ● indicates the nematic-isotropic transition, o the smectic-nematic transition and △ the smectic-smectic transition. Monotropic phases are marked in parentheses.

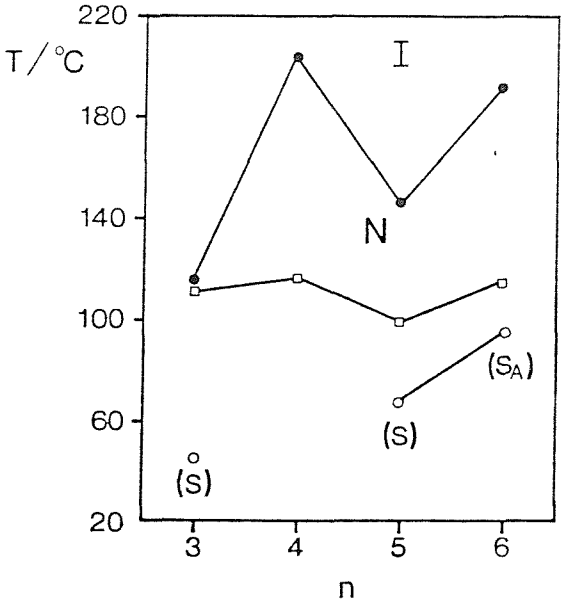

Figure 3.3.13 The dependence of the transition temperatures on the number of methylene units in the flexible alkyl core for the CB.OnO.6 series. The melting point is denoted by □ , ● indicates the nematic-isotropic transition and o the smectic-nematic transition. Monotropic phases are marked in parentheses.

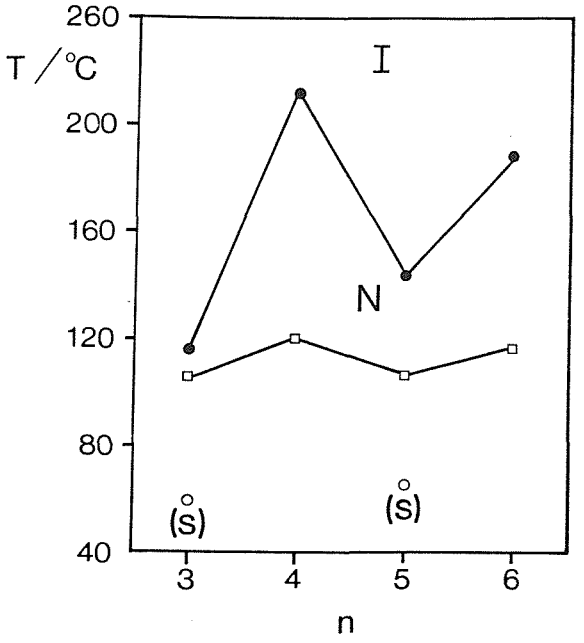

Figure 3.3.14 The dependence of the transition temperatures on the number of methylene units in the flexible alkyl core for the CB.OnO.7 series. The melting point is denoted by □ , ● indicates the nematic-isotropic transition and ○ the smectic-nematic transition. Monotropic phases are marked in parentheses.

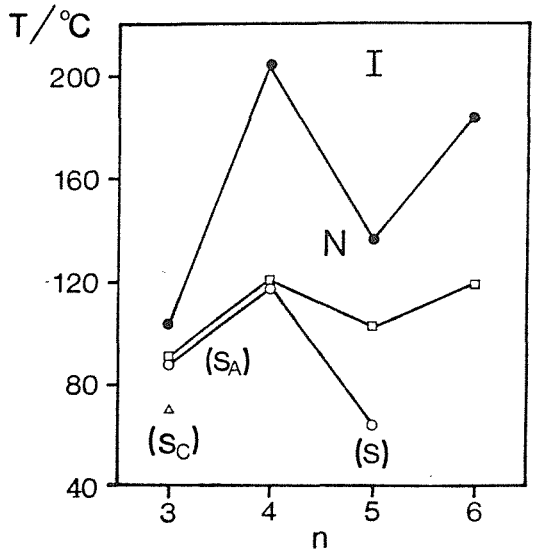

Figure 3.3.15 The dependence of the transition temperatures on the number of methylene units in the flexible alkyl core for the CB.OnO.8 series. The melting point is denoted by □ , ● indicates the nematic-isotropic transition, ○ the smectic-nematic transition and the smectic-smectic transition. Monotropic phases are marked in parentheses.

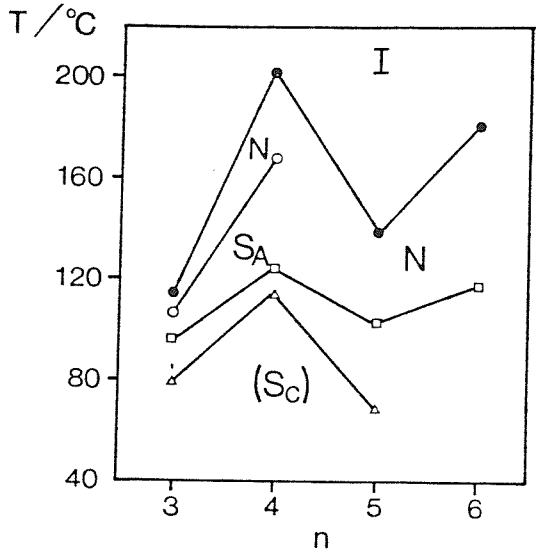

Figure 3.3.16 The dependence of the transition temperatures on the number of methylene units in the flexible alkyl core for the CB.OnO.9 series. The melting point is denoted by □ , ● indicates the nematic-isotropic transition, ○ the smectic-nematic transition and △ the smectic-smectic transition. Monotropic phases are marked in parentheses.

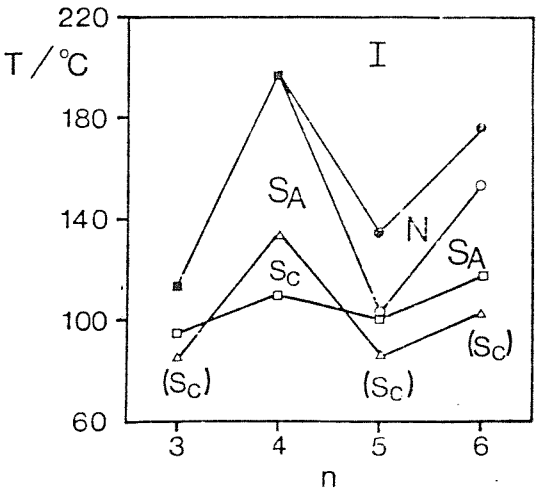

Figure 3.3.17 The dependence of the transition temperatures on the number of methylene units in the flexible alkyl core for the CB.OnO.10 series. The melting point is denoted by □ , ● indicates the nematic-isotropic transition, ■ the smectic A-isotropic transition, the smectic-nematic transition ○ and △ the smectic-smectic transition. Monotropic phases are marked in parentheses.

Summarising, therefore, the CB.OnO.m series exhibit properties that would largely have been anticipated with the exception of the dependence of the smectic-nematic transition temperatures upon the length of the terminal alkyl chain. This is particularly true for the CB.O4O.m and CB.O6O.m series for which T_{S_AN} initally rises, passing through a maxima then falls dramatically before reemerging as we increase m. In order to explain these observations it would seem reasonable to assume that the driving force precipitating smectic phase formation must differ as m is increased. In an attempt to clarify this situation we performed a limited number of X-ray diffraction experiments on selected CB.OnO.m compounds, the results of which are listed in table 3.3.5.

Compound	l/Å	T/T_{S_AN} T/T_{S_AI}	d/A	d/l
CB.O6O.2	34.5	0.97	16.6	0.5
CB.O6O.5	38.1	0.99	18.5	0.5
CB.O6O.10	44.0	0.96	78.4	1.8
CB.O3O.10	39.2	0.97	65.4	1.7

Table 3.3.5 The layer spacing, d, in the smectic A phases of selected CB.OnO.m compounds; l denotes the estimated all-trans molecular length.

Immediately apparent from the data listed in table 3.3.5 is that the structure of the smectic A phase exhibited by CB.O3O.10 and CB.O6O.10 is different to that observed for CB.O6O.2 and CB.O6O.5 and this is reflected in the ratio of the layer spacing to the all-trans molecular length. For CB.O3O.10 and CB.O6O.10 this ratio is 1.7 and 1.8 respectively and these are readily explained by invoking an

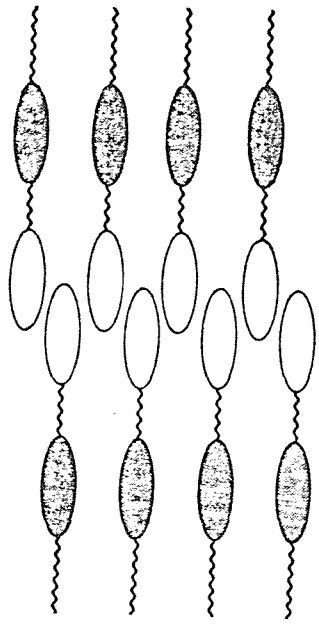

Figure 3.3.18 The interdigitated structure proposed for the smectic A phase of CB.030.10 and CB.060.10; the Schiff's base is shaded while the cyanobiphenyl group is not.

interdigitated bilayer structure in which the cyanobiphenyloxy moieties are aranged in an anti-parallel manner as shown in figure 3.3.18. The driving force for such dimerisation apears to be an electrostatic interaction between the polar and polarisable cyanobiphenyl groups while the smectic phase results from the molecular inhomogeniety produced by the long terminal alkyl chains. This structural modification of the smectic A phase is normally termed the interdigitated smectic A phase, S_{A_d}, [15] and is described in the introductory Chapter.

The ratio of the layer spacing to the all-trans molecular length for both CB.060.2 and CB.060.5 is approximately 0.5 and this can be explained in one of two ways. First, it may simply imply that the phase is actually tilted but this is not possible because optically a homeotropic texture is observed implying there to be no bulk tilt angle. Second, there has to be an interpenetration of the molecular layers in such a way that the length of the unit cell of the structure

is less than that of the molecule. To achieve this condition, the two different mesogenic groups of the asymmetric dimer must be associated. We describe this as an intercalated structure to distinguish it from an interdigitated arrangement in which the same groups of different molecules are interleaved. Figures 3.3.19(a) and 3.3.19(b) are schematic representations of two possible intercalated structures composed of asymmetric dimers that each result in a ratio of the layer spacing to the molecular length of approximately 0.5. The difference between the two structures is simply whether or not the arrangement of the molecules within the structure is random. If, however, the molecular arrangement is random, figure 3.3.19(a), then the ratio of the layer spacing to the molecular length is 0.5 only if the two different mesogenic moieties have similar electron density profiles, otherwise the layer spacing is simply the molecular length. We believe, however, that for the CB.OnO.m compounds the two semi-rigid units are sufficiently different to be distinguished within the resolution of our diffractometer. Thus, we propose that the molecules are not randomly arranged within the intercalated structure. This, however, implies that the sample should exhibit bulk ferroelectric properties and if this is not the case, we simply extend the model to allow for clusters such as that sketched in figure 3.3.19(b) to exist in both orientations with respect to the director and in statistically equal numbers. We shall discuss why the molecules intercalate in this manner later. It should be noted that an analogous structure has been proposed for the smectic A phase of compounds with lateral cyanophenyl groups;

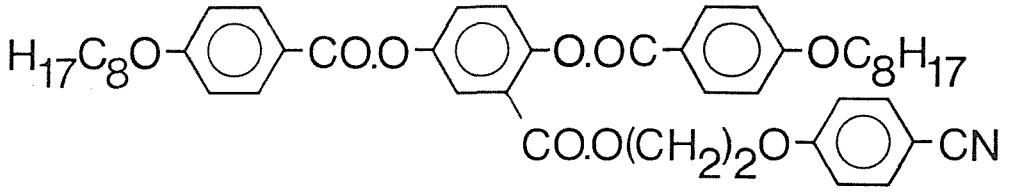

although the interpenetration of the layers is not so large [17].

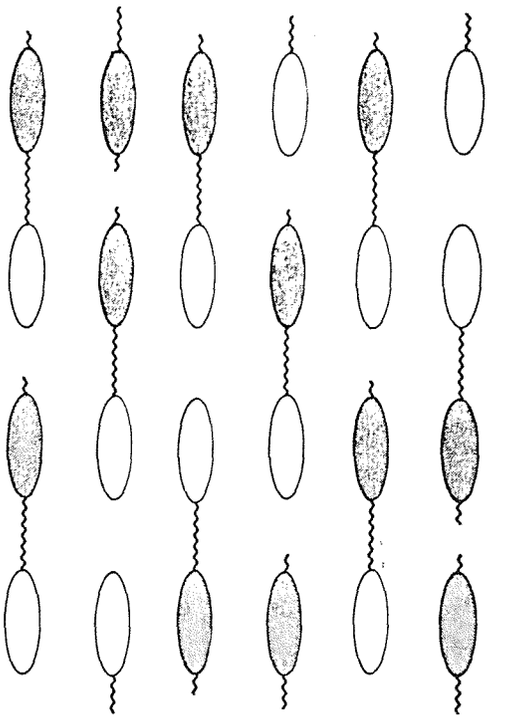

(a)

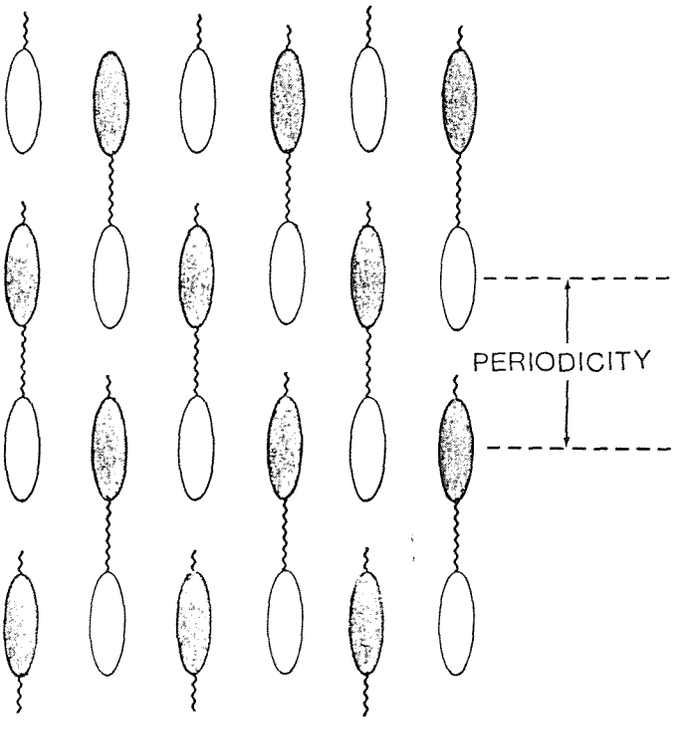

(b)

Figure 3.1.19 Two possible intercalated structures composed of an asymmetric dimer; (a) represents a random arrangement of the molecules and (b) a non-random arrangement. The Schiff's base is shaded while the cyanobiphenyl group is not.

The liquid crystal-isotropic transition temperatures of selected CB.OnO.m compounds are compared with those of the corresponding BCBO-n and m.OnO.m compounds in figures 3.3.20, 3.3.21 and 3.3.22. In all three plots the BCBO-n materials show the highest clearing temperatures. The CB.OnO.m compounds have transition temperatures intermediate between those of the corresponding BCBO-n and m.OnO.m materials providing the length of the terminal chain is short (m=1-4); this is shown in figure 3.3.20. A simplistic interpretation of this assumes that core-core interactions are dominant in determining the clearing temperature of a compound and that the cyanobiphenyloxy-cyanobiphenyloxy interaction is greater than the mixed core interaction which in turn is larger than the Schiff's base-Schiff's base interactions.

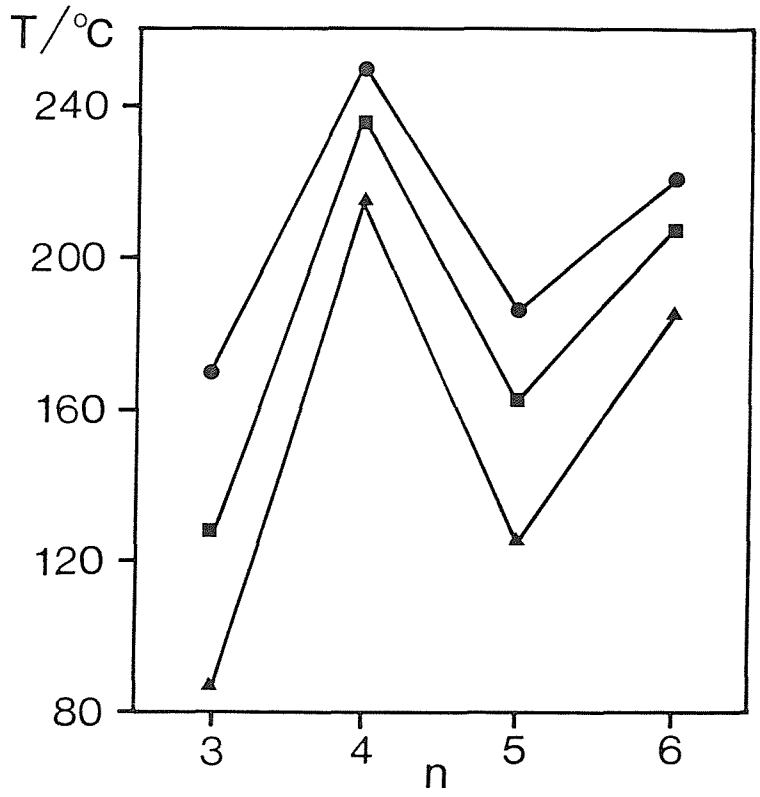

Figure 3.3.20 The dependence of the nematic-isotropic transition temperatures on the number of methylene groups in the flexible alkyl core for the BCBO-n (●), the 2.OnO.2 (▲) and the CB.OnO.2 (■) series.

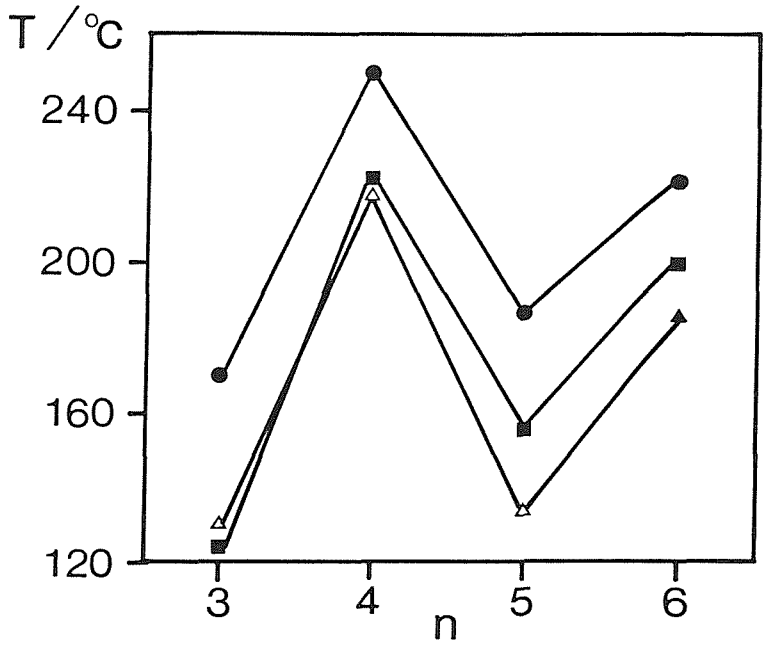

Figure 3.3.21 The dependence of the transition temperatures on the number of methylene groups in the flexible alkyl core for the BCBO-n (●), the 5.OnO.5 (▲) and the CB.OnO.5 (■) series; filled symbols indicate nematic-isotropic transitions and open symbols denote smectic-isotropic transitions.

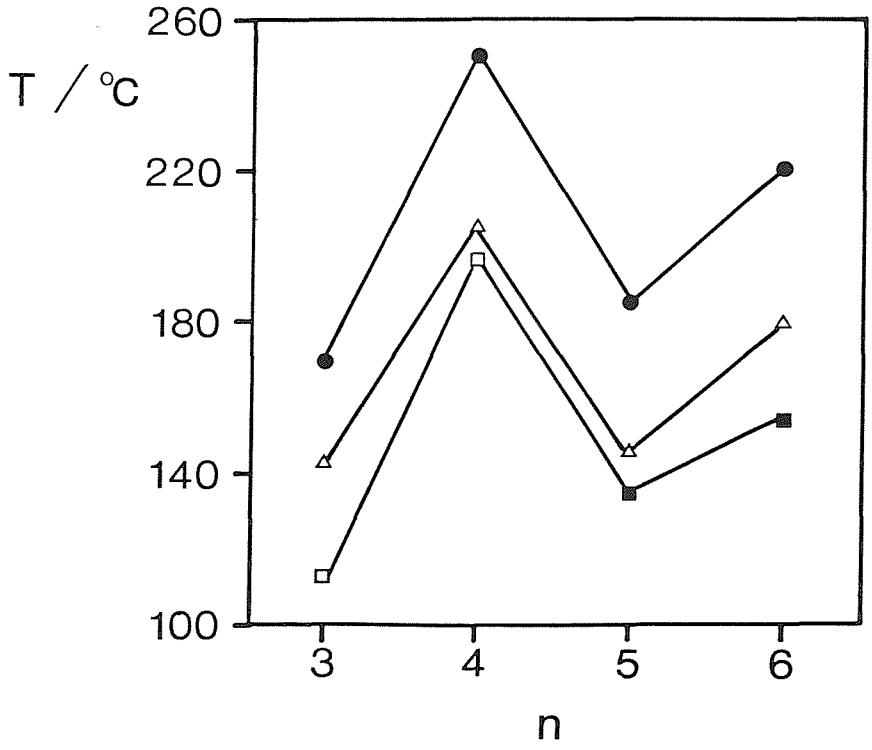

Figure 3.3.21 The dependence of the transition temperatures on the the number of methylene groups in the flexible alkyl core for the BCBO-n (●), the 10.OnO.10 (▲) and the CB.OnO.10 (■) series; filled symbols indicate nematic-isotropic transitions and open symbols denote smectic-isotropic transitions.

Figure 3.3.21, however, shows that 5.O3O.5 has a higher clearing temperature than CB.O3O.5 and in figure 3.3.20, all four compounds of the 10.OnO.10 series have higher liquid crystal-isotropic transition temperatures than those of the CB.OnO.10 series. This suggests that as m is increased, alkyl chain-alkyl chain interactions become increasingly important in stabilising the smectic phases formed by the m.OnO.m compounds. To further emphasise this cross-over of transition temperatures between the CB.OnO.m and the m.OnO.m series as m is increased, figures 3.3.23 to 3.3.26 give the dependence of the clearing temperatures upon m for both series. The plots clearly show that for low values of m, the CB.OnO.m compounds have higher clearing temperatures than the corresponding m.OnO.m materials but this is reversed as the terminal chain length is increased.

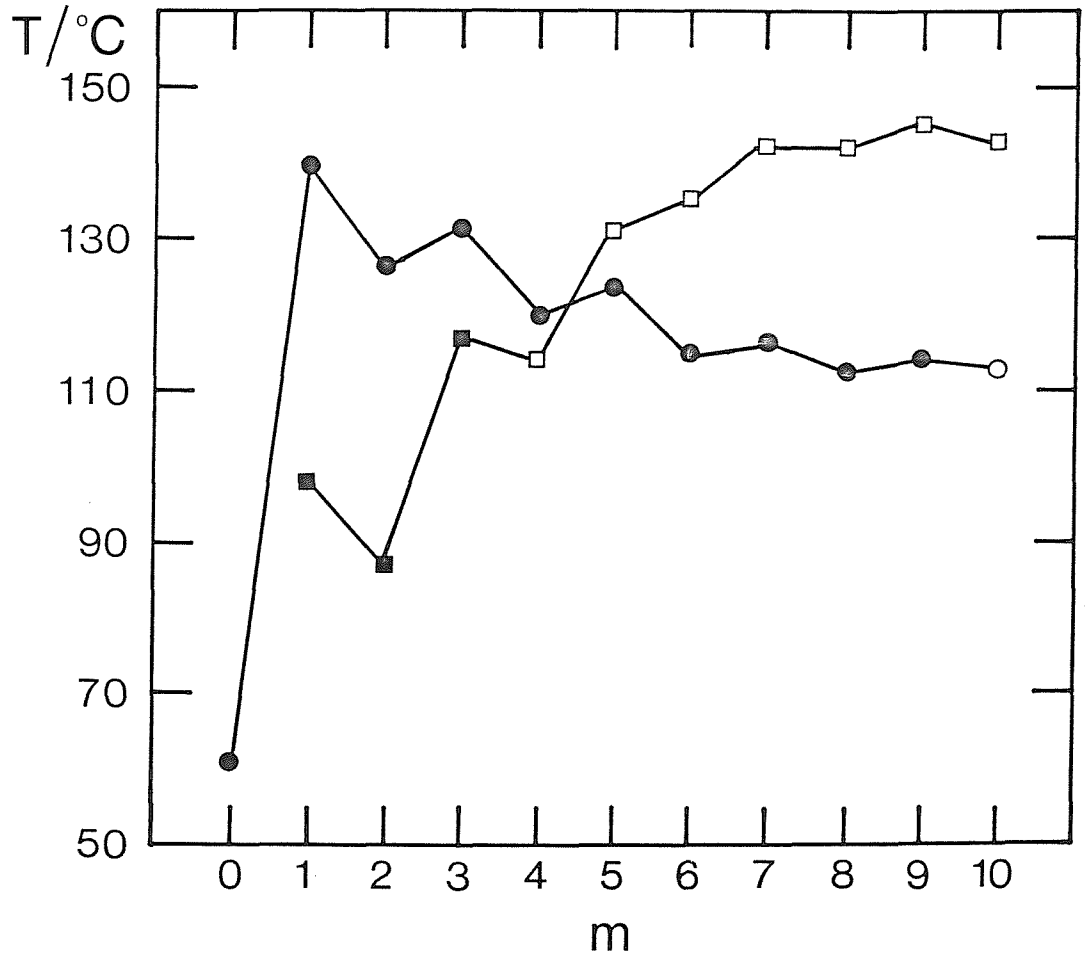

Figure 3.3.23 The dependence of the clearing temperatures on the length of the terminal alkyl chain for the CB.O3O.m (●) and the m.O3O.m (■) series; open symbols denote smectic-isotropic transitions and filled symbols indicate nematic-isotropic transitions.

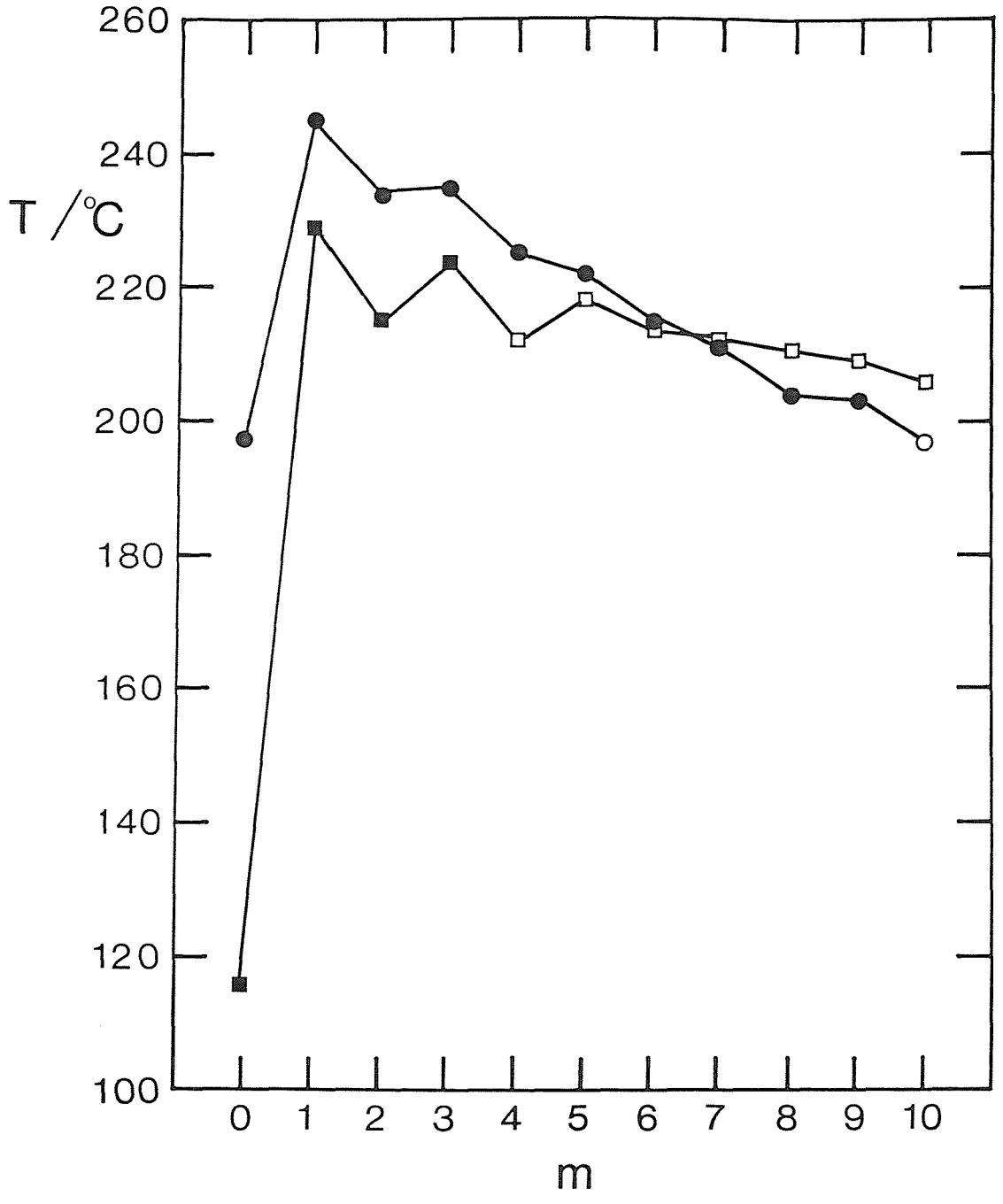

Figure 3.3.24 The dependence of the clearing temperatures on the length of the terminal alkyl chain for the CB.O4O.m (●) and the m.O4O.m (■) series; open symbols denote smectic-isotropic transitions and filled symbols indicate nematic-isotropic transitions.

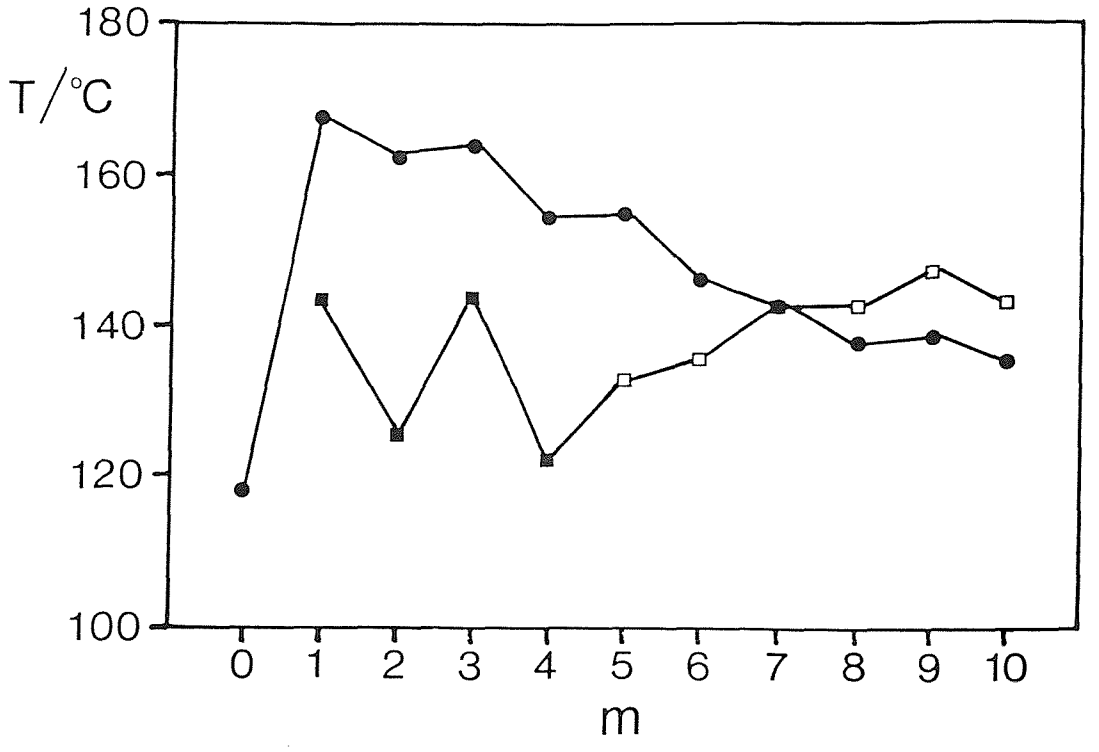

Figure 3.3.25 The dependence of the clearing temperatures on the length of the terminal alkyl chain for the CB.O5O.m (●) and the m.O5O.m (■) series; open symbols denote smectic-isotropic transitions and filled symbols indicate nematic-isotropic transitions.

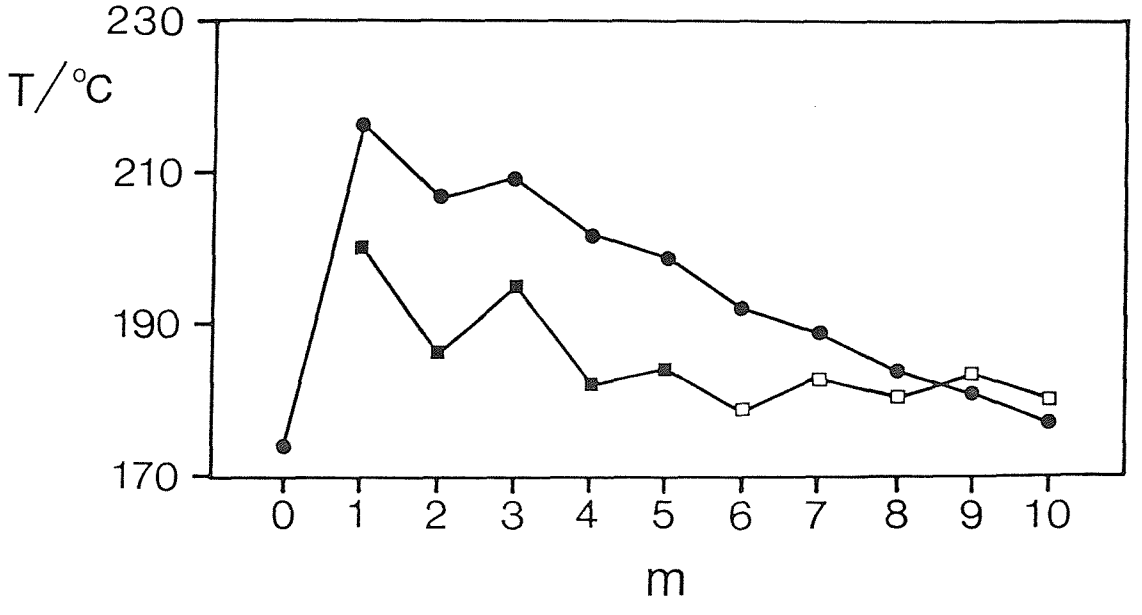

Figure 3.3.26 The dependence of the clearing temperatures on the length of the terminal alkyl chain for the CB.O6O.m (●) and the m.O6O.m (■) series; open symbols denote smectic-isotropic transitions and filled symbols indicate nematic-isotropic transitions.

A comparison of the entropies associated with the liquid crystal-isotropic transition for the CB.OnO.m compounds with those of the BCBO-n and m.OnO.m series is only posssible in a very limited number of cases because we must compare like transitions so effectively restricting the comparison to nematic-isotropic transitions. Figure 3.3.27 shows the dependence of the entropy change at the nematic-isotropic transition on the length of the flexible spacer for the BCBO-n, CB.OnO.2 and 2.OnO.2 compounds. The values of $\Delta S_{NI}/R$ for the CB.OnO.2 series are intermediate between those of the corresponding BCBO-n and 2.OnO.2 materials with the BCBO-n compounds always exhibiting the largest entropy change. This trend is also evident for compounds with m=1 and 3. This supports the view that core-core interactions are dominant for low values of m and that the mixed core interaction strength is intermediary between the two like core interactions.

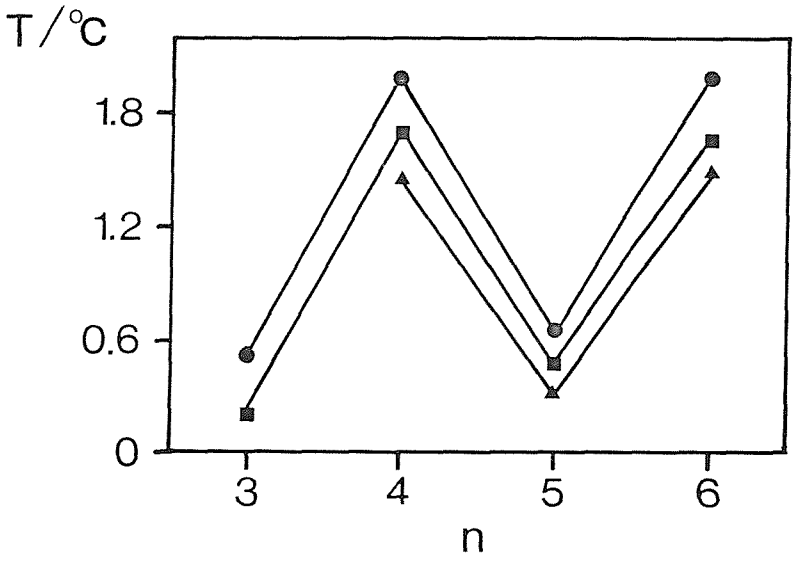

Figure 3.3.27 The dependence of the nematic-isotropic entropy of transition on the length of the flexible spacer for the BCBO-n (●), CB.OnO.2 (■) and the 2.OnO.2 (▲) series.

It should be noted that the entropy change associated with the smectic A-isotropic transition of CB.O3O.10 ($\Delta S/R=0.88$) is much smaller than that of 10.O3O.10 ($\Delta S/R=3.10$). It is not possible to compare the

entropy change associated with the smectic A-isotropic transition of CB.O4O.10 ($\Delta S/R=2.56$) with that of 10.O4O.10 because this exhibits a smectic C-isotropic transition but surprisingly, it is smaller than the entropy change associated with the smectic A-isotropic transition of 10.O3O.10 ($\Delta S/R=3.10$). This may imply that the contribution to $\Delta S/R$ from the change in the conformational disribution of the terminal alkyl chains is far more significant for the m.OnO.m series than it is for the CB.OnO.m compounds. If this is the case, then it is likely that the terminal alkyl chains of the m.OnO.m compounds are more ordered than their CB.OnO.m counterparts; this may be the effect of greater packing constraints in a monolayer as opposed to those in the interdigitated bilayer structure of the smectic A phase exhibited by CB.OnO.m compounds having large values of m.

We have seen that the transitional properties of the CB.OnO.m compounds are intermediate between those of the corresponding m.OnO.m and BCBO-n materials providing m is small. This prompts the obvious question; how do the properties of the asymmetric dimers compare to those of equimolar mixtures of the analogous symmetric dimers? Figure 3.3.28 gives the liquid-crystalline properties of CB.O5O.2, CB.O5O.6 and CB.O5O.10 alongside those of the corresponding symmetric dimers and equimolar mixtures of them. It should be noted that the mixtures gave biphasic regions varying from less than a degree up to approximately five degrees and so the uncertainties in the transition temperatures of the mixtures is, at worse, $\pm 3\,^{\circ}C$ but is often much less. It has become clear that the properties of the CB.OnO.m series are strongly dependent on the length of the terminal alkyl chain, m, and so in these comparisons we chose compounds having low (2), intermediate (6) and large (10) values of m. The most striking feature in figure 3.3.28 is probably the very similar clearing temperatures of the CB.OnO.m compounds and the analogous equimolar mixtures. The 2.O5O.2/BCBO-5 mixture has a nematic-isotropic transition temperature that is equal to the mean of the individual components and does not exhibit any smectic behaviour, whereas CB.O5O.2 possesses a marginally higher T_{NI} and has a monotropic smectic phase. On increasing m to six, the nematic-isotropic transition temperatures of CB.O5O.6 and the corresponding mixture are again similar. The stability of the smectic

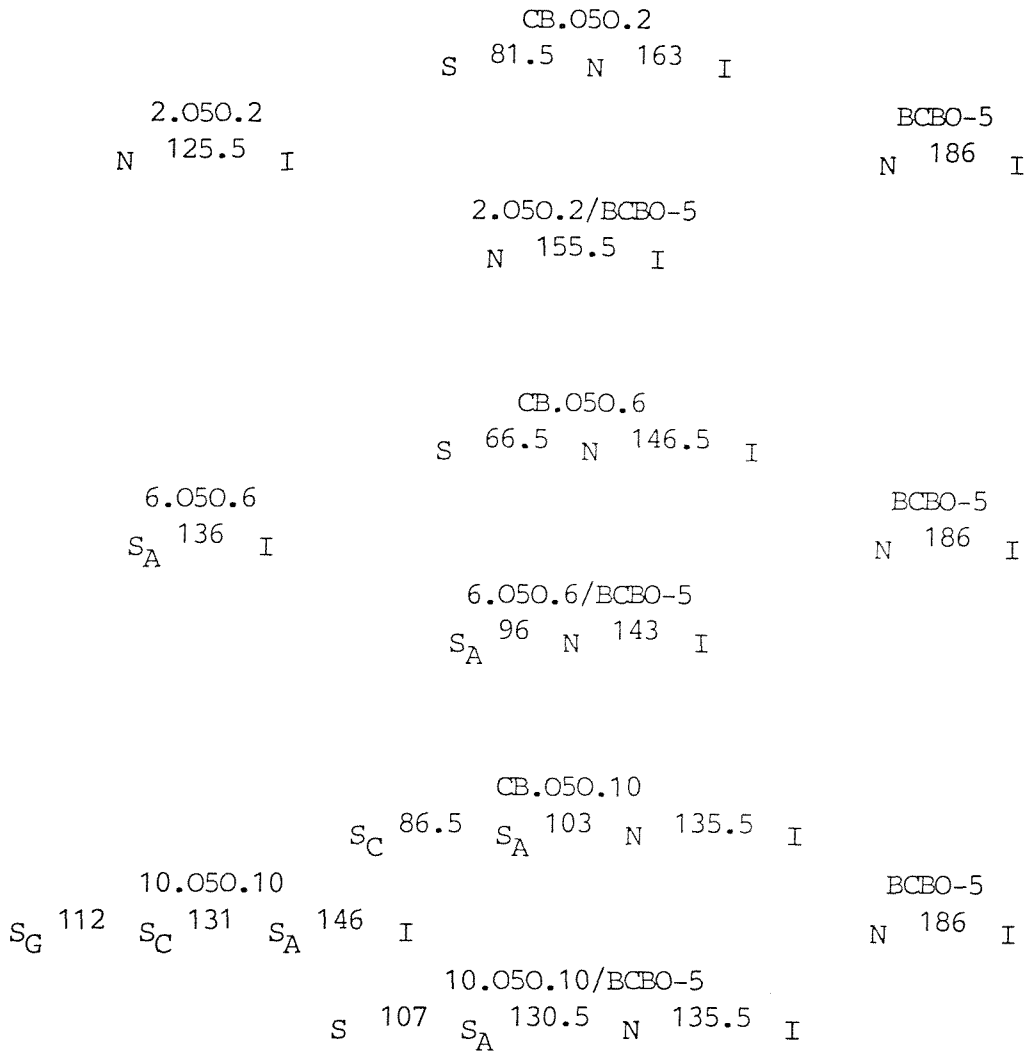

Figure 3.3.28 A comparison of the liquid-crystalline transition temperatures (°C) of the CB.OnO.m's with those of equimolar mixtures of the analogous BCBO-n [7] and m.OnO.m compounds.

phase exhibited by 6.O5O.6 is greatly reduced in the mixture. The BCBO-5/10.O5O.10 mixture has a nematic-isotropic transition temperature that is equal to that of CB.O5O.10 and which is lower than that observed for either of the symmetric dimers. The increase in smectic stability on increasing m from 6 to 10 in the mixtures is similar to that observed on passing from CB.O5O.6 to CB.O5O.10 and in both cases is approximately 30°C. The lower temperature smectic phase of the BCBO-5/10.O5O.10 mixture could not be assigned by its rather poorly defined focal-conic fan texture alone and rapid crystallisation of the sample prevented X-ray diffraction studies.

Figure 3.3.29 compares the transition temperatures of CB.O6O.2, CB.O6O.6 and CB.O6O.10 to those of the analogous symmetric dimers and equimolar mixtures of them. Again, there is a striking similarity in the clearing temperatures of the CB.OnO.m compounds and the corresponding mixtures. Indeed, the nematic-isotropic transition temperatures of CB.O6O.2 and the BCBO-2/2.O6O.2 mixture are equal and are approximately the mean of the T_{NI}'s of the symmetric dimers. In addition, the mixture and CB.O6O.2 have equal smectic A-nematic transition temperatures whereas neither 2.O6O.2 or BCBO-2 exhibit any smectic behaviour. The obvious question is do the symmetric dimers intercalate in the smectic A phase observed for the mixture in a similar fashion to that proposed in figure 3.3.19(a) for the S_A phase of CB.O6O.2 ? Unfortunately, the smectic A phase of the mixture crystallises within the duration of the X-ray diffraction experiment and hence, its layer spacing could not be obtained. However, an equimolar mixture of 2.O1OO.2 and BCBO.10 exhibits a smectic A phase which has a layer spacing of 19.4 Å [18] whereas the molecular lengths are 42 Å and 36.4 Å respectively. Therefore, it appears that the molecules in this mixture do indeed intercalate in a similar manner to that proposed for CB.O6O.2. On increasing m to six, the nematic-isotropic transition temperatures of CB.O6O.6 and the corresponding mixture are again very similar. The smectic A-nematic transition temperatures of the BCBO-6/6.O6O.6 and the BCBO-6/2.O6O.2 mixtures are approximately equal even though 6.O6O.6 exhibits solely smectic behaviour. It should be noted that on passing from CB.O6O.2 to CB.O6O.6 T_{SN} falls dramatically. On increasing m to ten, CB.O6O.10 and

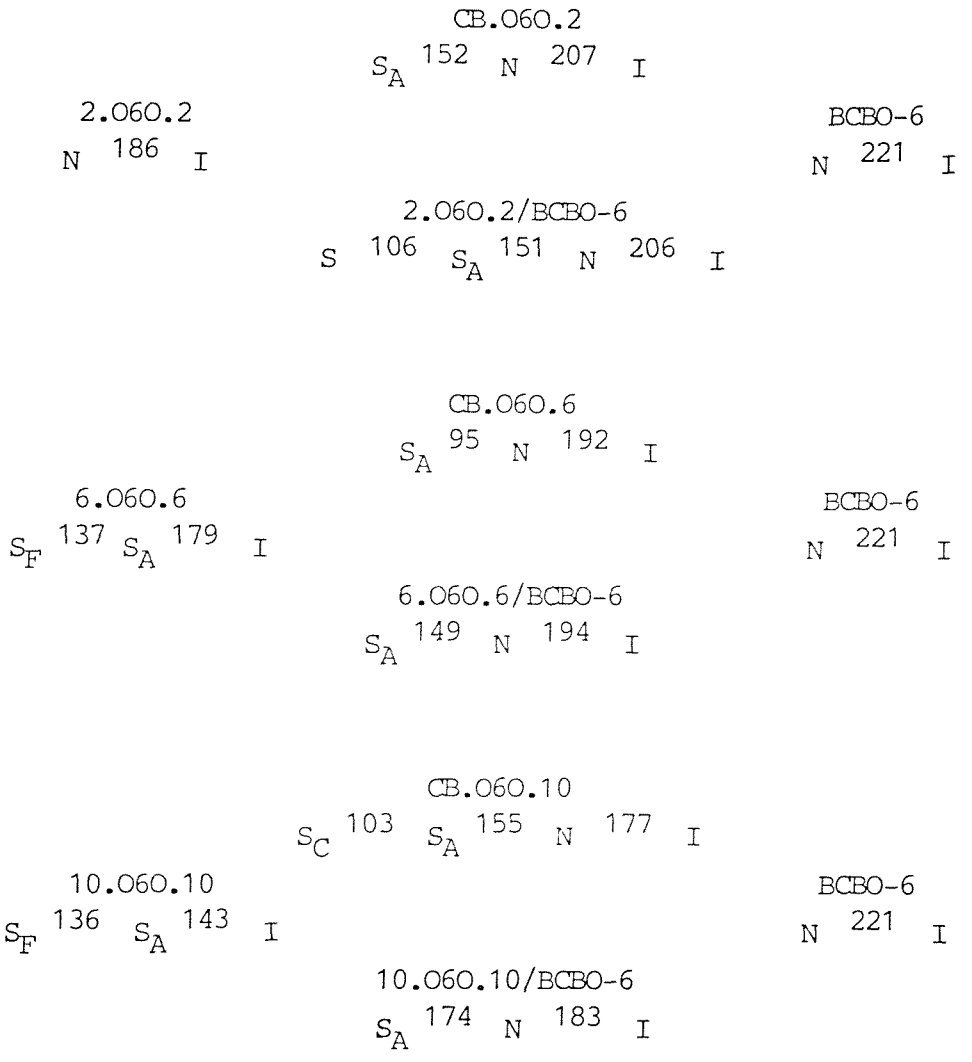

Figure 3.3.29 A comparison of the liquid-crystalline transition temperatures (°C) of the CB.OnO.m's with those of equimolar mixtures of the analogous BCBO-n [7] and m.OnO.m compounds.

the BCBO-10/10.O6O.10 mixture have similar nematic-isotropic transition temperatures and these are approximately equal to the mean of the clearing temperatures of 10.O6O.10 and BCBO-10. The thermal stability of the smectic A phase of the mixture has increased and this is also observed on passing from CB.O6O.6 to CB.O6O.10. Thus, the asymmetric dimers having both odd and even alkyl spacers mirror, to some extent, the behaviour shown by equimolar mixtures of the analogous symmetric dimers. This similarity in behaviour between the CB.OnO.m series and equimolar mixtures of the corresponding BCBO-n and m.OnO.m compounds suggests that the cores of the dimeric molecules are composed of three segments; two mesogenic units and an alkyl spacer. The interactions in the asymmetric dimer are, therefore, equivalent to those in the equimolar mixtures of the symmetric dimers and so similar behaviour would be anticipated and indeed is observed.

We now turn our attention to a comparison of the asymmetric dimers to equimolar mixtures of the constituent monomers. We chose to study the CB.OnO.4 series and considered them to be the dimeric analogues of the equimolar mixtures: EBBA (20.4)/1OCB, EBBA/2OCB, EBBA/3OCB and EBBA/4OCB. The liquid-crystalline transition temperatures of these mixtures are given in figure 3.3.30 alongside the transition temperatures of the monomers and the CB.OnO.4 compounds. The most striking feature of figure 3.3.30 is that the EBBA/2OCB, EBBA/3OCB and EBBA/4OCB mixtures exhibit smectic polymorphism whereas all the single components are exclusively nematics. The smectic phases have been assigned solely on the basis of their optical textures and so should be treated with some caution. The smectic A phase exhibited by the EBBA/2OCB and EBBA/4OCB mixtures was identified by the observation optically of both homeotropic areas and regions of focal-conic fan texture. On cooling the smectic A phase of the EBBA/2OCB mixture, the homeotropic regions remained but the focal-conic fan texture changed becoming truncated and almost mosaic-like. We assigned this lower temperature phase as a smectic B. On further cooling, the regions of truncated focal-conic fans become crossed by permanent bands that are unbroken and a platelet texture in which the plates apear to overlap develops from the regions of homeotropic alignment. This phase we assign as a smectic E. This phase sequence, S_A-S_B-S_E, is shown in

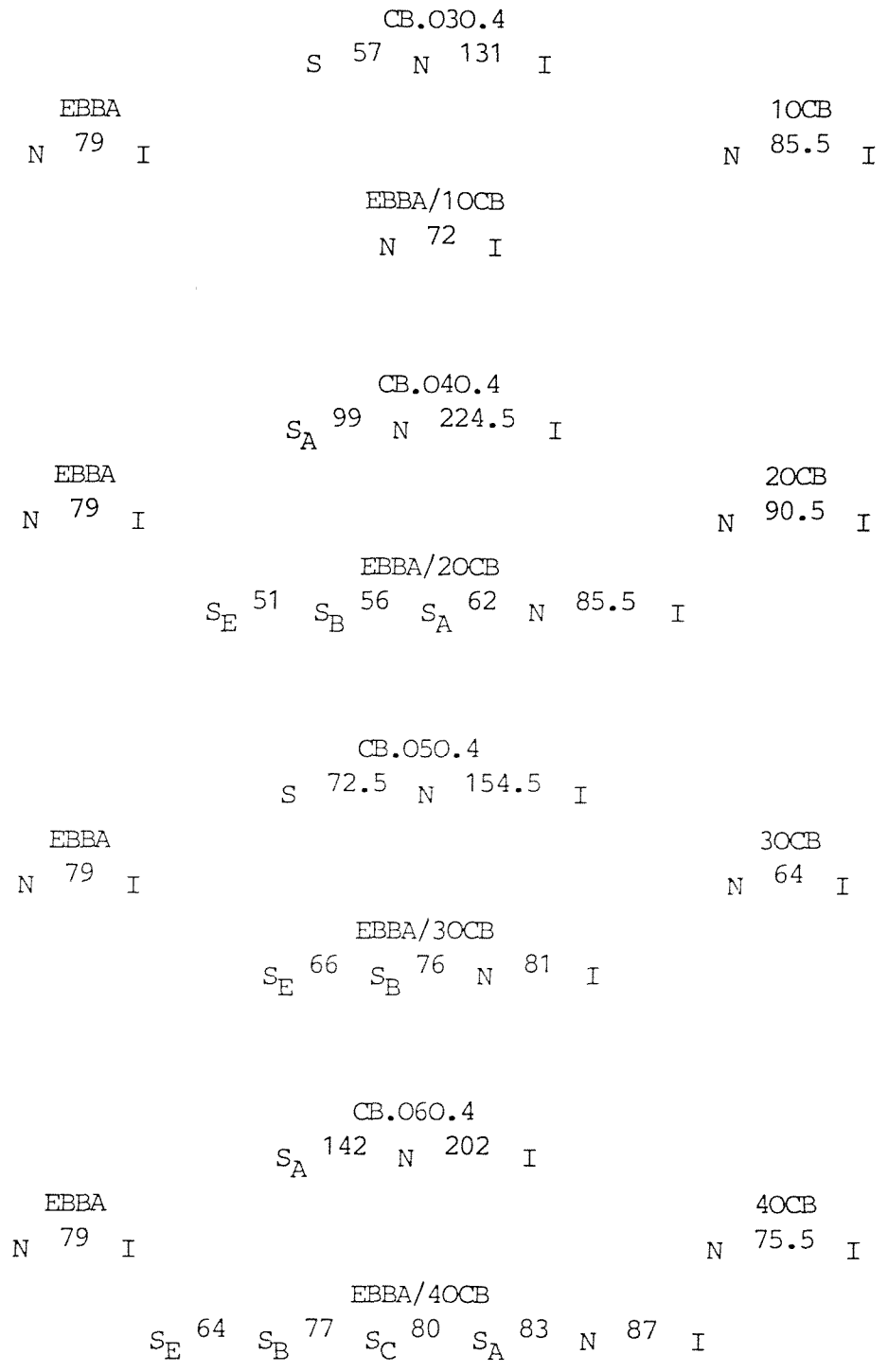

Figure 3.3.28 A comparison of the liquid-crystalline transition temperatures (°C) of the CB.OnO.m's with those of equimolar mixtures of EBBA and nOCB's.

plates 3.3.1, 3.3.2 and 3.3.3. The EBBA/4OCB mixture has a smectic C phase interjected between a smectic A and a smectic B phase and is identified on the basis of the homeotropic regions in the smectic A texture adopting a schlieren texture on cooling and also, the areas of focal-conic fans become somewhat broken and sanded. The smectic B phase has a similar texture to that described for the EBBA/2OCB mixture, shown in plate 3.3.2. On cooling the nematic phase of the EBBA/3OCB mixture 'H'-shaped platelets begin to grow and coalesce to form mosaic areas. This phase is assigned as a smectic B. On further cooling, these platelets become crossed by permanent lines characteristic of a smectic E phase. This phase sequence, N-S_B-S_E, is shown in plates 3.3.4, 3.3.5 and 3.3.6.

The occurence of induced smectic phases in these EBBA/nOCB mixtures tends to support the argument that the cyanobiphenyl-Schiff's base interaction is a driving force in smectic phase formation. The reasons for the appearance of injected smectic phases in mixtures composed of purely nematogenic compounds are generally not well understood but, for this particular example, it has been suggested that there is a favourable charge transfer interaction between a cyanobiphenyl group and a Schiff's base which may be responsible for the formation of induced smectic phases in mixtures containing these moieties [10,11,12].

We began investigating the properties of mixtures, in part, to rationalise the very unusual dependence of the smectic A-nematic transition temperatures on m for the CB.OnO.4 and CB.OnO.6 series. For mixtures of the monomeric analogues a charge transfer interaction is thought to be responsible for the formation of induced smectic phases. If this is also the case for the CB.OnO.m compounds then the driving force for the creation of the intercalated smectic A structure, proposed in figure 3.3.19(a), is easy to understand because such a structure maximises the overlap between the cyanobiphenyl group and the Schiff's base. This also explains why the smectic stability initially increases but subsequently decreases as the length of the terminal alkyl chain is increased. Initially, the short chains can pack with greater efficiency into the spaces between the layers. The

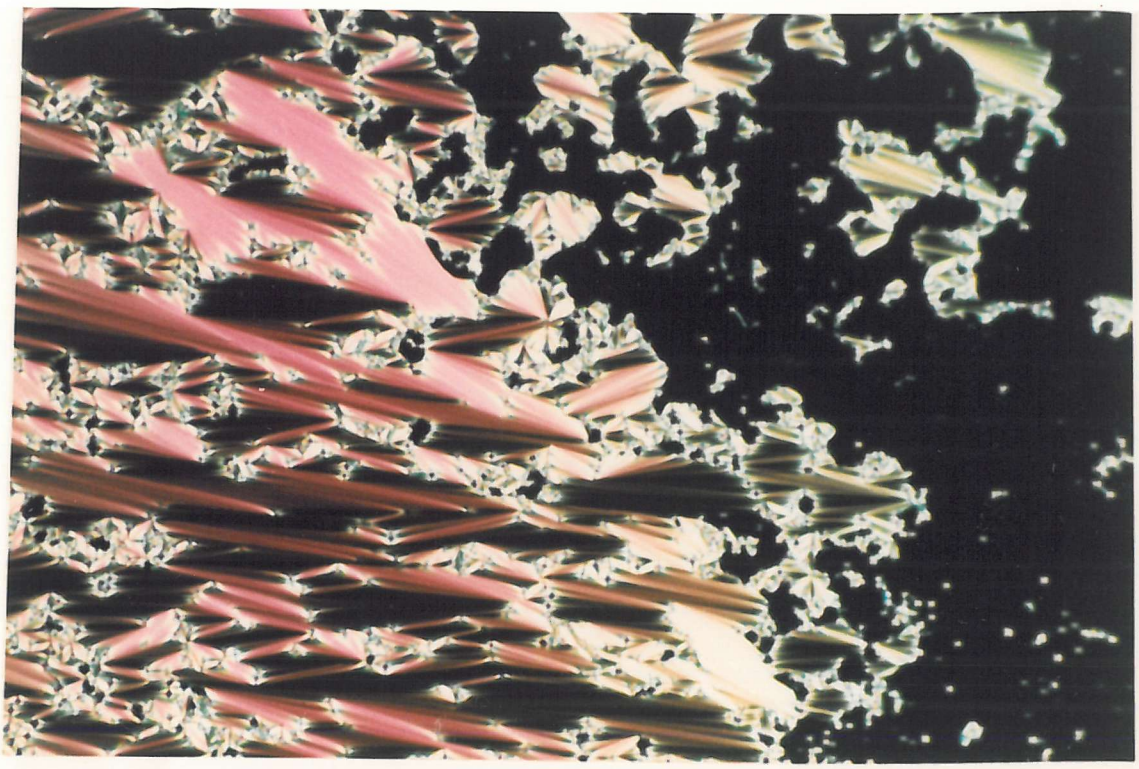

Plate 3.3.1 The focal-conic fan and homeotropic textures of the smectic A phase of an equimolar mixture of 20CB and EBBA (T=58 °C).

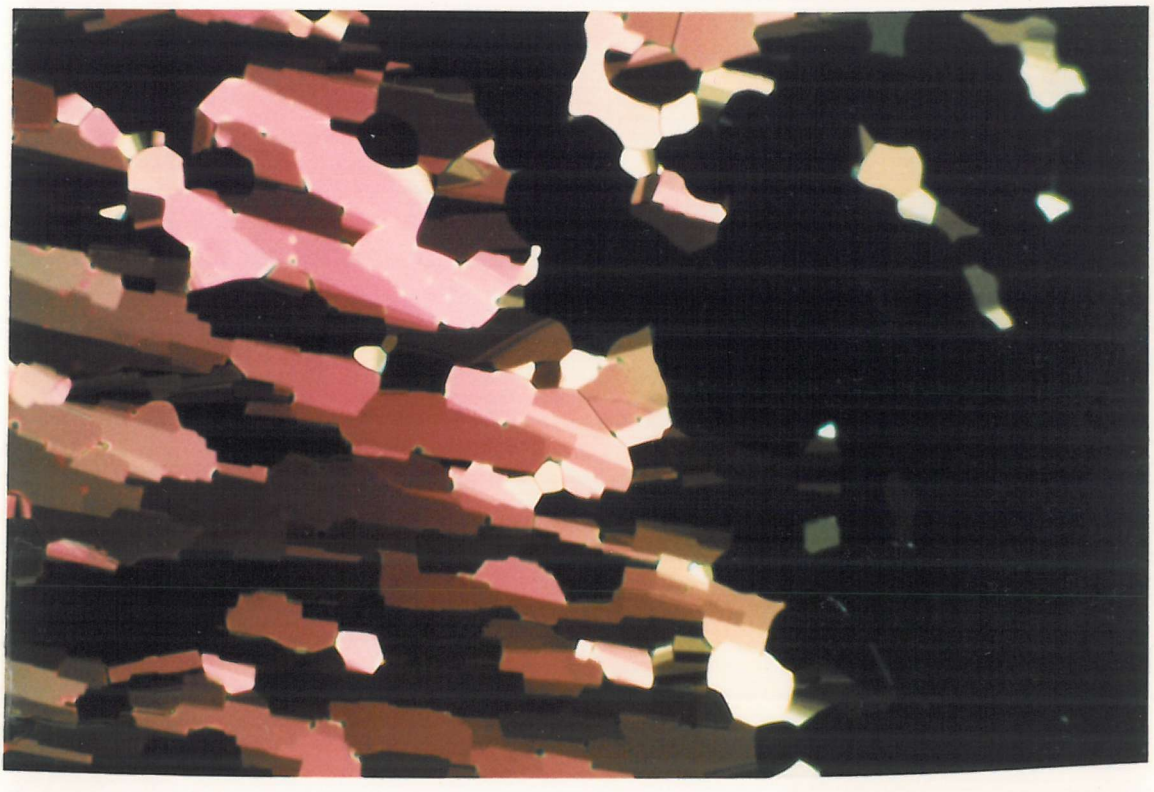

Plate 3.3.2 The paramorphotic focal-conic fan and homeotropic textures of the smectic B phase formed on cooling the smectic A phase of an equimolar mixture of 20CB and EBBA (T=54 °C).

Plate 3.3.3 The arced focal-conic fan and platelet textures of the smectic E phase formed on cooling the smectic B phase of an equimolar mixture of 20CB and EBBA (T=48 °C).

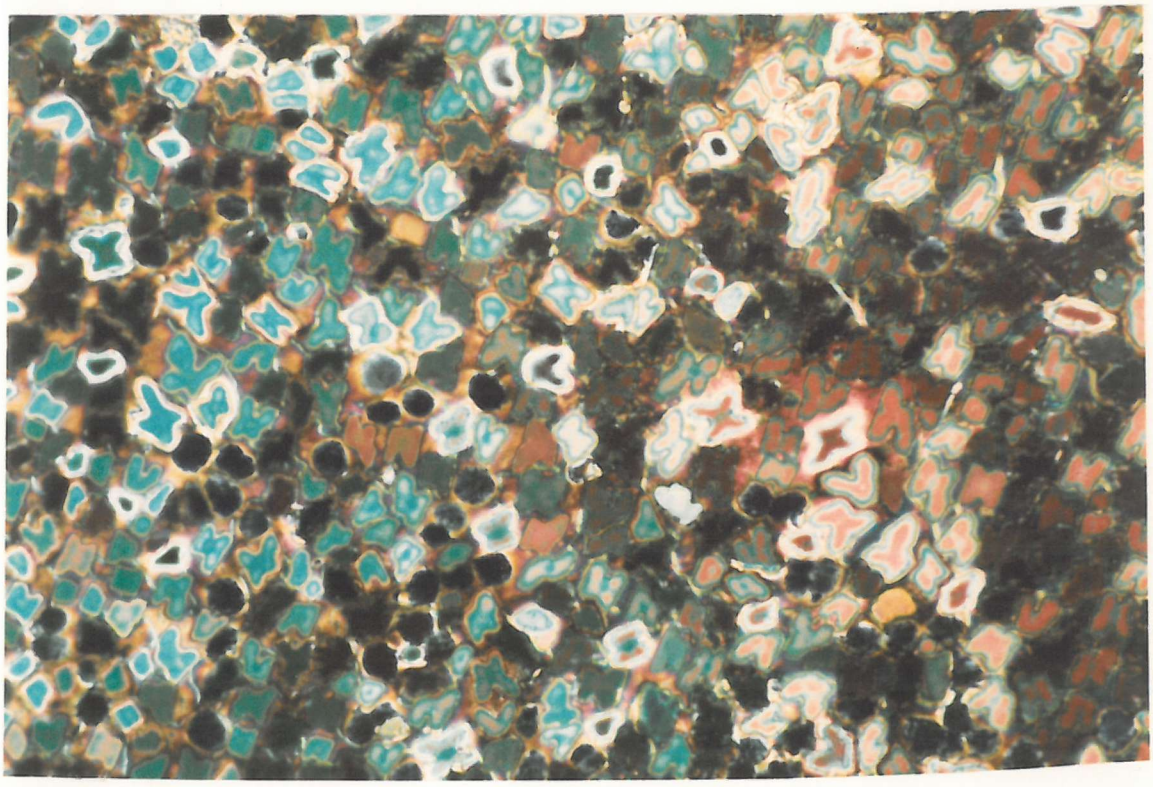

Plate 3.3.4 The mosaic texture of the smectic B phase separating from the nematic phase on cooling an equimolar mixture of 30CB and EBBA (T=75 °C).

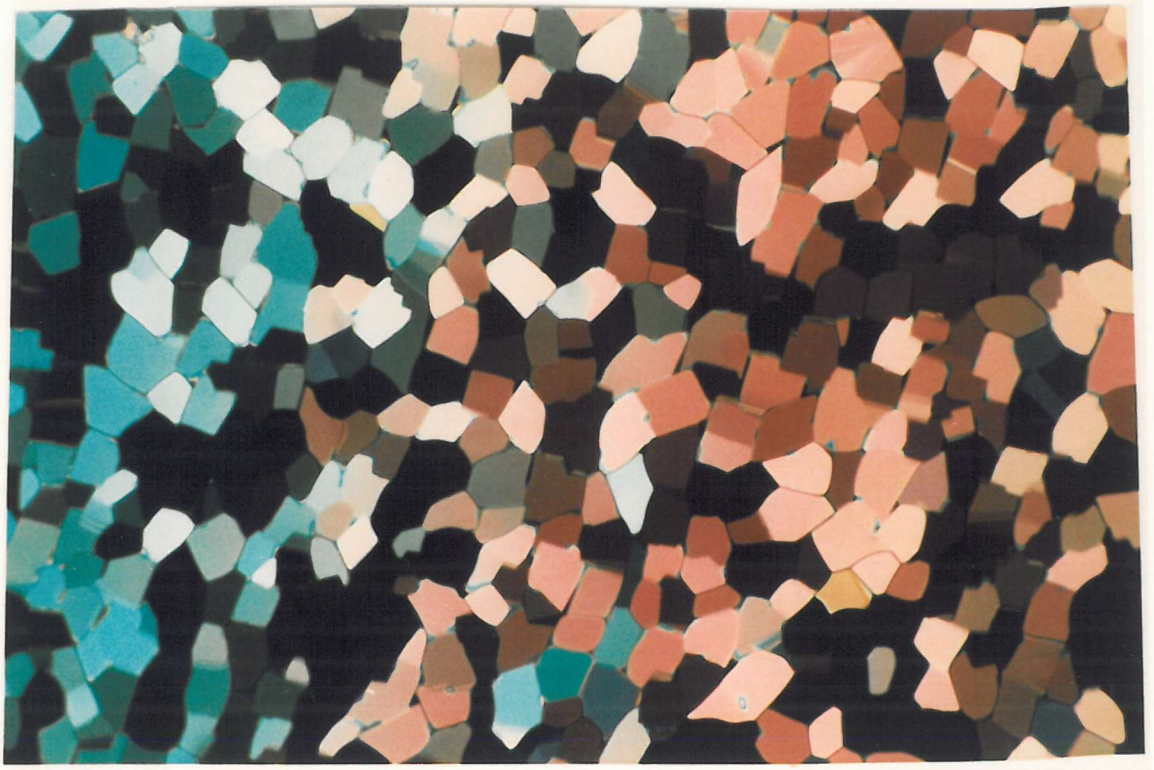

Plate 3.3.5 The mosaic texture of the smectic B phase formed on cooling the nematic phase of an equimolar mixture of 3OCB and EBBA (T=69 °C).

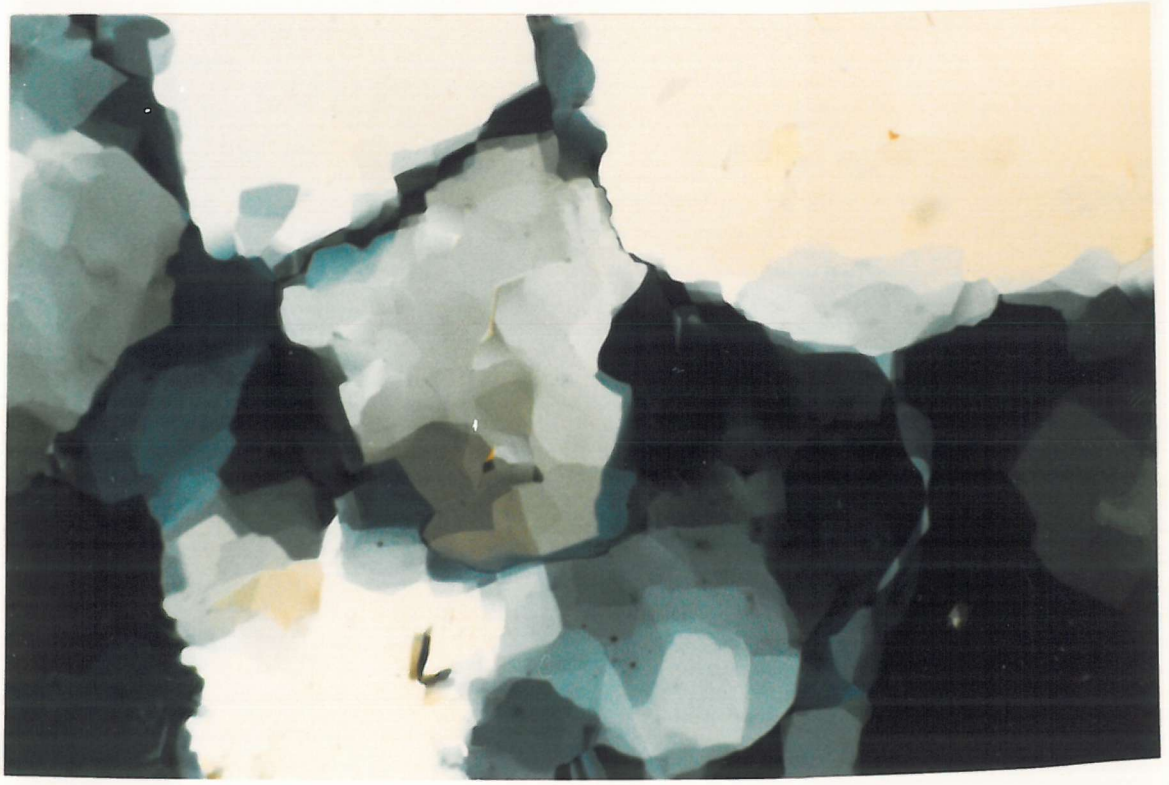

Plate 3.3.6 The platelet texture of the smectic E phase formed on cooling the mosaic texture of the smectic B phase for an equimolar mixture of 3OCB and EBBA (T=58 °C).

size of these spaces is dictated by the length of the alkyl spacer. Thus, as the terminal chain length increases there is insufficient space to accommodate the chains and so the layers are pushed apart so reducing the overlap and hence, the interaction between the cyanobiphenyl group and the Schiff's base. For long terminal alkyl chains the driving force responsible for the resurgence in smectic behaviour is not a charge transfer interaction but instead it is the electrostatic interaction between the polar and polarisable cyanobiphenyl groups resulting in the dimerisation of the molecules while the smectic phase results from the molecular inhomogeniety produced by the long terminal alkyl chains. This interpretation of the dependence of T_{SN} upon m also explains why the CB.O6O.m series exhibits smectic A phases of higher thermal stability than the corresponding CB.O4O.m compounds providing m is small. This arises simply because the size of the spaces in the intercalated structure are dependent upon the length of the alkyl spacer and hence, for a CB.O6O.m compound these spaces will be larger so accommodating the terminal chains more easily. The reduction in smectic behaviour for medium length terminal alkyl chains reflects the absence of any interactions that would tend to stabilise the conventional monolayer smectic A structure. Finally, it is clear why the dependence of T_{SN} upon m for the CB.O3O.m and CB.O5O.m series is much less dramatic and also, why the thermal stability of the smectic phases observed is lower than that of the even membered materials. Molecules having an odd length spacer can be thought of as being bent and so cannot pack efficiently into the intercalated structure proposed. Hence, the packing constraints in the structure are less severe than that in one composed of an even membered compound and so the dependence upon m would be anticipated to be less as indeed it is. It should be noted, however, that there is no evidence to suggest that the odd membered copounds adopt an intercalated structure in their smectic phases and it is impossible to establish this because the materials crystallise rapidly after forming the smectic phase.

3.4 Conclusions

This Chapter has introduced a new class of dimeric liquid crystals, the asymmetric dimer, in which two different mesogenic groups are linked through an alkyl spacer. The asymmetric dimers prepared, the CB.OnO.m series, exhibit properties that would largely have been anticipated with the exception of the dependence of the smectic-nematic transition temperatures upon m for, particularly, the CB.O4O.m and CB.O6O.m series. For these series, the thermal stability of the smectic A phase does not simply increase on lengthening the terminal alkyl chain but instead passes through a maximum before falling dramatically on increasing m. The smectic A phase subsequently reappears for long terminal alkyl chains. This behaviour was rationalised by proposing that the structure of the smectic A phase changes from being intercalated to interdigitated on increasing m and the cause of this is the difficulty in packing long alkyl chains into the proposed intercalated structure. For short alkyl chains the mixed core interaction, which is possibly a charge transfer interaction between the cyanobiphenyl group and the Schiff's base, is the driving force in the formation of an intercalated smectic A phase in which such interactions are maximised. As m is increased, however, the layers are pushed apart and so we see a reduction in T_{SN}. For long terminal chains the molecules dimerise, the driving force for this being the electrostatic interaction between the polar and polarisable cyanobiphenyl groups, and the smectic phase results from the molecular inhomogeniety produced by the long terminal alkyl chains. The dramatic fall in T_{SN} for compounds having intermediate values of m was attributed to the absence of any interactions that would stabilise the conventional monolayer structure of a smectic A phase.

3.5 References

[1] Saupe, A., 1966, Mol. Cryst., 1, 527.

[2] Burnell, E.E., and de Lange, C.A., 1982, J. Chem. Phys., 76, 3474.

[3] Robertson, J.C., Yim, C.T., and Gilson, D.F.R., 1971, Can. J. Chem., 49, 2345.

[4] Burnell, E.E., de Lange, C.A., and Snijders, J.G., 1982, Phys. Rev. A, 25, 2339.

[5] Barker, P.B., van der Est, A.J., Burnell, E.E., Patey, G.N., de Lange, C.A., and Snijders, J.G., 1984, Chem. Phys. Letts., 107, 426.

[6] Sachdev, H., 1987, PhD Thesis, University of Southampton.

[7] Emsley, J.W., Luckhurst, G.R., Shilstone, G.N., and Sage, I., 1984, Mol. Cryst. Liq. Cryst. Letts., 102, 223.

[8] see Chapter 2.

[9] Patey, G.N., Burnell, E.E., Snijders, J.G., and de Lange, C.A., 1983, Chem. Phys. Lett., 99, 271.

[10] Park, J.W., Bak, C.S., and Labes, M.M., 1975, J. Am. Chem. Soc., 97, 4398.

[11] Domon, M., and Billard, J., 1979, J. Phys. (Paris), 40, C3-413.

[12] Cladis, P.E., 1981, Mol. Cryst. Liq. Cryst., 67, 177.

[13] Keller, P., and Liebert, L., 1978, Solid State Phys. Suppl., 14, 19.

[14] Gray, G.W., 1979, The Molecular Physics of Liquid Crystals, edited by G.R. Luckhurst and G.W. Gray, Academic Press, Chapt. 1.

[15] Pohl, L., Eidenschink, R., Krause, J., and Weber, G., 1978, Phys. Lett., 65A, 169.

[16] Gray, G.W., and Goodby, J.W., 1984, Smectic Liquid Crystals - Textures and Structures, Leonard Hill.

[17] Diele, S., Weissflog, W., Pelz, G., Manke, H., and Demus, D., 1986, Liq. Cryst., 1, 101.

[18] Date, R.W., unpublished results.

CHAPTER 4 STRUCTURE-PROPERTY RELATIONSHIPS IN DIMERIC LIQUID CRYSTALS

4.1 Introduction

Dimeric liquid crystals are important for both fundamental and technological reasons and these have already been fully discussed in the introductory Chapter of this Thesis. The usefulness of such materials in both areas, however, has been largely restricted by the prohibitively high transition temperatures exhibited by the vast majority of dimeric compounds now known and consequently, the only properties that have been measured for dimers apart from transition temperatures and enthalpies of transition are order parameters [1]. The aim of this Chapter, therefore, was to investigate, by the synthesis of a range of new compounds, molecular structure-property relationships in dimers with a view, in particular, to reducing the transition temperatures.

It is well known that the lateral substitution of the mesogenic moiety in either monomeric or polymeric liquid crystals often results in the depression of the clearing temperatures [2]. For example, replacing a proton at position A by a methyl group in the ester:

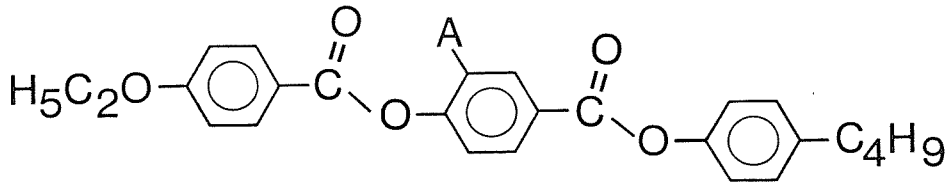

reduces the nematic-isotropic transition temperature from 231 °C to 179 °C [3]. Similarly, replacing the proton at position A by a methyl group in the polymer:

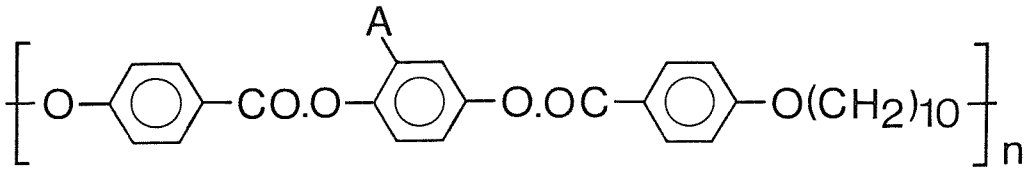

reduces the clearing temperature from 305 °C to 274 °C [4]. We note that although these depressions in mesophase stability appear large on the

centigrade scale, on an absolute scale they represent reductions in the clearing temperatures of only about 10% and 5% respectively. Nonetheless, lateral substitution is a means by which clearing temperatures may be reduced in monomeric and polymeric mesogens and it seemed reasonable to assume that such substitution would also reduce the transition temperatures of dimers. We synthesised, therefore, the α,ω-bis(2,4-dimethylanilinebenzylidine-4'-oxy)alkanes:

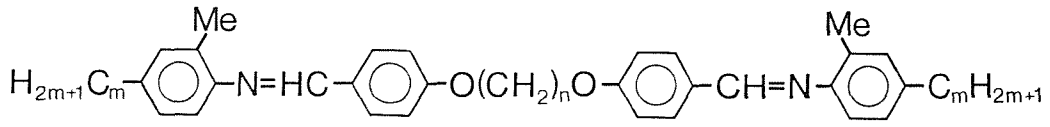

This particular series was chosen because the unsubstituted materials, the 1.On0.1 series, have been prepared and hence, the effect of the methyl substituents could be easily assessed. The mnemonic used for this series is 1(Me).On0.(Me)1 where n denotes the number of carbon atoms in the spacer. In addition, a series of laterally substituted asymmetric dimers have been synthesised, the α-(4-cyanobiphenyl-4'-oxy)-ω-(2,4-dimethylanilinebenzylidine-4'-oxy)alkanes:

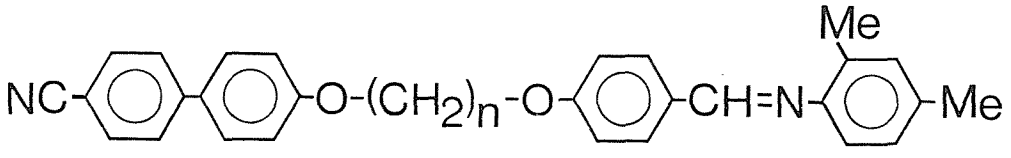

This series was chosen because the analogous unsubstituted materials, the CB.On0.1 series, are discussed in Chapter 3 and thus, the effect of a single lateral substituent could be determined. By analogy with the CB.On0.1 series, the mnemonic used for the laterally substituted compounds is CB.On0.(Me)1, in which n denotes the number of carbon atoms in the spacer.

Another method by which the transition temperatures of liquid-crystalline main-chain polymers have been reduced is the introduction of non-linear rigid groups into the main-chain. This acts to reduce the cylindrical shape of the backbone and by varying the percentage of comonomer, the liquid crystal-isotropic transition temperatures of the copolymer fall accordingly. For example, the transition temperatures

of the polyester:

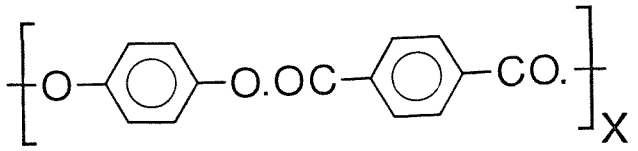

have been reduced by the insertion of napthalene [5]:

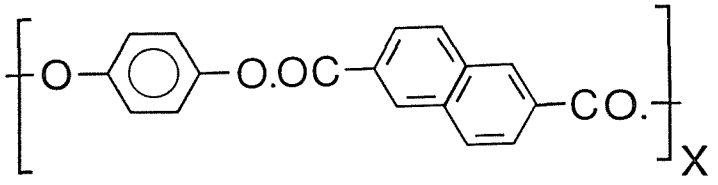

The replacement of a biphenyl unit by a napthalene group also acts to reduce the transition temperatures in monomeric liquid crystals. For example, the replacement of the biphenyl group in the ester:

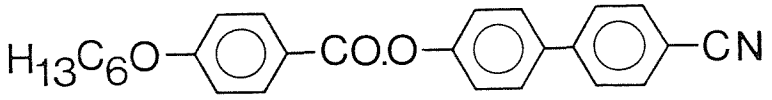

by napthalene:

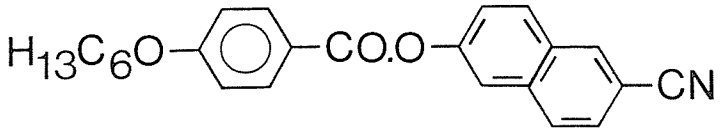

results in a reduction of the nematic-isotropic transition temperature of 86 °C but the effect of such substitution on melting points is less predictable [6]. In order to investigate the use of the napthalene moiety in dimers we synthesised two members of the homologous series, the α,ω-bis(6-cyanonapthalene-2-oxy)alkanes:

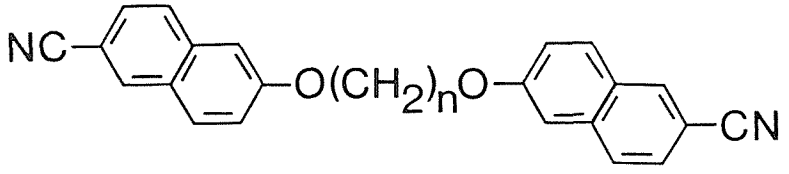

and use the mnemonic BCNO-n to describe them. The two homologues prepared were the fourth and fifth members and these were selected for two reasons; first, in a series of dimers the compound having four carbon atoms in the spacer has the second highest liquid crystal-

isotropic transtion temperature of the series but is more readily prepared than the second member which has the highest transition temperature and thus, if no mesogenic behaviour is observed for the fourth member, it is unlikely that the remaining will prove to be liquid-crystalline; secondly, it is always important to compare the properties of dimers possessing spacers of different parity and hence, the fifth member was prepared. This particular series was chosen because the analogous biphenyl dimers have been synthesised, the BCBO-n's [7] and hence, the effect of increasing the biaxialty of the mesogenic groups can be evaluated.

The chemical nature of the spacer in a semi-flexible main-chain polymer is known to exert a great influence on the liquid-crystalline properties of the material [4]. For example, if the spacer in:

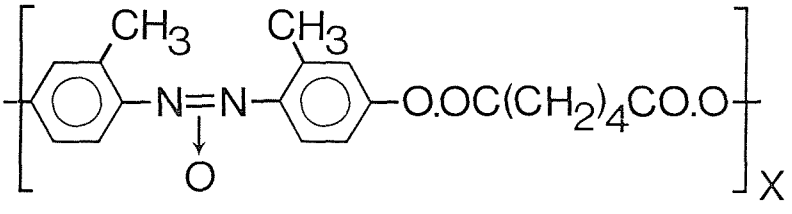

is branched by a methyl group:

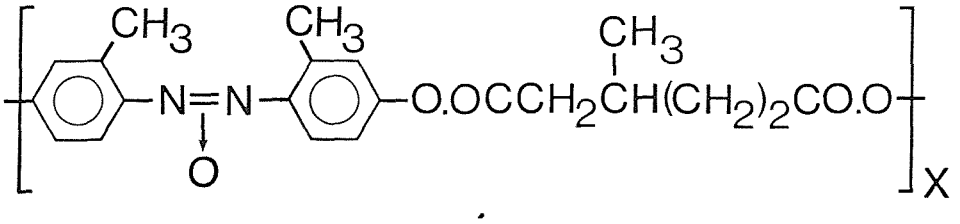

then the nematic-isotropic transition temperature is reduced by 45 °C [8]. In order to investigate whether a similar effect is observed in dimers we have synthesised 1,4-bis(4-cyanobiphenyl-4'-oxy)pentane (1,4-BCBO-5):

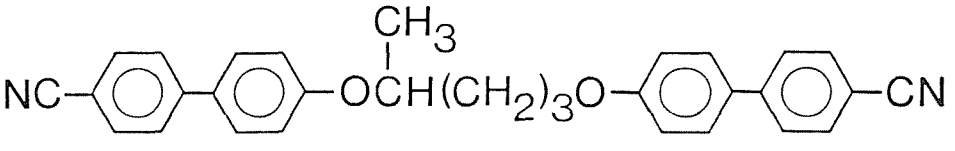

and compare its properties to those of the unbranched analogue BCBO-4 [7].

We have also synthesised a new class of dimer in which the mesogenic

groups are linked via an oligoethylene oxide spacer:

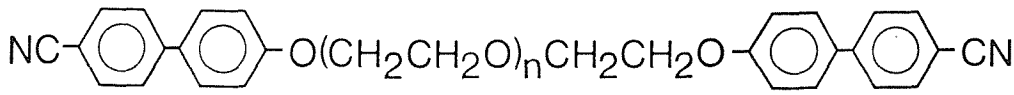

and the mnemonic used for this series is BCBO(EO)-n where n represents the number of ethylene oxide units in the spacer. This particular series was chosen for several reasons. First, the ground state conformations of a polyethyleneoxide chain are thought to differ from those of an alkyl chain [9]. Secondly, the corresponding mesogens possessing an alkyl spacer have been well studied [7]. Finally, polyethyleneoxide spacers have been incorporated into semi-flexible main-chain polymers [4,10].

For monomeric liquid crystals the effect of varying the central linkage in the mesogenic moiety on the liquid-crystalline properties of the compound is well documented [2]. This, however, is not the case for dimeric liquid crystals and so we synthesised the α,ω-bis(4,4'-cyanophenyloxycarboxyphenyloxy)alkanes:

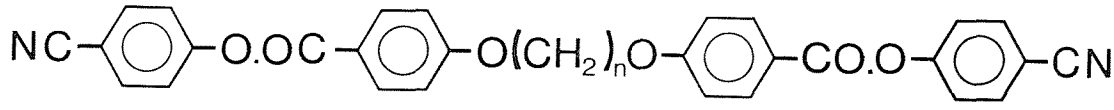

and compare their properties to those of the biphenyl analogues [7].

In monomeric liquid crystals, terminal alkyl chains serve to reduce the freezing point of a compound and so to investigate their effect in a dimer, we have synthesised the fourth and fifth members of the α,ω-bis(4-hexylbiphenyl-4'-oxy)alkanes:

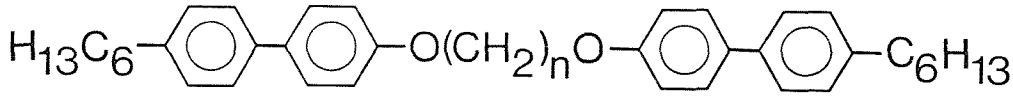

and use the mnemonic BHBO-n to describe this series. The preparation of just two homologues, BHBO-4 and BHBO-5, were for reasons identical to those offered for the BCNO-n series.

Finally, several asymmetric dimers of general structure;

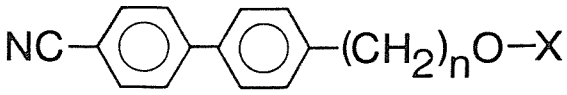

have been prepared and their properties are discussed. The mnemonic used to describe this series is CBnOX where n represents the number of carbon atoms in the spacer and X describes a semi-rigid group; Bip denotes biphenyl, CB represents cyanobiphenyl and BH indicates hexyl-biphenyl.

4.2 Experimental

4.2.1 α,ω-bis(2,4-dimethylanilinebenzylidine-4'-oxy)alkanes

The 1(Me).OnO.(Me)1 series was prepared in an analogous manner to that used for the m.OnO.m series described in Chapter 2. Thus, 2,4-dimethylaniline was added to a stirred solution of an α,ω-bis(4-formylphenyl-4'-oxy)alkane in hot ethanol. A few crystals of p-toluene sulphonic acid were added to the reaction mixture. This was stirred at room temperature for approximately four hours. The resulting white precipitate was filtered off, washed thoroughly with cold ethanol and dried. The compounds with odd length spacers were recrystallised twice from absolute ethanol with the exception of the third member which was recrystallised from ethyl acetate. The members possessing even length spacers were recrystallised twice from toluene. The yields in all cases exceeded 70%. Structural characterisation of the products was performed using ^{1}H-N.M.R. and I.R. spectroscopy.

Spectra

1(Me).O9O.(Me)1:

^{1}H-N.M.R.; δ ($CDCl_3$) 1.0-2.1 (m,7H), 2.3 (s,6H), 4.0 (t,2H), 6.7-7.0 (m,5H), 7.8 (d,2H), 8.2 (s,1H) ppm;

I.R.; ν 1620 cm^{-1}.

4.2.2 α-(4-cyanobiphenyl-4'-oxy)-ω-(2,4-dimethylanilinebenzylidine-4'-oxy)alkanes

The CB.OnO.(Me)1 series was prepared in an analagous manner to that used for the 1(Me).OnO.(Me)1 compounds described in the previous section. The synthesis of the α-(4-cyanobiphenyl-4'-oxy)-ω-(4-formylphenyl-4'-oxy)alkanes is described in Chapter 5. CB.030.(Me)1 and CB.050.(Me)1 were recrystallised twice from absolute ethanol and CB.040.(Me)1 and CB.060.(Me)1 were recrystallised twice from ethyl acetate. The yields for all four reactions exceeded 70% and structural characterisation of the products was performed using ^{1}H-N.M.R. and

I.R. spectroscopy.

Spectra

CB.030.(Me)1:

^{1}H-N.M.R.; δ ($CDCl_3$) 2.1-2.6 (m,8H), 4.2 (t,4H), 6.8-7.3 (m,7H), 7.4-8.1 (m,8H), 8.3 (s,1H) ppm.

I.R.; ν 1620, 2230 cm^{-1}.

4.2.3 α,ω-bis(4,4'-cyanophenyloxycarboxyphenyloxy)alkanes

The synthetic route for the preparation of these diesters involves four steps:

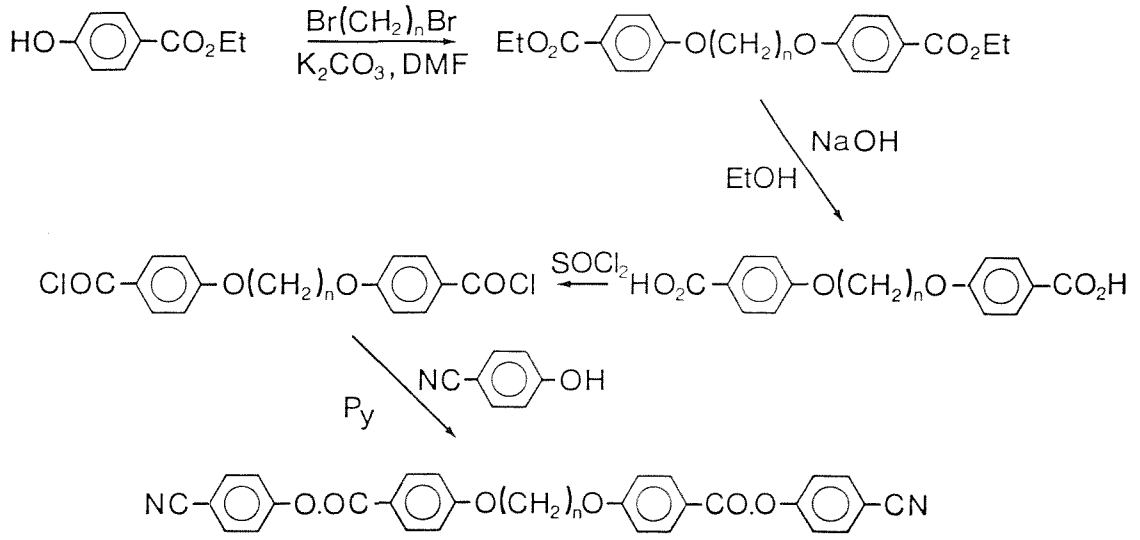

4,4'-Dicarbethoxy-α,ω-Diphenoxyalkanes

The method used for preparation of the 4,4'-dicarbethoxy-α,ω-diphenoxyalkanes was based upon that described by Griffin and Havers [11].

A mixture of ethyl 4-hydroxybenzoate (10g, 0.06mol), an α,ω-dibromoalkane (0.03mol) and potassium carbonate (12.5g, 0.09mol) in N,N-dimethylformamide (50ml) was stirred under reflux for four hours. The reaction mixture was allowed to cool and then poured into water

(500ml) and the resulting precipitate filtered off. The crude product was recrystallised from ethanol and yields ranged from 40% to 70%. Structural characterisation of the products was performed using ^{1}H-N.M.R. and I.R. spectroscopy and the melting points, listed in Table 4.2.3.1, agreed well with literature values [12].

Spectra

4,4'-dicarbethoxy-1,11-diphenoxyundecane:

^{1}H-N.M.R.; δ ($CDCl_3$) 0.9-1.7 (m,6H), 3.6 (t,1H), 4.0 (q,1H), 6.6 (d,1H), 7.7 (d,1H) ppm;

I.R.; ν 1710 cm^{-1}.

n	T_{CI}/ °C
2	104.5
3	107
4	100
5	92
6	130
7	93
8	101
9	85
10	109
11	84
12	86

Table 4.2.3.1 The melting points of the 4,4'-dicarbethoxy-α,ω-diphenoxyalkanes.

4,4'-Dicarboxy-α,ω-Diphenoxyalkanes

A 4,4'-dicarbethoxy-α,ω-diphenoxyalkane (c.a.10g) was added to a 10% solution of sodium hydroxide in 95% ethanol(100ml). The resulting

mixture was stirred under reflux for two hours. The reaction mixture was allowed to cool and then poured into cold water (500ml). This was heated to approximately 80 °C and if required more water was added in order to dissolve the sodium salt of the 4,4'-dicarboxy-α,ω-diphenoxy-alkane. The hot solution was acidified using concentrated hydrochloric acid and allowed to cool overnight. The resulting white precipitate was filtered off, washed thoroughly with water and recrystallised twice from aqueous ethanol. The yields ranged from 60% up to 80% and the melting points of the diacids, listed in Table 4.2.3.2, agree well with literature values [12]. Structural characterisation of the products was performed using I.R. spectroscopy.

Spectra

4,4'-dicarboxy-1,11-diphenoxyundecane:

I.R.; ν 1680, 2200-3200 cm^{-1}.

n	T_{CI}/ °C
2	357-359
3	330-332
4	343-346
5	289-291
6	290-292
7	245-248
8	286-288
9	254-256
10	272-274
11	247-249
12	256-260

Table 4.2.3.2 The melting points of the 4,4'-dicarboxy-α,ω-diphenoxyalkanes.

4,4'-Dichloroformyl-α,ω-Diphenoxyalkanes

A 4,4'-dicarboxy-α,ω-diphenoxyalkane (0.01 mol) was refluxed in freshly distilled thionyl chloride (0.1 mol) for two hours. The excess thionyl chloride was distilled off under vacuum. The resulting white solid was washed with dry petroleum ether and dried under a stream of dry nitrogen. The 4,4'-dichloroformyl-α,ω-diphenoxyalkane was used without further purification.

α,ω-bis(4,4'-cyanophenyloxycarboxyphenyloxy)alkanes

A 4,4'-dichloroformyl-α,ω-diphenoxyalkane (c.a. 0.01 mol) was added in small portions to a stirred solution of 4-cyanophenol (0.021 mol) in pyridine (40 ml) at 0 °C. The reaction mixture was allowed to warm to room temperature and stirred overnight. The mixture was poured over ice (100g) and acidified using concentrated hydrochloric acid. The resulting white precipitate was filtered off, washed thoroughly with water and dried. The crude product was recrystallised several times from a toluene/ethanol mixture. The yields were all in the range 65% to 80% and structural characterisation of the products was performed using I.R. spectroscopy.

Spectra

1,11-bis(4,4'-cyanophenyloxycarboxyphenyloxy)undecane:

I.R.; ν 1730, 2230 cm^{-1}.

4.2.4 BCBO(EO)-n

The BCBO(EO)-n compounds were prepared in two steps: first, the tosylation of diethylene glycol, triethylene glycol and tetraethylene glycol and second, the subsequent reaction of these with 4-cyano-hydroxybiphenyl.

Tosylation

A solution of toluene-4-sulphonyl chloride (540g) in pyridine (250ml)

and dichloromethane (50ml) was added dropwise to a stirred solution of the diol (1 mol) in pyridine (250ml) at 0°C. The temperature of the reaction mixture was kept below 40°C throughout this addition. The mixture was allowed to cool to room temperature and was stirred overnight. Water (50ml) was slowly added to the stirred mixture resulting in a sudden temperature increase and the reaction mixture was stirred for a further hour. This was then added to 6M hydrochloric acid (1.4 l) and the resulting mixture cooled causing the separation of an orange oil which was extracted using diethyl ether (3×200ml). The organic extracts were combined, dried over anhydrous sodium sulphate and the organic solvents were distilled off under reduced pressure to leave a white solid (yields 30%-40%). The ditosylates were not further purified for fear of decomposition. The products were characterised using I.R. spectroscopy which revealed strong bands at 1360 cm^{-1} and 1190cm^{-1} that corrrespond to S=O stretches and also, an aromatic band at 1600cm^{-1}. The spectra contained no bands in the region corresponding to O-H stretches.

BCBO(EO)-n

A mixture of a freshly prepared ditosylate (0.02 mol), 4-cyano-hydroxybiphenyl (9.7g, 0.05mol), potassium carbonate (9.7g, 0.07mol) and butanone (80ml) were refluxed with srirring overnight. The cooled reaction mixture was shaken thoroughly with water and extracted using dichloromethane (2×100ml). The combined organic extracts were dried using calcium chloride; the solvents were distilled off to leave a white solid that was recrystallised twice from ethyl acetate. The yields in all three cases were in the range 70%-80%. The products were characterised using ^{1}H-N.M.R. and I.R. spectroscopy. The purities of the BCBO(EO)-n compounds exceeded 99% as determined by differential scanning calorimetry.

Spectra

BCBO(EO)-3:

^{1}H-N.M.R.; δ ($CDCl_3$) 3.7 (s,2H), 3.9 (m, 1H), 4.1 (m,1H), 7.0 (d,1H), 7.5 (m,3H) ppm;

I.R.; ν 2230 cm^{-1}.

4.2.5 α,ω-bis(4-hexylbiphenyl-4'-oxy)alkanes

The two compounds of this series, BHBO-4 and BHBO-5, were prepared by refluxing a stirred mixture of 4-hexylhydroxbiphenyl (1g, 4mmol), an α,ω-dibromoalkane (2mmol) and potassium carbonate (2.21g 16mmol) in dimethylformamide (25ml) overnight. The reaction mixture was allowed to cool and then shaken thoroughly with water (200ml). The resulting white precipitate was filtered off, washed thoroughly with water and dried. The crude product was recrystallised twice from ethyl acetate (yields BHBO-4=70%; BHBO-5=65%). The products were characterised using I.R. spectroscopy which revealed no bands in the O-H stretching region and their purity was assessed by differential scanning calorimetry to be greater than 99%.

4.2.6 1,4-bis(4-cyanobiphenyl-4'-oxy)pentane

A mixture of 1,4-dibromopentane (10g, 0.04mol), 4-cyanohydroxybiphenyl (17.8g, 0.09mol), potassium carbonate (12.6g, 0.09mol) and sodium hydroxide (3.5g, 0.09mol) in dimethylformamide (30ml) was refluxed with stirring overnight. The reaction mixture was allowed to cool and then added to water (200ml). The resulting sticky white precipitate was extracted using dichloromethane (2×100ml); the combined organic extracts were washed with water (100ml), dried using calcium chloride and the solvents distilled off to leave a white solid. The crude product was purified by column chromatography using alumina as the adsorbate and dichloromethane as the eluent. The columned product was recrystallised from ethanol. The purity of the final product was checked using thin layer chromatography. The yield was 60% and the product was characterised using I.R. and ^{1}H-N.M.R. spectroscopy.

Spectra

1,4-BCBO-5:

^{1}H-N.M.R.; δ ($CDCl_3$) 1.4 (d,3H), 1.9 (m,4H), 4.1 (t,2H), 4.6 (m,1H), 7.0 (m,4H), 7.5 (d,4H), 7.6-7.8 (m,8H) ppm;

IR; ν 2210cm^{-1}.

4.2.7 α,ω-bis(6-cyanonapthalene-2-oxy)alkanes

6-cyano-2-hydroxynapthalene

6-cyano-2-hydroxynapthalene was prepared in 40% yield by the cyanation of 6-bromo-2-hydroxynapthalene. The cyanation proceedure used was identical to that described in detail in the following section. The crude 6-cyano-2-hydroxynapthalene was passed through silica gel using dichloromethane as eluent and subsequently recrystallised from aqueous ethanol. The melting point of the product (159 °C) agreed well with the literature value [6].

α,ω-bis(6-cyanonapthalene-2-oxy)alkanes

The two members of this homologous series were prepared in an analogous manner to that used for the BHBO-n compounds described in 4.2.5 by replacing 4-hexylhydroxybiphenyl with 6-cyano-2-hydroxynapthalene. The butyl homologue was recrystallised twice from toluene and the pentyl compound twice from ethyl acetate. Structural characterisation of the products was performed using I.R. spectroscopy which revealed a band at 2200cm^{-1} corresponding to the nitrile strectching mode.

4.2.8 α-(4-substitutedbiphenyl-4'-oxy)-ω-(4,4'-cyanpobiphenyl)alkanes

Several compounds belonging to this general class were synthesised via a four step synthetic route:

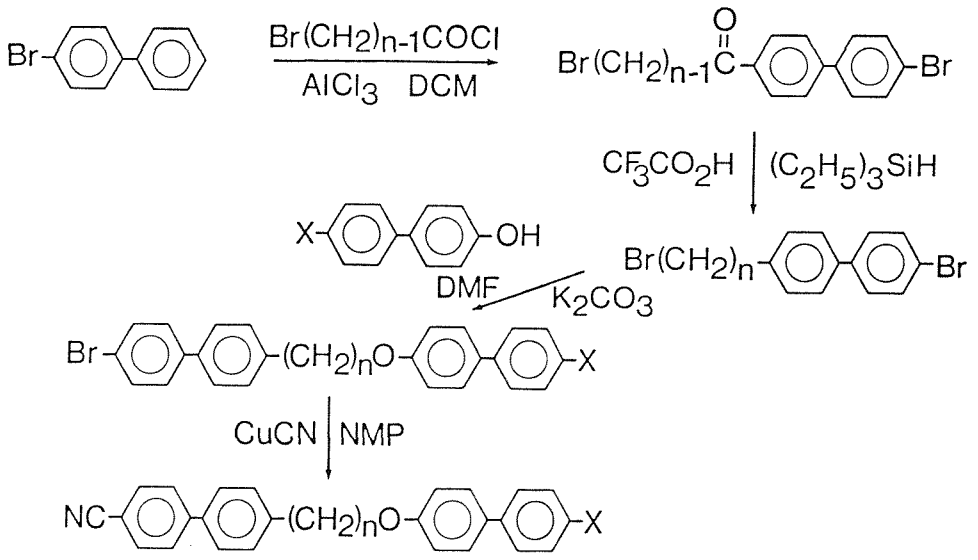

4-bromo-4'-(ω-bromoalkanoyl)biphenyl

The hexyl homologue was prepared using the commercially available 6-bromohexanoyl chloride which was redistilled immediately prior to use. 5-bromopentanoyl chloride was prepared by refluxing 5-bromopentanoic acid (50g) with freshly distilled thionyl chloride (125ml) for two hours. The excess thionyl chloride was then distilled off leaving 5-bromopentanoyl chloride which was purified by distillation under reduced pressure.

A solution of ω-bromoalkanoyl chloride (0.12 mol) and 4-bromobiphenyl (0.12 mol, 28g) in dichloromethane (30ml) was added dropwise to a stirred suspension of aluminium trichloride (0.12 mol, 16g) in dichloromethane at 0°C. The resulting mixture was alllowed to warm to room temperature and stirred overnight. The reaction mixture was added to water (250ml) and this was extracted using dichloromethane (3×100ml). The organic fractions were combined and dried using anhydrous calcium chloride. The dichloromethane was removed and the

crude product was passed through silica gel using a mixture of dichloromethane and petroleum ether (50:50) as eluent and recrystallised from ethanol. The products, 4-bromo-4'-(6-bromohexanoyl)biphenyl (yield 85%; C-N 75 °C; N-I 58 °C) and 4-bromo-4'-(5-bromopentanoyl)biphenyl (yield 80%; C-N 114 °C; N-I 56 °C), were characterised using ^{1}H-N.M.R. and I.R. spectroscopy.

Spectra

4-bromo-4'-(6-bromohexanoyl)biphenyl:

^{1}H-N.M.R.; δ ($CDCl_3$) 1.3-2.2 (m,3H), 3.0 (t,1H), 3.4 (t,1H), 7.4-7.7 (m,3H), 8.0 (d,1H) ppm;

I.R.; ν 1680cm^{-1}.

α-bromo-ω-(4,4'-bromobiphenyl)alkane

The carbonyl group in the Friedel-Crafts acylation product was reduced to a methylene unit using triethylsilane in trifluoroacetic acid [13]. Triethylsilane (0.14 mol, 22ml) was added dropwise to a stirred solution of 4-bromo-4'-(ω-bromoalkanoyl)biphenyl (0.06mol) in trifluoroacetic acid (0.44 mol, 34ml). During this addition care was taken to ensure that the temperature of the reaction mixture did not exceed 40 °C. This was stirred for a further three hours at room temperature and then shaken thoroughly with water (300ml). The resulting mixture was extracted using dichloromethane (2×100ml). The combined organic layers were dried using anhydrous calcium chloride and the solvent was removed to leave a white solid that was recrystallised from ethanol. The structures of 1-bromo-6-(4,4'-bromobiphenyl)hexane (yield 73%; C-I 75 °C) and 1-bromo-5-(4,4'-bromobiphenyl)pentane (yield 68%; C-I 73.5 °C) were verified using ^{1}H-N.M.R. and I.R. spectroscopy; the I.R. spectra of both compounds contained no bands in the carbonyl strectching region.

Spectra

1-bromo-6-(4,4'-bromobiphenyl)hexane:

^{1}H-N.M.R.; δ ($CDCl_3$) 1.2-2.1 (m,4H), 2.6 (t,1H), 3.4(t,1H), 7.1-7.7 (m,4H) ppm.

α-(4-substitutedbiphenyl-4'-oxy)-ω-(4,4'-bromobiphenyl)alkane

A mixture of α-bromo-ω-(4,4'-bromobiphenyl)alkane (0.012 mol), 4-hydroxy-4'-substitutedbiphenyl (0.012 mol), potassium carbonate (0.024 mol, 3.3g) and butanone (20ml) was refluxed with stirring for seven hours. The reaction mixture was then allowed to cool and added to water (150ml). This was extracted using dichloromethane (2×150ml) and the combined organic layers were dried using anhydrous calcium chloride. The solvents were subsequently distilled off and the crude product was recrystallised from ethyl acetate with the single exception of 1-(4-cyanobiphenyl-4'-oxy)-5-(4,4'-bromobiphenyl)pentane (yield 68%; C-I 220 °C; N-I 210 °C) which was recrystallised from toluene. The characterisation of the products was performed using ^{1}H-N.M.R. and I.R. spectroscopy.

Spectra

1-(4-biphenyl-4'-oxy)-6-(4,4'-bromobiphenyl)hexane (C-I 131 °C):
^{1}H-N.M.R.; δ ($CDCl_3$) 1.3-2.1 (m,8H), 2.7 (t,2H), 4.0 (t,2H), 6.9-7.7 (m,17H) ppm;

1-(4-hexylbiphenyl-4'-oxy)-6-(4,4'-bromobiphenyl)hexane (C-I 115 °C):
^{1}H-N.M.R.; δ ($CDCl_3$) 0.9 (t,3H), 1.1-2.1 (m,16H), 2.6 (t,4H), 3.9(t,2H), 6.8-7.6 (m,16H) ppm;

1-(4-cyanobiphenyl-4'-oxy)-6-(4,4'-bromobiphenyl)hexane (C-I 141.5 °C; N-I 124.5 °C):
^{1}H-N.M.R.; δ ($CDCl_3$) 1.2-2.0 (m,4H), 2.6 (t,1H), 4.0 (t,1H), 6.8-7.6 (m,8H) ppm;
I.R.; ν 2210cm^{-1}.

α-(4-substitutedbiphenyl-4'-oxy)-ω-(4,4'-cyanobiphenyl)alkane

The cyanation of the bromosubstituted compounds employed the method described by Coates and Gray [14].

A mixture of an α-(4-substitutedbiphenyl-4'-oxy)-ω-(4,4'-bromo-

biphenyl)alkane (0.006 mol), cuprous cyanide (0.0084 mol, 1.5g) and dry N-methyl 2-pyrrolidone (25ml) was stirred at 200°C for four hours. This was then cooled to 80°C and a solution of ferric chloride (5g) in water (10ml) and hydrochloric acid (4ml) was added. The reaction mixture was kept at 80°C for a further thirty minutes and then allowed to cool overnight. This was added to water (200ml) and extracted using dichloromethane (3×100ml). The combined organic layers were washed with water (3×100ml) and dried using anhydrous calcium chloride. The solvents were removed under vacuum and the crude product was passed through alumina and silica gel using dichloromethane as the eluent. All the products were recrystallised from ethanol with the exception of CB5OCB (yield 58%) which was recrystallised from toluene. The products were characterised using ^{1}H-N.M.R. and I.R. spectroscopy.

Spectra

1-(4-biphenyl-4'-oxy)-6-(4,4'-cyanobiphenyl)hexane:
^{1}H-N.M.R.; δ ($CDCl_3$) 1.1-2.1 (m,8H), 2.6 (t,2H), 3.9 (t,2H), 6.8-7.7 (m,17H) ppm;
I.R.; ν 2210 cm^{-1};

1-(4-hexylbiphenyl-4'-oxy)-6-(4,4'-cyanobiphenyl)hexane:
^{1}H-N.M.R.; δ ($CDCl_3$) 0.9 (t,3H), 1.1-2.0 (m,16H), 2.6 (t,4H), 3.9 (t,2H), 6.7-7.7 (m,16H) ppm;
I.R.; ν 2210cm^{-1};

1-(4-cyanobiphenyl-4'-oxy)-6-(4,4'-cyanobiphenyl)hexane;
^{1}H-N.M.R.; δ ($CDCl_3$) 1.3-1.9 (m,4H), 2.6 (t,1H), 3.9 (t,1H), 6.7-7.6 (m,8H) ppm;
I.R.; ν 2210cm^{-1}.

4.3 Results and Discussion

4.3.1 The α,ω-bis(2,4-dimethylanilinebenzylidine-4'-oxy)alkanes

The transitional properties of the 1(Me).OnO.(Me)1 series are listed in table 4.3.1.1; the compounds are monotropic nematogens with the exceptions of those having spacer lengths of 6, 8, 9 and 10 which are enantiotropic and 1(Me).O3O.(Me)1 for which no mesophase is observed. The nematic phase found for nine of the compounds was identified on the basis of the schlieren texture when viewed under the polarising microscope. The dependence of the transition temperatures upon the length of the flexible alkyl spacer is given in figure 4.3.1.1; both

n	T_{CI}/ °C †T_{CN}/ °C	T_{NI}/ °C	ΔH_{C-}/kJmol^{-1} ΔH_{NI}/kJmol^{-1}		ΔS_{C-}/R ΔS_{NI}/R	
3	134.5	(<87)	80.0	-	23.7	-
4	188.5	(163.5)	54.3	4.12	14.2	1.14
5	96	(71)	46.0	0.72	15.0	0.25
6	†135	145.5	44.3	5.19	13.1	1.49
7	103.5	(73.5)	32.7	0.88	10.5	0.30
8	†117.5	125	51.2	5.70	15.8	1.72
9	†81	83.5	35.5	1.72	12.1	0.58
10	†109	115	55.1	6.45	17.4	2.00
11	100	(90)	65.8	2.00	21.3	0.66
12	110.5	(105)	58.5	6.80	18.4	2.17

Table 4.3.1.1 The transition temperatures, enthalpies and entropies of transition of the 1(Me).OnO.(Me)1 series; ( ) denotes a monotropic transition. The uncertainties in the temperatures are ±1 °C and in the thermodynamic data are ±10%.

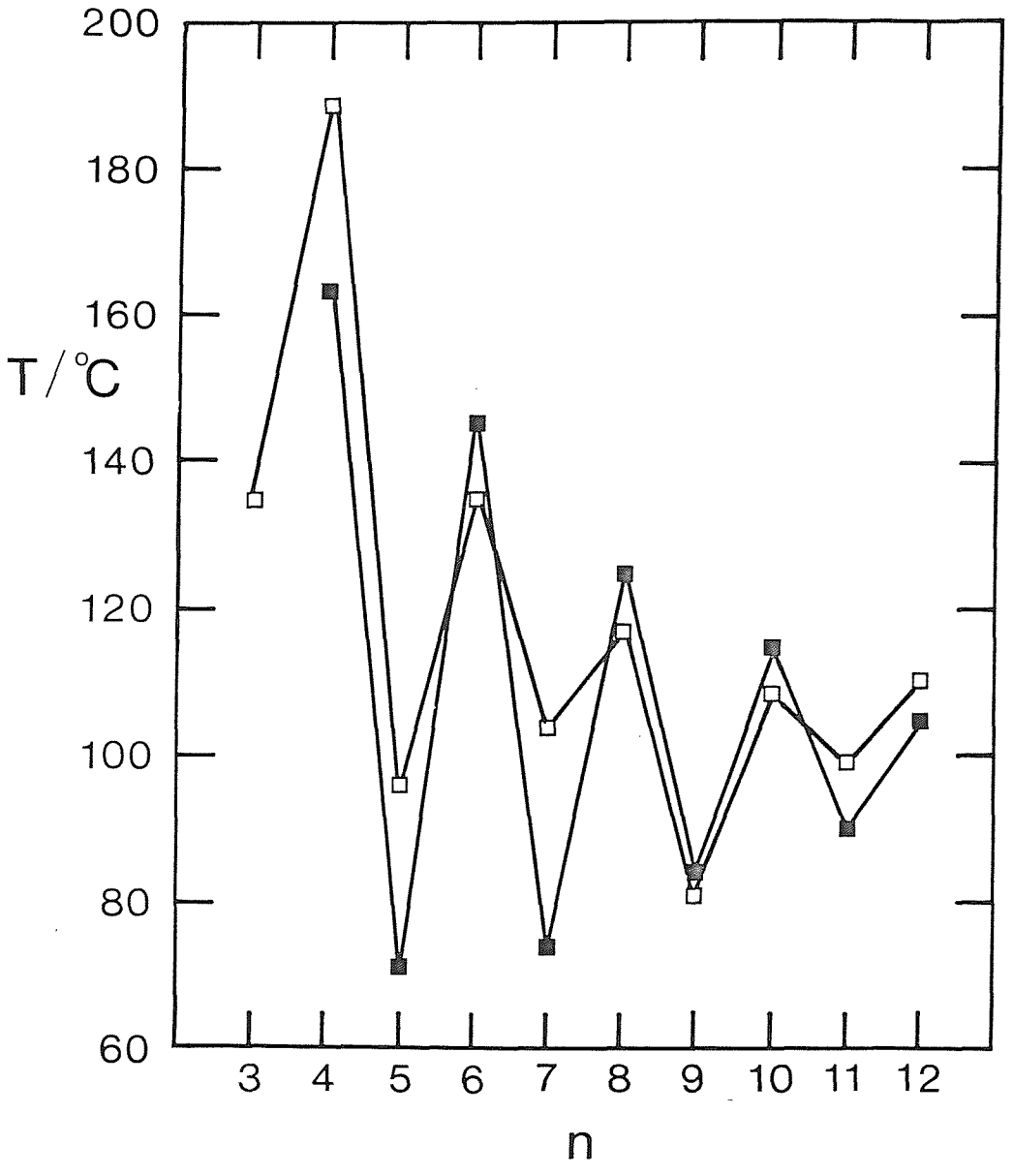

Figure 4.3.1.1 The dependence of the transition temperatures on the number of methylene groups in the flexible core for the 1(Me).OnO.(Me)1 series; □ indicates the melting points and ■ denotes the nematic-isotropic transitions.

the melting points and the nematic-isotropic transition temperatures show a pronounced odd-even effect with the compounds possessing an even length spacer having the higher values. The alternation in both sets of transition temperatures attenuates with increasing spacer length. Figure 4.3.1.2 compares the dependence of the transition temperatures upon the length of the flexible alkyl spacer for the 1(Me).OnO.(Me)1 and 1.OnO.1 series and this reveals that both the melting points and the nematic-isotropic transition temperatures are depressed by the addition of lateral methyl substituents. In all but two compounds the reduction of the nematic-isotropic transition temperature is greater than that of the melting point. This is emphasised in table 4.3.1.2 which lists the difference between the transition temperatures of the 1.OnO.1 and 1(Me).OnO.(Me)1 series.

n	ΔT_{C-} / °C	ΔT_{NI} / °C
3	28	>63
4	4	65.5
5	51.5	72.5
6	42	55
7	32.5	73.5
8	53	57
9	56	60
10	57.5	51
11	29.5	53
12	51.5	49.5

Table 4.3.1.2 The reductions in the transition temperatures of the 1.OnO.1 series upon the addition of two lateral methyl groups.

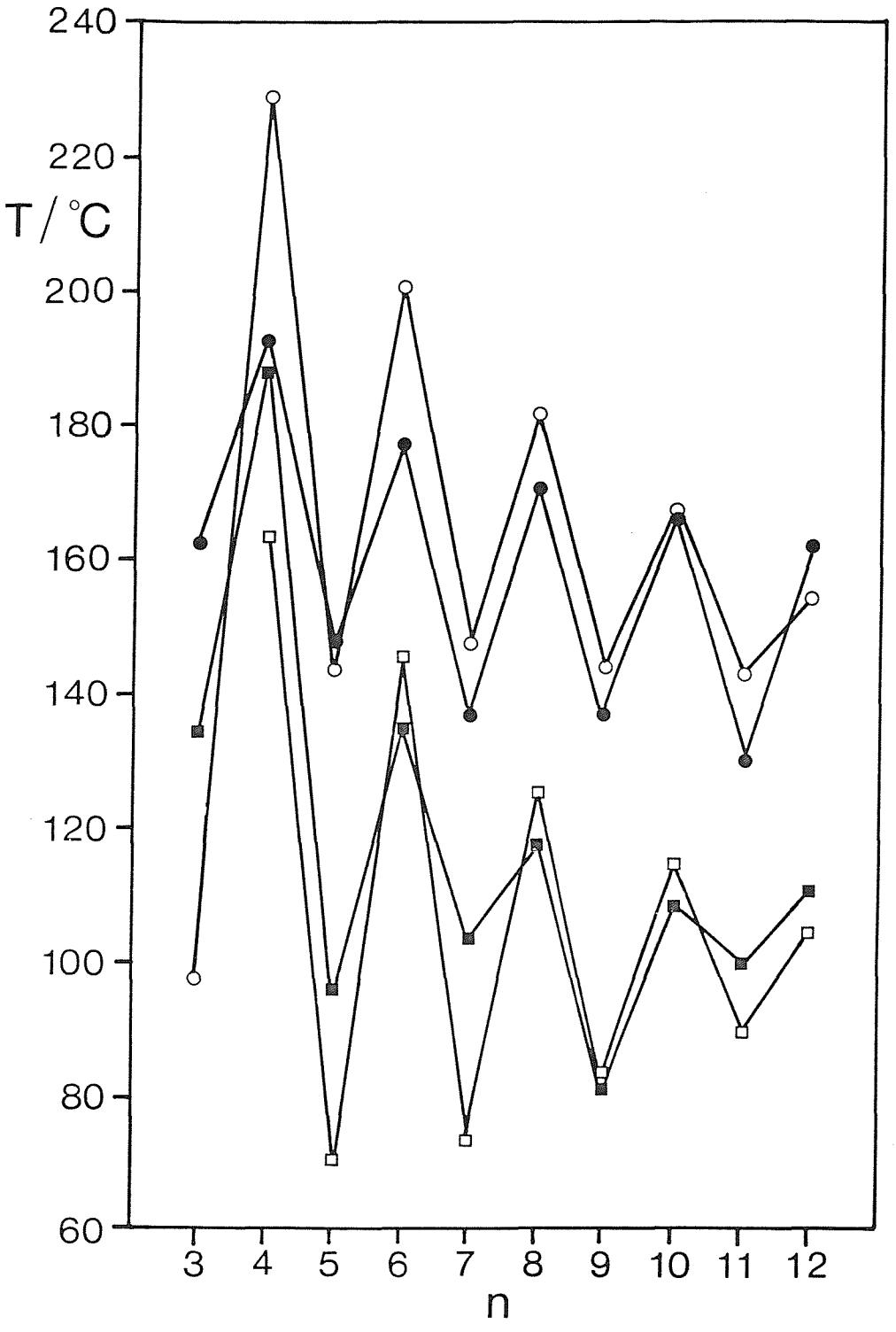

Figure 4.3.1.2 The dependence of the transition temperatures for the 1.OnO.1 and 1(Me).OnO.(Me)1 series on the number of methylene groups in the alkyl spacer; ● indicates the melting point and O denotes the nematic-isotropic transition for the 1.OnO.1 series and ■ represents the melting point and □ the nematic-isotropic transition for the 1(Me).OnO.(Me)1 series.

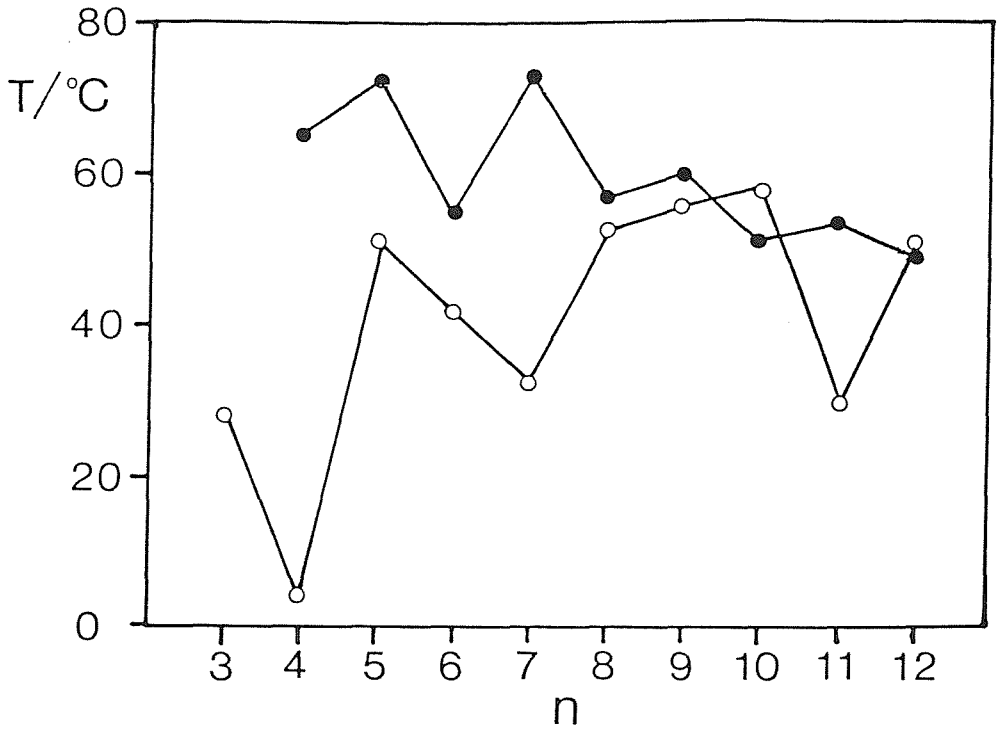

Figure 4.3.1.3 The dependence of the reduction of the melting points(o) and the nematic-isotropic-transition temperatures (●) on the number of methylene groups in the alkyl spacer on the addition of two lateral methyl groups to the 1.OnO.1 series.

Figure 4.3.1.3 shows the difference in transition temperatures between analogous homologues in the 1.OnO.1 and 1(Me).OnO.(Me)1 series. The reduction of the melting points of the 1.OnO.1 series on the lateral substitution of two methyl groups behaves irregularly on increasing the length of the alkyl spacer. The depressions in the nematic-isotropic transition temperatures, however, show an odd-even effect which attenuates on increasing n; the compounds with an even length spacer show a smaller reduction in nematic thermal stabilty upon lateral substitution than do those possessing an odd length spacer. It is interesting to note that for the monomeric analogues, the nO.m's, a lateral methyl substituent:

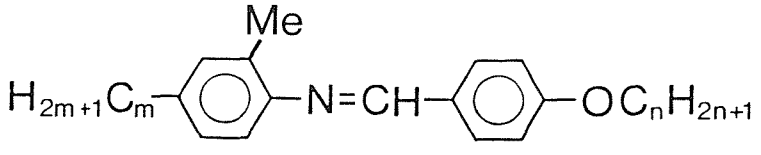

reduces the clearing temperature by about 56 °C, irrespective of the

values of n and m [15,16]. If we compare this value to those listed in table 4.3.1.2 it is evident that the reductions in the clearing temperatures of the dimers are similar to those observed for the monomers even though two lateral methyl groups have been incorporated into the dimeric structure. This will be discussed later.

Figure 4.3.1.4 shows the dependence of the entropy change associated with the nematic-isotropic transition upon the length of the flexible spacer for both the 1.OnO.1 and 1(Me).OnO.(Me)1 series and very similar behaviour is observed for both. The entropies show a very pronounced odd-even effect on varying n with the even membered compounds having the higher values. This alternation atenuates in a relative sense on increasing n for both series. Also, both sets of data show an underlying increase in the value of the entropy change on increasing the spacer length. It should be stressed that the entropy change measured for a 1(Me).OnO.(Me)1 compound is invariably less than that of the corresponding 1.OnO.1 member. This is a surprising result if compared to monomeric liquid crystals for which it is often found that lateral substitution increases the entropy change associated with the nematic-isoptropic transition [2]. The nematic-isotropic transition temperatures of the 1(Me).OnO.(Me)1 series are higher than predicted from the effects of lateral substitution in monomers and therefore, the entropy change at the transition will be smaller than expected. The observed decrease in $\Delta S/R$, however, is difficult to interpret unambiguously although presumably reflects, in part, the increase in the biaxiality of the mesogenic groups which results in the flexible spacer being less strongly 'anchored' at its ends and thus, the conformational entropy decreases.

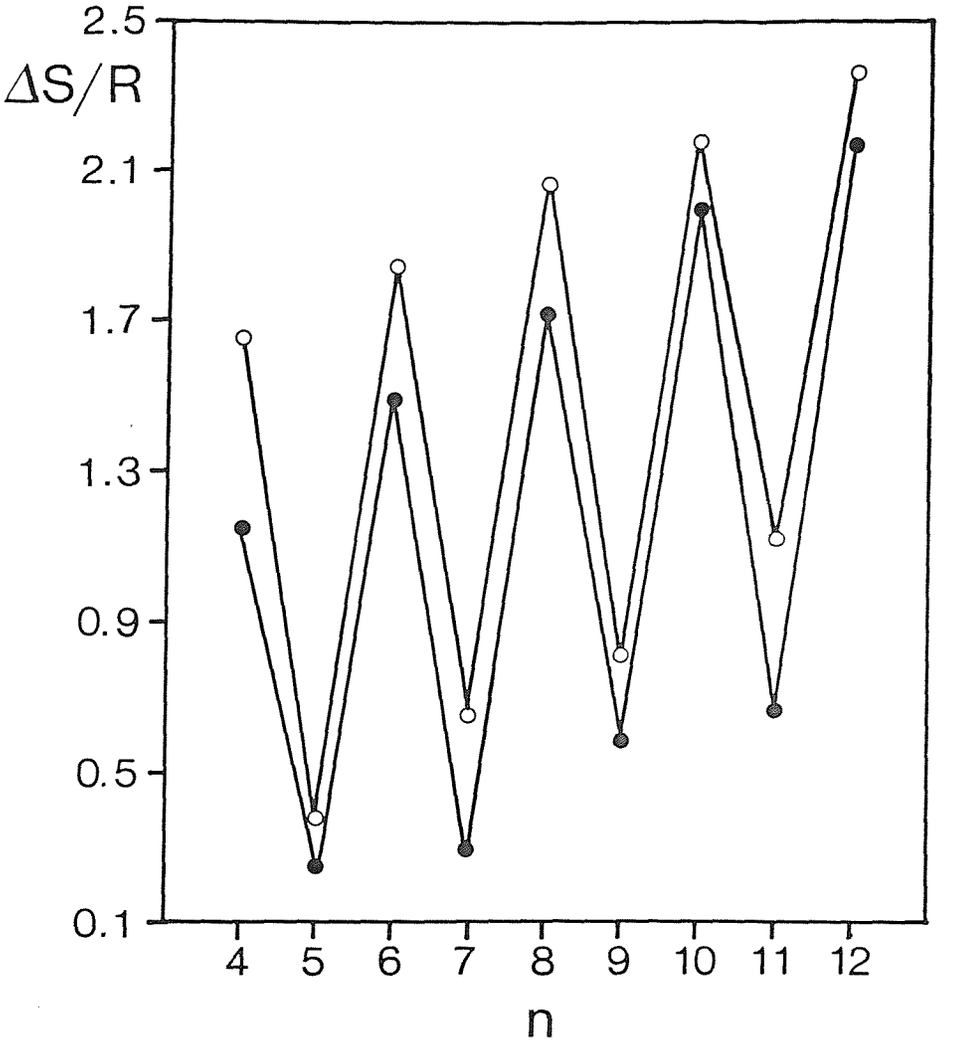

Figure 4.3.1.4 The dependence of the entropy change associated with the nematic-isotropic transition on the number of methylene groups in the alkyl spacer for the 1.OnO.1 (o) and 1(Me).OnO.(Me)1 (●) series.

4.3.2 The α-(4-cyanobiphenyl-4'-oxy)-ω-(2,4-dimethylaniline-benzylidine-4'-oxy)alkanes

The transitional properties of the CB.OnO.(Me)1 series are listed in table 4.3.2.1; the compounds are all enantiotropic nematogens with the exception of CB.O3O.(Me)1 which is monotropic. The dependence of the transition temperatures upon the length of the flexible spacer is shown in figure 4.3.2.1. The melting points show no regular behaviour on increasing n whereas the nematic-isotropic transition temperatures exhibit a very large odd-even effect.

n	T_{C-N} / °C †T_{C-I} / °C	T_{N-I} / °C	ΔH_{C-}/kJmol^{-1}	ΔH_{N-I}/kJmol^{-1}	ΔS_{C-}/R	ΔS_{N-I}/R
3	†137.0	(71.0)	38.6	0.30	11.4	0.11
4	131.5	203.5	40.7	6.26	12.1	1.58
5	124.5	132.5	29.7	1.29	8.99	0.38
6	133.0	176.5	34.0	6.04	10.1	1.62

Table 4.3.2.1 The transition temperatures, enthalpies and entropies of transition of the CB.OnO.(Me)1 series; () denotes a monotropic transition. The uncertainties in the temperatures are ±1 °C and in the thermodynamic data are ±10%.

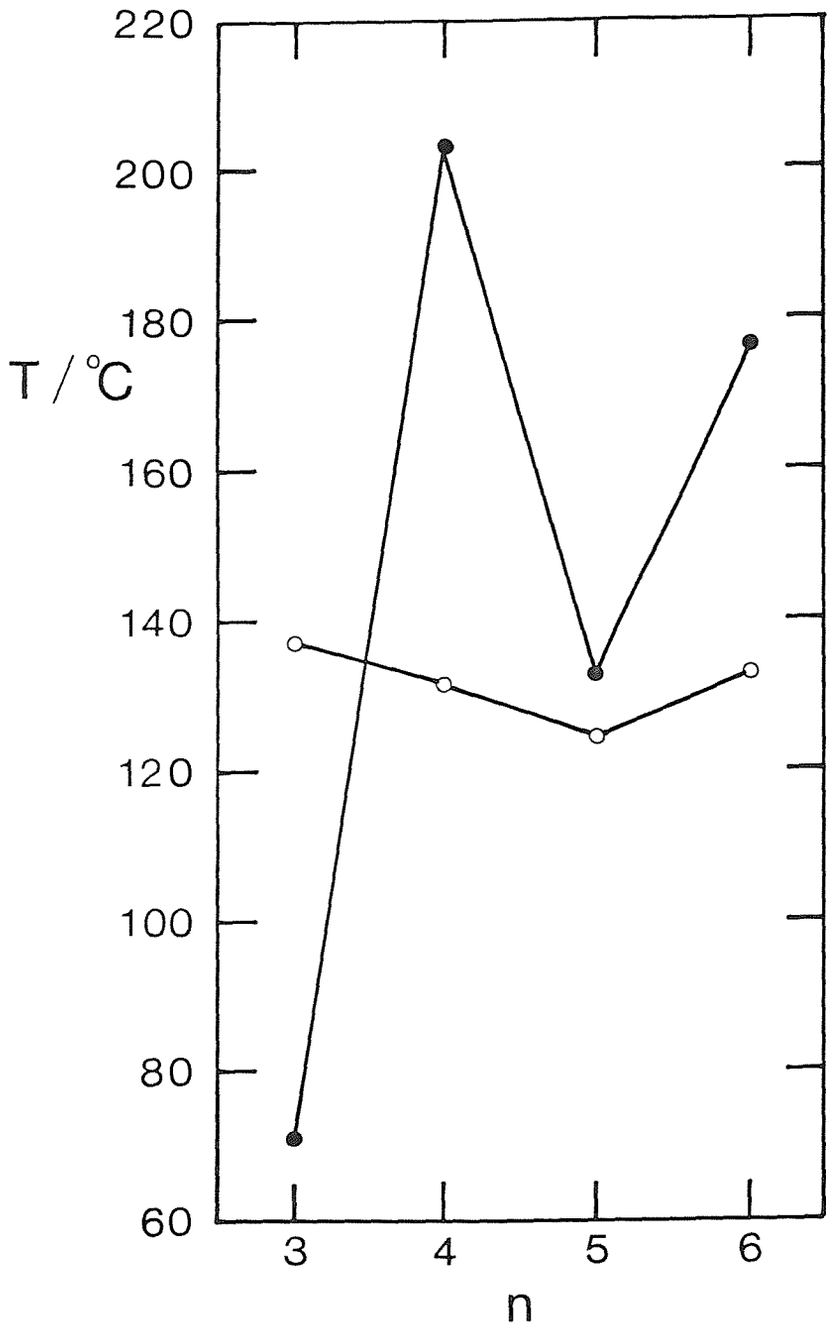

Figure 4.3.2.1 The dependence of the melting points (O) and the nematic-isotropic transition temperatures (●) on the length of the flexible spacer for the CB.OnO.(Me)1 series.

Figure 4.3.2.2 compares the melting points of the CB.OnO.(Me)1 series to their unsubstituted analogues, the CB.OnO.1 series, and reveals that lateral substitution of the CB.OnO.(Me)1 compounds is accompanied by a significant decrease in their melting points with the exception of CB.O5O.(Me)1 which has a slightly higher melting point than CB.O5O.1. A similar comparison of the nematic-istropic transition temperatures of the two series is shown in figure 4.3.2.3 and it is clear that the nematic thermal stability of the unsubstituted compounds is higher than that of the laterally substituted materials. However, this diference in the nematic-isotropic transition temperatures is not as large as would be anticipated on the basis of the monomeric examples [15,16] described in the preceeding section.

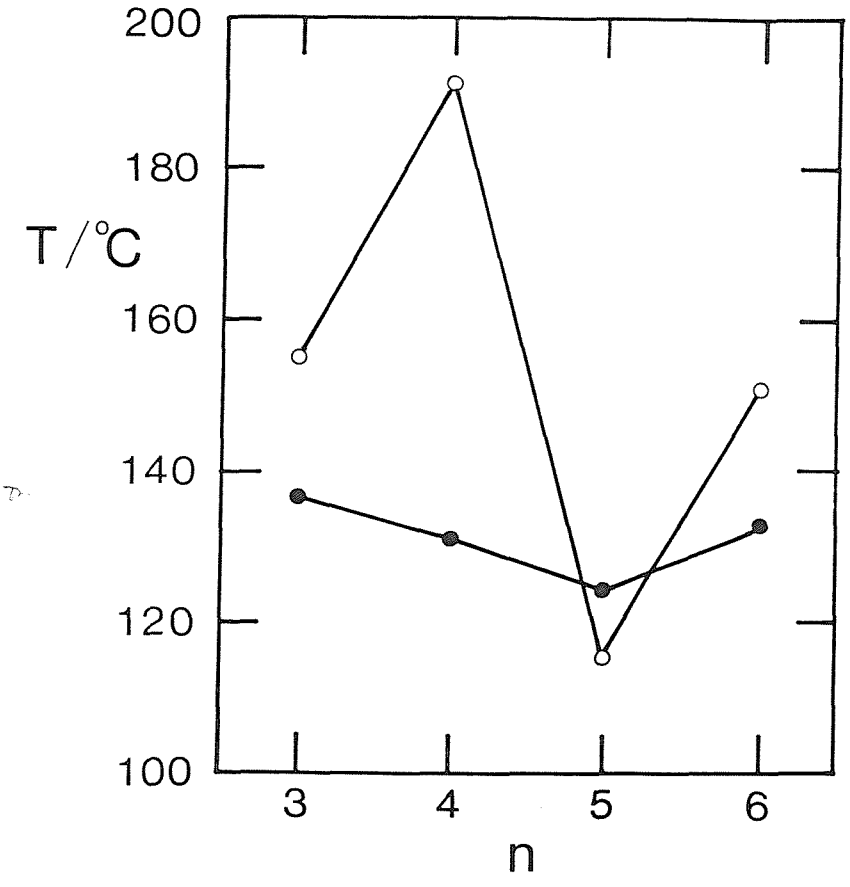

Figure 4.3.2.2 The dependence of the melting points on the number of methylene groups in the alkyl spacer for the CB.OnO.1 (O) and the CB.OnO.(Me)1 (●) series.

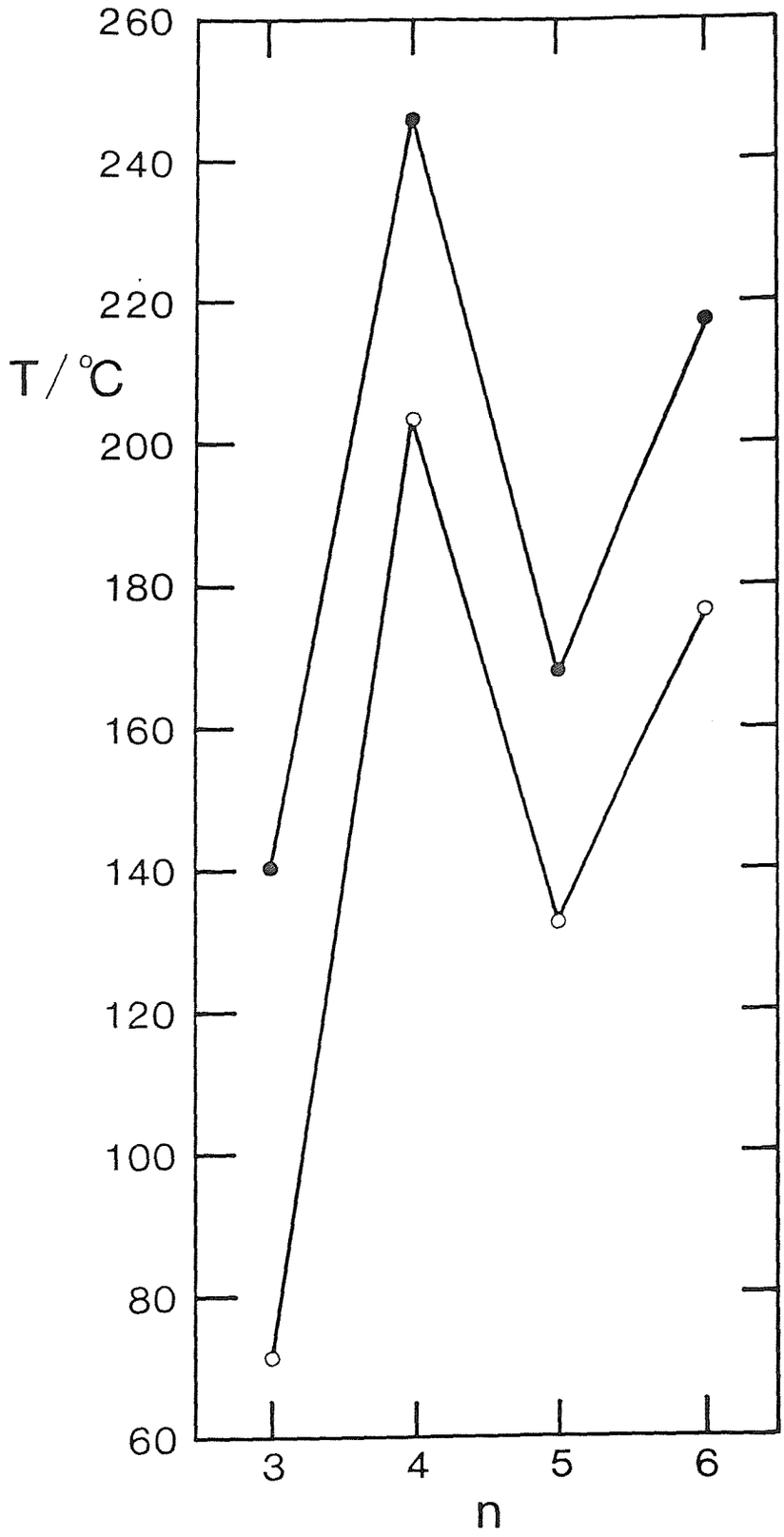

Figure 4.3.2.3 The dependence of the nematic-isotropic transition temperatures on the number of methylene groups in the flexible alkyl spacer for the CB.OnO.1 (●) and the CB.OnO.(Me)1 (O) series.

Figure 4.3.2.4 shows the dependence of the entropy change associated with the nematic-isotropic transition upon the length of the spacer for both the CB.OnO.(Me)1 and CB.OnO.1 series. A very large alternation in the entropy changes upon varying n is evident for both series. The entropy changes for the CB.OnO.1 compounds are all higher than the corresponding laterally substituted materials. This may be rationalised using exactly the same arguments offered in the preceeding section to explain the reduction in $\Delta S_{NI}/R$ on laterally substituting the 1.OnO.1 series. Further speculation concerning the CB.OnO.(Me)1 and 1(Me).OnO.(Me)1 series must await the results from theoretical calculations in which the change in the rigid group is modelled by reducing X_a and hence, increasing the ratio X_c/X_a.

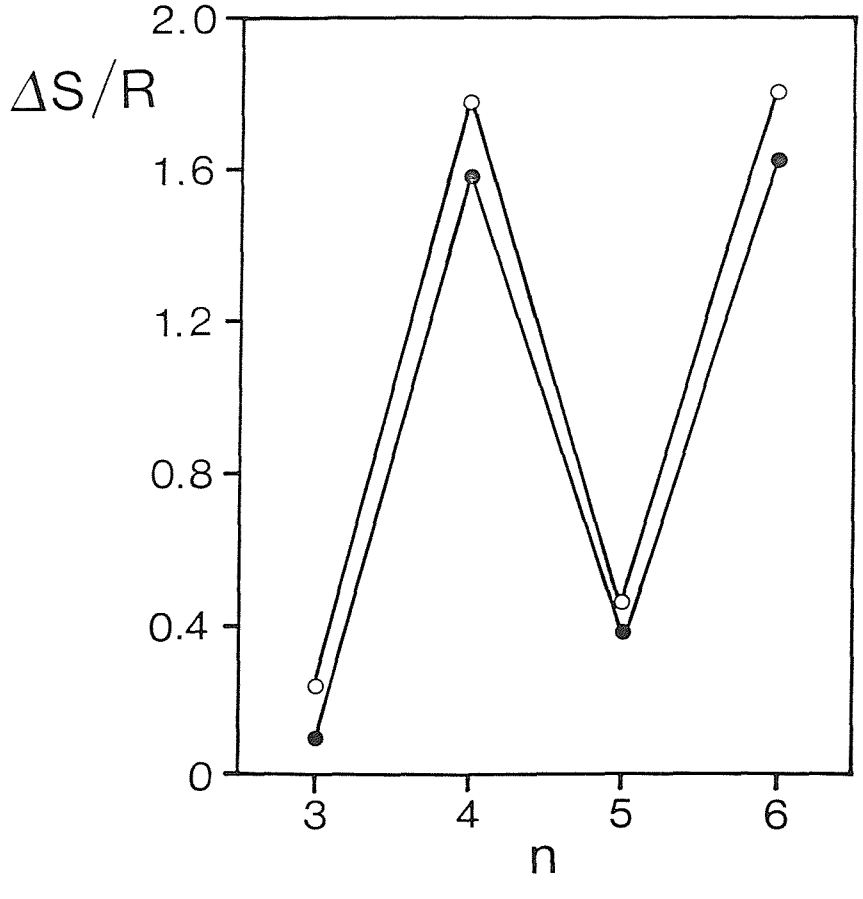

Figure 4.3.2.4 The dependence of the entropy change associated with the nematic-isotropic transition on the number of methylene groups in the alkyl spacer for the CB.OnO.1 (o) and the CB.OnO.(Me)1 (●) series.

The four CB.OnO.(Me)1 compounds are purely nematic whereas three of the corresponding CB.OnO.1 materials exhibit smectic phases. In fact, the nematic phases of CB.O4O.(Me)1 and CB.O6O.(Me)1 both supercool to approximately 35 °C and this represents a decrease in smectic phase stability of at least 60 °C. This observation is easy to understand remembering that in Chapter 3 the smectic phases of CB.O4O.1 and CB.O6O.1 are proposed to have intercalated structures that arise from the mixed core interaction. Lateral substitution of the Schiff's base group dilutes this interaction and causes steric problems. Thus, the smectic thermal stability would be predicted to decrease and this is indeed observed.

4.3.3 The α,ω-bis(4,4'-cyanophenyloxycarboxyphenyloxy)alkanes

The transitional properties of this homologous series are listed in table 4.3.3.1; all ten compounds are enantiotropic nematogens. After this work had been completed, Griffin et al [17] reported the transition temperatures of these compounds and the agreement between the two sets of data is very good. It should be noted that Jin et al [18] had earlier described the tenth member of this series but the nematic-isotropic transition temperature given is some 10 °C lower than that presented here.

Figure 4.3.3.1 shows the dependence of the transition temperatures upon the length of the flexible spacer, n, for the α,ω-bis(4,4'-cyanophenyloxycarboxyphenyloxy)alkanes. The melting points exhibit a pronounced odd-even effect up to the nonyl homologue. The nematic-isotropic transition temperatures also show a very large alternation upon varying the parity of n which attenuates with increasing n. Figure 4.3.3.2 illustrates the dependence of the entropy change associated with the nematic-isotropic transition on the length of the alkyl spacer for these diesters and also, for the BCBO-n's. The entropy change for both series of compounds exhibit a dramatic odd-even effect upon varying n, with an underlying increase in ΔS/R for both odd and even membered compounds. The entropy change for a diester possessing an odd number of carbon atoms in the spacer is larger than

n	T_{CN}/ °C	T_{NI}/ °C	$\Delta H_{C\_}$/kJmol^{-1}	ΔH_{NI}/kJmol^{-1}	$\Delta S_{C\_}$/R	ΔS_{NI}/R
3	183	190	22.2	2.92	5.87	0.76
4	220	247	45.7	7.18	11.2	1.66
5	158	204	32.4	3.88	9.05	0.98
6	200	223	47.1	7.23	12.0	1.76
7	171	193	66.3	4.04	18.0	1.05
8	186	204	42.7	7.25	11.2	1.83
9	162	182	51.1	4.82	14.2	1.28
10	161	193	47.6	7.78	7.66	2.01
11	136	171	54.2	5.09	15.4	1.38
12	155	184	45.4	7.79	6.73	2.05

Table 4.3.3.1 The transition temperatures, enthalpies and entropies of transition of the α,ω-bis(4,4'-cyanophenyloxycarboxyphenyloxy)-alkanes. The uncertainties in the temperatures are ±2 °C and in the thermodynamic data are ±10%.

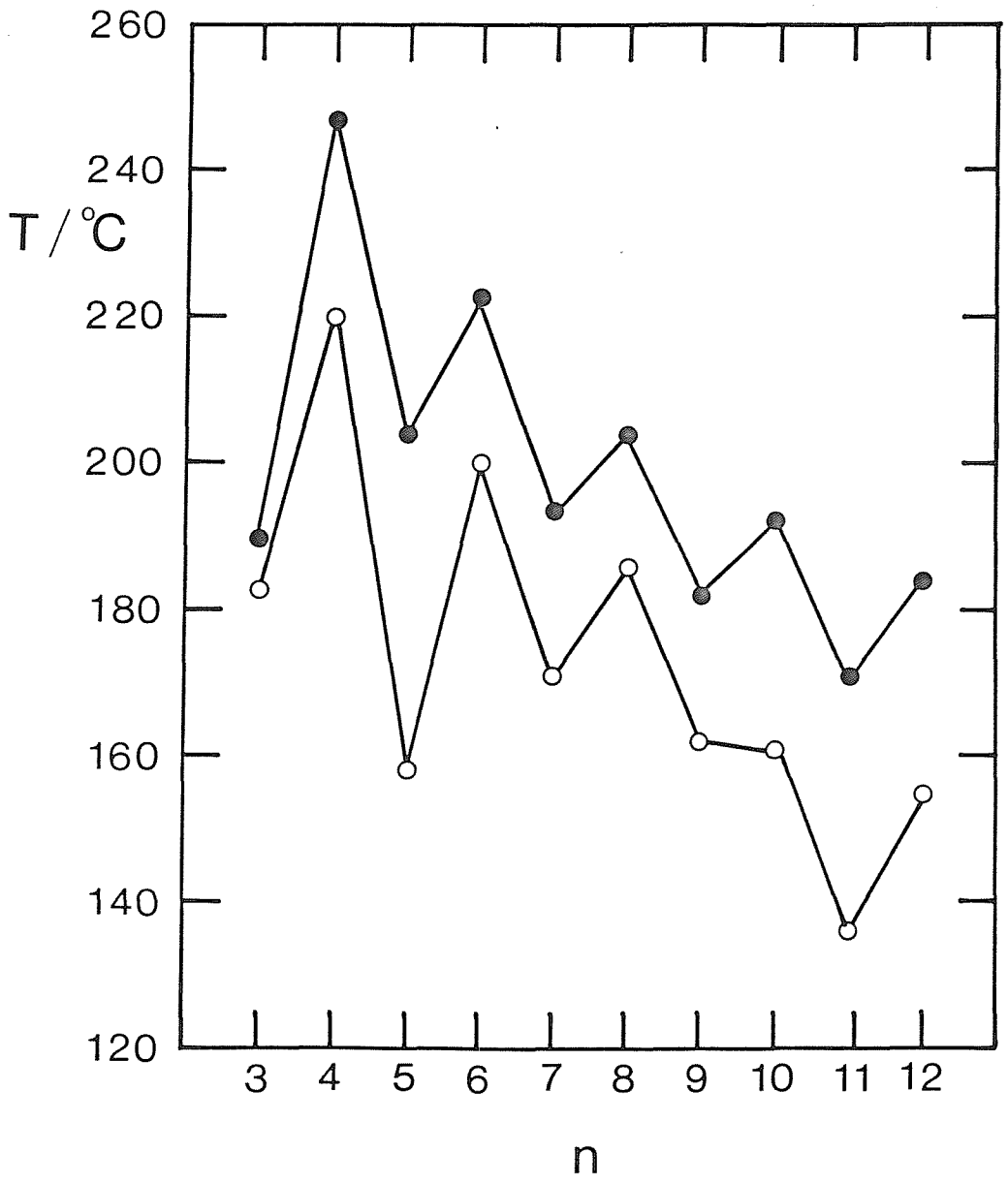

Figure 4.3.3.1 The dependence of the transition temperatures for the α,ω-bis(4,4'-cyanophenyloxycarboxyphenyloxy)alkanes on the number of methylene groups in the flexible spacer; O indicates the melting point while ● denotes the nematic-isotropic transition.

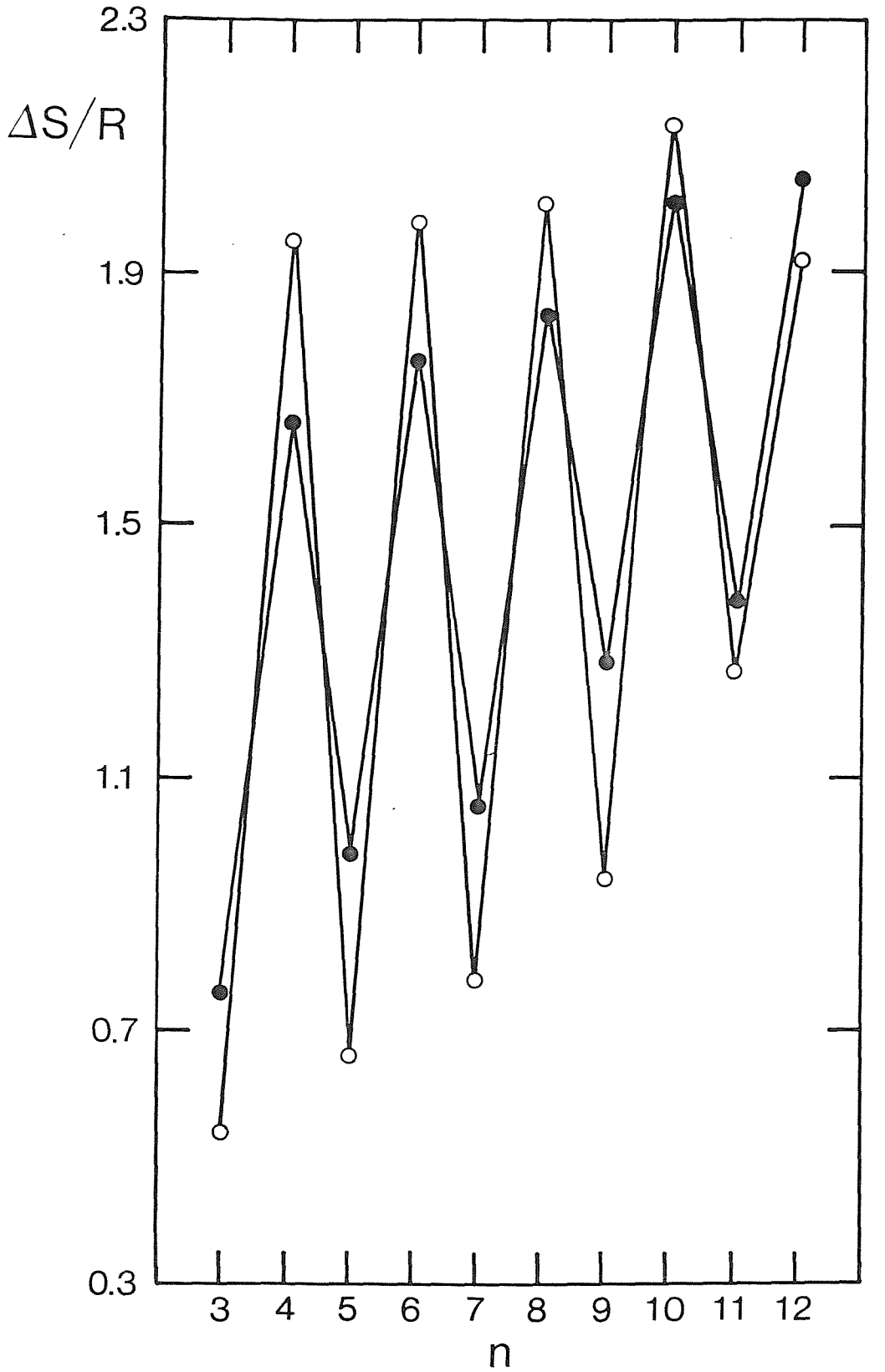

Figure 4.3.3.2 The dependence of the entropy change at the nematic-isotropic transition on the number of methylene groups in the flexible core for the α,ω-bis(4,4'-cyanophenyloxycarboxyphenyloxy)alkanes (●) and the BCBO-n's (o) [7].

even membered homologues. Consequently, the magnitude of the alternation exhibited by the entropy changes is larger for the BCBO-n series than for the diesters. This is a surprising result for it may be argued that the introduction of an ester linkage into the biphenyl unit increases the mesogenicity of the group and thus, should be more effective in 'anchoring' the ends of the flexible alkyl spacer resulting in a greater conformational entropy. This view, however, is not supported by the nematic-isotropic transition temperatures which, with just a single exception, are higher for the diesters than for the analogous BCBO-n compounds. Interpreting these results is very difficult for there are many competing factors and further speculation must await the results from model caculations in which X_a is increased.

Figure 4.3.3.3 shows the dependence of the nematic-isotropic transition temperatures upon the length of the alkyl spacer for the α,ω-bis(4-cyanobiphenyl-4'-oxy)alkanes (BCBO-n), the α,ω-bis(4,4'-cyanophenyloxycarboxyphenyloxy)alkanes (diesters), and the α,ω-bis(4-cyanoanilinebenzylidine-4'-oxy)alkanes (di-imines) [17]. After the sixth homologue the order of nematic thermal stability is:

di-imines > diesters > BCBO-n ;

and this is in agreement with the order found for comparable monomeric mesogens [2]. For spacer lengths of less than six carbon atoms this order is not observed. It should be stressed, however, that these inversions in the normal order are very small and within experimental error.

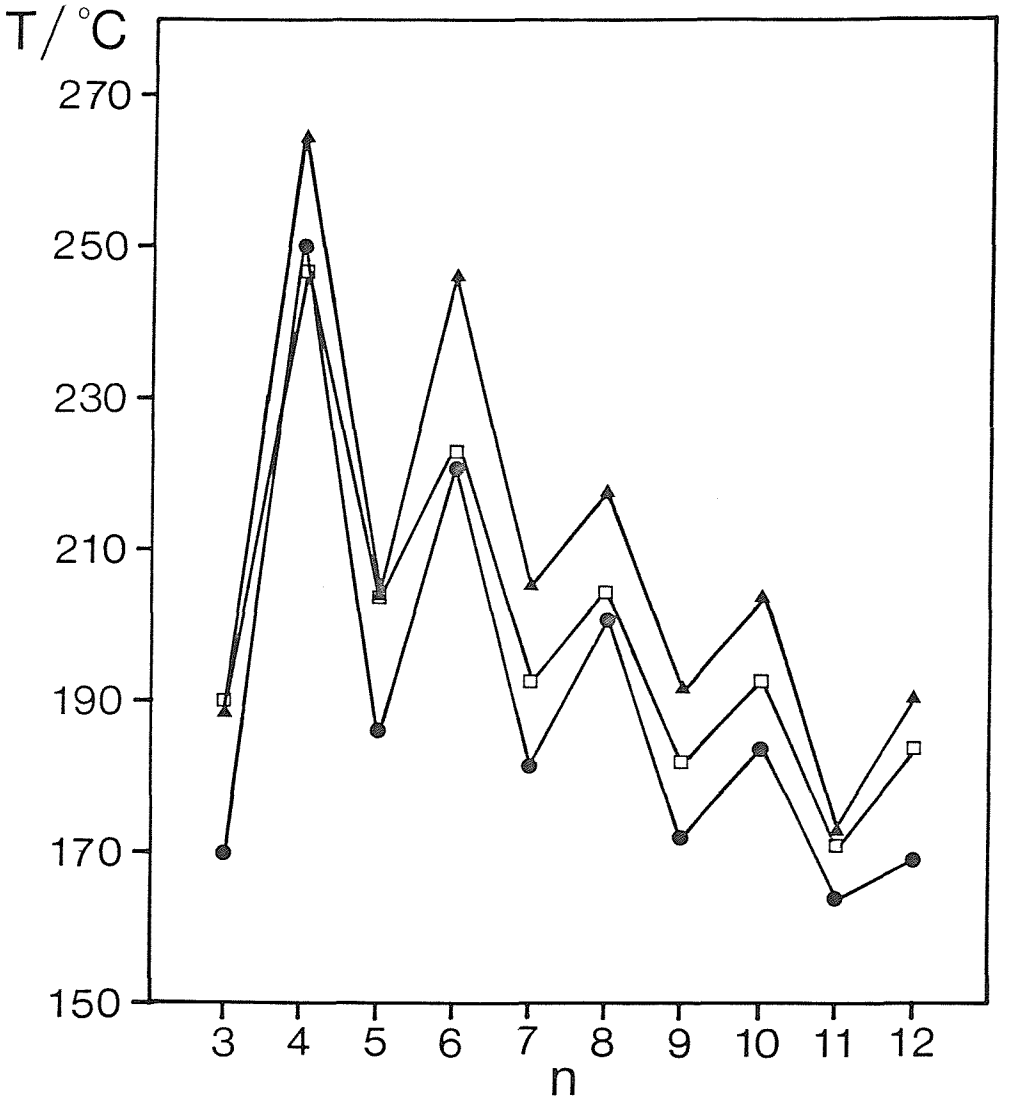

Figure 4.3.3.3 The dependence of the nematic-isotropic transition temperatures on the number of methylene groups in the alkyl spacer for the α,ω-bis(4,4'-cyanophenyloxycarboxyphenyloxy)alkanes (□), the α,ω-bis(4-cyanoanilinebenzylidine-4'-oxy)alkanes (▲) [17], and the α,ω-bis(4-cyanobiphenyl-4'-oxy)alkanes (●) [7].

4.3.4 The BCBO(EO)-n series

The transitional properties of three members of this homologous series are listed in table 4.3.4.1 together with those of the analogous BCBO-n compounds [7]. Also included in the table are the properties of BCBO-2 for it may be argued that this is the first member of the BCBO(EO)-n series with n=0. BCBO(EO)-2 and BCBO(EO)-3 exhibit monotropic nematic behaviour while BCBO(EO)-1 is an enantiotropic nematogen on the initial melting of a sample but this appears to be a metastable crystal form and subsequent meltings occur at a higher temperature and directly to the isotropic phase. The BCBO(EO)-n

Compound	T_{CN}/ °C †T_{CI}/ °C	T_{NI}/ °C	$\Delta H_{C\_}$/kJmol^{-1} ΔH_{NI}/kJmol^{-1}		$\Delta S_{C\_}$/R	ΔS_{NI}/R
BCBO-2	205	265	37.4	7.91	9.4	1.77
[1]BCBO(EO)-1	152.5	154	60.6	2.10	17.1	0.59
BCBO-5	137	186	30.2	2.53	8.8	0.66
BCBO(EO)-2	†161.5	(111)	63.0	-	19.7	-
BCBO-8	175	201	56.5	7.92	15.2	2.01
BCBO(EO)-3	†104	(70)	46.3	0.71	14.8	0.25
BCBO-11	123	164	52.0	4.63	15.8	1.27

Table 4.3.4.1 The transition temperatures, enthalpies and entropies of transition of the BCBO(EO)-n and BCBO-n [7] series; () denotes a monotropic transition. The uncertainties in the temperatures are ±1 °C and in the thermodynamic data are ±10%.

[1]First melting only; subsequent meltings occured at 159 °C, ΔH=51.4 kJmol^{-1}, $\Delta S/R$=14.3.

compounds have lower clearing points than their BCBO-n counterparts. For example, the nematic-isotropic transition temperature of BCBO(EO)-2 is 90°C lower than that of BCBO-8. On completion of this work we learnt of a similar study by Creed et al [19] who prepared two dimers having ethyleneoxide spacers. Of these, one was BCBO(EO)-1 and there is excellent agreement between the two sets of data. In the second compound, the ethylene oxide spacer links two 4-pentyloxyphenyl cinnamate groups:

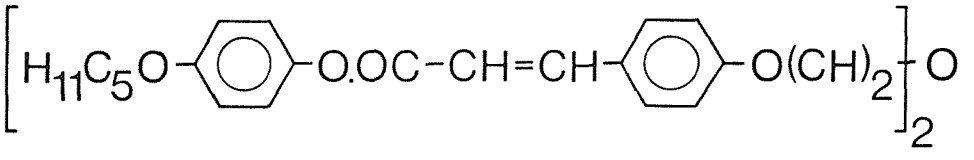

A further study incorporating oligoethylene oxide spacers has been performed by Chien et al [20] who prepared two compounds derived from triethyleneglycol:

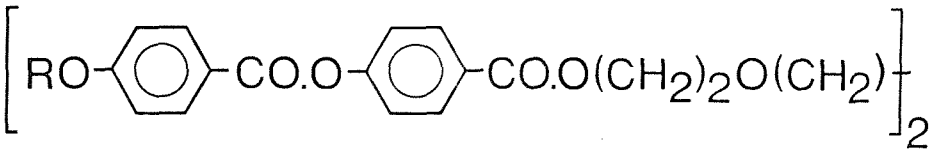

The general trend emerging from this small number of compounds is that replacing an alkyl spacer with one comprised of ethylene oxide units results in a reduction in the clearing temperature. This, however, is not the case for semi-flexible main-chain polymers. For example, replacement of the alkyl spacer in:

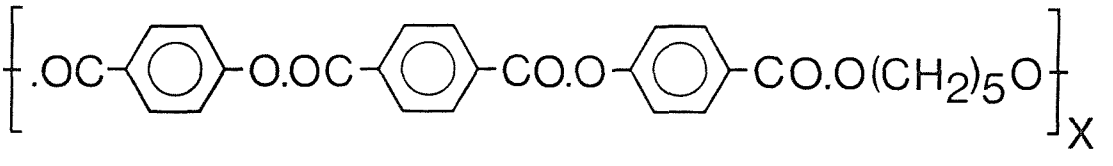

by an ethylene oxide spacer:

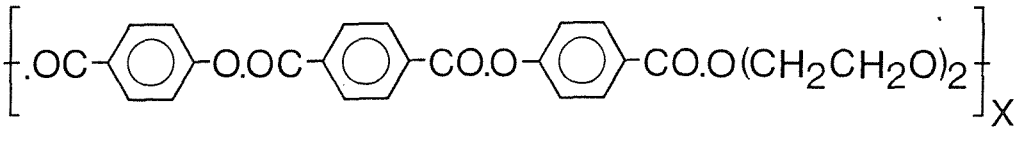

actually increases the clearing point by 21°C [4]. Also, replacing the octyl spacer by triethylene oxide serves to increase the clearing point by 37°C. It should be noted that in these examples the alkyl based polymers are purely smectic whereas those incorporating

oligoethylene oxide spacers exhibit smectic and nematic phases. In fact, the smectic phase stability decreases upon introducing oxygen atoms into the spacer and this suggests that the lateral intermolecular forces have been weakened by repulsive polar interactions between oxygen atoms. This may be simply thought of as a reduction in the molecular inhomogeniety.

In a polymeric system, therefore, an oligoethylene oxide spacer promotes liquid crystal phase formation relative to the analogous alkyl spacer whereas this is reversed for dimers. It is believed that in a polyoxyethylene chain the energy of the gauche conformer of the C-C bond is lower than that of the trans conformer [9]. The stabilisation of the gauche conformer is thought, in part, to be a result of O•••O interactions. It has been assumed that this preference for the gauche conformation is also applicable to oligoethylene oxide spacers in both dimers and polymers [18]. If this is the case and the conformational distribution of an oligoethylene oxide spacer does vary from that of an alkyl spacer we may expect to see this reflected in the entropies of transition although we really need the results from model calculations to assess the differences in the two conformational distributions. The entropy change associated with the nematic-isotropic transition was measured for BCBO(EO)-1 and BCBO(EO)-3 and these are listed in table 4.3.4.1. Unfortunately, BCBO(EO)-2 does not supercool sufficiently far to permit measurement of the enthalpy of transition. The values of the entropy change for BCBO(EO)-1 and BCBO-5 are equal within experimental error whereas those of BCBO(EO)-3 and BCBO-11 differ greatly with BCBO(EO)-3 having a much smaller value. These observations are difficult to rationalise but suggest that the conformational distribution of the spacer in BCBO(EO)-1 is very similar to that in BCBO-5 and the difference in transition temperatures is a consequence of differing intermolecular forces whereas, for BCBO(EO)-3 and BCBO-11 the conformational distributions of the spacers differ greatly, explaining the large difference in the entropy changes associated with the nematic-isotropic transition. Thus, the oligoethylene oxide spacers in BCBO(EO)-1 and BCBO(EO)-3 appear to behave differently. This may be explained remembering that the stabilisation of gauche linkages in polyoxyethylene chains derives

from interactions between oxygen atoms. The first member of the BCBO(EO)-n series, BCBO(EO)-0 (BCBO-2), has been modelled theoretically and the results clearly indicate that a very large proportion of the spacers exist in an all-trans conformation [21]. This presumably results from the steric effect of the two terminal groups. Clearly, therefore, the interaction between the two oxygen atoms in BCBO-2 is insufficient to stabilise the gauche conformer. In BCBO(EO)-1, the O•••O interaction is between an oxygen atom within the alkyl spacer with one forming part of the mesogenic group and this interaction, also, does not appear to significantly change the conformational distribution of the spacer. In the spacer of BCBO(EO)-3, however, there are O•••O interactions similar in nature to those found in polyoxyethylene and as expected, we now see a conformational distribution that differs from that of the undecyl spacer. This argument predicts that BCBO(EO)-2 would, also, have an entropy smaller than its analogous alkyl counterpart, BCBO-8. This line of reasoning is admittedly speculative in nature and opposes the opinions of Creed et al [19] who argue that the insertion of gauche linkages into the spacer of BCBO(EO)-1 serve to increase the colinearity of the two mesogenic groups. This argument was used to explain the fact that they measured the entropy change associated with the nematic-isotropic transition of BCBO(EO)-1 to be slightly higher than that of BCBO-5. They have failed to take into account that there are two very different types of oxygen atoms in the spacer of BCBO(EO)-1 and it is unreasonable to assume that they will interact in the same way as those in a polyoxyethylene chain. A greater understanding of the BCBO(EO)-n compounds requires them to be computer modelled.

4.3.5 The α,ω-bis(4-hexylbiphenyl-4'-oxy)alkanes

The two compounds prepared in this homologous series both have high melting points, given in figure 4.3.5.1, and neither exhibit liquid-crystalline behaviour.

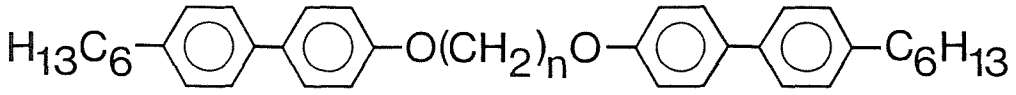

n = 4	n = 5
C-I 197 °C	C-I 154 °C
N-I <135 °C	N-I <130 °C

Figure 4.3.5.1 The melting points of BHBO-4 and BHBO-5.

The BHexBO-n series is an example for which the analogous monomer without the flexible spacer is known:

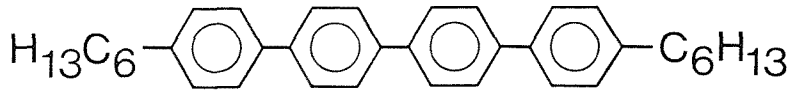

and this has a smectic A-isotropic transition temperature at 341 °C [22]. Therefore, the introduction of the flexible spacer has reduced the smectic thermal stability by at least 206 °C. The melting point has fallen by 97 °C for BHBO-4 and 140 °C for BHBO-5. The dramatic decrease in smectic stability upon introducing a flexible alkyl spacer presumably reflects the decrease in molecular inhomogeniety as well as the increase in molecular flexibility.

4.3.6 1,4-bis(4-cyanobiphenyl-4'-oxy)pentane

1,4-Bis(4-cyanobiphenyl-4'-oxy)pentane is an enantiotropic nematogen and its transitional properties are listed in figure 4.3.6.1 together with those of BCBO-4 [7]. Lateral substitution of the spacer has reduced both the melting point, by 77 °C, and the nematic-isotropic

transition temperature by 90 °C. This large reduction in the transition temperatures may be a result of the methyl group lowering the symmetry of the molecule. In a monomeric analogue, 5OCB, branching at the α-carbon atom in the alkoxy chain depresses the melting point by 43 °C and the nematic-isotropic transition temperature by 130.5 °C [23]. Thus, the decrease in the nematic thermal stability of the dimer is not as large as would have been predicted.

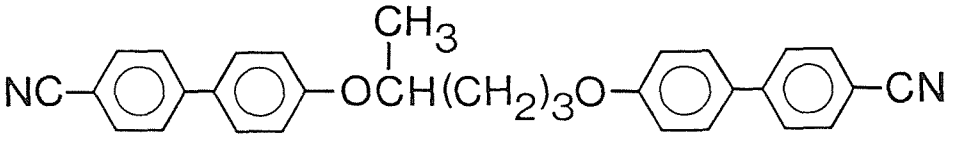

	132 °C	160 °C
	C -	N - I
ΔH/kJmol^{-1}	26.8	4.31
ΔS/R	7.95	1.20

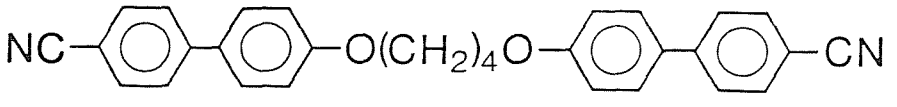

	209 °C	250 °C
	C -	N - I
ΔH/kJmol^{-1}	41.7	8.47
ΔS/R	10.4	1.95

Figure 4.3.6.1 The effect of branching the alkyl spacer of a dimeric liquid crystal.

The entropy change associated with the nematic-isotropic transition of BCBO-4 is greater than that of 1,4-BCBO-5 and this may reflect that the methyl branch acts to stabilise conformations which are unfavourable in the unsubstituted compound. It should be noted that the entropy change for 1,4-BCBO-5 is still considerably higher than that of monomeric analogues. The methyl branch has introduced a chiral centre into the molecule but in this investigation we have not attempted to resolve the optical isomers.

4.3.7 The α,ω-bis(6-cyanonapthalene-2-oxy)alkanes

The two members of this homologous series prepared, BCNO-4 (C-I 258 °C) and BCNO-5 (C-I 187 °C) are both high melting and exhibit no liquid-crystalline behaviour. The expectation that replacing the biphenyl unit in the BCBO-n series by a napthalene group would result in a depression of the melting points was not realised and indeed the melting point of BCNO-4 is 49 °C higher than that of BCBO-4 and similarly, BCNO-5 has a melting point 50 °C greater than BCBO-5. The 6-cyanonapthalene-2-oxy moiety is not recognised as promoting mesogenic behaviour. In the monomeric analogues, the nOCB's, replacing the biphenyl unit by a 6,2-substituted napthalene serves to increase the melting points while destroying liquid-crystalline behaviour [24]. This destruction of mesogenic behaviour in both monomeric and dimeric compounds presumably reflects the greater biaxiality of the napthalene unit as compared to biphenyl.

4.3.8 α-(4-substitutedbiphenyl-4'-oxy)-ω-(4,4'-cyanobiphenyl)alkanes

The transitional properties of four compounds belonging to this general class are listed in table 4.3.8.1; all four are nematogens. For the purposes of discussion, the CB6OX compounds will be referred to as having an odd length spacer and hence, for example, CB6OCB will be compared with BCBO-5. Similarly, CB5OCB is considered to be an even membered compound and thus, compared to BCBO-4. The most striking feature in table 4.3.8.1 is that CB6OCB exhibits a smectic phase and this is discussed separately. The differences in the nematic-isotropic transition temperatures between BCBO-5 and CB6OCB of 31.5 °C and between CBO5OBip and CB6OBip of 30.5 °C are in agreement with those observed for monomeric liquid crystals for which a reduction of between 30 °C and 40 °C is usually found on replacing the oxygen atom in an alkoxy chain by a methylene group [2]. The depression in the nematic-isotropic transition temperature on replacing an oxygen atom in BCBO-4, however, is only 10 °C. The entropy change associated with the nematic-isotropic transition of BCBO-5 is greater than that of CB6OCB whereas that of BCBO-4 is smaller than that of CB5OCB. These

Compound	$^{\dagger}T_{CI}$/°C T_{CN}/°C $^{1}T_{CS}$/°C	T_{SN}/°C	T_{NI}/°C	$\Delta H_{C\_}$/kJmol^{-1}	ΔH_{NI}/kJmol^{-1}	$\Delta S_{C\_}$/R	ΔS_{NI}/R
CB6OBip	†129	-	(70.5)	-	-	-	-
CBO5OBip	†161.5	-	(101)	-	-	-	-
CB6OBH	†110.5	-	(101)	-	-	-	-
[a]CB6OCB	^{1}99	109	154.5	31.9	1.68	10.3	0.47
BCBO-5	137	-	186	30.2	2.53	8.8	0.66
CB5OCB	175.5	-	240	31.7	9.31	8.52	2.18
BCBO-4	209	-	250	41.7	8.47	10.4	1.95

Table 4.3.8.1 The transition temperatures, enthalpies and entropies of transition for members of the CBOnX series; () denotes a monotropic transition. The uncertainties in the temperatures are ±1 °C and in the thermodynamic data are ±10%.
[a] ΔH_{SN}= 0.03 kJmol^{-1}; $\Delta S_{SN}/R$ = 0.01.

differences are small and so their unambiguous interpretation is dificult. However, the increase in conformational entropy on going from BCBO-4 to CB5OCB implies that the nematic-isotropic transition temperature will not fall as far as would be predicted and this is indeed observed. The relative efficiency of the terminal group in enhancing the thermal stability of the nematic phase in these asymmetric dimers is:

CN > Br > Hexyl > H;

and this is in accord with that found for monomeric liquid crystals[2].

4.3.9 The smectic phase of CB6OCB

The smectic phase of CB6OCB has been investigated using a number of techniques and the results obtained from each will be discussed in turn.

Polarising microscopy

The optical textures of this smectic phase are not standard. On cooling the nematic phase, the schlieren texture develops a pattern reminiscent of poorly defined focal-conic fans presumably implying either a smectic A or C phase. These textures are shown in plates 4.3.1 and 4.3.2 respectively. On further cooling, the texture does appear to change gradually; the rather square fans formed initially become somewhat rounded and this texture is shown in plate 4.3.3. It should be stressed that in these photographs the dark areas do not correspond to homeotropic alignment but instead are simply areas without sample. Attempts to produce homeotropic alignment of the sample failed.

Differential scanning calorimetry

The transition from the smectic phase to the nematic phase is very weakly first order ($\Delta S/R = 0.01$) and this suggests that the phase is either a smectic A or C. No other transition was detected within the smectic range.

X-ray diffraction

The X-ray diffraction pattern of the smectic phase is very curious for it contains only diffuse wide angle scattering with no apparent evidence of any low angle diffraction. The relevance of this is unclear but there are several possible explanations. First, the X-ray diffraction pattern does not represent a powder pattern but instead the sample had spontaneously formed a monodomain. This, however, is an unlikely explanation for the experiment was repeated with sample rotation and no low angle diffraction was observed. Secondly, a

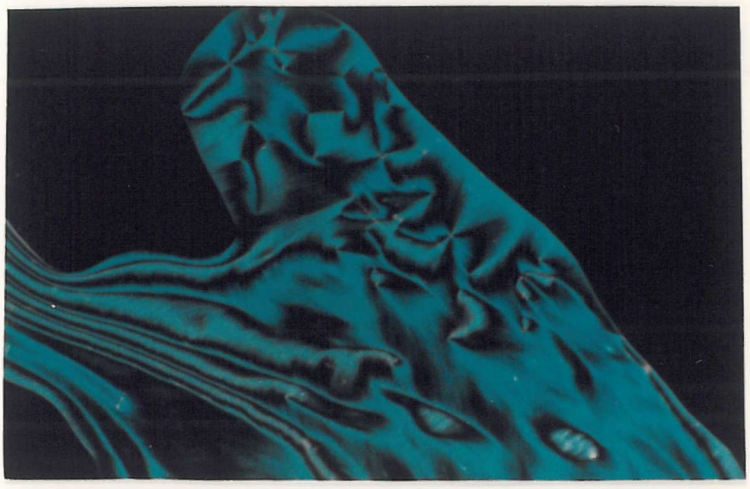

Plate 4.3.1 The schlieren texture of the nematic phase of CB6OCB (T=112 ℃).

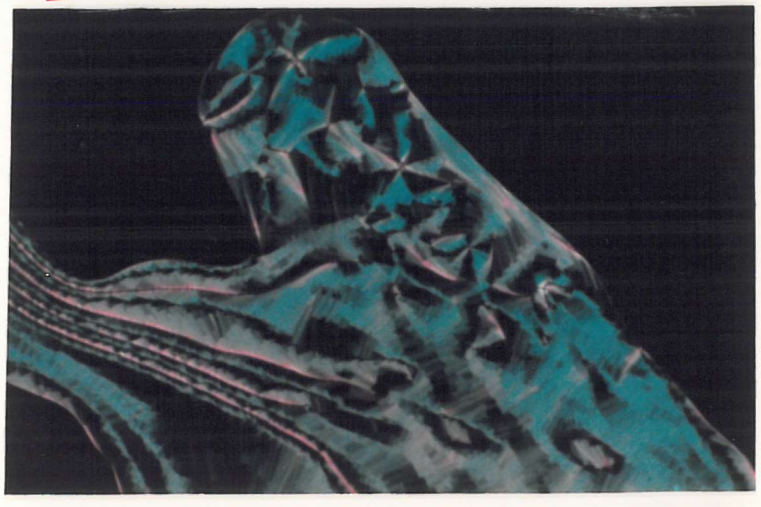

Plate 4.3.2 The poorly defined focal-conic fan texture formed on cooling the nematic phase of CB6OCB (T=107 ℃).

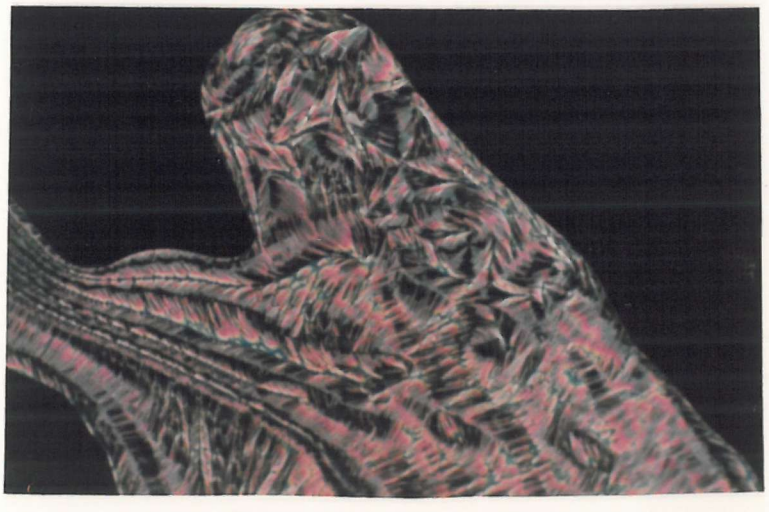

Plate 4.3.3 The texture formed on cooling the smectic phase of CB6OCB (T=99 ℃).

diffraction pattern represents the convolution of an underlying continuous Fourier transform arising from the contents of the unit cell, with an interference function derived from the unit cell dimensions. If this interference function occurs at a node on the continuous Fourier transform no diffraction pattern will be observed. The structural implications of this are far from clear. Third, the structure of the smectic phase may be such that it possesses a symmetry that gives rise to absences of the odd orders of reflection and again, the structural implications are unclear. Finally, the layer spacing may simply be so large that the first order of layer reflection falls outside the experimental limits. This implies a layer spacing of greater than 100 Å and this is difficult to rationalise with the estimated all-trans length of CB6OCB of 31 Å. Summarising, therefore, X-ray diffraction has provided no positive structural information on the smectic phase of CB6OCB.

Electron spin resonance spectroscopy

The smectic phase of CB6OCB has been investigated using two different spin probes [25] and the results for each are in excellent agreement. In both the isotropic and nematic phases a three line spectrum is observed and for the nematic phase this corresponds to a well aligned sample; an example is shown in figure 4.3.9.1(a). On lowering the temperature of the sample so that it is just within the smectic phase, a three line spectrum is observed and hence the monodomain has been preserved, see figure 4.3.9.1(b). On lowering the temperature further, however, two extra lines appear in the spectrum implying that the director is no longer uniformly aligned with respect to the field; an example of this five line spectrum is shown in figure 4.3.9.1(c). Lowering the temperature still further, the spectrum still has five lines but the intensities of these have changed, see figure 4.3.9.1(d). It should be noted that these spectral changes are all reversible. The inner two lines of the spectra derive from the director lying parallel to the field and the outer two lines from the director being perpendicular to the field. Therfore, initially the smectic phase appears to have a smectic A type structure. As the

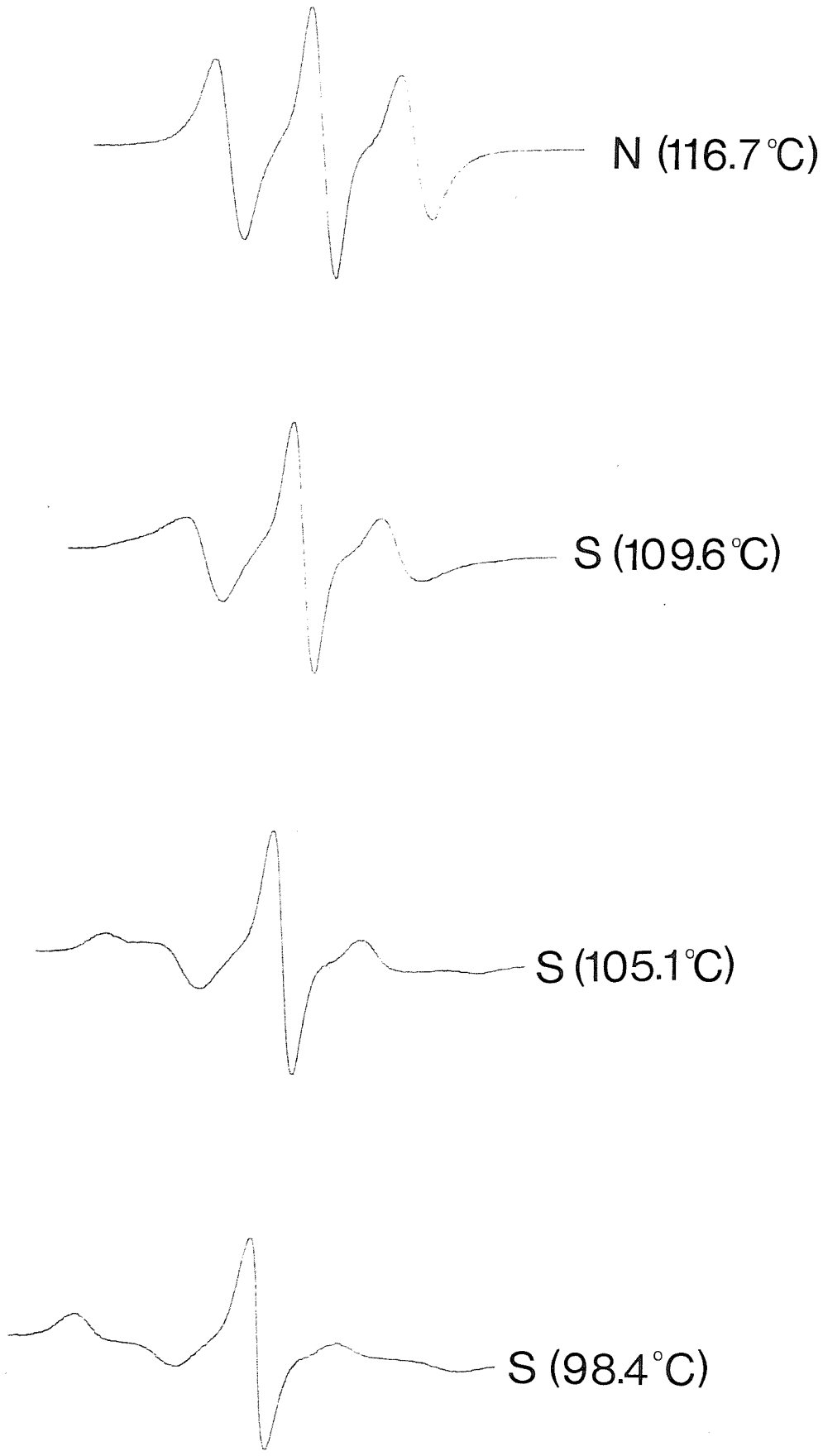

Figure 4.3.9.1 The dependence of the E.S.R. spectrum of a cholestane probe dissolved in CB06CB on temperature.

temperature is lowered the director is no longer uniformly aligned with respect to the field but instead appears to be lying both parallel and at an angle, α, to the field. This may be explained by allowing the smectic A layers to ripple. Lowering the temperature still further , a greater fraction of the molecules lie at an angle with respect to the field and this angle increases tending towards 90° with decreasing temperature. This is consistent with an undulation of the layers and is represented schematically in figure 4.3.9.2.

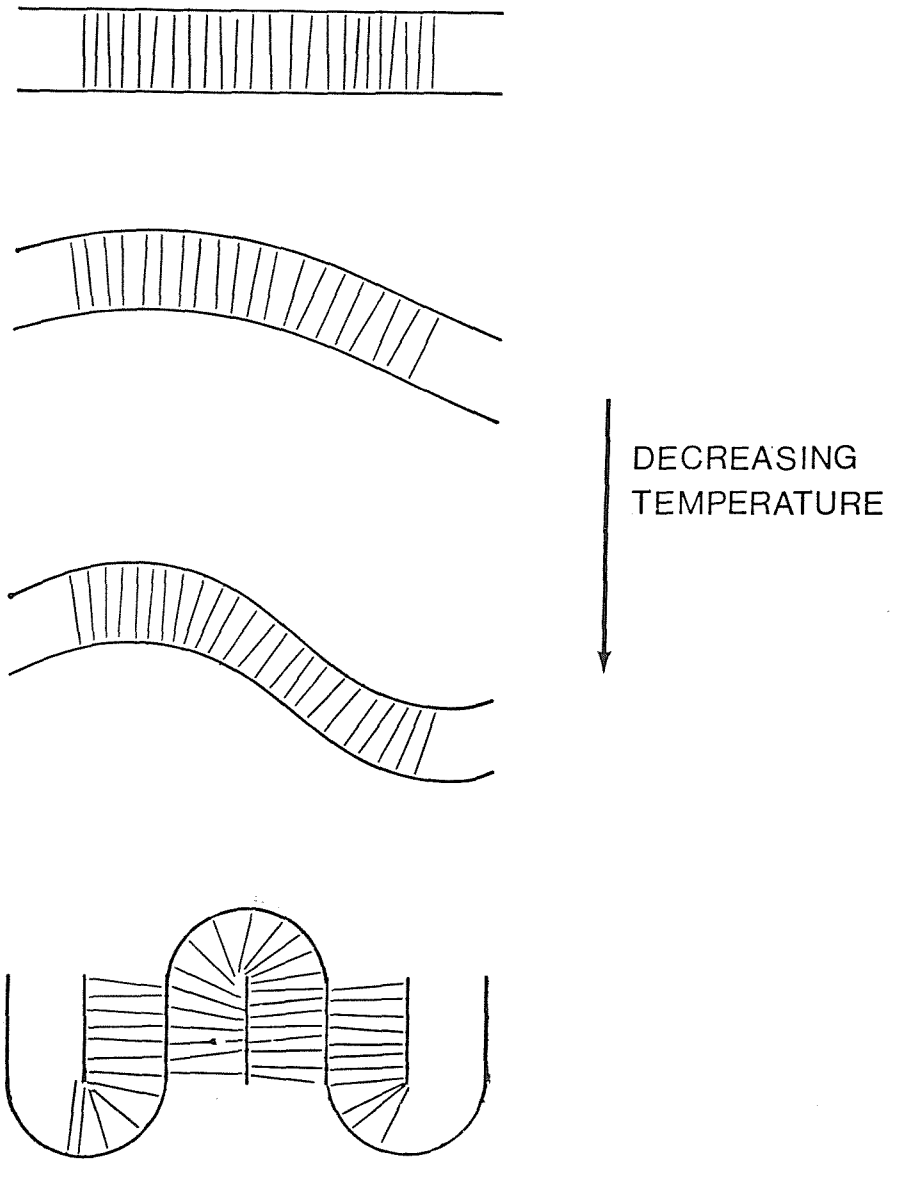

Figure 4.3.9.2 A schematic representation of the dependence of the structure of the smectic phase of CB6OCB on temperature.

Deuterium nuclear magnetic resonance spectroscopy (D-N.M.R.)

A deuteriated solute, anthracene-d_{10}, was used as a probe to study the smectic phase of CB6OCB using D-N.M.R. [25]. The spectral shapes obtained did not vary with temperature although the splittings do change. There are two possible explanations for this. First, D-N.M.R. employs a higher magnetic field strength than E.S.R. and this may be sufficiently large to maintain director alignment throughout the temperature range of the smectic phase. Secondly, the difference in frequencies used to observe the transition in D-N.M.R. and E.S.R. differ greatly and the D-N.M.R. results actually represent an average motion of the director.

The D-N.M.R. results are very difficult to rationalise on the basis of existing theories. In particular, the dependence of S_{ZZ} upon temperature is puzzling because on decreasing the temperature S_{ZZ} measured in the nematic phase increases as would be expected but on entering the smectic phase remains approximately constant with temperature. Also, the dependence of S_{ZZ} upon S_{XX-YY} represented schematically in figure 4.3.9.3 differs from that generally observed. The relevance of this unusual behaviour is not clear.

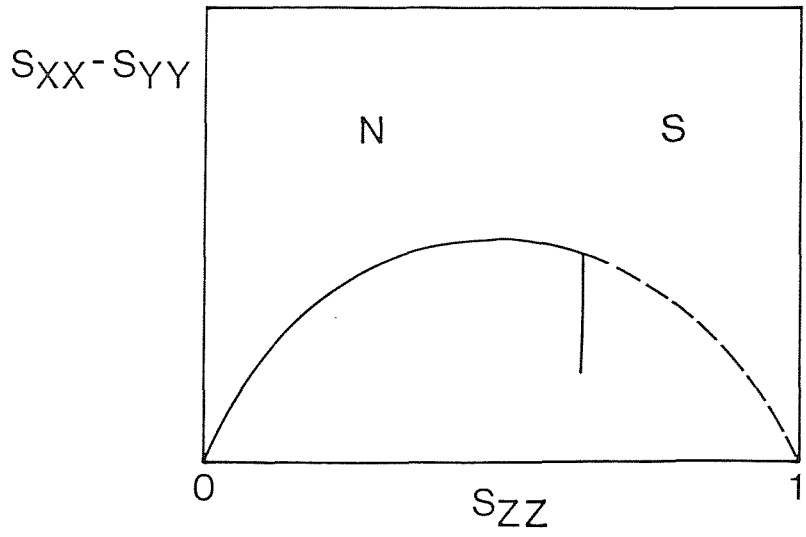

Figure 4.3.9.3 The dependence of S_{ZZ} on S_{XX-YY} measured for anthracene-d_{10} dissolved in CB6OCB. The solid line represents the experimental data and the dotted line is the generally observed behaviour.

4.4 Conclusions

This Chapter has shown that structure-property relationships in dimers, where applicable, are similar to those developed for monomeric compounds. For example, a lateral methyl substituent on the mesogenic group reduces the nematic-isotropic transition temperature in both monomeric and dimeric liquid crystals. It should be noted, however, that such substitution decreases the entropy change at the transition for dimers but tends to increase it for monomers. The CB.OnO.(Me)1 series illustrates that lateral substitution also serves to depress smectic stability. The relative effect of a terminal substituent in increasing nematic thermal stability was established to be the same for asymmetric dimers as it is for monomers. Varying the link in the aromatic groups of a dimer also appears to reflect the effects of such change in monomers except in the case of dimers having short spacer lengths.

The properties of a dimer have been shown to depend critically upon the length, parity and chemical structure of the spacer. Dimers incorporating oligoethylene oxide spacers have significantly lower nematic-isotropic transition temperatures and also, lower entropies of transition compared with the analogous compounds possessing alkyl spacers. Branching the spacer also reduces both the temperatures and entropies of transition.

Finally, the asymmetric dimer, CB6OCB, exhibits a smectic phase that possesses several unique properties; however, further investigations must be performed in order to establish its structure.

4.5 References

[1] Emsley, J.W., Luckhurst, G.R., and Shilstone, G.N., 1984, Molec. Phys., 53, 1023.

[2] Gray, G.W., 1979, The Molecular Physics of Liquid Crystals, edited by G.R. Luckhurst and G.W. Gray, Academic Press, Chap. 1.

[3] Young, W.R., Haller, I., and Green, D.C., 1972, J. Org. Chem., 37, 3707.

[4] Lenz, R.W., 1985, Faraday Discuss. Chem. Soc., 79, 21.

[5] Finkelmann, H.,1987, Thermotropic Liquid Crystals, edited by G.W. Gray, Wiley, Chap. 6.

[6] Coates, D., and Gray, G.W., 1976, Mol. Cryst. Liq. Cryst., 37, 249.

[7] Emsley, J.W., Luckhurst, G.R., Shilstone, G.N., and Sage, I., 1984, Mol. Cryst. Liq. Cryst. Lett., 102, 223.

[8] Blumstein, A., 1985, Polym. J., 17, 277.

[9] Flory, P.J., 1969, Statistical Mechanics of Chain Molecules, Interscience, Chap. 5.

[10] Yoon, D.Y., Bruckner, S., Volksen, W., Scott, J.C., and Griffin, A.C., 1985, Faraday Discuss. Chem. Soc., 79, 41.

[11] Griffin, A.C., and Havens, S.J., 1981, J. Polym. Sci. Polym. Phys. Ed., 19, 951.

[12] Donahoe, H.B., Benjamin, L.E., Fennoy, L.V., and Greiff, D., 1961, J. Org. Chem., 26, 474.

[13] Kursanov, D.N., Parnes, Z.N., and Loim, N.M., 1974, Synthesis, 663.

[14] Coates, D., and Gray, G.W., 1976, J. Chem. Soc. Perkin 2, 863.

[15] Smith, G.W., Garlund, Z.G., and Curtis, R.J., 1973, Mol. Cryst. Liq. Cryst., 19, 327.

[16] Gardlund, Z.G., Curtis, R.J., and Smith, G.W., 1973, J. Chem. Soc. Chem. Comm., 202.

[17] Griffin, A.C., Vaidya, S.R., Hung, R.S.L., and Gorman, S., 1985, Mol. Cryst. Liq. Cryst. Lett., 1, 131.

[18] Jin, J.I., Chung, Y.S., Lenz, R.W., and Ober, C., 1983, Bull. Korean Chem. Soc., 4, 143.

[19] Creed, D., Gross, J.R.D., Sullivan, S.L., Griffin, A.C., and Hoyle, C.E., 1987, Mol. Cryst. Liq. Cryst., 149, 185.

[20] Chien, J.C.W., Zhou, R., and Lillya, C.P., 1987, Macromolecules, 20, 2341.

[21] Heaton, N.J., 1986, Ph.D. Thesis, University of Southampton.

[22] Demus, D., Demus, H., and Zaschke, H., 1974, Flussige Kristalle in Tabellen, V.E.B. Deutscher Verlag fur Grundstoffindustrie.

[23] Gray, G.W., and Kelly, S.M., 1984, Mol. Cryst. Liq. Cryst., 104, 335.

[24] von Lauk, U.H., Skrabal, P., and Zollinger, H., 1985, Helv. Chim. Acta, 68, 1406.

[25] Chiu, F.S.M., 1985, Third Year Project Report, University of Southampton.

CHAPTER 5 THE PREPARATION AND PROPERTIES OF MODEL COMPOUNDS OF DIMERIC LIQUID CRYSTALS

5.1 Introduction

We have already seen in the preceeding three chapters that a characteristic property of a homologous series of dimeric liquid crystals, in which the length of the alkyl spacer is varied, is the very pronounced odd-even effect in their thermodynamic properties at the liquid crystal-isotropic transition [1]. There are, however, other examples of low molar mass mesogens which exhibit similarly large alternations in their transition temperatures; the majority of these compounds have a common molecular architecture comprising an anisometric terminal group, often a phenylene ring, attached to a mesogenic moiety via a flexible alkyl chain [2]. Such a structure is termed dimeric if the anisometric group is itself a mesogenic group and thus, this class of compounds are structurally intermediate between monomers and dimers. The primary aim of this Chapter was to investigate to what extent such molecules mimic the behaviour of dimeric liquid crystals. Gray et al [2-5] have performed detailed investigations of the liquid-crystalline properties of the phenyl and ω-phenylalkyl 4-(4'-substituted-benzylideneamino)cinnamates:

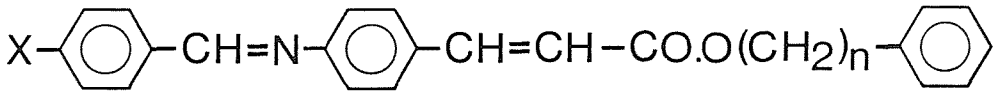

The dependence of the transition temperatures upon the length of the alkyl chain for the ω-phenylalkyl 4-(4'-cyanobenzylidineamino)-cinnamates [2] is shown in figure 5.1.1; a very pronounced alternation in the nematic-isotropic transition temperatures is immediately apparent. This odd-even effect appears to attenuate with increasing chain length and so is very similar to the behaviour observed for dimers [1]. This alternation was attributed to the fact that for even members of the series the terminal phenyl ring is collinear with the semi-rigid core whereas for odd members the two anisometric units are no longer collinear [3]; this is represented diagrammatically in figure 5.1.2.

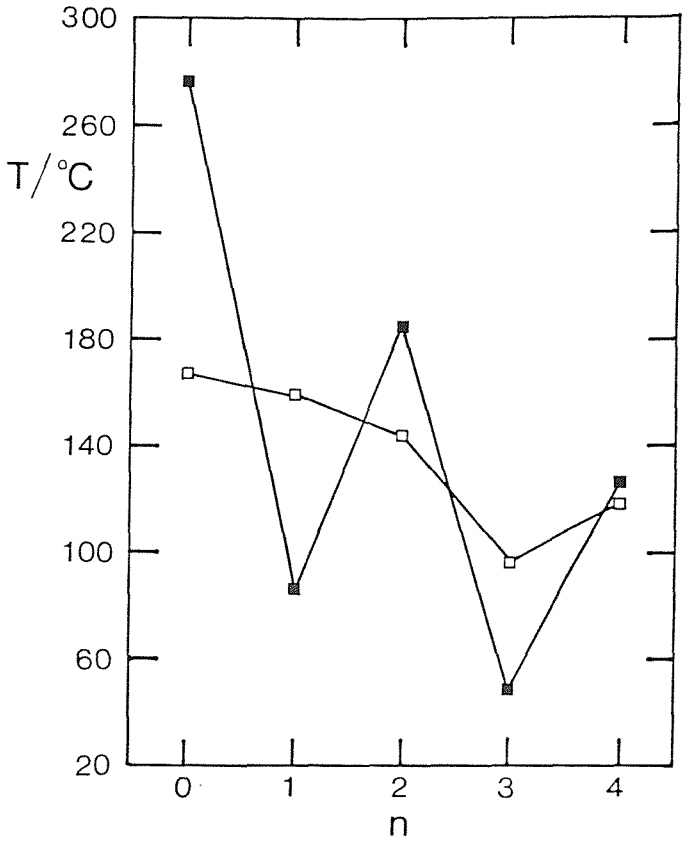

Figure 5.1.1 The dependence of the transition temperatures on the number of carbon atoms in the alkyl chain for the ω-phenylalkyl 4(4'-cyanobenzylideneamino)cinnamates; □ indicates the melting point and ■ denotes the nematic-isotropic transition temperature.

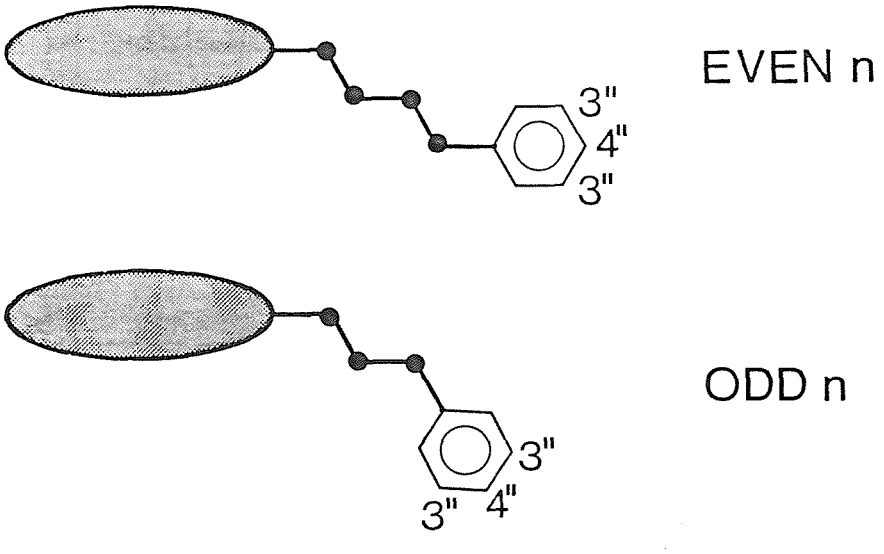

Figure 5.1.2 A diagrammatic representation of a molecular structure comprising a rigid core and a phenyl ring linked via an alkyl chain in the all-trans conformation.

In order to test this somewhat simplistic but nonetheless appealing explanation that the large alternation in the nematic-isotropic transition temperatures reflects the smaller anisometric unit moving on and off the long axis of the rest of the molecule, Gray et al [4,5] synthesised esters containing 4"-chloro, 4"-methyl, 3"-chloro or 3"-methyl substituents on the terminal phenyl ring; these positions are shown in figure 5.1.2. The effect of substition in the 4"-position on the clearing temperature was found to be related to the parity of the alkyl chain; for even members such substitution enhances the thermal stability of the nematic phase whereas for the odd members nematic stability is reduced. This is totally consistent with the view that for even members the molecule is essentially linear so that a 4"-sustituent increases the length to breadth ratio of the molecule and hence, increases the nematic-isotropic transition temperature. For odd values of n, however, substitution in the 4"-position broadens the molecule because the phenyl ring is lying off the molecular long axis; hence, a reduction in the nematic-isotropic transition temperature is anticipated and indeed observed.

Furthermore, substitution in the 3"-position generally decreases the nematic-isotropic transition temperatures for both even and odd membered compounds. However, this effect is sometimes smaller for the odd members and in one example an increase in the nematic thermal stability is observed [4]. To explain these observations, Gray [4] noted that if rotation about the O-ring (n=0) or CH_2-ring bonds is possible then for substitution in the 3"-position there are two extreme molecular conformations when the ring is coplanar with the rest of the molecule. For an even member, irrespective of which conformation is adopted, a 3"-substituent broadens the molecule and thus, a decrease in nematic thermal stability is easily understood. For an odd member, however, a substituent in the three position can actually lengthen the molecule and so an increase in the nematic thermal stability would be predicted. Gray further commented that since there is no consistent effect for substitution in the 3"-position with an odd member then it is unlikely that free rotation can occur about the CH_2-ring bond in the nematic phase and that the amounts of the different rotational conformers differ with substituent

type and alkyl chain length. This is somewhat surprising as the rotation of a phenyl group is normally expected to occur. However, the experimental results appear to have been fully explained by restricting the alkyl chain to essentially the all-trans conformer and then, considering the relative spatial dispositions of the anisometric groups.

It should be remembered that both methyl and chloro terminal substituents stabilise nematic behaviour relative to the analogous unsubstituted compound and that a chloro substituent is normally more effective in this than a methyl group [6]. If compounds possessing a small anisometric group are to be considered structurally intermediate between monomers and dimers then as the mesogenicity of the terminal anisometric group is increased, the resulting transition temperatures would be expected to tend towards those of the dimer. This, however, is only observed for compounds possessing an even length spacer and so the logical extension of Gray's arguments [4] is that a dimer having an odd length spacer should have a lower nematic-isotropic transition temperature than the analogous compound possessing only a single mesogenic group. This is not the case and instead, large increases in the nematic-isotropic transition temperatures are observed on substituting a mesogenic moiety for a terminal proton in the alkyl chain of a conventional monomer; for example, 5OCB has a T_{NI} of 48 °C whereas BCBO-5 has a T_{NI} of 186 °C. This apparent contradiction is discussed later.

As we have seen, compounds possessing a semi-rigid core and a small anisometric group linked via an alkyl chain appear to mimic the large alternation in transition temperatures observed on varying the parity of the spacer in dimeric liquid crystals. The obvious question is whether the large alternation in the entropy change associated with the nematic-isotropic transition exhibited by dimers is also reproduced in these compounds. Ennulat and Brown [7] prepared the cholesteryl ω-phenylalkanoates and reported both the transition temperatures and the entropies of transition for this series. Figure 5.1.3 shows the dependence of the transition temperatures on the length of the alkyl chain for these esters; a very large alternation

in the cholesteric-isotropic transition temperature on varying n is immediately apparent. This alternation attenuates with increasing n and thus, appears to mimic the behaviour observed for dimeric compounds. Figure 5.1.4 gives the dependence of the entropy change associated with the cholesteric-isotropic transition upon n for the cholesteryl ω-phenylalkanoates; a large odd-even effect is evident with the even members having the higher values. It should be noted also that the even members have larger values of ΔS/R for the cholesteric-isotropic transiton than the corresponding cholesteryl alkanoates [7]. Thus, the behaviour of the cholesteryl ω-phenyl-alkanoates does indeed seem intermediate between that of monomeric and dimeric liquid crystals.

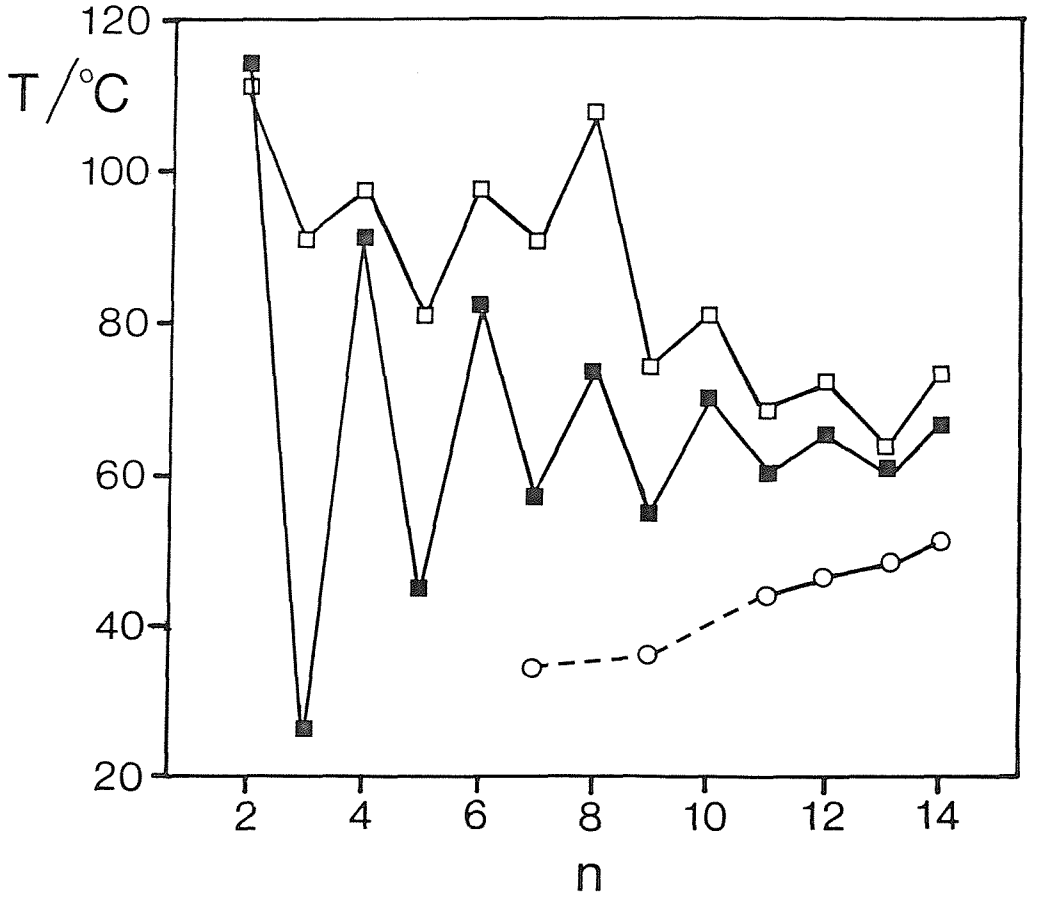

Figure 5.1.3 The dependence of the transition temperatures on the number of carbon atoms in the alkyl chain for the cholesteryl ω-phenylalkanoates [7]; □ indicates the melting point, ■ denotes the cholesteric-isotropic transition, and ○ the smectic-cholesteric transition.

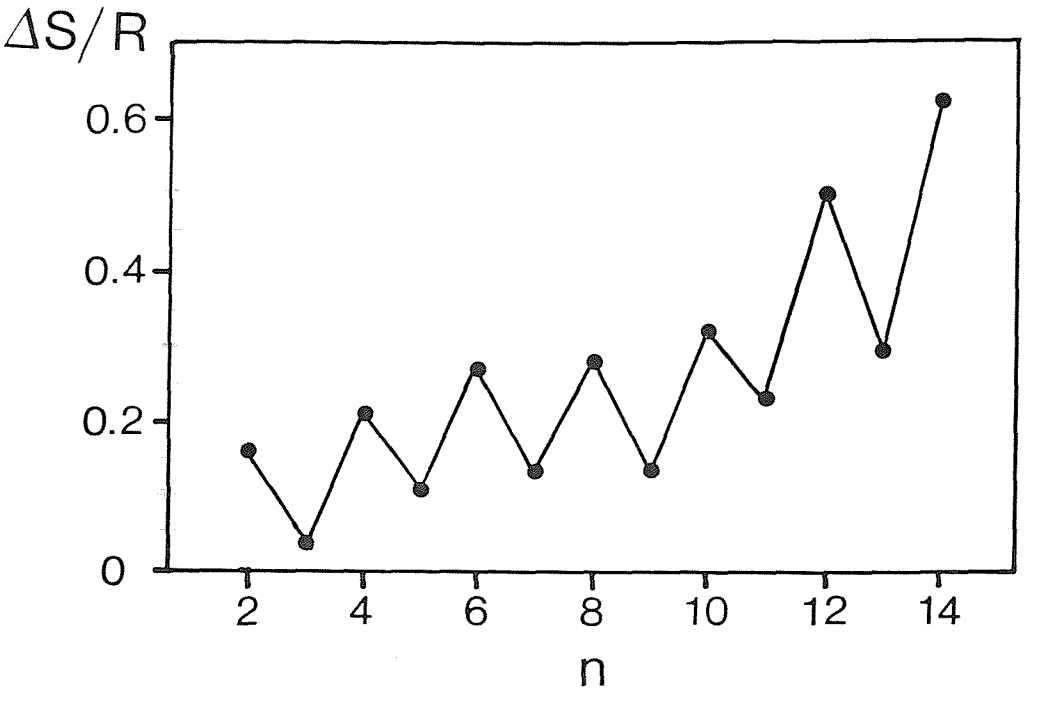

Figure 5.1.4 The dependence of the entropy change at the cholesteric-isotropic transition on the number of carbon atoms in the alkyl chain for the cholesteryl ω-phenylalkanoates.

A theoretical description of nematogens possessing a small anisometric terminal group

The unsually pronounced odd-even effect exhibited by the ω-phenylalkyl 4-(4'-substituted benzylideneamino)cinnamates reported by Gray et al [2] has recently been theoretically modelled by Mukherjee et al [8]. It should be noted, however, that Luckhurst [9] had previously successfully modelled the large alternation in the transition temperatures of dimeric liquid crystals. At the root of the theory developed by Mukherjee et al [8] from that of Marcelja [10] are the assumptions that the molecule consists of three distinct components; namely the semi-rigid core, an alkyl chain and the terminal anisometric group. Secondly, the alkyl chain is assumed to interact only very weakly with the field and hence, this may be ignored. Thus, they considered the system to be composed of molecules containing two distinct segments that interact with all other similar molecules via a Maier-Saupe dispersion force. Strictly, this does not need to be a

dispersion force but instead the important assumption is the second rank nature of the potential of mean torque for each conformer. The dispersion energy of a molecule in a particular conformation can be written as;

$$E_{dis} = - [X_a P_2(\cos\theta_a) + X_b P_2(\cos\theta_b(\phi))]$$

where the subscript a refers to the core and b to the terminal anisometric group. The angles θ_a and θ_b are the respective polar angles between a component and the direction of the molecular field or director. X_a and X_b are the interaction strength parameters and ϕ is the angle of rotation of the anisometric group, assumed to be cylindrically symmetric, about the rigid core.

For a mixture of different rod-like molecules the molecular field experienced by one molecule depends on the order parameter of the second species, the strengths of the anisotropic interactions and the composition of the mixture. Mukherjee et al [8] uses the rigorous results obtained from multicomponent mixtures [11] and by analogy defines the strength parameters for this system as ;

$$X_a = \varepsilon_{aa} C_a(N) V_a^{-1} \eta_a + \varepsilon_{ab} C_b(N) V_b^{-1} \eta_b$$

$$X_b = \varepsilon_{ab} C_a(N) V_a^{-1} \eta_a + \varepsilon_{bb} C_b(N) V_b^{-1} \eta_b$$

where C(N) is the volume fraction of the N^{th} member of the homologous series and V is the molecular volume of the basic segments. ε_{aa}, ε_{ab} and ε_{bb} are the coupling constants resulting from the core-core, core-anisometric group and anisometric group-anisometric group interactions respectively. The volume fraction and the molecular volumes are both known whereas the coupling constants are not. However, Mukherjee et al [8] apply Berthelot's combining for binary mixtures of nematogenic molecules [11] even though this was proposed only for scalar and not anisotropic interactions, and obtain;

$$\varepsilon_{ab} = (\varepsilon_{aa} \times \varepsilon_{bb})^{1/2}$$

leaving only ε_{aa} and ε_{bb} as adjustable parameters; these were

assigned using the nematic-isotropic transition temperatures of two members of the series.

The order parameters of the two segments were obtained at a particular temperature, T, using the self-consistent equations;

$$\eta_a = Z^{-1} \sum_{\substack{\text{all} \\ \text{conf.}}} \int_0^{2\pi} \int_0^1 P_2(\cos\theta_a) \exp[-(E_{dis}+E_{con})/kT] d(\cos\theta) d\phi$$

and

$$\eta_b = Z^{-1} \sum_{\substack{\text{all} \\ \text{conf.}}} \int_0^{2\pi} \int_0^1 P_2(\cos\theta_b(\phi)) \exp[-(E_{dis}+E_{con})/kT] d(\cos\theta) d\phi$$

where E_{con} is the conformational internal energy of the molecule and Z is the total partition function. Thus, θ_b and E_{con} have to be determined for all possible conformations of the molecule which were generated using the internal angles, and the corresponding orientations with respect to the laboratory-frame were calculated for a given ϕ. The Helmholtz free energy per particle for a nematic with respect to the isotropic is, within the molecular field appproximation;

$$A = (X_a\eta_a + X_b\eta_b)/2 - kT\ln(Z/Z_I)$$

where Z_I is the partition function in the isotropic phase and is obtained by setting the order parameters equal to zero. The calculated values of the nematic-isotropic transition temperatures using this theory appear to differ by between 10 K and 20 K from the observed experimental values. It should be noted, however, that the transition temperatures of the ω-phenylalkyl 4-(4'-cyanobenzylideneamino)-cinnamates originally published by Gray and Harrison [2] differ from those later reported by Gray [4] and that Mukherjee et al [8] use the transition temperatures in the earlier report. The largest discrepancy between the two sets of temperatures is for n=1 which in the first

account has a nematic-isotropic transition temperature of 87 °C [2] but in the later paper is given as 38.5 °C [4]. Unfortunately, Mukherjee et al [9] used the earlier value in assigning values for ε_{aa} and ε_{bb} and so have unwittingly introduced significant errors into their calculations. Thus, it is unclear how well their theory describes the behaviour of these compounds.

The aims of this Chapter were to investigate structure-property relationships in this class of molecules possessing a small terminal anisometric group by the synthesis of new compounds and then to compare these to those of dimeric liquid crystals. Thus, we have synthesised several series of α-(4-cyanobiphenyl-4'-oxy)-ω-(4-substitutedphenyloxy)alkanes:

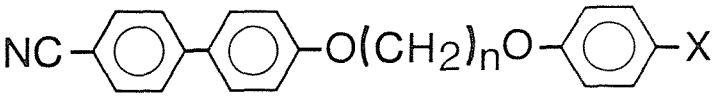

X=H: n=2-6

X= CN, CHO, Ph: n=3-6.

This particular set of compounds was chosen because with X=PhCN the structure is that of the dimeric BCBO-n's [1] and without the terminal anisometric group we simply have the nOCB's. Therefore, these new compounds may be considered to have structures which are intermediate between the monomeric nOCB series and the dimeric BCBO-n series and both of these have been well studied.

5.2 Experimental

The reaction scheme for the preparation of the α-(4-cyanobiphenyl-4'-oxy)-ω-(4-substitutedphenyloxy)alkanes involves two steps; first, the reaction of an α-chloro-ω-iodoalkane with 4-cyanohydroxybiphenyl to produce an α-chloro-ω-(4-cyanobiphenyl-4'-oxy)alkane and the subsequent reaction of this with a 4-substitutedphenol to yield the final product.

α-chloro-ω-(4-cyanobiphenyl-4'-oxy)alkanes

A mixture of an α-chloro-ω-iodoalkane (0.035mol), 4-cyanohydroxybiphenyl (0.035mol,6.8g) and sodium hydroxide (0.035mol,1.4g) in dimethylsulphoxide (40ml) was stirred at room temperature overnight. The reaction mixture was shaken thoroughly with water (300ml); the resulting white precipitate was filtered off, washed with water and dried. The crude product was passed through silica gel using dichloromethane as the eluent and recrystallised from ethanol. The yields were in the range 65% to 78%. The products were characterised using mass spectroscopy which identified the molecular ion, as well as I.R. and ^{1}H-N.M.R. spectroscopy.

Spectra

1-Chloro-4-(4-cyanobiphenyl-4'-oxy)butane:

^{1}H-N.M.R.; δ ($CDCl_3$) 1.9-2.2 (m,2H), 3.6 (t,1H), 4.0(t,1H), 6.9-7.7 (m,4H) ppm;

I.R.; ν 2210 cm^{-1}.

α-(4-cyanobiphenyl-4'-oxy)-ω-(4-substitutedphenyloxy)alkanes

A mixture of an α-chloro-ω-(4-cyanobiphenyl-4'-oxy)alkane (0.005mol), a 4-substitutedphenol (0.005mol), potassium carbonate (0.015mol,2.1g) and sodium iodide (0.0005mol,0.075g) in dimethylformamide (25ml) was refluxed with stirring for three hours. The reaction mixture was allowed to cool and then added to water (150ml). The resulting white precipitate was filtered off, washed thoroughly with water and dried.

The crude products were recrystallised from ethanol with several exceptions; ethyl acetate was used to recrystallise 1-(4-cyanobiphenyl-4'-oxy)-6-(4-phenyloxy)hexane, the odd membered compounds derived from 4-phenylphenol and all four compounds prepared using 4-cyanophenol. The even membered materials derived from 4-phenylphenol were recrystallised from toluene. The yields of all these reactions exceeded 70% and the purity of the final products was checked using thin layer chromatography. The structural characterisation of these compounds was performed using mass spectroscopy which identified the molecular ion in each case, as well as I.R. and ^{1}H-N.M.R. spectroscopy.

Spectra

1-(4-cyanobiphenyl-4'-oxy)-5-(4-phenyloxy)pentane;
^{1}H-N.M.R.; δ ($CDCl_3$) 1.6-2.1 (m,6H), 4.0 (t,4H), 6.7-7.7 (m,13H) ppm;
I.R.; ν 2210 cm^{-1}.

1-(4-cyanobiphenyl-4'-oxy)-6-(4-formylphenyloxy)hexane;
^{1}H-N.M.R.; δ ($CDCl_3$) 1.3-2.2 (m,8H), 4.0 (t,4H), 6.8-7.1 (m,4H), 7.4-7.9 (m,8H), 9.9 (s,1H) ppm;
I.R.; ν 1680, 2210 cm^{-1}.

1-(4-cyanobiphenyl-4'-oxy)-5-(4-cyanophenyloxy)pentane;
^{1}H-N.M.R.; δ ($CDCl_3$) 1.6-2.1 (m,3H), 4.0(t,2H), 6.8-7.1 (m,2H), 7.3-7.7 (m,4H) ppm;
I.R.; ν 2210 cm^{-1}.

1-(4-cyanobiphenyl-4'-oxy)-5-(4-phenylphenyloxy)pentane;
I.R.; ν 2210 cm^{-1}.

Thermal characterisation

The thermal properties of these compounds were determined using a Perkin-Elmer DSC-2C differential scanning calorimeter as well as a Nikon polarising microscope equipped with a Linkam hot stage. This was also employed to investigate the optical textures of the liquid-crystalline phases.

5.3 Results and Discussion

The α-chloro-ω-(4-cyanobiphenyl-4'-oxy)alkanes

The four members of this homologous series, prepared as intermediates in the synthesis of the α-(4-cyaonbiphenyl-4'-oxy)-ω-(4-substituted phenyloxy)alkanes, all exhibit monotropic nematic phases and their transitional properties are listed in table 5.3.1.

n	T_{CI}/°C	T_{NI}/°C	ΔH_{CI}/kJmol^{-1}	$\Delta S_{CI}/R$	ΔH_{NI}/kJmol^{-1}	$\Delta S_{NI}/R$
3	74	(43.5)	19.7	0.32	6.82	0.12
4	63.5	(62.5)	21.5	0.31	7.68	0.11
5	71	(60)	28.2	0.50	9.85	0.18
6	80.5	(65.5)	31.5	0.57	10.7	0.20

Table 5.3.1 The transition temperatures, enthalpies and entropies of transition for the α-chloro-ω-(4-cyano-biphenyl-4'-oxy)alkanes; n indicates the number of carbon atoms in the alkoxy chain and () denotes a monotropic transition. The uncertainties in the transition temperatures are ±1 °C and in the thermodynamic data are ±10%.

The dependence of the transition temperatures on the length of the alkoxy chain for the α-chloro-ω-(4-cyanobiphenyl-4'-oxy)alkanes is shown in figure 5.3.1. The melting points do not exhibit a regular dependence on n but the nematic-isotropic transition temperatures do

alternate on increasing n. Comparing the behaviour of these chlorine substituted compounds with those of the unsubstituted analogues, the nOCB's, reveals a decrease in nematic thermal stability on substituting a chlorine atom for a methyl proton. This may simply be a consequence of the reduction in the anisometric properties of the molecule.

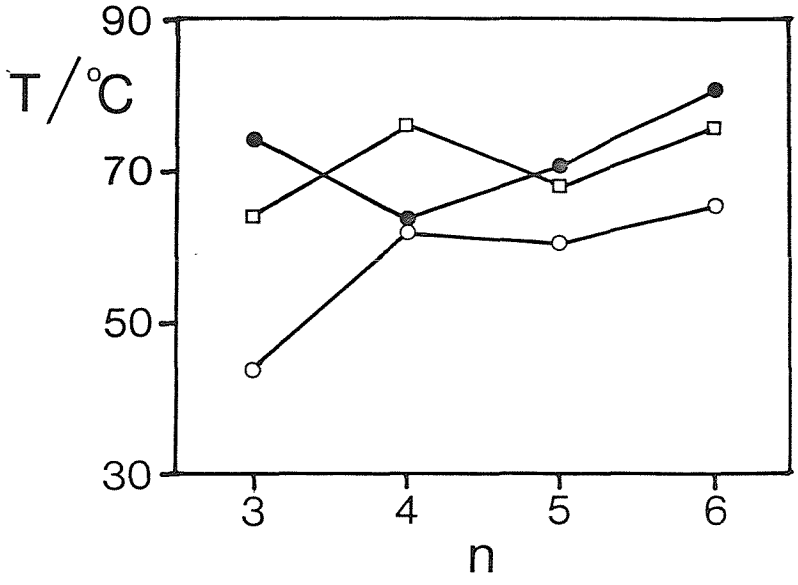

Figure 5.3.1 The dependence of the melting points (●) and the nematic-isotropic transition temperatures (o) on the number of carbon atoms in the alkyl chain for the α-chloro-ω-(4-cyanobiphenyl-4'-oxy)alkanes. The nematic-isotropic transition temperatures (□) of the 4-n-alkoxycyanobiphenyls are also shown.

The α-(4-cyanobiphenyl-4'-oxy)-ω-(4-phenyloxy)alkanes

The transitional properties of five members of this series are listed in table 5.3.2; all five compounds exhibit monotropic nematic phases with the exception of the third member for which no mesophase was observed above 25 °C. The dependence of the transition temperatures upon the length of the alkyl chain for these compounds is shown in figure 5.3.2. Both the melting points and nematic-isotropic transition temperatures exhibit a large odd-even effect on increasing n. The

similarity of this behaviour with that exhibited by nematic dimers [1] should be noted. Figure 5.3.2 also shows the nematic-isotropic transition temperatures of the analogous nOCB compounds and it is immediately apparent that substitution of a terminal methyl proton by a phenyloxy group increases the nematic thermal stability for even members but depresses it for odd members. This result will be discussed later.

n	T_{CI}/ °C	T_{NI}/ °C	ΔH_{CI}/kJmol^{-1}	ΔH_{NI}/kJmol^{-1}	ΔS_{CI}/R	ΔS_{NI}/R
2	163	(92.5)	46.4	-	12.8	-
3	87	<25	29.5	-	9.84	-
4	127	(91.5)	43.2	-	13.0	-
5	90	(38.5)	33.6	-	11.1	-
6	101	(84.5)	37.9	2.42	12.2	0.81

Table 5.3.2 The transition temperatures, enthalpies and entropies of transition for the α-(4-cyanobiphenyl-4'-oxy)-ω-(4-phenyloxy)alkanes; n indicates the number of carbon atoms in the alkoxy chain and () denotes a monotropic transition. The uncertainties in the transition temperatures are ±1 °C and in the thermodynamic data are ±10%.

Unfortunately, for this series only the value of the entropy change associated with the nematic-isotropic transition for the hexyl homologue could be determined because crystallisation prevented measurements for the other homologues. Significantly, however, the value of $\Delta S_{NI}/R$ for the hexyl homologue is larger than that normally

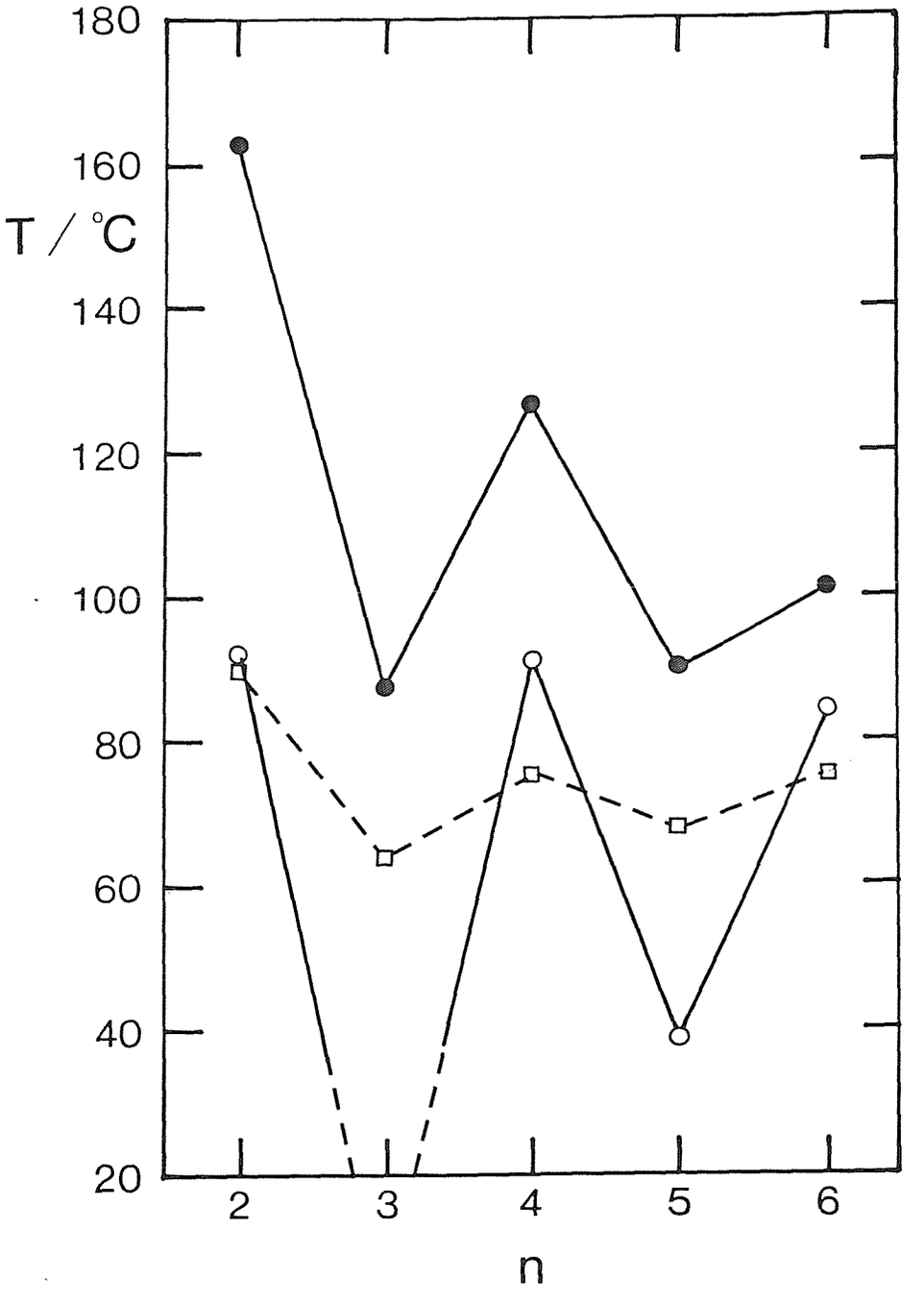

Figure 5.3.2 The dependence of the melting points (●) and the nematic-isotropic transition temperatures (○) on the number of carbon atoms in the alkyl chain for the α-(4-cyanobiphenyl-4'-oxy)-ω-(4-phenyloxy)alkanes. The nematic-isotropic transition temperatures of the 4-n-alkoxycyanobiphenyls (□) are also shown where n now refers to the number of carbon atoms in the alkoxy chain.

quoted for monomeric liquid crystals but smaller than that of dimeric compounds containing even length spacers. Therefore, and not surprisingly, this series appears to have transitional properties which are intermediate between those of monomers and dimers.

The α-(4-cyanobiphenyl-4'-oxy)-ω-(4-formylphenyloxy)alkanes

The transitional properties of the four members prepared from this series are listed in table 5.3.3; all four compounds exhibit nematic phases and the odd members are monotropic.

n	T_{CI}/°C †T_{CN}/°C	T_{NI}/°C	ΔH_{CI}/kJmol^{-1}	ΔH_{NI}/kJmol^{-1}	ΔS_{CI}/R	ΔS_{NI}/R
3	112	(38)	25.7	-	8.04	-
4	†110	137	28.9	2.79	9.07	0.82
5	99	(80)	31.6	-	10.2	-
6	†85	121	25.8	3.87	8.68	1.18

Table 5.3.3 The transition temperatures, enthalpies and entropies of transition for the α-(4-cyanobiphenyl-4'-oxy)-ω-(4-formylphenyloxy)alkanes; n indicates the number of carbon atoms in the alkoxy chain and () denotes a monotropic transition. The uncertainties in the transition temperatures are ±1 °C and in the thermodynamic data are ±10%.

The dependence of the transition temperatures upon the length of the alkoxy chain for the α-(4-cyanobiphenyl-4'-oxy)-ω-(4-formylphenyloxy)alkanes is shown in figure 5.5.3. The melting points of this

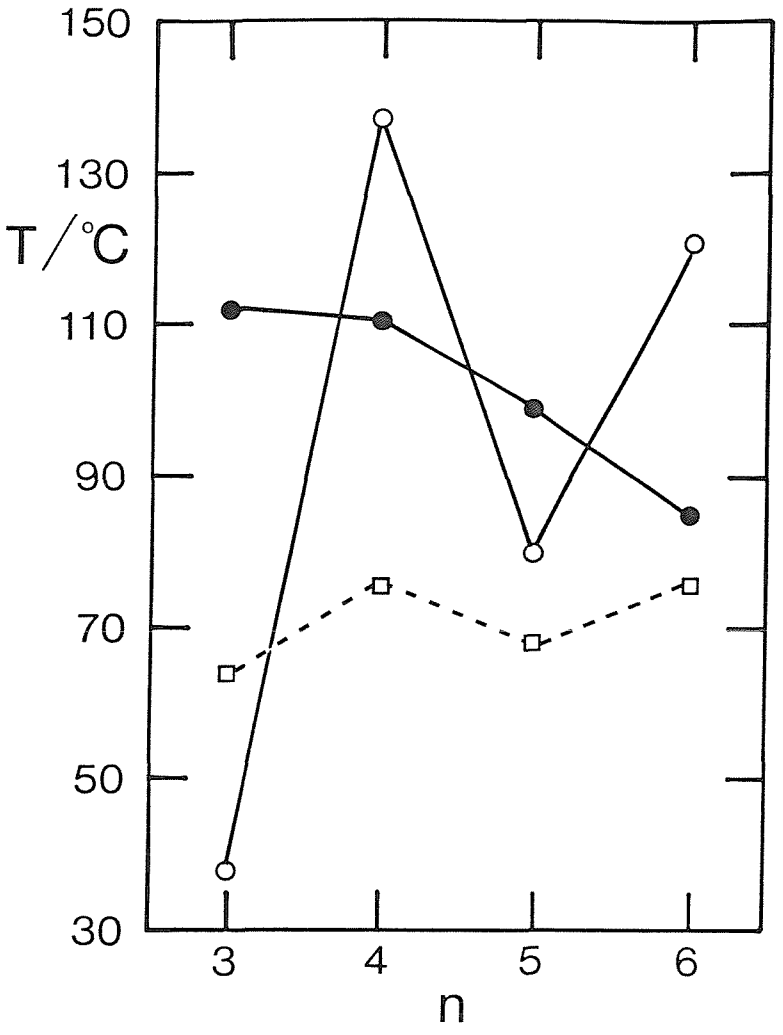

Figure 5.3.3 The dependence of the melting points (●) and the nematic-isotropic transition temperatures (O) on the number of carbon atoms in the alkyl chain for the α-(4-cyanobiphenyl-4'-oxy)-ω-(4-formylphenyloxy)alkanes. The clearing temperatures (□) of the 4-n-alkoxycyanobiphenyls are also shown where n now refers to the number of carbon atoms in the alkoxy chain.

series do not exhibit an alternation on increasing n but instead simply decrease. The nematic-isotropic transition temperatures, however, show a very pronounced alternation on varying n and is comparable to the behaviour of dimeric compounds. Only the propyl homologue has a nematic-isotropic transition temperature lower than the corresponding nOCB compound.

For this series the entropy change associated with the nematic-isotropic transition was determined for both even members and the two values of $\Delta S_{NI}/R$ obtained are intermediate between those of monomeric and even membered dimeric mesogens. Also, the hexyl homologue has a value of $\Delta S_{NI}/R$ larger than that of the butyl compound and this is in accord with the general result obtained for dimers that increasing the spacer length for a given parity increases the entropy change associated with the nematic-isotropic transition. Therefore, the α-(4-cyanobiphenyl-4'-oxy)-ω-(4-formylphenyloxy)alkanes also have properties intermediate between those of monomeric and dimeric compounds.

The α-(4-cyanobiphenyl-4'-oxy)-ω-(4-cyanophenyloxy)alkanes

The transitional properties of the α-(4-cyanobiphenyl-4'-oxy)-ω-(4-cyanophenyloxy)alkanes are listed in table 5.3.4. The even members of this series are enantiotropic nematogens, the pentyl homologue exhibits a monotropic nematic phase and no mesophase is observed for the propyl member above 80 °C.

The dependence of the transition temperatures upon the length of the alkoxy chain for these cyano substituted compounds is given in figure 5.3.4. The melting points do not show an alternation on varying n but instead simply decrease with increasing n as was observed for the formyl substituted compounds. The nematic-isotropic transition temperatures exhibit a very large odd-even effect on increasing n and again, this is reminiscent of the behaviour of dimers. The entropy change associated with the nematic-isotropic transition could only be measured for the even members and as with the formyl substituted compounds, both values of $\Delta S_{NI}/R$ are larger than those exhibited by monomeric mesogens and the value for the hexyl homologue is the greater of the two.

n	$^{\dagger}T_{CI}$/°C T_{CN}/°C	T_{NI}/°C	ΔH_{CI}/kJmol^{-1}	ΔH_{NI}/kJmol^{-1}	ΔS_{CI}/R	ΔS_{NI}/R
3	†152	<80	41.4	-	11.7	-
4	144.5	149	36.7	4.27	10.7	1.22
5	†134	(84)	47.7	-	14.1	-
6	127	133.5	36.3	4.64	11.3	1.38

Table 5.3.4 The transition temperatures, enthalpies and entropies of transition for the α-(4-cyanobiphenyl-4'-oxy)-ω-(4-cyanophenyloxy)-alkanes; () denotes a monotropic transition. The uncertainties in the transition temperatures are ±1 °C and in the thermodynamic data are ±10%.

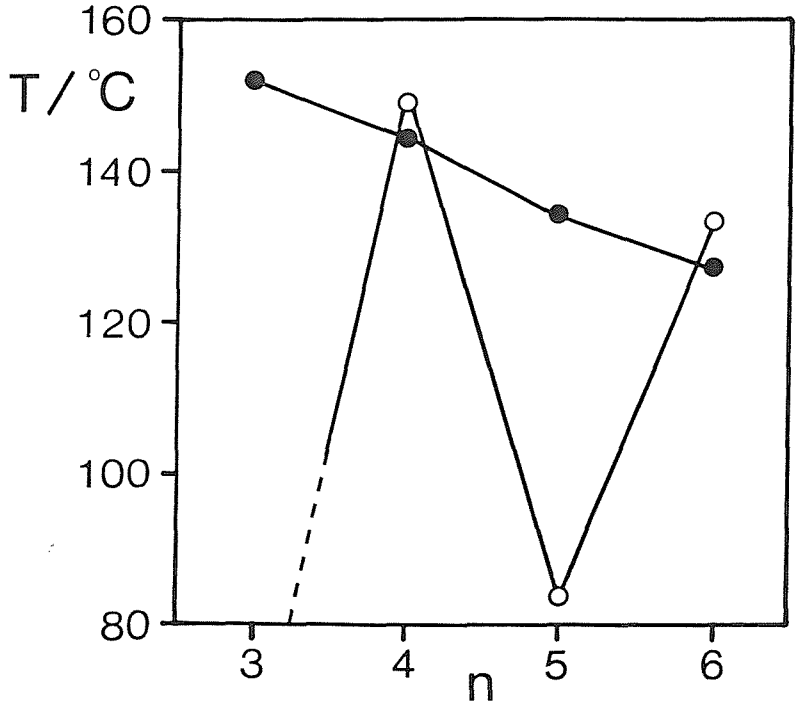

Figure 5.3.4 The dependence of the melting points (●) and the nematic-isotropic transition temperatures (O) on the number of carbon atoms in the alkyl chain for the α-(4-cyanobiphenyl-4'-oxy)-ω-(4-cyanophenyloxy)alkanes.

The α-(4-cyanobiphenyl-4'-oxy)-ω-(4-phenylphenyl-4'-oxy)alkanes

The transition temperatures of the α-(4-cyanobiphenyl-4'-oxy)-ω-(4-phenylphenyl-4'-oxy)alkanes are listed in table 5.3.5. The butyl, pentyl and hexyl homologues are monotropic nematogens and no mesophase is observed for the propyl homologue above 120 °C. In addition, the two even members also exhibit a monotropic smectic A phase which was identified on the basis of its optical texture; namely, regions of both focal-conic fans and homeotropic alignment.

n	T_{CI}/°C	T_{S_AN}/°C	T_{NI}/°C
3	144	-	<120
4	213	(159.5)	(183)
5	161.5	-	(101)
6	188	(152)	(162.5)

Table 5.3.5 The transition temperatures of the α-(4-cyanobiphenyl-4'-oxy)-ω-(4-phenylphenyl-4'-oxy)alkanes; () denotes a monotropic transition. The uncertainties in the transition temperatures are ±1 °C.

Figure 5.3.5 shows the dependence of the transition temperatures upon the length of the alkoxy chain for the α-(4-cyanobiphenyl-4'-oxy)-ω-(4-phenylphenyl-4'-oxy)alkanes and again, the very pronounced alternation in the nematic-isotropic transition temperatures on varying the parity of the alkoxy chain is immediately apparent. The melting points of this series also appear to exhibit a large odd-even effect. Unfortunately, all these compounds required extensive supercooling to obtain the nematic phase rendering the measurment of the nematic-isotropic enthalpy of transition impossible.

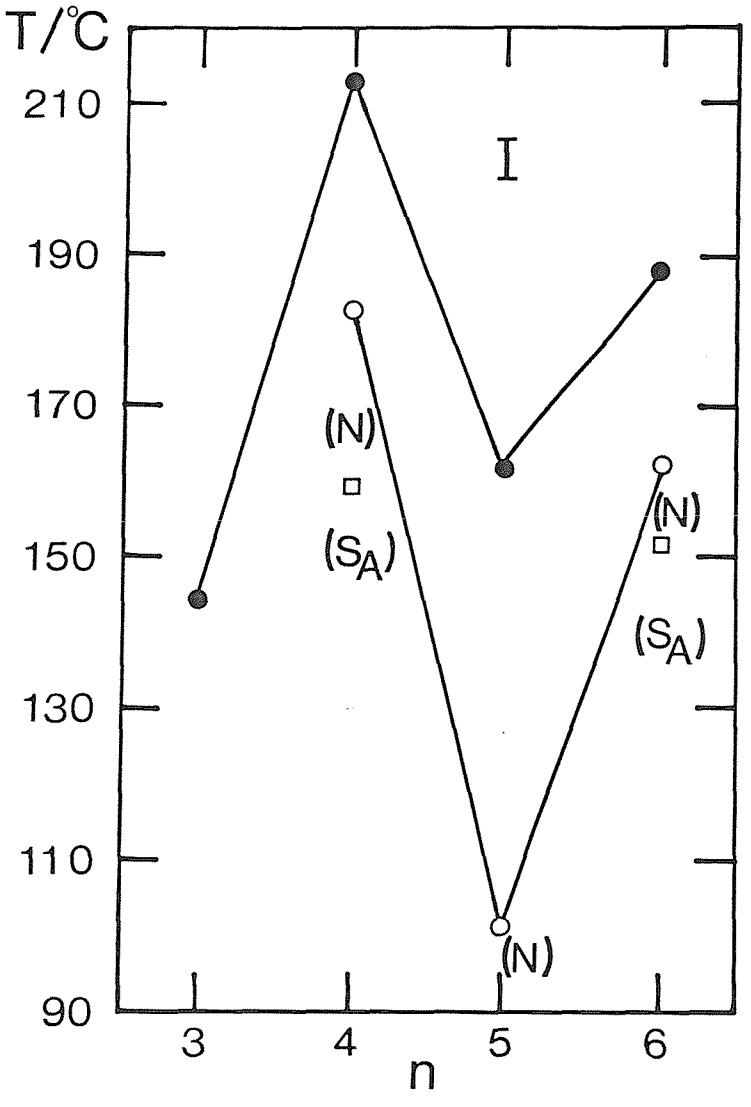

Figure 5.3.5 The dependence of the transition temperatures on the number of carbon atoms in the alkyl chain for the α-(4-cyanobiphenyl-4'-oxy)-ω-(4-phenylphenyl-4'-oxy)alkanes; ● indicates the melting points, O denotes the nematic-isotropic transition and □ the smectic A-isotropic transition. Monotropic transitions are marked in parentheses.

All four new series of mesogens possessing a small terminal anisometric group appear to have properties intermediate between those of a monomer and a dimer. In order to examine the influence of varying the 4-substituent, figure 5.3.6 shows the dependence of the nematic-isotropic transition temperatures on the length of the alkoxy chain for all four series as well as for the analogous nOCB and BCBO-n compounds. It is apparent from figure 5.3.6 that the efficiency of the 4-substituent in increasing the thermal stability of the nematic phase for both odd and even membered compounds is;

$$PhCN > Ph > CN > CHO > H;$$

and this is in complete accord with that generally observed for terminal substitution in monomeric liquid crystals [6]. This appears to contradict Gray's findings for the 4"-substituted-ω-phenylalkyl 4-(4'-cyanobenzylideneamino)cinnamates [4,5] in which a 4"-substituent was found to lower the nematic-isotropic transition temperature for odd members. To understand this difference one must consider the size, polarity and polarisabilty of the terminal groups employed in the various studies. The Hull group chose to use methyl and chloro substituents, both of which are small and conjugate only weakly with the phenyl ring so making only a small contribution to the anisometric properties of the molecules, for example the anisotropy in the polarisability. Thus, the increase in the interaction of the terminal anisometric group with the molecular field is more than offset by the increase in molecular volume and so the overall effect is a destabilisation of the nematic phase for the odd membered materials. In this study, however, the substituents used, CN, CHO and Ph, are readily polarisable and capable of interacting strongly with the terminal phenyl ring and thus, make a far larger contribution to the anisotropic properties of the molecule than either a chloro or a methyl substituent. Therefore, the increase in the volume of the terminal anisometric group is now offset by the increased interaction of the segment with the molecular field so resulting in increased nematic thermal stability for both odd and even membered compounds.

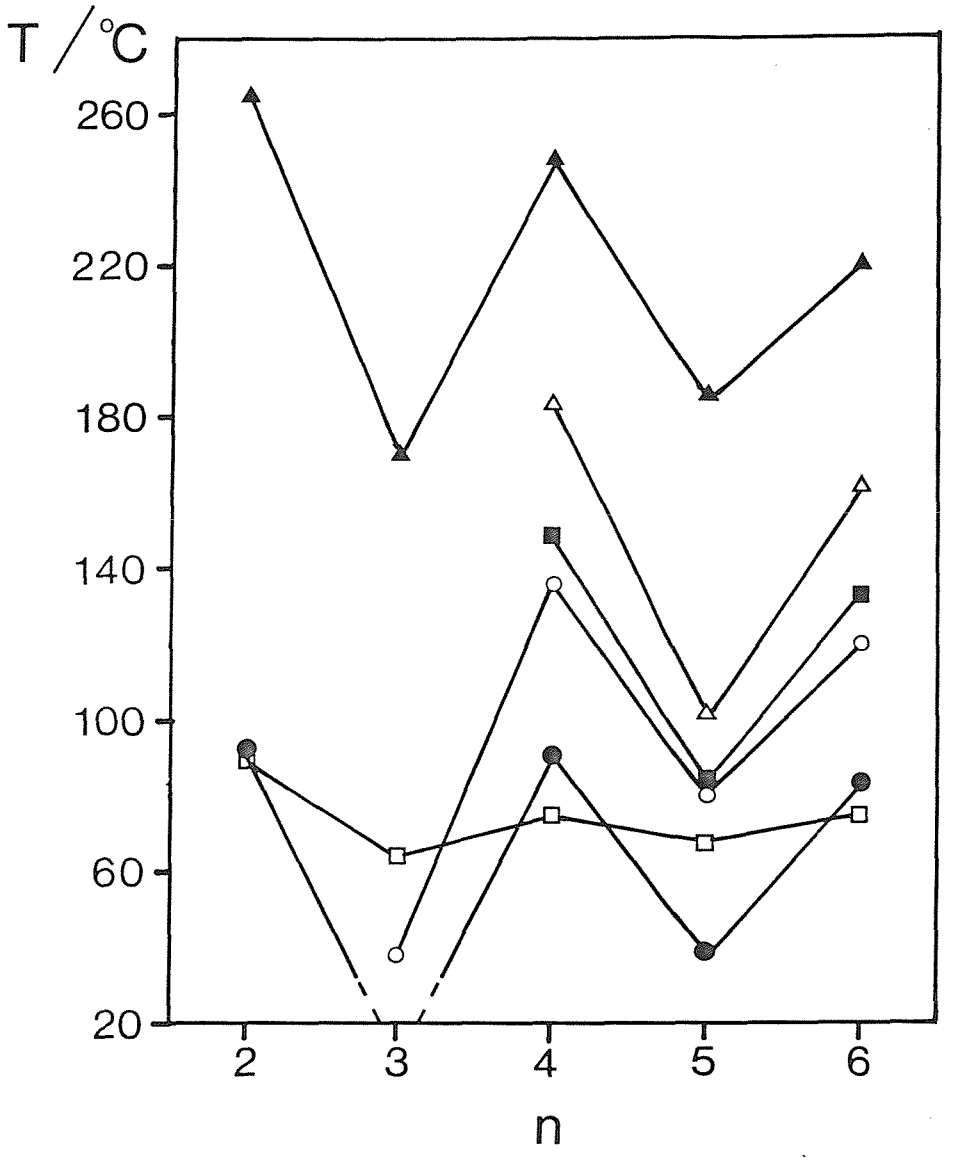

Figure 5.3.6 The dependence of the nematic-isotropic transition temperatures upon the number of carbon atoms in the alkyl chains for the α-(4-cyanobiphenyl-4'-oxy)-ω-(4-substitutedphenyloxy)alkanes. The unsubstituted series is denoted by ● , ○ indicates the formyl substituted, ■ the cyano substituted and △ the phenyl substituted compounds. Also shown are the transition temperatures of the 4-n-alkoxycyanobiphenyls (□) and the BCBO-n series (▲) [1].

A comparison of the nematic-isotropic transition temperatures of the nOCB's and their dimeric counterparts, the BCBO-n's, with their structural intermediates is presented in figure 5.3.7. An interesting feature of this comparison is that for even membered compounds it makes little difference whether or not the addition of a 4-substituent changes the terminal anisometric group into a recognisable mesogenic moiety. For example, adding CN to the unsubstituted phenyl ring increases the nematic-isotropic transition temperature by 49 °C whereas adding CN to the phenyl substituted compound, so creating a mesogenic moiety, increases the T_{NI} by 58.5 °C and this is a small difference on an absolute scale. For an odd member, however, creating a mesogenic moiety has a far more marked effect on the nematic thermal stability. Again using the addition of CN as an example, the difference between the cyano substituted and the unsubstituted compounds is 45.5 °C but between the cyanophenyl and the phenyl substituted materials is 85.5 °C. This is difficult to understand although presumably reflects the increased interaction of the more anisometric terminal group with the molecular field. Further speculation must await the results of theoretical calculations in which the increased anisometry of the terminal group is modelled by increasing X_b.

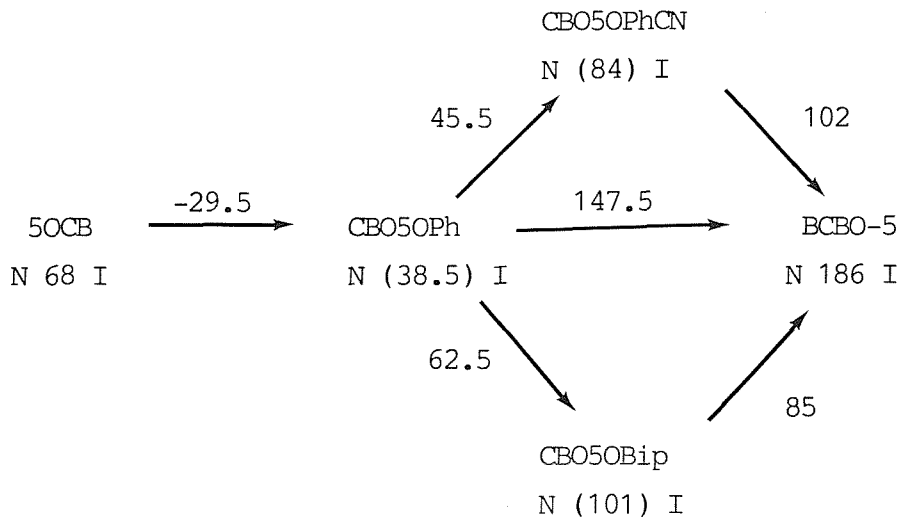

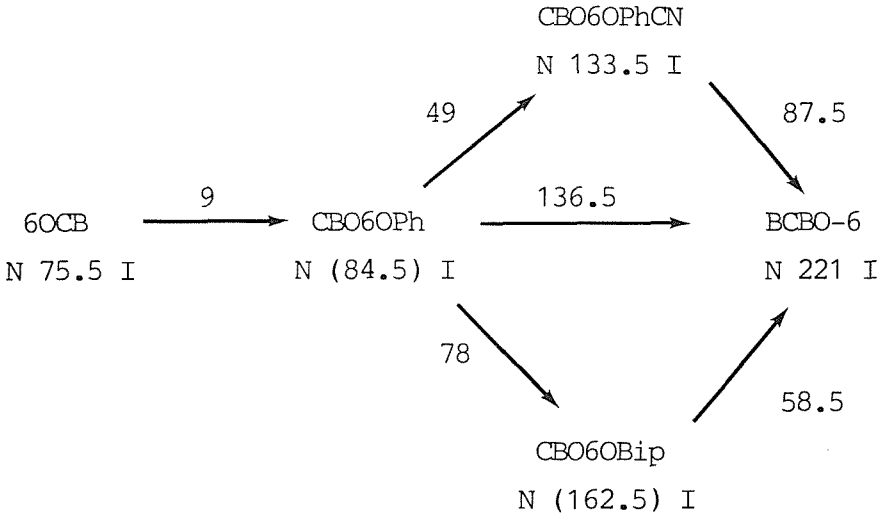

Figure 5.3.7 A comparison of the nematic-isotropic transition temperatures (°C) of the nOCB's and their analogous dimers, the BCBO-n's [1] with structural intermediates.

5.4 Conclusions

This Chapter has shown that liquid crystals comprising a semi-rigid core and a small terminal anisometric group linked via an alkyl chain possess properties intermediate between those of a monomer and a dimer. For example, the pronounced alternation in transition temperatures upon varying the parity of the spacer in a homologous series of dimers is also a characteristic feature in compounds possessing a small terminal anisometric group. Whether this alternation in transition temperatures is also mirrored in the entropies associated with the nematic-isotropic transition was not determined although the indications seem to suggest it is. Indeed, Ennulat and Brown [8] have shown that the entropies associated with the cholesteric-isotropic transition for the cholesteryl ω-phenyl-alkanoates do exhibit a more pronounced alternation than their monomeric counterparts. Therefore, it is proposed that molecules possessing terminal anisometric groups can be considered structural precursors to dimeric compounds and that there is a continuum of liquid-crystalline behaviour from the monomer through these intermediate structures to the dimer.

The compounds presented in this Chapter serve as a warning against attempting to predict or explain liquid-crystalline behaviour solely in terms of a single conformation of the molecule. For example, in an odd membered compound a 4-substituent on the terminal anisometric group serves to decrease the length to breadth ratio of the molecule if we consider only the all-trans conformation and hence, the nematic thermal stability is predicted to decrease. This, however, is not always observed and instead attention must also be given to other anisotropic molecular properties such as the polarisability anisotropy and the contribution of these to the molecular field. Therefore, attempts to rationalise the behaviour of dimeric compounds in terms of the spatial disposition of the mesogenic groups resulting from the all-trans conformation of the spacer [12] should be treated with some caution.

5.5 References

[1] see for example Emsley, J.W., Luckhurst, G.R., Shilstone, G.N., and Sage, I., 1984, Mol. Cryst. Liq. Cryst. Lett., 102, 223.

[2] see for example Gray, G.W., and Harrison, K.J., 1971, Mol. Cryst. Liq. Cryst., 13, 37.

[3] Gray, G.W., and Harrison, K.J., 1971, Symposia of the Faraday Soc., 5, 54.

[4] Gray, G.W., 1975, J. Phys. (Paris), 36, 337.

[5] Coates, D., and Gray, G.W., 1975, J. Phys. (Paris), 36, 365.

[6] Gray, G.W., 1979, The Molecular Physics of Liquid Crystals, edited by G.R. Luckhurst and G.W. Gray, Academic Press, Chap. 1.

[7] Ennulat, R.D., and Brown, A.J., 1971, Mol. Cryst. Liq. Cryst., 12, 367.

[8] Mukherjee, C.D., Bose, T.R., Ghosh, D., Roy, M.K., and Saha, M., 1986, Mol. Cryst. Liq. Cryst., 140, 205.

[9] Luckhurst, G.R., 1985, Recent Advances in Liquid Crystalline Polymers, edited by L.L. Chapoy, Elsvier Applied Science Publishers, Chap. 7.

[10] Marcjela, S.J., 1974, J. Chem. Phys., 60, 3599.

[11] Humphries, R.L., James, P.G., and Luckhurst, G.R., 1971, Symposium of the Faraday Soc., 5, 107.

[12] Jin, J.I., and Park, J.H., 1984, Mol. Cryst. Liq. Cryst., 110, 293.

CHAPTER 6 THE SYNTHESIS AND CHARACTERISATION OF LOW MOLAR MASS LIQUID CRYSTALS POSSESSING LATERAL ALKYL CHAINS

6.1 Introduction

For many years, it was generally believed that a lateral substituent on the rigid core of a liquid crystal depresses the nematic-isotropic transition temperature according to the size of the substituent, irrespective of its other properties such as polarisibility and polarity [1]. For example, Osman [2] has shown that the nematic-isotropic transition temperatures of a series of laterally substituted 1,4-bis(4-trans-pentylcyclohexyl)-benzenes:

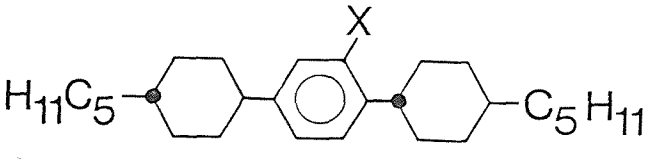

decrease according to the substituent X in the order:

$$F > Cl > CH_3 > Br > CN > NO_2.$$

Exceptions to this knowledge-based rule were known but these could easily be understood. For example, a 5-bromo-substituent in the 6-n-alkoxy-2-napthoic acids actually increases the nematic thermal stability [3] and this can be rationalised in terms of the substituent being shielded:

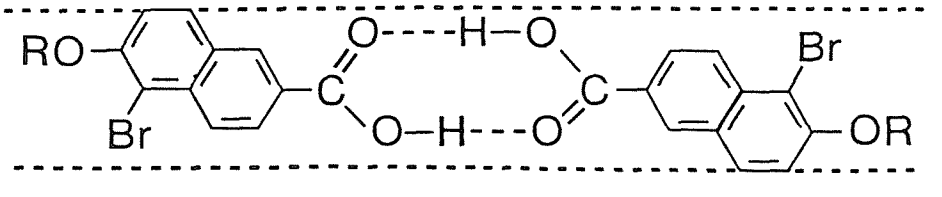

and thus does not change the length to breadth ratio of the molecule. This explanation, however, does not satisfactorily account for the increase in the nematic-isotropic transition temperature. A second example of a lateral substituent increasing the nematic-isotropic transition is if the substituent can form intra-molecular hydrogen

bonds as is the case for a series of hydroxy-substituted azo-compounds [4]:

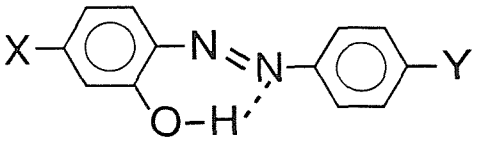

The increase in the nematic thermal stability can be attributed, in part, to the reduction of rotational motion within the molecule as a result of the hydrogen bond and this increases the planarity of the molecule. Hence, the molecular polarisability ansotropy is larger and therefore, the dispersion forces between molecules are greater.

The knowledge-based rule stating that only relatively small lateral substituents may be incorporated into the molecular structure of a liquid crystal without destroying the mesophase appeared to be quite general with only a few well understood exceptions. It came as a great surprise, therefore, when Weissflog and Demus [5,6] demonstrated that the 1,4-bis-(4-n-octyloxybenzoyloxy)-2-n-alkyl-benzenes:

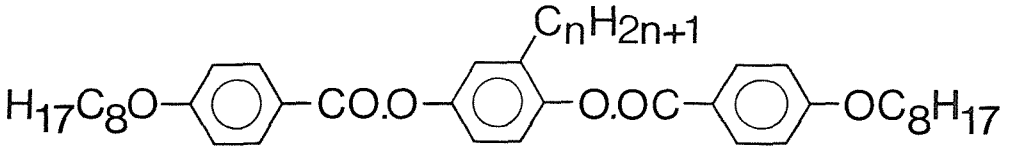

are enantiotropic nematogens even with lateral alkyl chains of up to sixteen carbon atoms in length. The nematic-isotropic transition temperatures of this series decrease for early members but then appear to converge to a given value without the alternation between odd and even alkyl chain lengths found if the terminal chain length is varied. In order to confirm these observations and to investigate other properties of laterally branched mesogens we have synthesised the 1,4-bis-(4-n-hexyloxybenzoyloxy)-2-n-alkyloxycarboxylbenzenes:

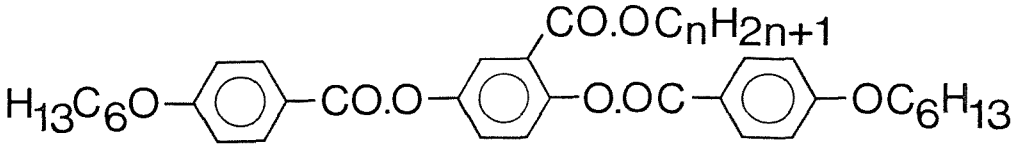

n = 1 - 12.

Recently, Tinh et al [7] reported the transitional properties of two new series of compounds composed of molecules having two alkyl chains attached to the same terminal phenyl ring of the core:

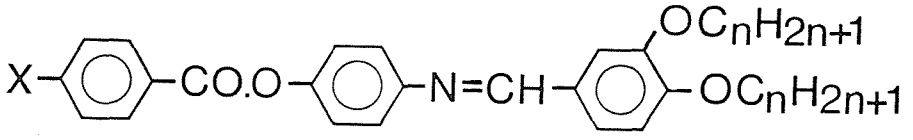

n = 6-12; X = CN, NO_2.

They termed this class of compounds forked polar mesogens and all fourteen compounds exhibit enantiotropic smectic A_d behaviour. The reduction in the clearing points on introduction of the meta-alkoxy chain is about 130 °C for the cyano-substituted compounds and 120 °C for the nitro-substituted series [7,8]. This difference in reduction results in the nitro-substituted forked compounds having higher smectic-isotropic transition temperatures than their cyano-substituted counterparts. This inversion of the thermal stability was attributed to a greater packing efficiency of the nitro-substituted compounds in the smectic phase [7]. Weissflog et al [9] reported the only other examples of forked mesogens currently known; namely, the 4-(3,4-di-alkoxy-benzylideneamino)-4'-cyanobiphenyls:

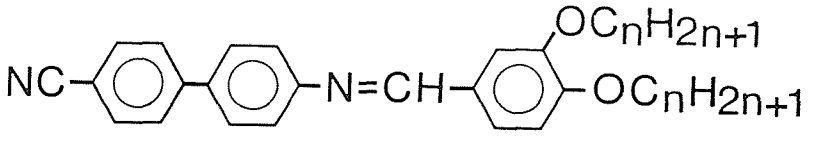

n = 1-8.

The first three members of this series are solely nematics and nematic behaviour is extinguished after the pentyl homologue. It is interesting to note that Weissflog and Demus [10] had previously concluded that a lateral chain substituent attached to the centre of the core strongly suppresses smectic behaviour whereas a topologically equivalent chain at the end of the core actually promotes smectic tendencies. This will be discussed fully later.

Tinh et al [7] suggested that the observation of liquid-crystalline behaviour in forked compounds implies that the meta-alkoxy chain is, to some extent, adopting conformations in which it lies parallel to the para-chain. This argument, if extended to consider a molecule that possesses only a single alkyl chain but in the meta-position, predicts that the chain should align along the major axis of the core and therefore, liquid-crystallinity may be observed. It is, however, a widely held view that moving an alkyl chain from the para position into the meta in a liquid crystal will result in the destruction of the mesophase. Indeed, as early as 1935 Jones [11] showed that the 4-n-alkoxybenzoic acids are mesogenic but the 3-n-alkoxybenzoic acids are not. In order to investigate this further, we have prepared the 4-cyano-4'-biphenylyl 3"-n-alkoxybenzoates;

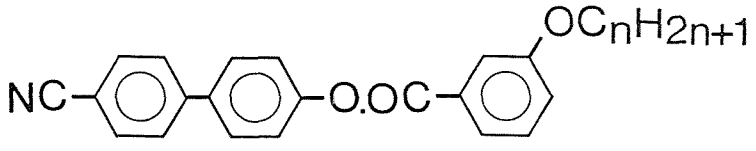

n = 1-12

mesogenic behaviour is observed for all twelve homologues. The mnemonic 3-n is used to describe this series in which n represents the number of carbon atoms in the alkoxy chain. We then proceeded to prepare the analogous forked materials, the 4-cyanobiphenylyl 3",4"-di-n-alkoxybenzoates:

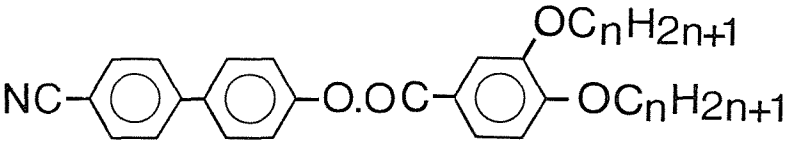

n = 1-12.

and all twelve homologues of this series also show mesogenic behaviour; by analogy we use the mnemonic 3,4-n to describe this series.

Finally, we decided to investigate the effect of incorporating a

second meta alkoxy chain into the molecular structure by preparing the first three homologues of the series, the 4-cyano-4'-biphenylyl 3",4",5"-tri-n-alkoxybezoates:

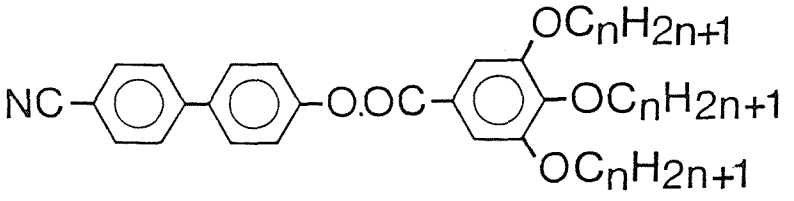

The mnemonic used for this series is 3,4,5-n and it should be noted that these tri-substituted materials are structurally intermediate between the conventional structure of a monomer and that of the recently reported phasmids [12]. A phasmidic liquid crystal is composed of molecules having six terminal alkyl chains, for example [12];

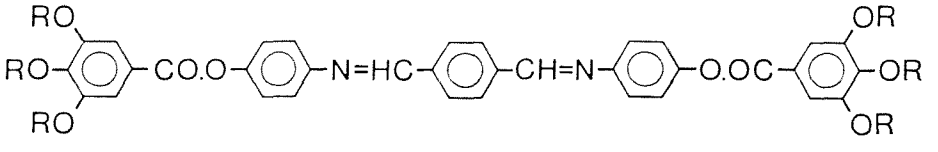

6.2 Experimental

6.2.1 1,4-bis-(4-n-hexyloxybenzoyloxy)-2-n-alkyloxycarboxylbenzenes

This homologous series of liquid crystals possessing a lateral alkyl chain was synthesised in two steps; first, 2,5-dihydroxybenzoic acid was esterified using an n-alcohol and this ester was reacted with 4-hexyloxybenzoyl chloride to yield the final products.

Alkyl 2,5-dihydroxybenzoate

A mixture of 2,5-dihydroxybenzoic acid (20g, 0.13mol), an n-alcohol (0.75mol), benzene (10ml) or, for alcohols heavier than butanol, toluene (10ml) and a few crystals of p-toluenesulphonic acid was refluxed with the azeotropic removal of water for 72 hours. The excess alcohol was removed under vacuum and to the residue was added dichloromethane (100ml). The resulting solution was washed using a 5% solution of sodium hydrogen carbonate and then dried using anhydrous calcium chloride. The dichloromethane was removed and the crude ester distilled under vacuum with the exceptions of the methyl, ethyl and butyl esters which instead were recrystallised from a mixture of chloroform and petroleum ether. The yields in all cases exceeded 80% and table 6.2.1.1 lists the melting points and distillation temperatures of the esters. The products were characterised using ^{1}H-N.M.R. and I.R. spectroscopy.

Spectra

Propyl 2,5-dihydroxybenzoate;
^{1}H-N.M.R.; δ ($CDCl_3$) 0.9 (t,3H), 1.4-2.0 (m,2H), 4.1 (t,2H), 4.8-5.7 (bs,2H), 6.7-7.0 (m,2H), 7.2 (d,1H) ppm;
I.R.; ν 1670, 3100-3600 cm^{-1}.

n	$^{\dagger}T_{CI}$/ °C T_{5mmHg}/ °C
1	[1]†87
2	†77
3	185-188
4	†63
5	180
6	[2]200-205
7	208-210
8	211-214
9	215
10	220-225
11	210-215
12	235-240

Table 6.2.1.1 The melting points or the distillation temperatures of the alkyl 2,5-dihydroxybenzoates; n indicates the number of carbon atoms in the alkyl chain.

[1] Lit. value 86-87 °C [13].

[2] Lit. value 185 °C at 1mmHg [14].

1,4-bis-(4-n-hexyloxybenzoyloxy)-2-n-alkoxycarboxylbenzenes

Hexyloxybenzoyl chloride (5g, 0.02mol) was added slowly to a stirred solution of an alkyl 2,5-dihydroxybenzoate (0.01mol) in pyridine (30ml) at 0 °C. The reaction mixture was allowed to warm to room temperature and stirred overnight. This was poured over ice (100g) and then acidified using concentrated hydrochloric acid. The resulting white precipitate was filtered off, washed thoroughly with water,

dried and recrystallised twice from absolute ethanol. Acidification of the hexyl and octyl homologue reaction mixtures yielded oils and these were extracted using dichloromethane. This was washed several times using dilute hydrochloric acid and then water. The excess dichloromethane was removed and the crude product recrystallised twice from absolute ethanol. The yields in all cases were in excess of 75% and the products were characterised using ^{1}H-N.M.R. and I.R. spectroscopy. The purity of the products was checked using thin layer chromatography.

Spectra

1,4-bis(4-n-hexyloxybenzoyloxy)-2-n-propyloxycarboxylbenzenes;
^{1}H-N.M.R.; δ ($CDCl_3$) 0.8-1.2 (m,9H), 1.2-2.2 (m,18H), 3.9-4.3 (m,6H), 7.0 (d,4H), 7.1-7.4 (m,2H), 7.9 (d,1H), 8.1 (d,4H) ppm;
I.R.; ν 1720 cm^{-1}.

6.2.2 The 3-n, 3,4-n and 3,4,5-n series

The 3-n, 3,4-n and 3,4,5-n series were all prepared using essentially the same reaction scheme consisting of four steps;

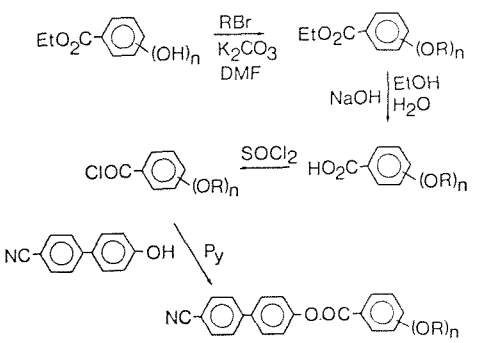

Ethyl 3-n-alkoxybenzoates

A mixture of ethyl 3-hydroxybenzoate (10g, 0.06mol), an alkyl bromide (0.066mol) and anhydrous potassium carbonate (12.5g, 0.09mol) in dimethylformamide (50ml) was refluxed with stirring for 5 hours. The reaction mixture was allowed to cool, added to water (200ml) and extracted using dichloromethane (3×50ml). The organic extracts were combined, washed with water (2×50ml) and dried using anhydrous calcium

chloride. The dichloromethane was removed and the crude product was distilled under vacuum. The distillation temperatures of the ethyl 3-n-alkoxybenzoates are recorded in table 6.2.2.1 and the yields in all cases were in excess of 70%. For the preparation of ethyl 3-methoxybenzoate, methyl iodide was used in preference to methyl bromide for reasons of reactivity. Structural characterisation of the products was performed using ^{1}H-N.M.R. and I.R. spectroscopy.

Spectra

Ethyl 3-n-butyloxybenzoate;

^{1}H-N.M.R.; δ ($CDCl_3$) 0.9 (t,3H), 1.1-2.0 (m,7H), 3.8 (t,2H), 4.2,(q,2H), 6.8-7.6 (m,4H) ppm;

I.R.; ν 1710 cm^{-1}.

n	T_{5mmHg}/ °C
1	118
2	98
3	128
4	130
5	129
6	160
7	150
8	166
9	158
10	162
11	210
12	200

Table 6.2.2.1 The distillation temperatures of the ethyl 3-n-alkoxybenzoates under reduced pressure (5mmHg); n refers to the number of carbon atoms in the alkoxy chain.

3-n-alkoxybenzoic acids

A solution of ethyl 3-n-alkoxybenzoate (10g) in 10% ethanolic sodium hydroxide (70ml) was refluxed with stirring for 2 hours. The reaction mixture was allowed to cool resulting in the precipitation of the sodium salt of the acid. The reaction mixture was added to water (200ml) in which the sodium salt dissolved and the solution was acidified to congo red using concentrated hydrochloric acid. The resulting white precipitate, the acid, was filtered off, washed thoroughly with water and recrystallised from aqueous ethanol. The yields of the pure acids were all in excess of 80% and their melting points are listed in table 6.2.2.2. The structural characterisation of the final products was performed using ^{1}H-N.M.R. and I.R. spectroscopy.

Spectra

3-n-butyloxybenzoic acid;

^{1}H-N.M.R.; δ ($CDCl_3$) 1.0 (t,3H), 1.3-2.1 (m,4H), 4.0 (t,2H), 6.9-7.7 (m,4H), 11.8 (s,1H) ppm;

I.R.; ν 1700, 2400-3200 cm^{-1}.

n	T_{CI} / °C
1	106.5
2	139
3	72
4	61.5
5	70.5
6	71
7	77.5
8	73.5
9	82.5
10	82
11	89.5
12	91

Table 6.2.2.2 The melting points of the 3-n-alkoxybenzoic acids.

3-n-alkoxybenzoyl chloride

A solution of a 3-n-alkoxybenzoic acid (5g) in freshly distilled thionyl chloride (10mol equivalent) was refluxed with stirring for 2 hours. The thionyl chloride was removed and the acid chloride distilled under reduced pressure. The yields in all cases exceeded 80% and the distillation temperatures are listed in table 6.2.2.3.

n	T/ °C	P/mmHg
1	205	30
2	180	30
3	138	30
4	190	10
5	170	10
6	220	30
7	185	10
8	196	30
9	210	30
10	230	30
11	260	30
12	240	30

Table 6.2.2.3 The distillation temperatures at a reduced pressure P of the 3-n-alkoxybenzoyl chlorides; n refers to the number of carbon atoms in the alkoxy chain.

4-cyano-4'-biphenylyl 3"-n-alkoxybenzoates

A 3-n-alkoxybenzoyl chloride (c.a. 4.4g, 0.02 mol) was added slowly to a stirred solution of 4-cyanohydroxybiphenyl (4g, 0.02mol) in pyridine (30ml) at 0 °C. The reaction mixture was allowed to warm to room temperature and stirred overnight. The reaction mixture was added to a mixture of ice and water (c.a. 100ml) and this was acidified using concentrated hydrochloric acid. The resulting white precipitate was filtered off, washed thoroughly with water and dried under vacuum. The crude product was recrystallised from an ethanol and chloroform mixture and the yields all exceeded 70%. The products were characterised using I.R. and ^{1}H-N.M.R. spectroscopy and their purity was checked using thin layer chromatography.

Spectra

4-cyano-4'-biphenylyl 3"-n-butyloxybenzoate;

^{1}H-N.M.R.; δ ($CDCl_3$) 0.9 (t,3H), 1.1-1.9 (m,4H), 4.0 (t,2H), 7.1-7.9 (m,12H) ppm;

I.R.; ν 1720, 2210 cm^{-1}.

Ethyl 3,4-di-n-alkoxybenzoates

The ethyl 3,4-di-n-alkoxybenzoates were prepared in an analogous manner to that described for the ethyl 3-n-alkoxybenzoates, replacing ethyl 3-hydroxbenzoate with ethyl 3,4-dihydroxybenzoate. Thus, a mixture of ethyl 3,4-dihydroxybenzoate (8g, 0.044mol), a bromoalkane (0.1mol) and anhydrous potassium carbonate (21.2g, 0.15mol) in dimethylformamide (50ml) was refluxed with stirring overnight. The work-up and purification proceedures were identical to those described for the ethyl 3-n-alkoxybenzoates. Methyl iodide was used in the preparation of ethyl 3,4-dimethoxybezoate. The yields all exceeded 70% and the distillation temperatures are listed in table 6.2.2.4. The structural characterisation of these esters was performed using ^{1}H-N.M.R. and I.R. spectroscopy.

Spectra

Ethyl 3,4-di-n-hexyloxybenzoate;

^{1}H-N.M.R.; δ ($CDCl_3$) 0.9 (t,6H), 1.1-2.1 (m,19H), 4.0 (t,4H), 4.3 (q,2H), 6.8 (d,1H), 7.4-7.7 (m,2H) ppm;

I.R.; ν 1710 cm^{-1}.

n	T/ °C
1	155
2	177
3	175
4	190
5	205
6	240
7	210
8	215
9	220
10	240
11	230
12	210

Table 6.2.2.4 The distillation temperatures of the ethyl 3,4-di-n-alkoxybenzoates under a reduced pressure of 5mmHg.

3,4-di-n-alkoxybenzoic acids

The hydrolysis of the ethyl 3,4-di-n-alkoxybenzoates was performed in an analogous manner to that described for the 3-n-alkoxybenzoates. However, the sodium salts of the 3,4-di-n-alkoxybenzoic acids were less soluble in water than those of the 3-n-alkoxybenzoic acids and the pentyl homologue and above were soluble only in hot water (11). The crude products were recrystallised from aqueous ethanol. The yields in all cases exceeded 75% and the melting points of the acids are listed in table 6.2.2.5. The structural characterisation of the acids was performed using ^{1}H-N.M.R. and I.R. spectroscopy.

Spectra

3,4-di-n-propyloxybenzoic acid;

^{1}H-N.M.R.; δ (DMSO-d_6) 0.9 (t,6H), 1.6 (m,4H), 3.8 (t,4H), 6.8 (d,1H), 7.2-7.4 (m,2H) ppm;

I.R.; ν 1670, 2300-3200 cm^{-1}.

n	T_{CI}/ °C
1	182.5
2	167.5
3	155.5
4	138.5
5	136.5
6	125.5
7	125.0
8	120.0
9	121.0
10	118.5
11	119.5
12	118.0

Table 6.2.2.5 The melting points of the 3,4-di-n-alkoxybenzoic acids.

3,4-di-n-alkoxybenzoyl chlorides

The 3,4-di-n-alkoxybenzoyl chlorides were prepared in an analogous manner to that described for the 3-n-alkoxybenzoyl chlorides. The distillation temperatures of the first seven homologues are listed in table 6.2.2.6. The higher homologues were not distilled because decomposition occurs below their distillation temperatures.

n	T/ °C
1	120
2	145-150
3	145-150
4	190
5	155-160
6	225-230
7	183-190

Table 6.2.2.6 The distillation temperatures of the 3,4-di-n-alkoxybenzoyl chlorides at a reduced pressure of 10mmHg.

4-cyano-4'-biphenylyl 3",4"-di-n-alkoxybenzoates

The 4-cyano-4'-biphenylyl 3",4"-di-n-alkoxybenzoates were prepared using the same method as described for the 4-cyano-4'-biphenylyl 3"-n-alkoxybenzoates. The crude products were recrystallised twice from an ethanol/chloroform mixture and their purity was checked using thin layer chromatography. The structural characterisation of this homologous series was performed using ^{1}H-N.M.R. and I.R. spectroscopy.

Spectra

4-cyano-4'-biphenylyl 3",4"-di-n-propyloxybenzoates;

^{1}H-N.M.R.; δ ($CDCl_3$) 1.0 (t,6H), 1.7 (m,4H), 4.0 (t,4H), 6.9 (d,1H), 7.1-7.9 (m,10H) ppm;

I.R.; ν 1710, 2210 cm^{-1}.

Methyl 3,4,5-tri-n-alkoxybenzoates

The methyl 3,4,5-tri-n-alkoxybenzoates were prepared in an analogous manner to that described for the ethyl 3-n-alkoxybenzoates. Thus, a mixture of methyl 3,4,5-trihydroxybenzoate (8g, 0.04mol), an alkyl bromide (0.13mol), potassium carbonate (30g,0.22mol) and dimethylformamide (50ml) was refluxed with stirring overnight. The methyl homologue was prepared using methyl iodide. The work-up and purification proceedures were identical to those described for the ethyl 3-n-alkoxybenzoates. The crude products were distilled under a reduced pressure of 5mmHg: methyl 3,4,5-trimethoxybenzoate (b.p. 130°C, yield 78%); methyl 3,4,5-triethoxybenzoate (b.p. 135°C, yield 78%); methyl 3,4,5-tri-n-propyloxybenzoate (b.p. 206°C; yield 68%). The structural characterisation of these products was performed using ^{1}H-N.M.R. and I.R. spectroscopy.

Spectra

Methyl 3,4,5-triethoxybenzoate;

^{1}H-N.M.R.; δ ($CDCl_3$) 1.3-1.7 (m,9H), 3.9 (s,3H), 4.2 (q,6H), 7.3 (s,2H) ppm;

I.R.; ν 1710 cm^{-1}.

3,4,5-tri-n-alkoxybenzoic acids

The hydrolysis of the methyl 3,4,5-tri-n-alkoxybenzoates using ethanolic sodium hydroxide was performed in an identical manner to that described in the preparation of the 3-n-alkoxybenzoic acids. The three acids prepared were recrystallised twice from aqueous ethanol: 3,4,5-trimethoxybenzoic acid (m.p. 170°C, yield 75%); 3,4,5-triethoxybenzoic acid (m.p. 113°C, yield 79%); 3,4,5-tri-n-propyloxybenzoic acid (m.p. 92°C, yield 82%). Structural characterisation of the products was performed using ^{1}H-N.M.R. and I.R. spectroscopy.

Spectra

3,4,5-triethoxybenzoic acid;

^{1}H-N.M.R.; δ (DMSO-d_6) 1.0 (q,9H), 3.5-4.0 (m,6H), 6.9 (s,2H) ppm;

I.R.; 1680, 2400-3200 cm^{-1}.

3,4,5-tri-n-alkoxybenzoyl chlorides

The 3,4,5-tri-n-alkoxybenzoyl chlorides were prepared in an analogous manner to that described for the 3-n-alkoxybenzoyl chlorides. All three acid chlorides were distilled under a reduced pressure of 5mmHg: 3,4,5-trimethoxybenzoyl chloride (b.p. 150°C, yield 85%); 3,4,5-triethoxybenzoyl chloride (b.p. 145°C, yield 90%); 3,4,5-tri-n-propyloxybenzoyl chloride (b.p. 155°C, yield 92%).

4-cyano-4'-biphenylyl 3",4",5"-tri-n-alkoxybenzoates

The 4-cyano-4'-biphenylyl 3",4",5"-tri-n-alkoxybenzoates were prepared using the method described for the 4-cyano-4'-biphenyl 3"-n-alkoxybenzoates. The crude products were recrystallised twice from an ethanol/chloroform mixture and their resulting purity was checked using thin layer chromatography. The structural characterisation of the final products was performed using ^{1}H-N.M.R. and I.R. spectroscopy.

Spectra

4-cyano-4'-biphenylyl 3",4",5"-triethoxybenzoate;
^{1}H-N.M.R.; δ ($CDCl_3$) 1.1-1.8(m,9H), 3.8-4.4(m,6H), 7.1-7.9(m,10H) ppm;
I.R.; ν 1710, 2210 cm^{-1}.

Thermal Characterisation

The thermal properties of these compounds were determined using a Perkin-Elmer DSC-2C differential scanning calorimeter as well as a Nikon polarising microscope equipped with a Linkam hot stage. This was also employed to investigate the optical textures of the liquid-crystalline phases. Selected examples of the smectic phases were studied further by X-ray diffraction with a Guinier camera fitted with a bent quartz monochromator using $CuK_{\alpha 1}$ radiation (λ=0.15405nm).

6.3 Results and Discussion

6.3.1 1,4-bis-(4-n-hexyloxybenzoyloxy)-2-n-alkoxycarboxylbenzenes

The transitional properties of the 1,4-bis-(4-n-hexyloxybenzoyloxy)-2-n-alkoxycarboxyl benzenes are listed in table 6.3.1. All the members of this series are enantiotropic nematogens with the sole exception of the third member which is monotropic. Figure 6.3.1.1 illustrates the dependence of the nematic-isotropic transition temperature upon the length of the lateral alkyl chain. As would be expected the transition temperature decreases with increasing chain length for the early members but then appears to begin to converge to a given value without the alternation found if the terminal alkyl chain length is varied. Molecular statistical theories of biaxial particles predict that the nematic-isotropic transition temperature should decrease by a small amount with a decreasing length to breadth ratio for the molecule. If the results presented in figure 6.3.1.1 are interpreted in this manner then it is clear that the length to breadth ratio of the molecule initially decreases and then tends to a constant value with increasing alkyl chain length. This may be explained by considering the conformations of the lateral alkyl chain. If the chain is considered to be all-trans then increasing the chain length would decrease monotonically the length to breadth ratio of the molecule. If, however, the lateral chain adopts a conformation in which it lies parallel to the molecular axis then the length to breadth ratio would indeed remain constant over a range of chain lengths. This can also be considered as the dilution of the semi-rigid cores becomes constant as the lateral chain length increases.

n	T_{CN}/°C T_{NI}/°C †T_{CI}/°C	ΔH_{C-}/kJmol^{-1} ΔH_{NI}/kJmol^{-1}	ΔS_{C-}/R ΔS_{NI}/R
1	98.5 135	33.5 10.9	2.25 0.67
2	85.5 124.5	35.5 11.9	2.47 0.75
3	†111.5 (106.5)	31.5 9.84	2.15 0.68
4	100.5 104.5	28.8 9.25	2.00 0.64
[1]5	67.5 101	23.1 8.18	1.87 0.60
6	75 101	35.0 12.1	1.83 0.60
7	70.5 97.5	36.7 12.9	1.76 0.58
8	70.5 94.5	34.5 12.1	1.91 0.63
9	58.5 90.5	34.5 12.5	1.73 0.57
10	63 89	44.4 15.9	1.85 0.62
11	67 87.5	37.2 13.2	1.83 0.62
12	70 86.5	57.3 20.1	1.94 0.65

Table 6.3.1 The transition temperatures and enthalpies and entropies of transition of the 1,4-bis-(4-n-hexyloxy-benzoyloxy)-2-n-alkoxycarboxylbenzenes; () indicates a monotropic transition. The uncertainties in the transition temperatures are ±1 °C and in the thermodynamic data are ±10%.
[1] Lit. values: T_{CN} 67 °C; T_{NI} 99.5 °C [10].

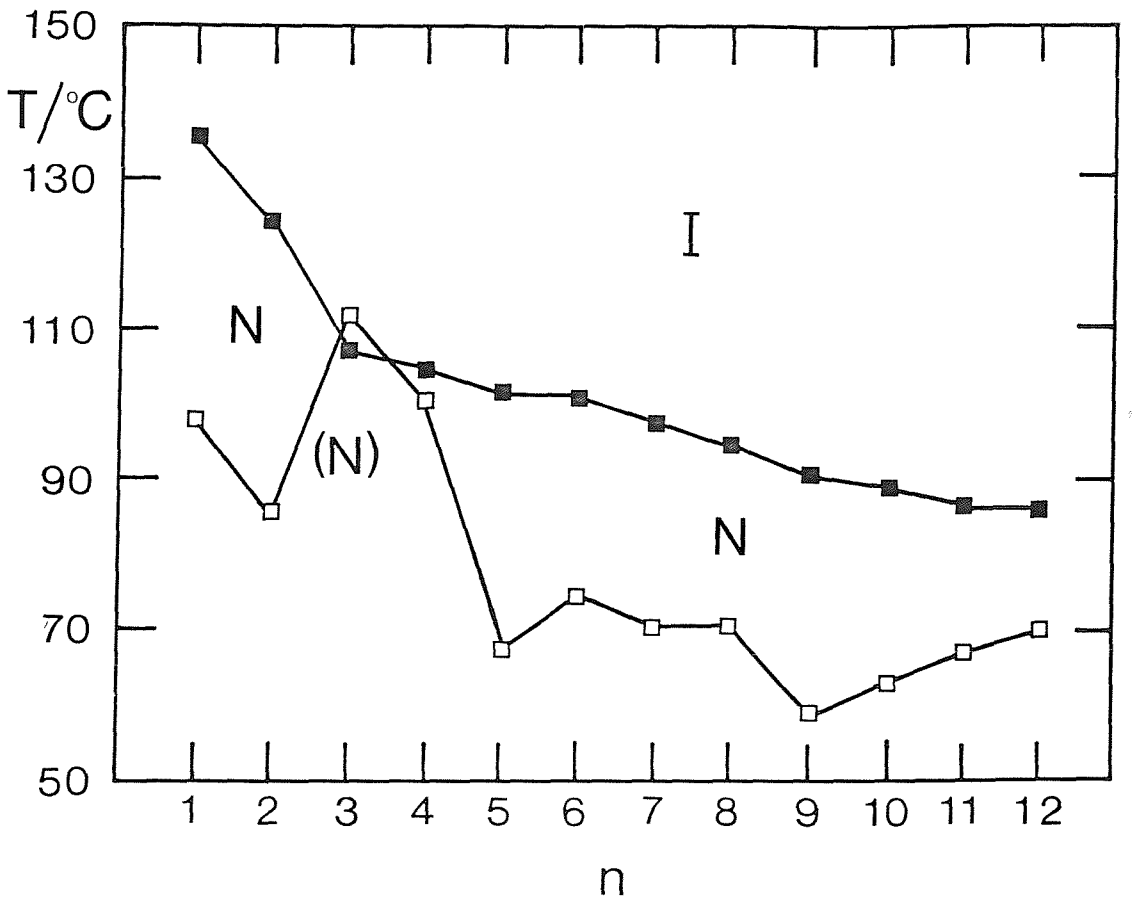

Figure 6.3.1.1 The dependence of the melting points (□) and the nematic-isotropic transition temperatures (■) on the number of carbon atoms in the lateral alkyl chain for the 1,4-bis-(4-n-hexyloxy-benzoyloxy)-2-n-alkoxycarboxylbenzenes.

The dependence of the entropies associated with the nematic-isotropic transition upon the length of the lateral alkyl chain is shown in figure 6.3.1.2. The entropies initially fall, pass through a minima and then rise again as the lateral alkyl chain length is increased. It is interesting to note that similar behaviour was reported by Demus et al [15] for the entropies of transition of the 1,4-bis-(4-n-octyloxy-benzoyloxy)-2-n-alkylbenzenes and this is shown in figure 6.3.1.3. This suggests that the nature of the link between the lateral alkyl chain and the semi-rigid core is not important in determining the value of the entropy change at the nematic-isotropic transition. It should be noted that the entropy changes shown in figure 6.3.1.3 are typically twice as large as those observed for conventional monomeric

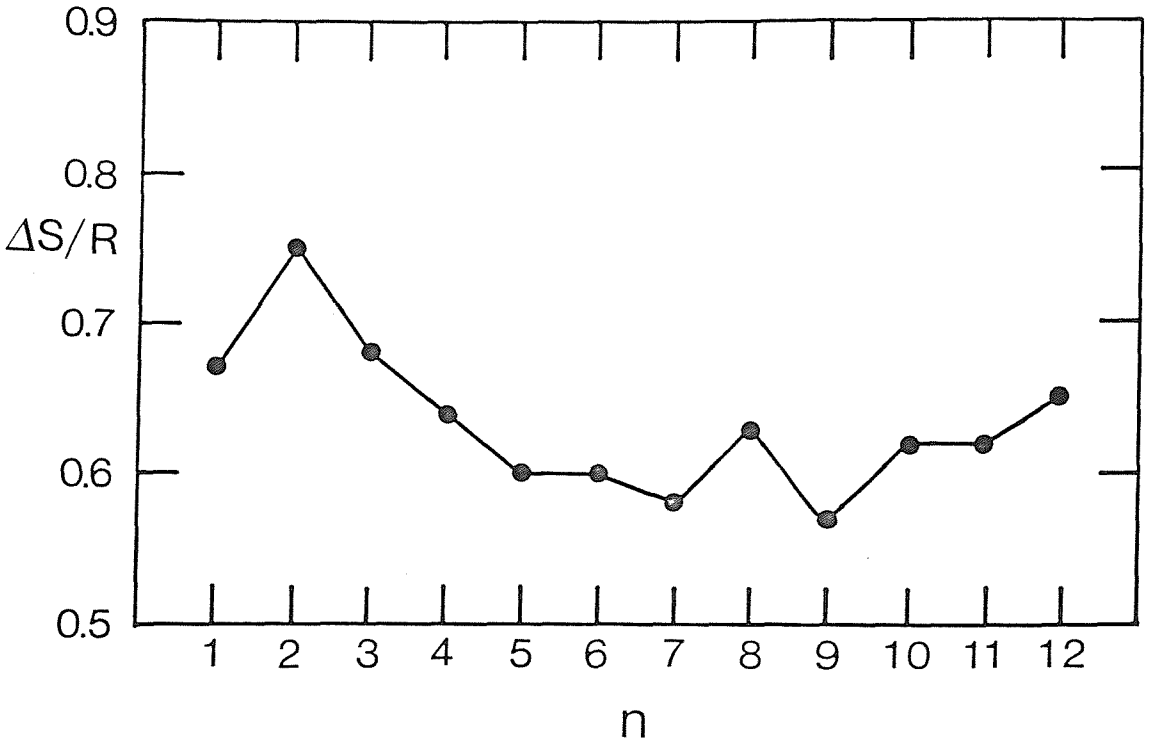

Figure 6.3.1.2 The dependence of the entropy change associated with the nematic-isotropic transition on the number of carbon atoms in the lateral alkyl chain for the 1,4-bis-(4-n-hexyloxybenzoyloxy)-2-n-alkoxycarboxylbenzenes.

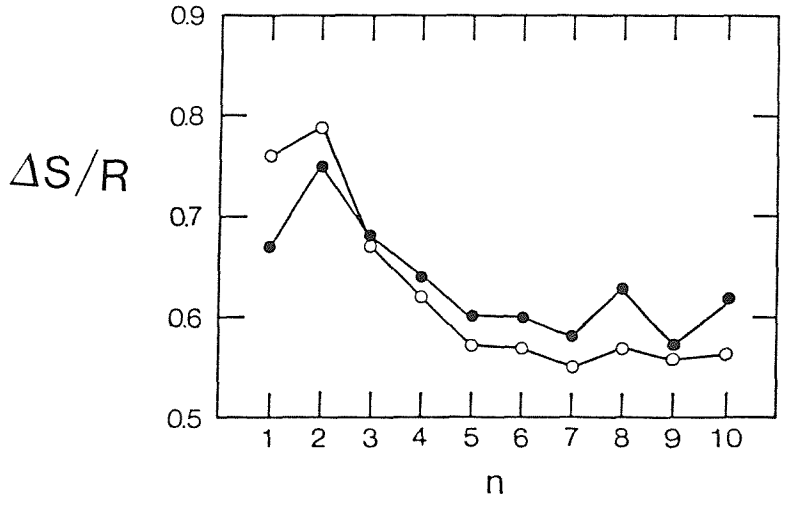

Figure 6.3.1.2 The dependence of the nematic-isotropic transition entropy on the number of carbon atoms in the lateral alkyl chain for the 1,4-bis-(4-hexyloxybenzoyloxy)-2-n-alkoxycarboxylbenzenes (●) and for the 1,4-bis-(4-n-octyloxybenzoyloxy)-2-n-alkylbenzenes (o) [15] where (n+2) now represents the total number of carbon atoms in the lateral alkyl chain.

mesogens. This may be due, in part, to the increase in the conformational contribution to the entropy change arising from the lateral alkyl chain. We stress, however, that the entropy changes are small and so their unambiguous interpretation is difficult. The fall in the entropy of transition with increasing chain length, shown in figure 6.3.1.3, is surprising since quite the opposite behaviour is observed if the length of a terminal chain is increased. This unexpected initial decrease may result from an increase in the molecular biaxiality but further speculation awaits the results from model calculations that allow for chain conformations as well as further experiments to measure the orientational order of mesogens possessing lateral alkyl chains.

6.3.2 4-cyano-4'-biphenylyl 3''-n-alkoxybenzoates

The transitional properties of the 3-n series are listed in table 6.3.2. All the members of this series are monotropic with the sole exception of 3-11 which exhibits an enantiotropic smectic A phase. The first four homologues are purely nematic; the fifth, sixth and seventh members exhibit both nematic and smectic A phases. The higher homologues show only smectic A behaviour. The smectic A phase was identified on the basis of its optical texture being composed of regions of homeotropic and focal-conic fan texture.

Figure 6.3.2.1 shows the dependence of the transition temperatures on the length of the alkoxy chain for the 3-n series. The nematic-isotropic transition temperature curve falls with increasing chain length, then appears to begin to converge but is intersected by the smectic A-isotropic transition temperature curve which rises with increasing chain length. The nematic-isotropic transition of the core, 4-cyano-4'-biphenylyl benzoate, is 195 °C [16]. Thus, the introduction of the 3-methoxy substituent has decreased the nematic thermal stability by 65.5 °C and this seems to be somewhat disproportionately large when compared simply with the decrease in the length to breadth ratio of the molecule. The initial decrease in the nematic-isotropic transition temperature for the early members of the 3-n series may be

n	T_{CI}/°C $^{\dagger}T_{CS_A}$/°C	T_{S_AN}/°C	T_{NI}/°C $^{\dagger}T_{S_AI}$/°C
1	155.5	-	(132)
2	127.5	-	(93.5)
3	154	-	(81)
4	111	-	(67)
5	98.5	(38)	(65.5)
6	80	(53.5)	(61.5)
7	78.5	(62.5)	(63.5)
8	86.5	-	†(65.5)
9	77	-	†(70.5)
10	88.5	-	†(73.5)
11	†69.5	-	†76
12	84.5	-	†(78.5)

Table 6.3.2 The transition temperatures of the 4-cyano-4'-biphenylyl 3"-n-alkoxybenzoates; ( ) denotes a monotropic transition. The uncertainties in the temperatures are ±1 °C.

attributed to the decrease in the length to breadth ratio of the molecule on increasing the chain length. However, a longer alkoxy chain may adopt conformations in which it lies parallel to the major axis of the core and hence, the monotonical decrease in the length to breadth ratio of the molecule is halted and may indeed be reversed. The obvious question now concerns the energetic cost of the alkoxy chain adopting such conformations. These elongated conformers will be more favoured in the nematic environment but further speculation awaits the results from model calculations which allow for these specific conformations.

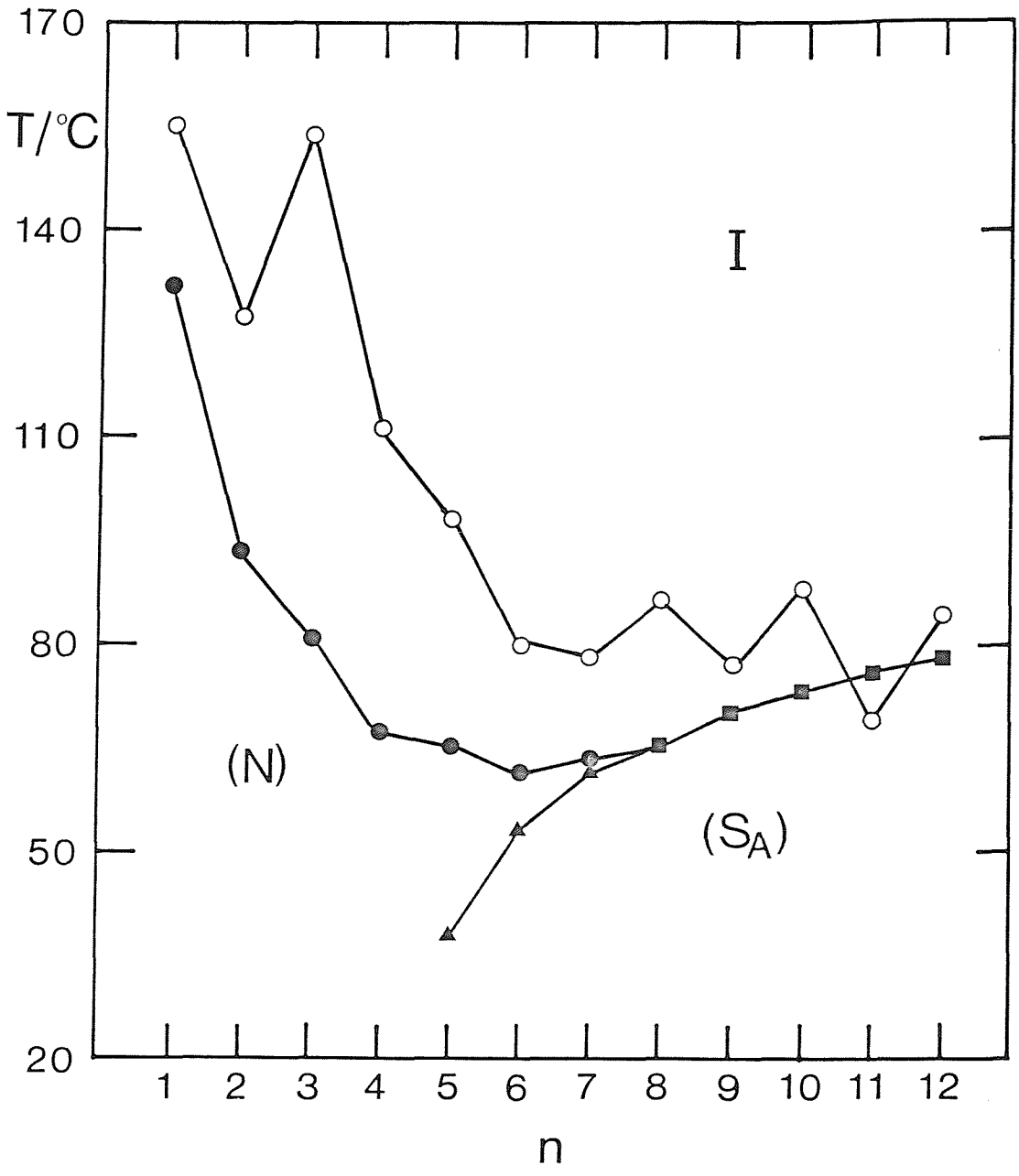

Figure 6.3.2.1 The dependence of the transition temperatures on the number of carbon atoms in the alkoxy chain for the 4-cyano-4'-biphenylyl 3''-n-alkoxybenzoates. The melting point is denoted by o, ● indicates the nematic-isotropic transition, ▲ the smectic A-nematic transition and ■ the smectic A-isotropic transition. Monotropic transitions are marked in parentheses.

It is interesting to note that a lateral alkyl chain positioned at the centre of the core greatly suppresses smectic phase stability whereas a topologically equivalent chain at the end of the core actually enhances smectic properties relative to nematic. This is shown in figure 6.3.2.2 which compares the clearing temperatures of the 3-n series with those of the 4-cyano-4'-biphenylyl 4''-n-alkoxybenzoates [16] which using our terminology may be referred to as the 4-n series; it is evident that the nematic properties of the 3-n series are extinguished at shorter chain lengths than in the 4-n series. The topological equivalence of the two lateral chains implies that theory would predict that the properties of the two different series should be comparable and this is clearly not the case. The difference in properties, however, is easily understood. A lateral chain attached to the centre of the core dilutes core-core interactions by forming a sheath around the core and this effectively reduces the molecular inhomogeniety as well as core-core interactions and in consequence, the smectic tendencies of the molecule are greatly reduced. This example serves to illustrate the shortcomings of theories that do not allow for the spatial position of the alkyl chain being modelled. The increase in the relative stability of the smectic phase on moving the alkoxy chain from the 4''-position to the 3''-position may arise from the associated lowering of the transition temperatures.

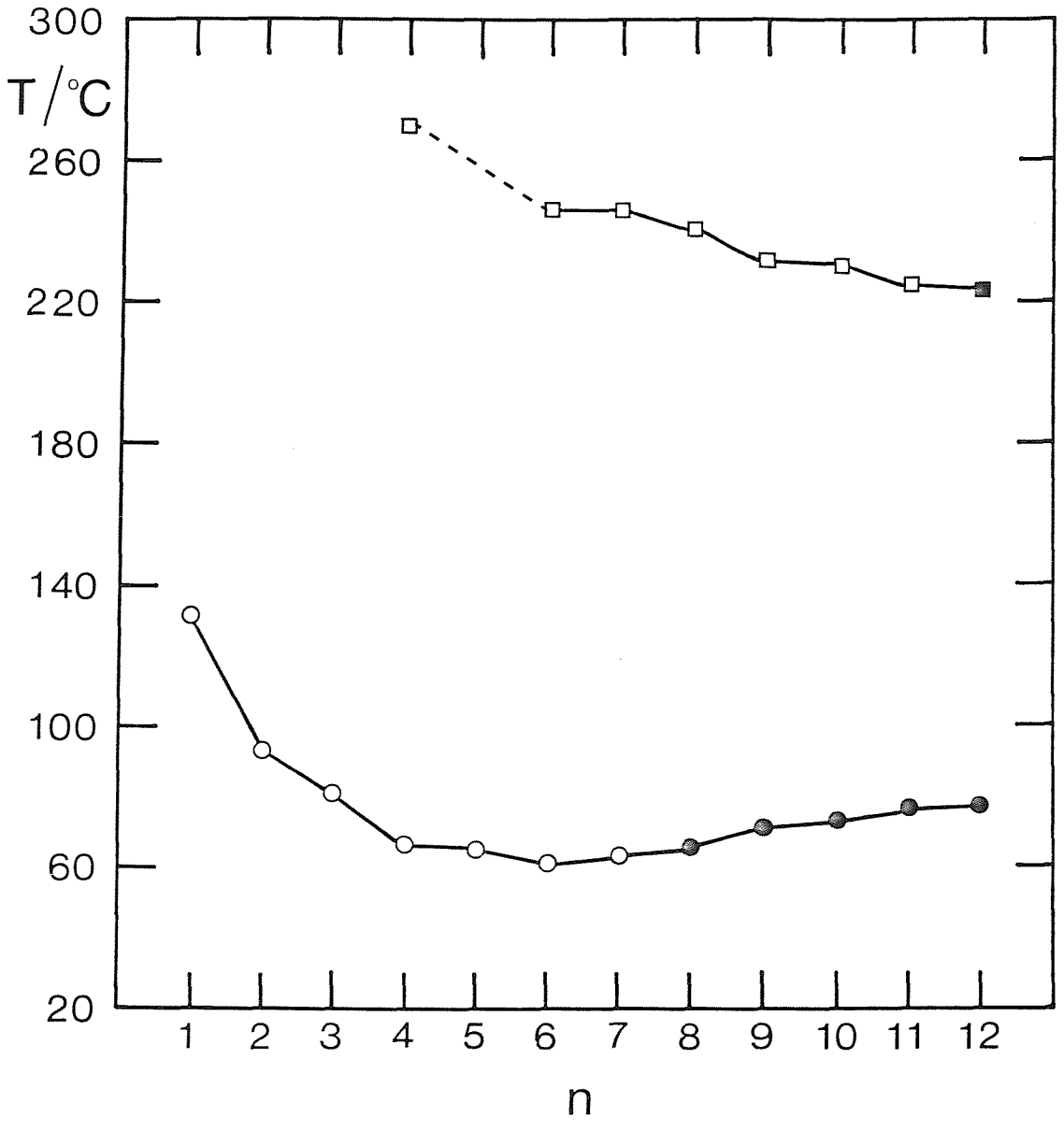

Figure 6.3.2.2 The dependence of the liquid crystal-isotropic transition temperature on the number of carbon atoms in the alkoxy chain for the 4-cyano-4'-biphenylyl 3"-n-alkoxybenzoates indicated by circles and for the 4-cyano-4'-biphenylyl 4"-n-alkoxybenzoates [16] denoted by squares. Open symbols represent nematic-isotropic transitions and filled symbols indicate smectic A-isotropic transitions.

6.3.3 4-cyano-4'-biphenylyl 3",4"-di-n-alkoxybenzoates

The transitional properties of the 3,4-n series are listed in table 6.3.3.1. Eight homologues exhibit enatiotropic mesophases, the exceptions are the second, third, fourth and fifth members for which monotropic behaviour is observed. The early members are solely nematogens; 3,4-4 exhibits both smectic A and nematic phases; the remaining homologues are exclusively smectogenic. 3,4-10, 3,4-11 and 3,4-12 exhibit a smectic C phase as well as a smectic A phase. The smectic A phase was identified as such on the basis of the optical textures observed when viewed under a polarising microscope; namely, regions of both homeotropic and focal-conic fan texture. On cooling the smectic A phase, the homeotropic regions adopted a schlieren texture and the focal-conic fans became broken and somewhat sanded. In consequence, this new phase was assigned as a smectic C.

Figure 6.3.3.1 shows the dependence of the transition temperatures on the number of carbon atoms in the terminal alkoxy chains for the 3,4-n series. The melting points show a decrease for the early members and then appear to converge with increasing chain length. The clearing points also decrease for the early members then begin to converge at which point, the smectic A-isotropic curve intersects the nematic-isotropic curve resulting in a slight increase in the clearing temperatures before they appear to converge to a given value. The 3,4-n compounds represent only the fourth series of forked mesogens to be reported and provide the only example for which as many as twelve homologues have been characterised. Figure 6.3.3.2 shows the dependence of the clearing temperatures on the number of carbon atoms in the alkoxy chains for the four different series of forked mesogens and the similarity in behaviour is striking. The observation of liquid-crystalline behaviour in compounds of this general molecular structure presumably implies that the meta-alkoxy chain to some extent adopts conformations in which it lies parallel to the para-alkoxy chain. These conformations presumably result in interactions between the two chains and the importance of such interactions is unclear.

n	$^1T_{CI}$/°C $^2T_{CN}$/°C T_{CS_A}/°C	$^1T_{S_AN}$/°C $T_{S_CS_A}$/°C	$^1T_{NI}$/°C T_{S_AI}/°C	$^1\Delta H_{NI}$/kJmol^{-1} $\Delta H_{C_}$/kJmol^{-1} ΔH_{S_AI}/kJmol^{-1}		$^1\Delta S_{NI}$/R $\Delta S_{C\_}$/R ΔS_{S_AI}/R	
1	^{2}187.5	-	^{1}191	35.7	^{1}0.82	9.33	^{1}0.22
2	^{1}171	-	^{1}(167)	51.3	^{1}0.73	13.9	^{1}0.20
3	^{1}163	-	^{1}(141.5)	42.7	-	11.8	-
4	^{1}154	^{1}(138)	^{1}(143)	45.9	^{1}1.50	13.0	^{1}0.43
5	143.5	-	(142.5)	44.0	4.31	12.7	1.25
6	138.5	-	147	43.5	5.12	12.7	1.47
7	133.5	-	145.5	43.0	5.46	12.7	1.57
8	131	-	146	48.7	6.23	14.6	1.79
9	130.5	-	144	52.1	6.10	15.5	1.76
10	130.5	(115)	143	53.2	6.46	15.9	1.87
11	128.5	(118)	139.5	54.3	6.30	16.3	1.84
12	130	(113)	142.5	58.0	7.34	17.3	2.15

Table 6.3.3.1 The transition temperatures, enthalpies and entropies of transition for the 4-cyano-4'-biphenylyly 3",4"-di-n-alkoxy-benzoates; () denotes a monotropic transition. The uncertainties in the temperatures are ±1°C and in the thermodynamic data are ±10%.

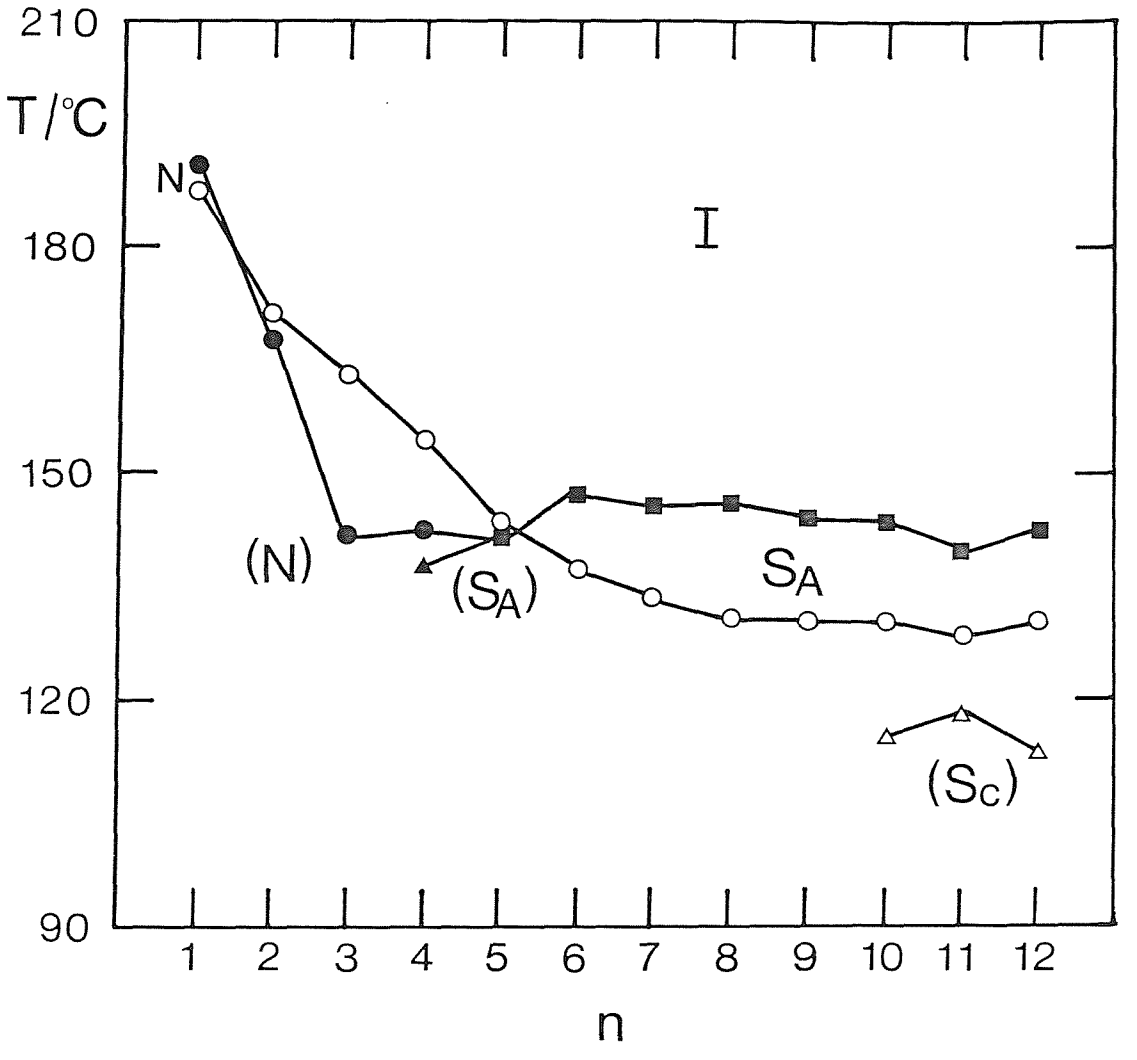

Figure 6.3.3.1 The dependence of the transition temperatures on the number of carbon atoms in the alkoxy chains for the 4-cyano-4'-biphenylyl 3",4"-di-n-alkoxybenzoates. The melting point is denoted by o , ● indicates the nematic-isotropic transition, ▲ the smectic A- nematic transition, △ the smectic A-smectic C transition and ■ the smectic A-isotropic transition. Monotropic phases are marked in parentheses.

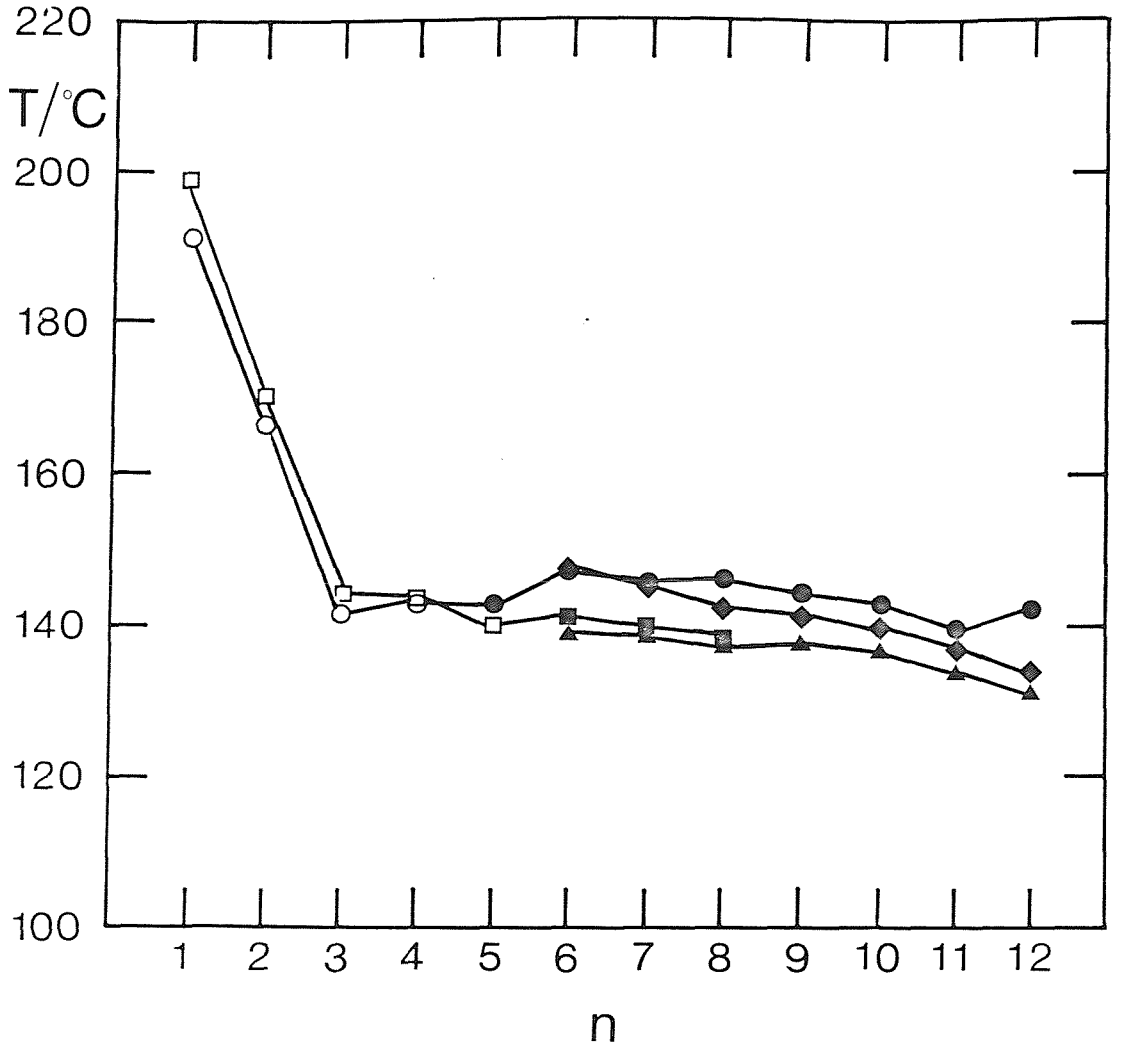

Figure 6.3.3.2 The dependence of the liquid crystal-isotropic transition temperatures on the number of carbon atoms in the alkoxy chains for the 4-cyano-4'-biphenylyl 3",4"-di-n-alkoxybenzoates denoted by circles, the 4-(3,4-di-n-alkoxybenzylideneamino)-4'-cyano-biphenyls [9] represented by squares, the 3,4-di-alkoxybenzylidene-4'-(4"-cyanobenzoyloxy)anilines [7] indicated by triangles and the 3,4-di-n-alkoxybenzylidene-4'-(4"nitrobenzoyloxy)anilines [7] denoted by diamonds. Open symbols represent nematic-isotropic transitions and filled symbols indicate smectic A-isotropic transitions.

The introduction of the meta-alkoxy chain has promoted smectic behaviour relative to nematic and this is shown in figure 6.3.3.3 which compares the clearing temperatures of the 3,4-n series with those of the 4-n series [16]. The layer spacings for several of the smectic A phases exhibited by members of the 3,4-n series have been measured using X-ray diffraction [17] and the results are summarised in table 6.3.3.2.

n	T/T_{S_AI}	d / Å	d / l
6	0.98	34.4	1.25
7	0.98	36.0	1.25
8	0.97	37.7	1.26
9	0.97	39.5	1.27
10	0.97	40.3	1.24
11	0.97	42.1	1.25
12	0.98	41.0	1.18

Table 6.3.3.2 The smectic layer spacings, d, and the ratios of the layer spacing to the estimated all-trans molecular length, d/l, for the 3,4-n series.

The ratio of the layer spacing to the estimated all-trans molecular length is almost constant and equal to 1.25 although the value of d/l for 3,4-12 appears to be somewhat smaller. These measurements suggest that the smectic A phase is of the S_{A_d} type in which the cyanobiphenyl groups are interdigitated.

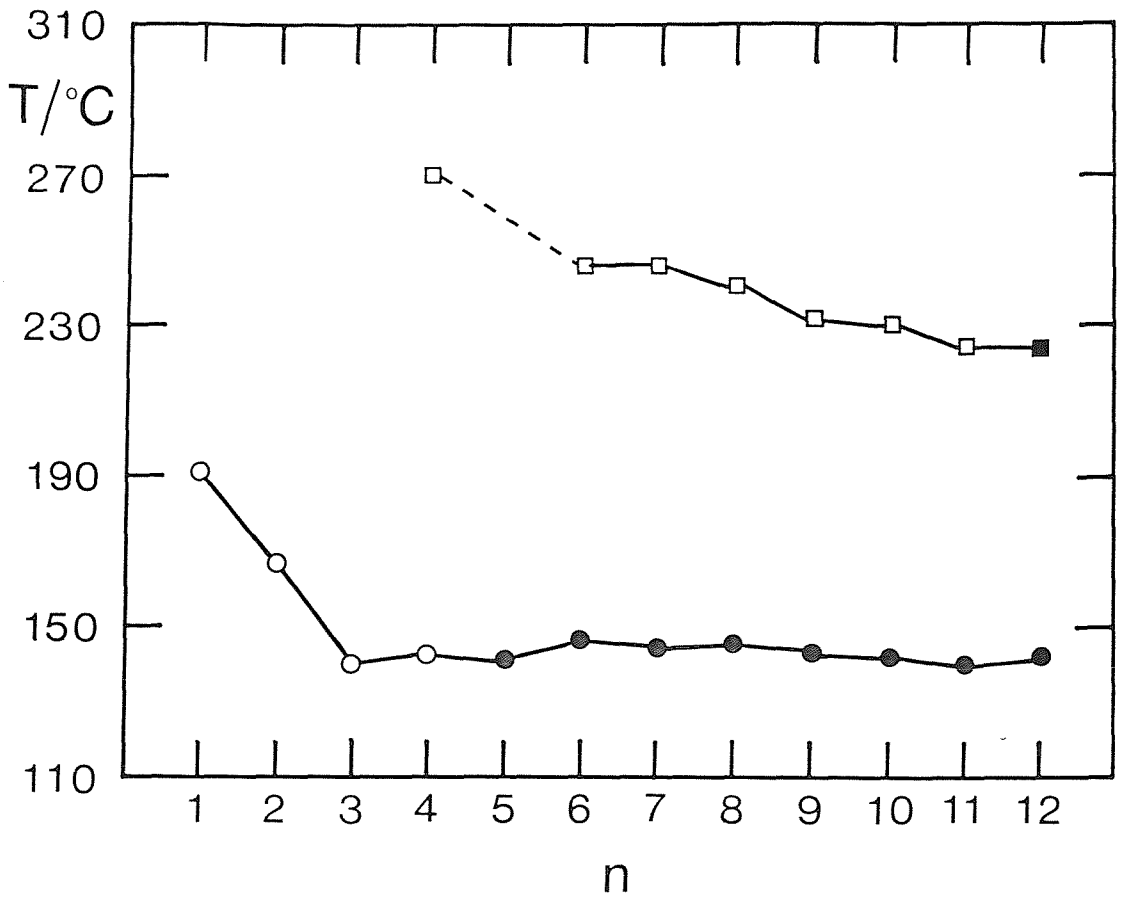

Figure 6.3.3.3 The dependence of the liquid crystal-isotropic transition temperature on the number of carbon atoms in the alkoxy chains for the 3,4-n series represented by circles and the 4-n series [16] denoted by squares. Open symbols indicate nematic-isotropic transitions and filled symbols indicate smectic A-isotropic transitions.

Figure 6.3.3.4 shows the dependence of the entropy change associated with the liquid crystal-isotropic transition on the number of carbon atoms in the alkoxy chains for the 3,4-n series. The value of $\Delta S_{NI}/R$ for 3,4-3 could not be measured, for the compound does not supercool sufficiently far. The entropies associated with the smectic A-isotropic transition increase on increasing the length of the alkoxy chains and this presumably reflects both a greater conformational entropy change and an increased ordering of the molecules.

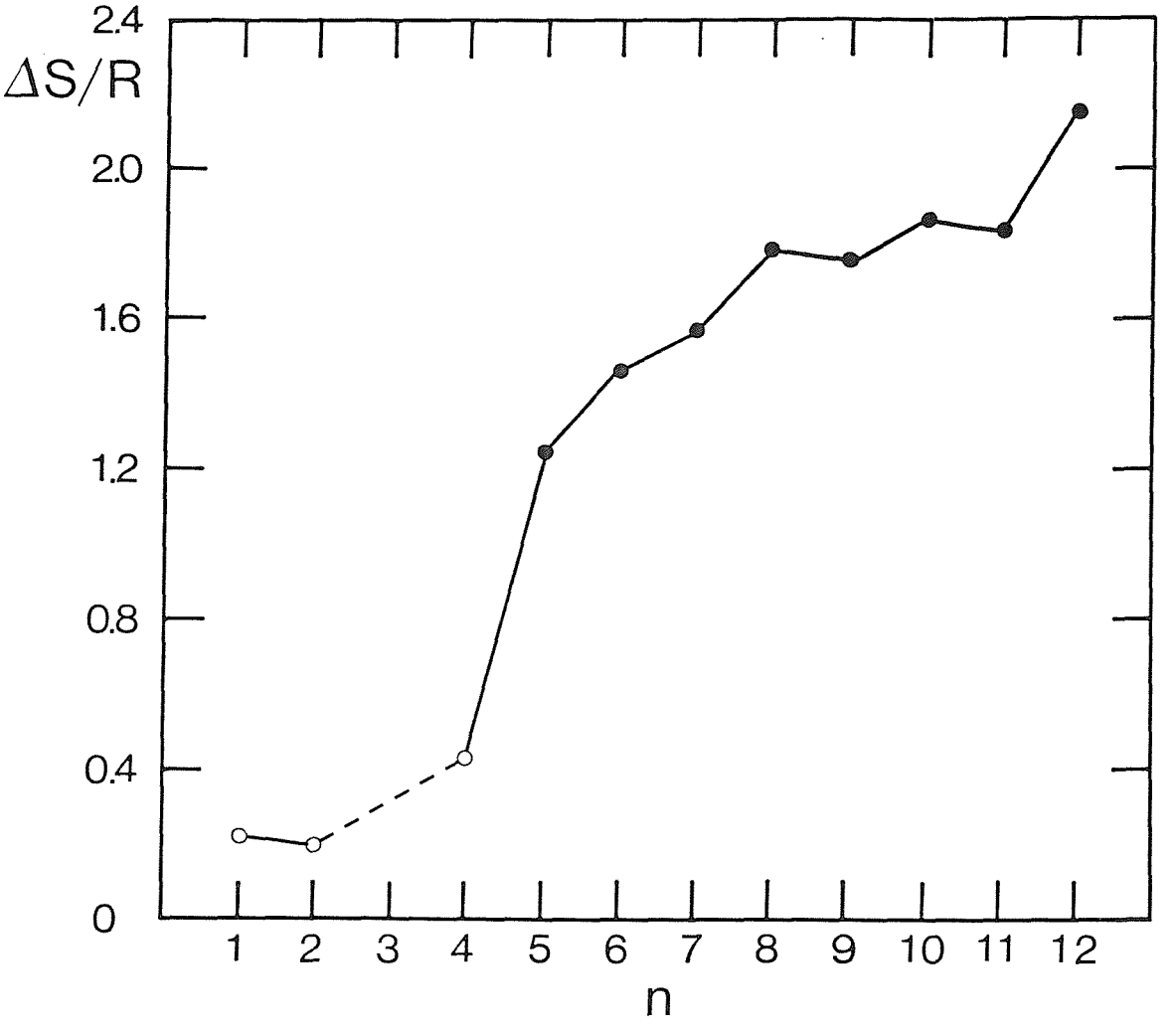

Figure 6.3.3.4 The entropy change associated with the liquid crystal-isotropic transition for the 3,4-n series as a function of the number of carbon atoms in the alkoxy chains. Open circles indicate nematic-isotropic transitions and filled symbols represent smectic A-isotropic transitions.

6.3.4 4-cyano-4'-biphenylyl 3",4",5"-tri-n-alkoxybenzoates

The first three members of the 3,4,5-n series have been characterised and their melting points are listed in table 6.3.4. These compounds do not exhibit mesogenic behaviour. This observation is not surprising because the introduction of one meta-alkoxy chain reduces the nematic-isotropic transition temperature by about 120 °C for the early members and if we assume that the introduction of a second meta-alkoxy chain will have the same effect then, the predicted transition temperatures for the early members of the 3,4,5-n series lie between 20 °C and 70 °C. This range is well below both the melting points of the compounds and the temperature to which the isotropic liquid supercools. In order to observe mesogenic behaviour for this class of molecular structure it will probably be necessary to incorporate a fourth benzene ring into the core structure to enhance the nematic-isotropic transition temperature.

n	T_{CI} / °C	T_{NI} / °C
1	173.5	<100
2	158.5	<100
3	134.5	<70

Table 6.3.4 The melting points of the 3,4,5-n series and the extent to which the isotropic liquid supercools.

6.4 Conclusions

We have described three different types of mesogens each of which are composed of molecules having alkyl chains that lie off the major axis of the rest of the molecule. This general molecular architecture is contrary to the popular belief that alkyl chains must be sited at the terminal positions of the molecule if the compound is to be mesogenic. However, by adopting non-all-trans conformations, lateral alkyl chains can lie parallel to the molecular long axis and hence, preserve a high length to breadth ratio for the molecule. Thus, although mesogens possessing lateral alkyl chains appear to challenge the classical rules of structure-property relationships in low molar mass liquid crystals, more careful thought shows that their properties may be understood within the established framework.

It appears that lateral alkyl chains which are, to a first approximation, topologically equivalent but in different spatial positions, can have a profoundly different influence upon mesogenic behaviour. A lateral alkyl chain attached to the centre of the semi-rigid core is extremely effective in destroying smectic behaviour. This is presumably a result of the chain forming a sheath around the core so reducing the core-core interactions that are essential to smectic phase formation. A lateral chain attached to the end of the core , however, promotes smectic behaviour and this possibly is a consequence of increased molecular inhomogeniety and reduced transition temperatures. This illustrates the shortcomings of theories that attempt to model alkyl chains without allowing for their position within the molecule.

6.5 References

[1] Gray, G.W., 1979, The Molecular Physics of Liquid Crystals, edited by G.R. Luckhurst and G.W. Gray, Academic Press, Chap. 1.

[2] Osman, M.A., 1985, Mol. Cryst. Liq. Cryst., 128, 45.

[3] Gray, G.W., and Jones, B., 1955, J. Chem. Soc., 236.

[4] van der Veen, J., and Hegge, T.C.J.M., 1974, Angew. Chem., 86, 378.

[5] Weissflog, W., and Demus, D., 1983, Cryst. Res. Techn., 18, 21.

[6] Weissflog, W., and Demus, D., 1984, Cryst. Res. Techn., 19, 55.

[7] Tinh, N.H., Malthete, J., and Destrade, C., 1985, Mol. Cryst. Liq. Cryst. Letts., 2, 133.

[8] Tinh, N.H., Gasparoux, H., Malthete, J., and Destrade, C., 1984, Mol Cryst. Liq. Cryst., 114, 19.

[9] Weissflog, W., Diele, S., and Demus, D., 1986, Mater. Chem. Phys., 15, 475.

[10] Weissflog, W., and Demus, D., 1985, Mol. Cryst. Liq. Cryst., 129, 235.

[11] Jones, B., 1935, J. Chem. Soc., 1874.

[12] see for example Malthete, J., Levelut, A.M., and Tinh, N.H., 1985, J. de Phys. Lett., 46, L875.

[13] Forrest, J., and Petrow, V., 1950, J. Chem. Soc., 2340.

[14] Jarvi, E.T., and Whitlock, H.W., 1980, J. Am. Chem. Soc., 102, 657.

[15] Demus, D., Diele, S., Hauser, A., Latif, I., Selbmann, Ch., and Weissflog, W., 1985, Cryst. Res. Techn., 20, 1547.

[16] Demus, D., and Zaschke, H., 1984, Flussige Kristalle in Tabellen, 2, Deutscher Verlag fur Grundstoffindustrie.

[17] Taylor, L, unpublished results.